

**SCHOOL OF CHEMISTRY**

**CARDIFF UNIVERSITY**



---

# **THE SYNTHESIS AND STUDY OF FLUORESCENT DENDRITIC MOLECULES**

---

A thesis submitted to Cardiff University for the degree of Doctor of  
Philosophy By:

**Alaa El-Betany**

**Supervisor: Neil B. McKeown**

**2010**

UMI Number: U564496

All rights reserved

INFORMATION TO ALL USERS

The quality of this reproduction is dependent upon the quality of the copy submitted.

In the unlikely event that the author did not send a complete manuscript and there are missing pages, these will be noted. Also, if material had to be removed, a note will indicate the deletion.



UMI U564496

Published by ProQuest LLC 2013. Copyright in the Dissertation held by the Author.  
Microform Edition © ProQuest LLC.

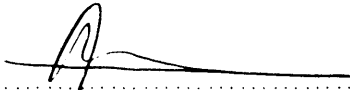
All rights reserved. This work is protected against  
unauthorized copying under Title 17, United States Code.



ProQuest LLC  
789 East Eisenhower Parkway  
P.O. Box 1346  
Ann Arbor, MI 48106-1346

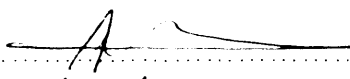
## DECLARATION

This work has not previously been accepted in substance for any degree and is not concurrently submitted in candidature for any degree.

Signed  (Candidate)  
Date 5/4/2012

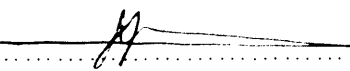
### STATEMENT 1

This thesis is being submitted in partial fulfilment of the requirements for the degree of Doctor of Philosophy.

Signed  (Candidate)  
Date 5/4/2012

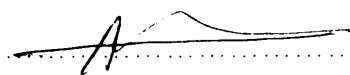
### STATEMENT 2

This thesis is the result of my own independent work/investigation, except where otherwise stated. Other sources are acknowledged by explicit references.

Signed  (Candidate)  
Date 5/4/2012

### STATEMENT 3

I hereby give consent for my thesis, if accepted, to be available for photocopying and for interlibrary loan, and for the title and summary to be made available to outside organisations.

Signed  (Candidate)  
Date 5/4/2012

## **DEDICATION**

To my late mother, father and grandmothers

To my sister and brothers and

To my wife

To my children, Yasmin and Nour

## ACKNOWLEDGEMENT

I would like to thank my supervisor, Professor Neil McKeown, for his help, guidance, and mentorship throughout the years. He has been a great advisor, supporter, and mostly a friend. I thank him from the bottom of my heart for his understanding, trust, and encouragement through the challenges that faced me whilst I've been completing my Ph.D. Without his trust and support, I would never be writing these very lines.

Thank you to the collaborators that I have had the pleasure of working with on this project: especially Dr Mark Gumbleton (Welsh School of Pharmacy) for his advice, and for helping and supporting me during my PhD and his group (Ghaith, Dr Chris, and Mat), Also Dr Niek Burmma, Dr. Peter Griffiths and Dr Simon Pope, and their PhD students: Abdulhakim, Irina, Craig and Ismail, Cardiff School of Chemistry. I would also like to thank Dr Alison Paul, Prof Kenneth Harris and Dr Mark Bagley for their support during viva and report time, and for showing a genuine and sincere interest in how things have been going generally.

Of course, thanks also goes to all my co-workers in McKown's group (especially Dr Kadhum for helping and supporting in the laboratory; Dr Bader, Dr Lino, Dr Grazia, Dr Yulia, Jono, Ryth, Alex, Mohamed, James, and a special thanks goes to Rupert and Matthew for their help in proofreading). A very special thanks goes to Dr. Robert Mart for everything, keeping me sane and on track (most of the time) and for always making yourself available, and of course for proofreading most of this work. An extended thanks goes to the technical staff in the School of Chemistry, especially for Terrie Dumelow in the Student Support Office, Cardiff School of Chemistry.

Many thanks to all my friends Verónica, Piotr and Thomas who have participated and enjoyed my studies. Also, many thanks to Non for her warm friendship and for helping and advising with the English language. I also would like to thank my employer and the whole Egyptian nation, for funding my studies. I would like to thank all my family especially my sister for her endless patience and understanding throughout the course of this study.

...Most importantly, I would like to thank my wife Mrs Enas Behiry for the simple fact to exist. You have always been ready to support my choices and make personal sacrifices to see me live them through. I could not have gotten this far without you, that's team work!...

Before finally, really I missing my mother too much...

Finally, this study could not have been completed without the help, guidance and inspiration of Allah.

## ABSTRACT

Researchers in visualisation and diagnostic imaging for biological applications regard water soluble fluorescent dendrimers as potentially useful materials. Described in this thesis is research with the aim of preparing and investigating a new series of fluorescent polyamidoamine (PAMAM) dendrons with an imidazole naphthalimide derivative (i.e. *7H*-benz[*de*]benzimidazo[2,1-*a*]isoquinoline-7-one ) as the fluorescent core.

After an introduction to the use of dendrimers and dendritic compounds in biology (Chapter 1), we describe work to prepare and optimise potential fluorophore cores, which are based on *N*-alkylamino, *N*-arylamino or imidazole naphthalimide derivatives (Chapter 2). The fluorescence intensity of most of these aromatic systems is weak due to the efficient intramolecular photoinduced electron transfer process (PET). However, derivatives of *7H*-benz[*de*]benzimidazo[2,1-*a*]isoquinoline-7-one proved encouraging and it was decided to use this readily modifiable fluorophore as the core in the design of highly fluorescent dendrons.

In the second experimental part of the thesis (Chapter 3), we designed and prepared several new water soluble fluorescent PAMAM dendrons based on *7H*-benz[*de*]benzimidazo[2,1-*a*]isoquinoline-7-one as fluorescent core and studied their photochemical and physicochemical properties. The dendrons are all fluorescent due to the core but in some cases this is modulated by the PET process, which increases with higher PAMAM dendron generation. For all dendrons the fluorescence is linearly correlated with concentration and the pH of the aqueous solvent has a significant effect for both UV absorbance (ground state) and fluorescent emission (excited state). In strong acidic media this is due to protonation of the core, while in

basic media the fluorescent emission is quenched due to presence of the PET process involving the tertiary amine groups within the PAMAM units. The strongest fluorescent emission of all carboxylate-terminated dendrons was pH 6. Physicochemical studies using the Pulsed Gradient Spin Echo Nuclear Magnetic Resonance (PGSE-NMR) technique indicate that the self-diffusion coefficient and hydrodynamic radii are unaffected by concentration suggesting that there is no aggregation. The confirmed properties (i.e. water solubility, high fluorescence at near neutral pH, and no aggregation) suggest these new dendrons are promising for applications in biological studies.

The next part of the thesis describes new avenues of research using these dendrons and similar materials are suggested in the final chapter (Chapter 5).

Finally, the appendix part of the thesis describes experimental work to assess the transport of the dendrons through biological barriers and their binding to DNA (Appendix A). This work was carried out in collaboration with other research groups. Initial studies suggest that the permeability of fluorescent core PAMAM dendrons across MDCK cell monolayers appear to be a function of the size of the dendrons. These studies pave the way for future detailed mechanistic and morphological studies to elucidate the nature of the interaction of fluorescent core PAMAM dendrons with epithelial cells. Preliminary studies also show that the fluorescent core binds to DNA, presumably by intercalation of the aromatic core. Addition of negatively charged dendrons results in a strong decrease in affinity for DNA. The affinity is not restored by esterification, highlighting contributions of both electrostatic repulsion but particularly steric interactions in blocking interactions. Coupling the fluorescent core

to positively charged dendrons leads to strong binding accompanied by precipitation of the DNA complex.

## Abbreviations

<b>Abs.</b>	Absorbance
<b>AcOH</b>	Acetic acid (CH <sub>3</sub> COOH)
<b>AcONa</b>	Sodium acetate (CH <sub>3</sub> COONa)
<b>Anal.</b>	Analytical
<b>BBB</b>	Blood–Brain Barrier
<b>BLQ</b>	Below level of quantitates
<b>C-4 subst.</b>	substituent attached to Carbon atom in position number 4
<b>Caco-2 cells</b>	Human colonic carcinoma cell line
<b>Calcd</b>	calculated
<b>CDCl<sub>3</sub></b>	Deuterated chloroform
<b>CHCl<sub>3</sub></b>	Chloroform
<b>(CH<sub>3</sub>COO)<sub>2</sub>Zn</b>	Zinc acetate
<b>Conc. H<sub>2</sub>SO<sub>4</sub></b>	Concentrated sulphuric acid
<b>COOH</b>	Carboxylic acid group
<b>COOMe</b>	Methyl carboxylate group
<b>COONa</b>	Sodium carboxylic acid salt
<b>D<sub>s</sub></b>	Self-diffusion Coefficient
<b>D<sub>2</sub>O</b>	Deuterated water
<b>DCM</b>	Dichloromethane
<b>DMEM</b>	Dulbecco's Modified Eagle's Medium
<b>DMF</b>	Dimethylformamide
<b>DMSO-d<sub>6</sub></b>	deuterated dimethyl sulfoxide
<b>DNA</b>	Deoxyribonucleic acid
<b>EDA</b>	Ethylene diamine
<b>EDTA</b>	Ethylenediaminetetraacetic acid,
<b>EI-MS</b>	Electron Ionization-Mass Spectroscopy
<b>Em</b>	Emission
<b>ESA</b>	Excited State Absorption
<b>EtOH</b>	Ethanol
<b>EVOM</b>	Epithelial voltohmmeter

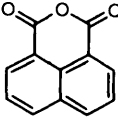
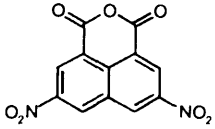
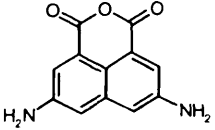
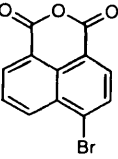
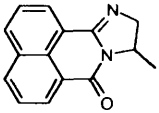
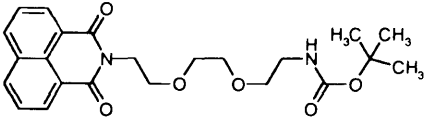
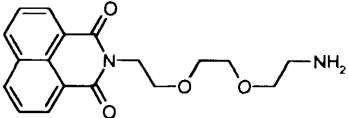
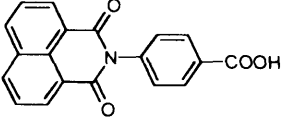
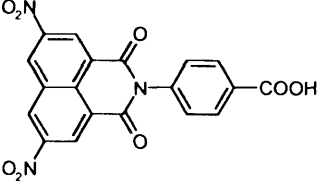
---

<b>FITC</b>	fluoresceine isothiocyanate
<b>Flu</b>	Fluorescence
<b>FT-IR</b>	Fourier Transform Infra-Red
<b>G</b>	Generation of dendrimers
<b>h</b>	Hour
<b>HPLC</b>	High-performance liquid chromatography
<b>HRMS</b>	High Resolution Mass Spectroscopy
<b>IC</b>	Internal Conversion
<b>ICT</b>	internal charge transfer
<b>In-Vitro</b>	Latin for "in glass," the term in vitro refers to experiments that are performed outside an organism's body
<b>in Vivo</b>	In vivo (Latin for "within the living") is experimentation using a whole, living organism as opposed to a partial or dead organism. OR Literally = "in life" ie in a living animal or human.
<b>ISC</b>	intersystem crossing
<b>Lit.</b>	Literature
<b>LLQ</b>	Low Latency Queuing OR Left lower quadrant
<b>LRMS</b>	Low Resolution Mass Spectroscopy
<b>MALDI-TOF</b>	Matrix Assisted Laser Desorption/Ionization Time-of-Flight
<b>Max.</b>	Maximum
<b>MDCK</b>	Madin–Darby canine kidney
<b>MeCN</b>	Acetonitrile
<b>MeOD</b>	Deuterated methanol
<b>MHz</b>	megahertz
<b>MOPS</b>	3-(N-morpholino)propanesulfonic acid
<b>mp</b>	Melting Point
<b>MTX</b>	methotrexate
<b>NBD chloride</b>	4-Chloro-7-nitro-2,1,3-benzoxadiazole
<b>nm</b>	nanometer
<b>nM</b>	nanomolar, ( $10^{-9}$ molar) of concentration
<b>NMR</b>	Nuclear Magnetic Resonance

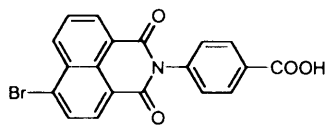
---

<b>n-<math>\pi^*</math> transition</b>	An electronic transition described approximately as <u>promotion</u> of an electron from a 'non-bonding' (lone-pair) n orbital to an 'antibonding' $\pi$ orbital designated as $\pi^*$ .
<b>OG<sub>488</sub></b>	Oregon Green 488
<b><math>P_{app}</math></b>	apparent permeability coefficients
<b>PAMAM</b>	polyamidoamine
<b>Pd/C</b>	Palladium on Activated Charcoal also known as Palladium on Carbon (Pd on C) is a mild hydrogenation catalyst
<b>PET</b>	photoinduced electron transfer process
<b>PETIM</b>	poly(propyl ether imine)
<b>P-gp</b>	p-glycoprotein
<b>PGSE-NMR</b>	Pulsed Gradient Spin Echo Nuclear Magnetic Resonance
<b>PIET</b>	Photoinduced Internal Electron Transfer process
<b>PPI</b>	poly(propyleneimine)
<b>ppm</b>	part per million
<b>RFI</b>	Relative Fluorescence Intensity
<b><math>R_h</math></b>	Hydrodynamic radii
<b>RT</b>	Room Temperature
<b>6-TAMRA</b>	6-carboxy tetramethyl rhodamine succinic ester
<b>TEER</b>	Transepithelial electrical resistance
<b>TFA</b>	Trifluoroacetic acid
<b>TLC</b>	Thin Layer Chromatography
<b>TMS</b>	tetramethylsilane
<b>UV-vis</b>	Ultraviolet-visible
<b><math>\Phi_F</math></b>	Fluorescence Quantum Yield
<b><math>\pi</math>-<math>\pi^*</math> transition</b>	An electronic transition described approximately as a promotion of an electron from a 'bonding' $\pi$ orbital to an 'antibonding' $\pi$ orbital designated as $\pi^*$
<b><math>\Omega</math></b>	The <b>ohm</b> (symbol: $\Omega$ ) is the <u>SI</u> unit of electrical resistance

## List of molecules

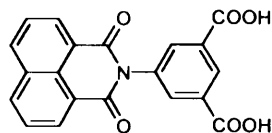
Short name	Structure	No.
1,8-naphthalic anhydride		1
3,6-dinitro-1,8-naphthalic anhydride		2
3,6-diamino-1,8-naphthalic anhydride		3
4-bromo-1,8-naphthalic anhydride		4
2-(1-aminopropan-2-yl)-1H-benzo[de]isoquinoline-1,3(2H)-dione.		CF2
tert-butyl 2-(2-(2-(1,3-dioxo-1H benzo[de]isoquinolin-2(3H)yl)ethoxy)ethoxy)ethylcarbamate.		FC3Boc
2-(2-(2-(2-aminoethoxy)ethoxy)ethyl)-1H-benzo[de]isoquinoline-1,3(2H)-dione.		CF3
4-(1,3-dioxo-1H,3H-benzo[de]isoquinolin-2-yl)-benzoic acid.		A1
4-(5,8-dinitro-1,3-dioxo-1H,3H-benzo[de]isoquinolin-2-yl)-benzoic acid.		A2

4-(6-bromo-1,3-dioxo-1H-benzo[de]isoquinolin-2(3H)-yl)benzoic acid.



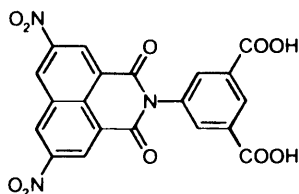
A4

5-(1,3-dioxo-1H,3H-benzo[de]isoquinolin-2-yl)-isophthalic acid.



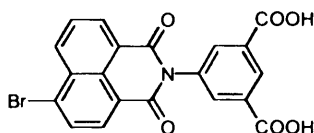
B1

5-(5,8-dinitro-1,3-dioxo-1H,3H-benzo[de]isoquinolin-2-yl)-isophthalic acid.



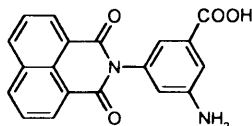
B2

5-(6-bromo-1,3-dioxo-1H-benzo[de]isoquinolin-2(3H)-yl)isophthalic acid.



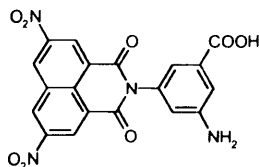
B4

3-amino-5-(1,3-dioxo-1H,3H-benzo[de]isoquinolin-2-yl)-benzoic acid.



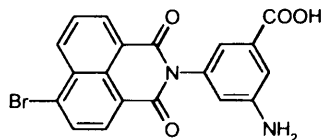
C1

3-amino-5-(5,8-dinitro-1,3-dioxo-1H,3H-benzo[de]isoquinolin-2-yl)-benzoic acid.



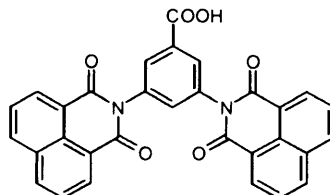
C2

3-amino-5-(6-bromo-1,3-dioxo-1H-benzo[de]isoquinolin-2(3H)-yl)benzoic acid.



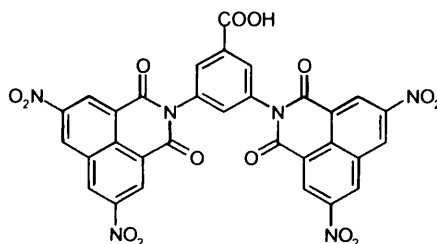
C4

3,5-bis-(1,3-dioxo-1H,3H-benzo[de]isoquinolin-2-yl)-benzoic acid.



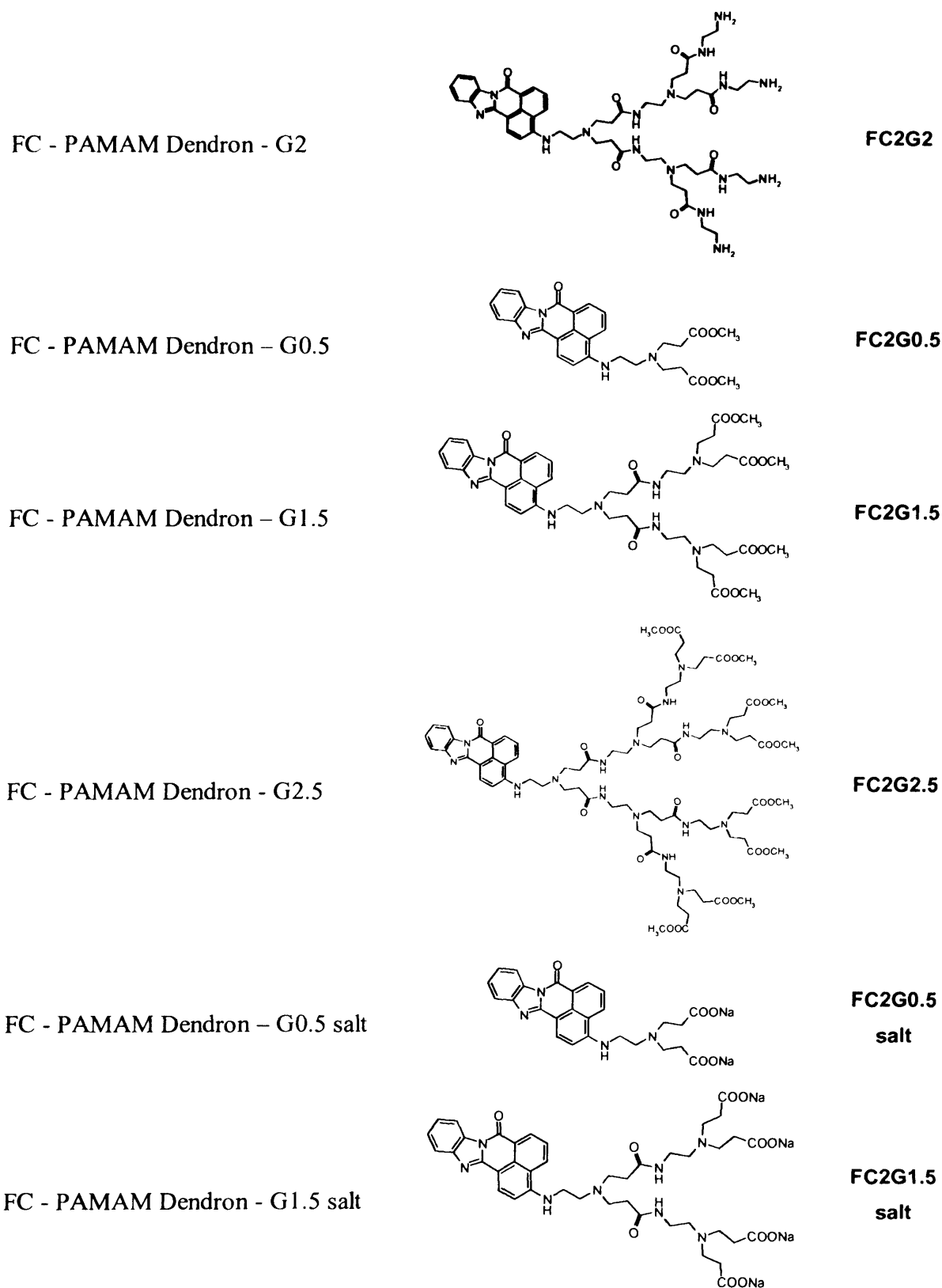
C11

3,5-bis-(5,8-dinitro-1,3-dioxo-1H,3H-benzo[de]isoquinolin-2-yl)-benzoic acid.

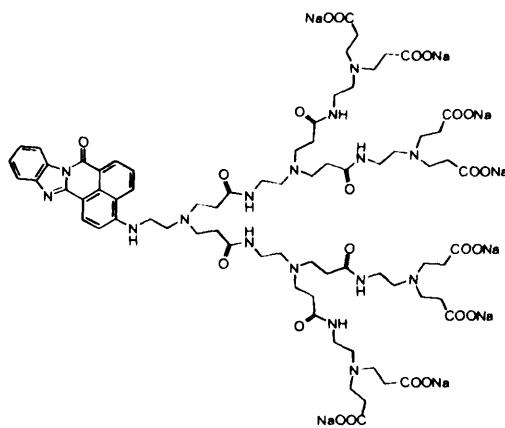


C22

<p>3,5-bis(6-bromo-1,3-dioxo-1H-benzo[de]isoquinolin-2(3H)-yl)benzoic acid.</p>		<p><b>C44</b></p>
<p>4-(5,8-diamino-1,3-dioxo-1H,3H-benzo[de]isoquinolin-2-yl)-benzoic acid.</p>		<p><b>A3</b></p>
<p>5-(5,8-diamino-1,3-dioxo-1H,3H-benzo[de]isoquinolin-2-yl)-isophthalic acid.</p>		<p><b>B3</b></p>
<p>3-amino-5-(5,8-diamino-1,3-dioxo-1H-benzo[de]isoquinolin-2(3H)-yl)benzoic acid.</p>		<p><b>C3</b></p>
<p>3,5-bis(5,8-diamino-1,3-dioxo-1H-benzo[de]isoquinolin-2(3H)-yl)benzoic acid.</p>		<p><b>C33</b></p>
<p>3-bromo-7H-benz[de]benzimidazo[2,1-a]isoquinoline-7-one.</p>		<p><b>FC2</b></p>
<p>3-(2-aminoethylamino)-7H-benz[de]benzimidazo[2,1-a]isoquinoline-7-one.</p>		<p><b>FC2G0</b></p>
<p>FC - PAMAM Dendron - G1</p>		<p><b>FC2G1</b></p>



FC - PAMAM Dendron - G2.5 salt



**FC2G2.5**  
**salt**



1.1.4.2. Mechanisms of drug loading onto dendrimer carriers..	8
1.1.4.3. Dendrimers as imaging agents.....	9
1.1.4.4. Pharmacokinetics.....	9
<b>1.2. Dendrimers Containing Fluorescent Labeling .....</b>	<b>10</b>
1.2.1. Type .....	11
1.2.1.1. Intrinsically Fluorescent Dendrimers.....	11
1.2.1.2. Multiply Labelled Dendritic Structures.....	11
1.2.1.3. Statistically Labelled Dendritic Structures.....	13
1.2.1.4. Dendrimers with Fluorescent Cores.....	14
1.2.1.5. Dendritic Wedges with Fluorescent ‘Cores’.....	14
1.2.2. Applications of fluorescent dendrimers .....	15
<b>1.3. Fluorescent Compounds .....</b>	<b>16</b>
1.3.1. Principles of fluorescence spectroscopy.....	16
1.3.1.1. Fluorescence.....	16
1.3.1.2. Structural factors that determine fluorescence.....	17
1.3.2. PAMAM conjugation to naphthalic anhydride derivatives .....	18
1.3.2.1. Synthesis and Photoluminescence properties.....	18
1.3.2.2. PAMAM conjugates.....	19
1.3.2.3. Chemotherapeutic applications.....	21
<b>1.4. Aims of the project .....</b>	<b>22</b>
<b>2. Chapter Two: Fluorescent Cores .....</b>	<b>24</b>
<b>2.1. Synthesis .....</b>	<b>24</b>
2.1.1. N-alkyl-1,8-naphthalic anhydride derivatives.....	24
2.1.2. N-aryl-1,8-naphthalic anhydride derivatives.....	25
<b>2.2. Photophysical studies .....</b>	<b>29</b>
2.2.1. UV-vis absorption spectra.....	29

2.2.2.	Relative fluorescence intensity (RFI).....	30
2.2.3.	Fluorescence quantum yield ( $\Phi_F$ ).....	35
<b>2.3.</b>	<b>Conclusions.....</b>	<b>36</b>
<b>3.</b>	<b>Chapter Three: Fluorescent PAMAM Carriers .....</b>	<b>37</b>
<b>3.1.</b>	<b>Design and synthesis .....</b>	<b>37</b>
3.1.1.	Synthesis of fluorophore core (FC2G0).....	37
3.1.2.	Synthesis of fluorescent PAMAM dendritic wedges ( COOMe, NH <sub>2</sub> ).....	40
3.1.3.	Synthesis of fluorescent PAMAM dendritic wedge salts (COONa).....	43
<b>3.2.</b>	<b>Photophysical characterization .....</b>	<b>46</b>
3.2.1.	UV-vis absorption properties.....	46
3.2.2.	Fluorescence measurements.....	47
3.2.2.1.	Relative intensity of fluorescence for PAMAM terminated (-COOMe, -NH <sub>2</sub> ).....	47
3.2.2.2.	Relative intensity for fluorescent PAMAM terminated [-COONa].....	51
3.2.3.	Effect of concentration on fluorescence emission intensity .....	52
3.2.4.	Influence of pH on the absorption and fluorescence characteristics.....	53
3.2.4.1.	UV-visible absorption spectra.....	53
3.2.4.1.	Influence of pH on the fluorescence of FC2G0.5, FC2G1.5 and FC2G2.5 salts.....	56
<b>3.3.</b>	<b>Physicochemical characterization studies .....</b>	<b>59</b>
3.3.1.	Pulsed Gradient Spin Echo - NMR ((PGSE) – NMR).....	59
3.3.1.1.	Self-diffusion coefficient (Ds).....	59
3.3.1.2.	Hydrodynamic radii (Rh).....	61
<b>3.4.</b>	<b>Conclusion.....</b>	<b>62</b>

<b>4. Chapter Four: Experimental .....</b>	<b>64</b>
<b>4.1. Experimental techniques .....</b>	<b>64</b>
<b>4.2. General experimental procedures.....</b>	<b>66</b>
4.2.1. Photolumiscence study procedures .....	66
<b>4.3. Experimental procedures .....</b>	<b>68</b>
4.3.1. Organic synthesis procedures.....	68
<b>4.4. Experimental Appendix .....</b>	<b>97</b>
<b>5. Chapter Five: Future Work .....</b>	<b>104</b>
<b>5.1. Design and synthesis.....</b>	<b>104</b>
5.1.1. Synthesis of new fluorescent dendritic wedges.....	104
5.1.2. Synthesis of fluorescent PAMAM dendritic multi-wedges.....	105
5.1.3. Self assembly core of fluorescent PAMAM dendritic wedges....	106
<b>6.2. Chemotherapeutic applications .....</b>	<b>107</b>
6.2.1. Inhibitor of protein aggregation .....	107
6.2.2. Anticancer activity studies.....	110
<b>References .....</b>	<b>112</b>
<b>Appendices.....</b>	<b>128</b>
<b>A Appendix A: Chemotherapeutic Applications .....</b>	<b>128</b>
<b>A.1 In-Vitro Permeability studies .....</b>	<b>128</b>
A.1.1. Introduction.....	128
A.1.2. Results and Discussions.....	130

A.1.2.1	Permeability of fluorescent core PAMAM dendrons across MDCK I, II cell monolayers.....	130
A.1.2.2	Effect on monolayer integrity by measuring transepithelial electrical resistance (TEER).....	132
A.1.3.	Summary.....	134
<b>A.2</b>	<b>DNA binding studies .....</b>	<b>135</b>
A.2.1.	Introduction.....	135
A.2.2.	Results and discussion.....	136
A.2.3.	Summary.....	141

# CHAPTER ONE

## INTRODUCTION

<b>1.1 Dendrimers .....</b>	<b>1</b>
<b>1.2 Dendrimers Containing Fluorescent Labelling.....</b>	<b>10</b>
<b>1.3 Fluorescent Compounds.....</b>	<b>16</b>
<b>1.4 Aims of the project.....</b>	<b>22</b>

## 1.1. Dendrimers

### 1.1.1. Background

Dendrimers can be considered one of the more attractive recent discoveries in the field of organic and polymer synthesis. They are exciting because they have an exceptional three-dimensional structure comprising three distinct components: core (or focal point), branching point and periphery (Figure 1.1). The story of the development of dendrimers starts in 1978 when Vögtle<sup>[1]</sup> reported his first steps towards an iterative synthesis of “cascade molecules” with branched architectures. Two distinct synthetic approaches are now established for these three-dimensional macromolecules; Tomalia *et al.* pioneered the divergent synthesis involving an “inside-out” approach,<sup>[2-3]</sup> while Hawker and Fréchet<sup>[4]</sup> pioneered convergent synthesis involving an “outside-in” approach.

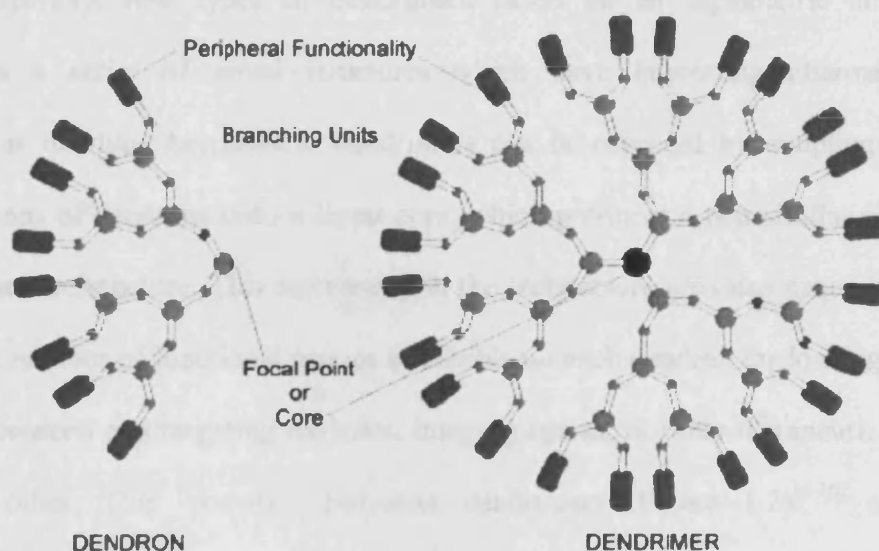


**Figure [1.1]:** Schematic diagram of the structure of a dendron and a dendrimer, highlighting the focal point or core (black) surrounded by rings of branching units (gray circles) and end-groups (rectangles).<sup>[5]</sup>

## 1.1.2. Variations of dendrimer structure

In 2005, Fréchet reported various designs of low polydispersity combinations of dendrons and linear polymers<sup>[6]</sup> such as linear-dendritic hybrids,<sup>[6-8]</sup> bow-tie dendrimers,<sup>[9-10]</sup> and dendronized polymers.<sup>[6, 11-13]</sup> Recently these new dendritic polymers have been applied in drug delivery and other biomedical applications.<sup>[14]</sup> In 2009, El-Sayed and co-workers reviewed the field,<sup>[15]</sup> cataloging the dendrimer families which have been used as carriers in chemotherapeutic applications such as biodegradable ester dendrimers,<sup>[16-19]</sup> amino acid-based dendrimers,<sup>[20-21]</sup> glycodendrimers,<sup>[22]</sup> hydrophobic dendrimers,<sup>[23]</sup> in addition to other, less important types.

### 1.1.2.1. Asymmetric dendrimers

Although the symmetric architecture of dendrimers has produced polymers with high monodispersity, new types of dendrimers based on an asymmetric architecture provides a series of novel structures which have interesting pharmacokinetic behaviour in vivo. Asymmetric dendrimers can be prepared by coupling different generations of dendrons onto a linear core, which produces a non-similar orthogonal dendrimer architecture. This asymmetry in the architecture provides exquisite control over the number of functional groups accessible on each dendron for loading of drugs in one dendron and targeting moieties, imaging agents, or other therapeutic moieties in the other. The “bow-tie” polyester dendrimers (Figure 1.2)<sup>[9-10]</sup> are noted asymmetric dendrimers first synthesized by Fréchet and co-workers. Lee and co-workers also reported another class of asymmetric dendrimers, using “click” chemistry to couple a propargyl G4 dendron to an azide functionalized G3 dendron, forming a triazole core.<sup>[24]</sup>

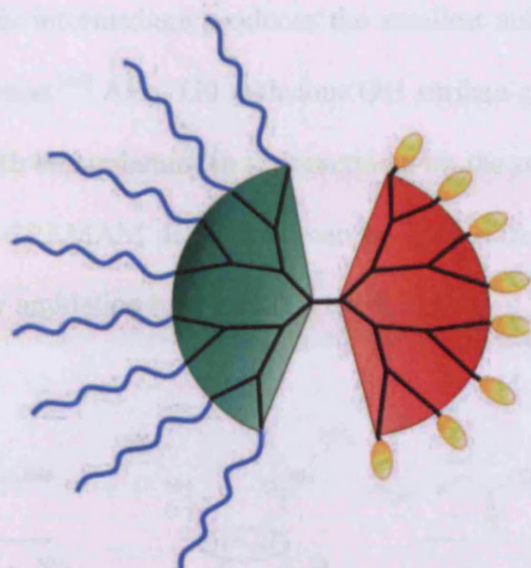


**Figure [1.2]:** represent “bow-tie” polyester dendrimer reported by Szoka and Fréchet.<sup>[10]</sup> The green dendron is functionalized with PEG arms (blue lines) to increase the dendrimer’s solubility and *in-vitro* half life, whereas the other red dendron can be used for the loading of anticancer drug molecules (yellow ovals).<sup>[15]</sup>

#### 1.1.2.2. Divergent synthesis of PAMAM dendrimers

As well as being the first dendrimers synthesised,<sup>[25]</sup> poly(amidoamine) (PAMAM) dendrimers are also considered one of the best potential drug delivery carriers due to their high biocompatibility. They are: hydrophilic, nanostructured, mimics of globular proteins,<sup>[25]</sup> are transported across the epithelial barrier of the gut,<sup>[26-28]</sup> inhibit protein-protein binding,<sup>[29]</sup> and have intrinsically fluorescent behaviour under acidic conditions,<sup>[30]</sup> in addition to their ability to load fluorescent compounds in their core and/or peripheries.<sup>[31-39]</sup> The synthesis of PAMAM dendrimers is mainly dependant on iterative steps, initially Michael addition onto an alkyldiamine core (e.g., ethylene diamine; EDA) using methyl acrylate monomers to yield a branched intermediate, which can be converted to the smallest PAMAM dendrimer generations with  $\text{NH}_2$ ,  $\text{COOH}$  or  $\text{OH}$  terminal groups.<sup>[40]</sup> Amidation is the second step, this smallest branched intermediate is reacted with excess EDA to produce G0 with four  $\text{NH}_2$  surface groups. Addition of methyl acrylate and then hydrolysis of the methyl ester

COOMe group in this intermediate produces the smallest anionic dendrimer (G0.5) with four COOH groups.<sup>[40]</sup> Also, G0 with four OH surface groups can be produced by replacing EDA with ethanolamine in the reaction with the smallest intermediate.<sup>[41]</sup> Higher generations of PAMAM dendrimers can be synthesized by repeated Michael additions followed by amidation reactions (Figure 1.3).

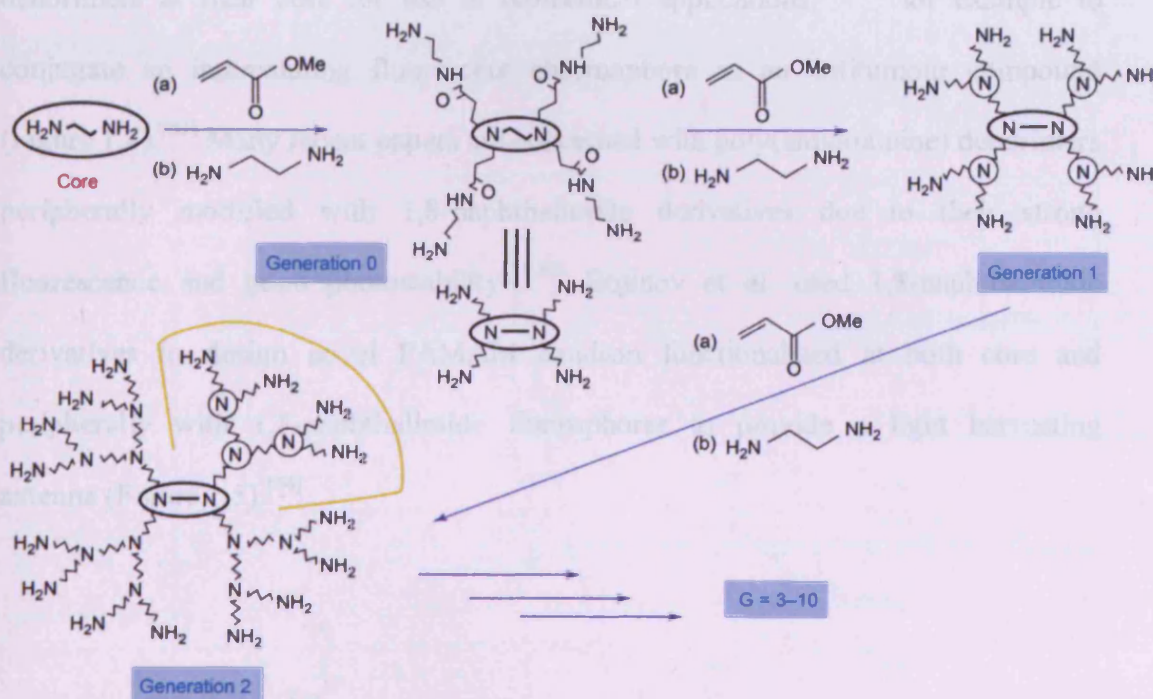


**Figure [1.3]:** Synthesis of tetra-functional poly(amidoamine) (PAMAM) dendrimers: exhaustive Michael addition of amino groups with methyl acrylate, followed by amidation of the resulting esters with ethylenediamine.<sup>[25]</sup>

### 1.1.2.3. Convergent synthesis

Although convergent synthetic strategy pioneered by Hawker and Fréchet overcame the problem of many divergent side-by-products, relatively few methods are recorded to synthesise PAMAM dendrimer,<sup>[42]</sup> especially few in the solution phase<sup>[43-48]</sup> where the use of different dendrons in solution needs large excesses of reagent which is impracticable. So Lee et al and co-workers (2006) presented the first synthesis of

poly(amidoamine) (PAMAM) dendrons in high yields by convergent synthesis<sup>[49]</sup> and by using click chemistry.<sup>[50]</sup> Furthermore, this method can afford PAMAM dendrimers possessing unsymmetrical branches with size-differentiation.<sup>[24]</sup>

#### 1.1.2.4. Modification of pre-made PAMAM dendrimers

A literature survey revealed many reports about synthetic modification of PAMAM dendrimers at their core for use in biomedical applications,<sup>[51-52]</sup> for example to conjugate an intercalating fluorescent chromophore as an antitumour compound (Figure 1.4).<sup>[53]</sup> Many recent papers are concerned with poly(amidoamine) dendrimers peripherally modified with 1,8-naphthalimide derivatives due to their strong fluorescence and good photostability<sup>[31-37]</sup> Bojinov et al. used 1,8-naphthalimide derivatives to design novel PAMAM dendron functionalized at both core and peripherally with 1,8-naphthalimide fluorophores to provide a light harvesting antenna (Figure 1.5).<sup>[54]</sup>

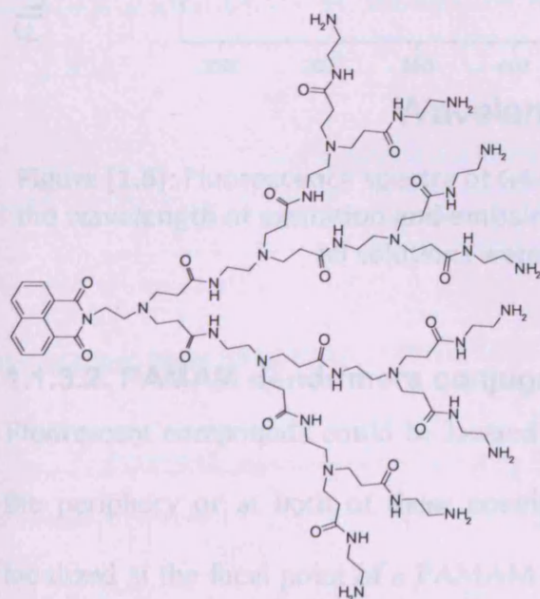


Figure [1.4]: PAMAM dendritic polyamines–(imide–DNA intercalator).<sup>[53]</sup>

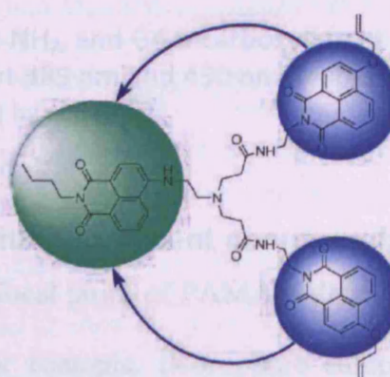
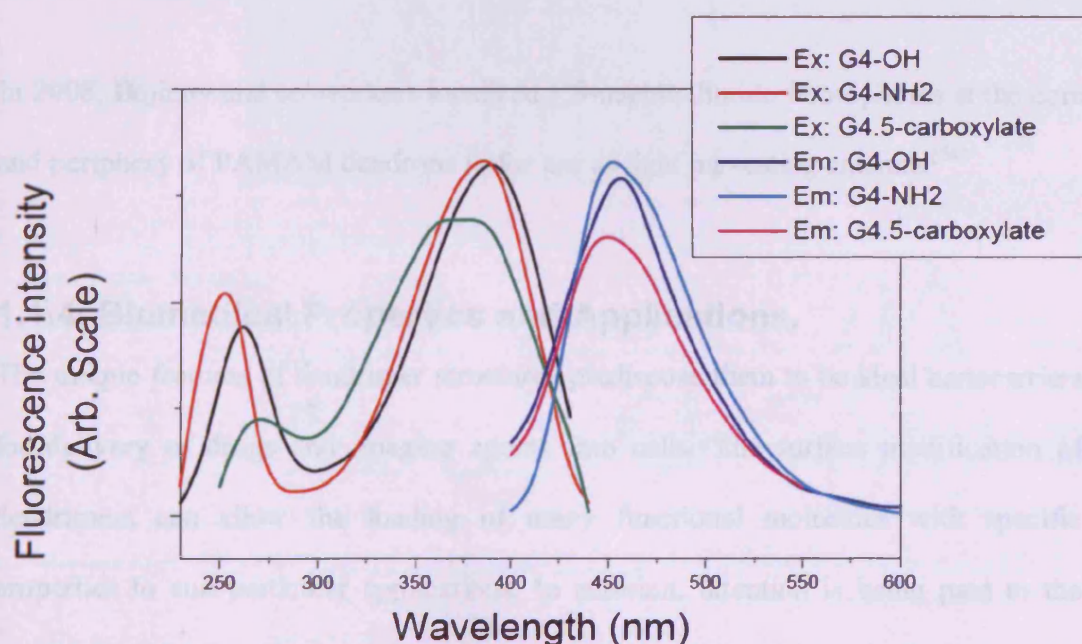


Figure [1.5]: PAMAM dendron functionalized at both core and peripherally with 1,8-naphthalimide fluorophores.<sup>[54]</sup>

### 1.1.3. Photophysical properties of PAMAM dendrimers

#### 1.1.3.1. Intrinsically fluorescent behaviour

Poly(amido amine) (PAMAM) dendrimers with different terminal groups ( $\text{NH}_2$ , OH, and COONa) show high fluorescence emission under different parameters and conditions. The fluorescent emission increases linearly with dendrimer concentration, or is rapidly increased by high temperature or at low pH, which may be attributed to the protonation of the tertiary amine groups (Figure 1.6).<sup>[30, 55]</sup>



**Figure [1.6]:** Fluorescence spectra of G4-OH, G4-NH<sub>2</sub>, and G4.5-carboxylate at pH 6, the wavelength of excitation and emission was at 385 nm and 450 nm, respectively. All solutions were 0.7 nM in water.<sup>[55]</sup>

#### 1.1.3.2. PAMAM dendrimers conjugated with fluorescent compounds

Fluorescent compounds could be located at the focal point of PAMAM dendrons, at the periphery or at both of these positions. For example, fluorophore compounds localized at the focal point of a PAMAM dendron like a fullerene (fullerodendron)<sup>[56-57]</sup> carbazole or pyrene moiety have been studied and demonstrate self-assembly behaviour.<sup>[58]</sup>

Many recent papers have concerned PAMAM dendrimers peripherally modified with 1,8-naphthalimide derivatives due to their strong fluorescence.<sup>[31-37]</sup> PAMAM dendrons of G1–G3 generations have been modified with naphthyl groups at the periphery and a dansyl group at the focal point.<sup>[38]</sup> Other examples include the coupling of dansyl chloride, sulforhodamine B2 acid fluoride, coumarin-343, NBD chloride, and 5(6)-carboxyfluorescein pentafluorophenyl ester to dendritic PAMAM structures for use as new oligomeric fluorescent labelling compounds.<sup>[39]</sup>

In 2008, Bojinov and co-workers localized 1,8-naphthalimide fluorophores at the core and periphery of PAMAM dendrons to for use as light harvesting antenna.<sup>[54]</sup>

#### **1.1.4. Biomedical Properties and Applications.**

The unique features of dendrimer structures predispose them to be ideal nanocarriers for delivery of drugs and imaging agents into cells. The surface modification of dendrimers can allow the loading of many functional molecules with specific properties to suit particular applications. In addition, attention is being paid to the potential use of dendrimer carriers to cross biological barriers, especially the blood–brain barrier (BBB) or gastrointestinal tract. It is expected that upcoming work in biomedical application of existing dendrimers will be also concerned with dendrimer toxicity and biocompatibility.<sup>[59-60]</sup>

##### **1.1.4.1. PAMAM dendrimers as potential drug delivery carriers**

The unique properties of PAMAM dendrimers are water solubility, nanosize and a well defined macromolecule structure.<sup>[40, 61-62]</sup> The uniform expansion of size<sup>[62]</sup> during generation increase make PAMAM dendrimers interesting mimics to globular proteins (Figure 1.7). There are many applications of PAMAM dendrimers in drug

delivery,<sup>[63]</sup> gene delivery,<sup>[64]</sup> and antisense oligonucleotide delivery.<sup>[65]</sup> Researchers still investigate and seek to understand the relationship between PAMAM dendrimer structural properties (size and charge)<sup>[27]</sup> and their ability to permeate cells that make up biological barriers.

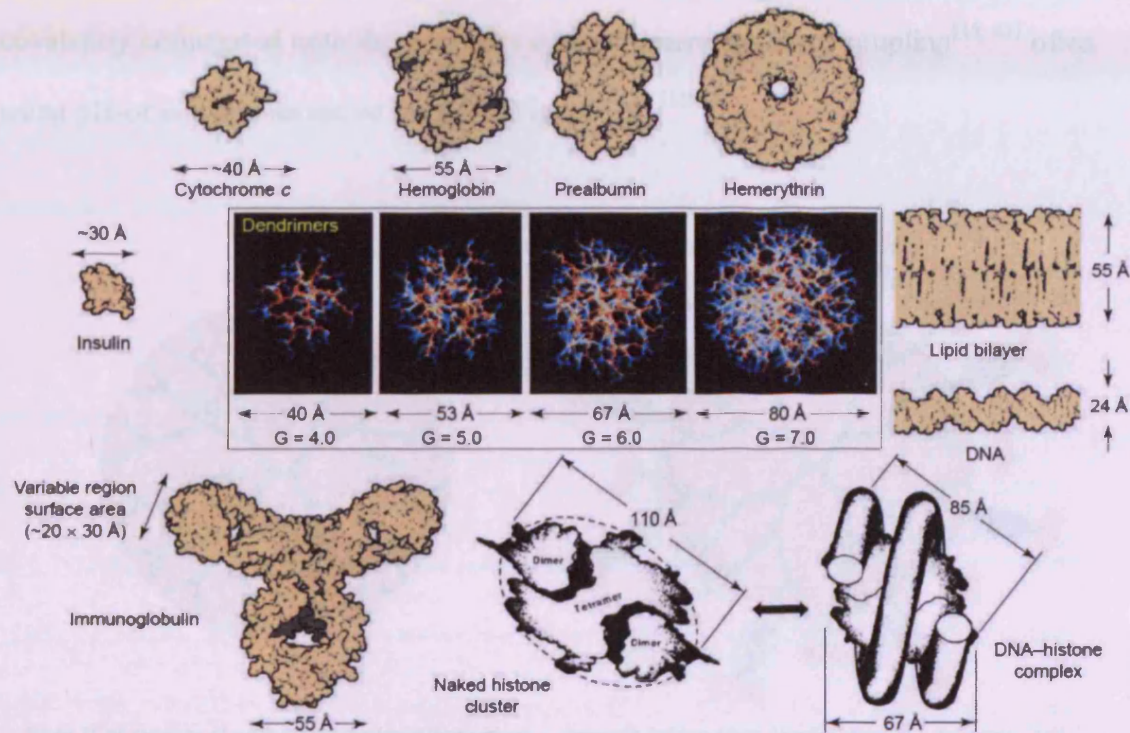


**Figure [1.7]:** A dimensionally scaled comparison of a series of poly(amidoamine) (PAMAM) dendrimers (NH<sub>3</sub> core; G = 4–7) with a variety of proteins, a typical lipid-bilayer membrane and DNA, indicating the closely matched size and contours of important proteins and bioassemblies.<sup>[25]</sup>

#### 1.1.4.2. Mechanisms of drug loading onto dendrimer carriers

##### 1.1.4.2.1. Physical encapsulation of drug molecules

Vögtle and co-workers investigated the trapping of guest molecules into branched polymers<sup>[66]</sup> by physical encapsulation of insoluble drug molecules to improve their aqueous solubility and control their release profile (Figure 1.8).<sup>[3, 16, 67-70]</sup> Insertion of hydrophobic molecules into dendrimers is usually achieved by mixing of drug

solutions with the polymer, where the nonpolar core links with the hydrophobic drug by hydrophobic interactions.<sup>[3, 16, 69-70]</sup>

#### 1.1.4.2.2. Chemical conjugation of drug molecules

On the other hand, different drugs, imaging agents, and/or targeting ligands can be covalently conjugated onto the periphery of dendrimers by direct coupling<sup>[15, 63]</sup> often using pH- or enzyme-sensitive linkages (Figure 1.9).<sup>[15, 71]</sup>



**Figure [1.8]:** Drawing of a dendrimer carrier encapsulating hydrophobic drug molecules in the dendrimer's voids to increase their aqueous solubility and control their release rate.<sup>[15]</sup>

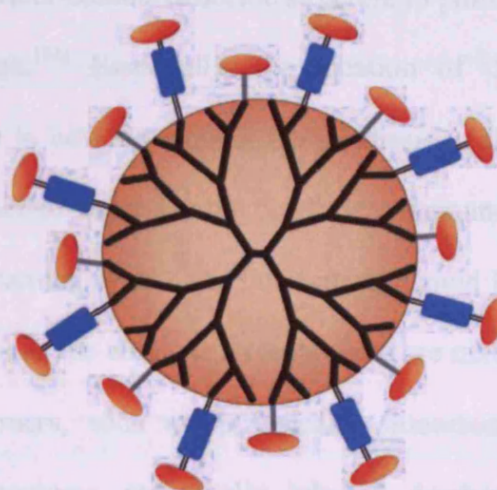


**Figure [1.9]:** Schematic drawing showing a dendrimer-drug conjugate where the drug molecules (red ovals) are either directly coupled (solid line) to dendrimer's surface groups or via a pH-sensitive linkage (blue rectangle).<sup>[15]</sup>

#### 1.1.4.3. Dendrimers as imaging agents

One of the first uses of dendrimers *in vivo* was as carriers for magnetic resonance imaging contrast reagents<sup>[72-73]</sup> Another imaging application involves photonic oxygen sensing<sup>[74]</sup>. Dendrimers with solubilizing and steric-stabilizing core-shell architecture have been developed for new photophysical technology, and offers promise for accurate, noninvasive optical imaging.<sup>[75]</sup>

#### 1.1.4.4. Pharmacokinetics

Investigation of dendrimer pharmacokinetics parameter are now essential for any further biomedical applications, because toxicity and bioavailability of any drug or

imaging agent loading to dendrimers will depend on their release rates from dendrimers and elimination rates.<sup>[76]</sup>

## 1.2. Dendrimers containing Fluorescent Labels.

Recent literature surveys indicate continuing interest in water soluble fluorescent dendrimers for visualisation and diagnostic imaging applications.<sup>[75, 77-81]</sup> As most fluorophores are quenched in aqueous media due to aggregation of the hydrophobic fluorophore, the concept is to use the bulky water-soluble dendritic structure to protect the fluorophore and hinder self-association.<sup>[81]</sup> Essentially, the location of the fluorophore(s) has played an important role in both controlling the synthesis of the dendrimer and its properties. The fluorescence of water-soluble dendritic compounds can be due to the entire macromolecular structure, or discrete fluorophores could be used as peripheral groups, as branch points or as the core. As a result, there are many types of water soluble fluorescent dendrimers, such as intrinsically fluorescent dendrimers, multiply labelled dendritic structures, statistically labelled dendritic structures, or dendrimers with fluorescent cores (Figure 1.10).<sup>[81]</sup>

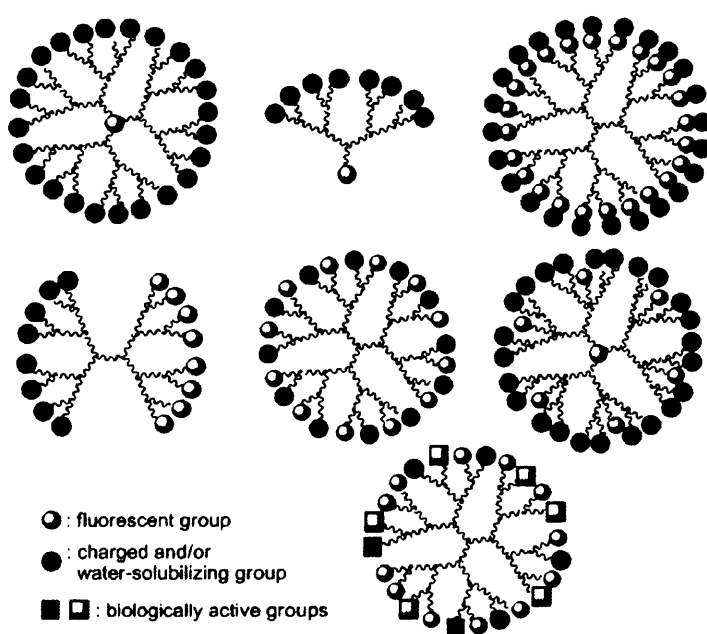


**Figure [1.10]:** Schematic representation of type of fluorescent dendrimers.<sup>[81]</sup>

## 1.2.1. Type

### 1.2.1.1. Intrinsically fluorescent dendrimers

Until recently, there were no reports of fluorescent PAMAM dendrimers.<sup>[82]</sup> This is due to its structure lacking any classical fluorophores but after more than 15 years from their first disclosure, the fluorescent properties of –COOH terminated PAMAM were investigated and were attributed to  $n-\pi^*$  transition of amido groups.<sup>[83]</sup> Also blue fluorescent emission was noticed due to the oxidation of  $\text{NH}_2$ - or OH -terminal groups<sup>[84]</sup> and a well-defined dependency of the fluorescence with the pH especially in acidic media,<sup>[55, 85]</sup> Recently, all poly(propyleneimine) (PPI),<sup>[30]</sup> poly(propyl ether imine) (PETIM) dendrimers,<sup>[86]</sup> and polylysine  $\text{NH}_2$ -terminated dendrimers were also revealed to be intrinsically fluorescent.<sup>[87]</sup>

### 1.2.1.2. Multiply labelled dendritic structures

Most fluorescent labelled compounds are water-insoluble due to the presence of aromatic groups in their structure, so the solubility of fluorescently-labelled dendrimers decreases as the number of fluorescent aromatic compounds increase. There are two main ways to overcome these disadvantages. The first is to use water-soluble compounds as an inner part of the dendrimer, or by using water soluble compounds as terminal groups in addition to fluorescent compounds.<sup>[81]</sup>

Many types of 1,8-naphthalimide derivatives have been conjugated to PAMAM dendrimers as terminal groups to provide cationic sensors in polar solvents except water (Figure 1.11).<sup>[32]</sup> In addition, dansyl, naphthyl, or pyrenyl fluorescent terminal groups were loaded onto PAMAM dendrimers of 0-5 generations but studies indicate strong aggregation behaviour in water.<sup>[88]</sup>

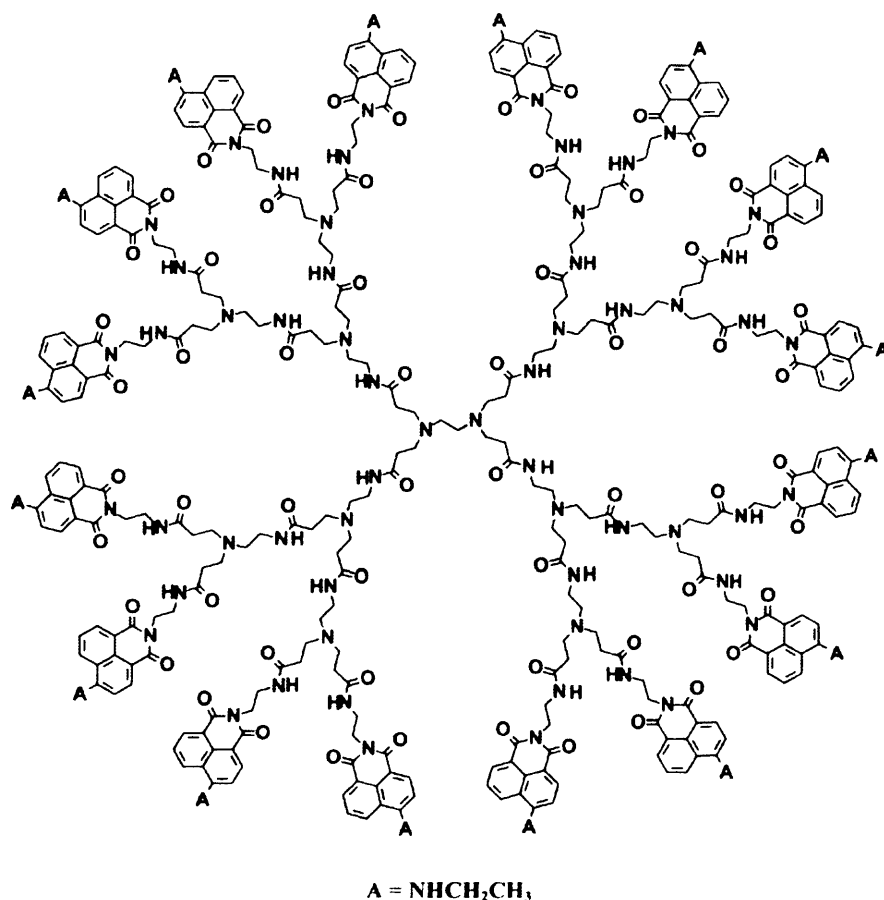


**Figure [1.11]:** 4-Ethylamino-1,8-naphthalimide-labeled PAMAM dendrimers.<sup>[32]</sup>

Another strategy to achieve a combination of water-solubility and fluorescence is to have two dissimilar kinds of terminal groups, one for water solubility and one for fluorescence. This approach can be achieved in two ways: the first by grafting the two types of groups onto two distinct areas of the dendritic periphery (so-called “Janus”-type dendrimers),<sup>[89]</sup> and the second by linking both monomers simultaneously to each terminal branching point. Another approach consists of having the two different types of functional groups linked to the branching points, leading to “multi-pluri-functionalised” compounds.<sup>[90]</sup> In the case of water-soluble fluorescent dendrimers, this approach was primary applied to ammonium groups and dansyl derivatives.<sup>[91]</sup>

### 1.2.1.3. Statistically labelled dendritic structures

In biological trials on water soluble dendrimers; especially PAMAM dendrimers, the statistical conjugation of a few fluorophores as terminal groups has gained prominence. For example, fluoresceine isothiocyanate (FITC) and Oregon Green 488 (OG<sub>488</sub>; Figure 1.12) fluorophores two closely related compounds have been incorporated by statistical couplings on the terminal groups of dendrimers.<sup>[81]</sup> These conjugated fluorophores do not appear to alter the biological activity or transport of the dendrimers.<sup>[92-93]</sup>

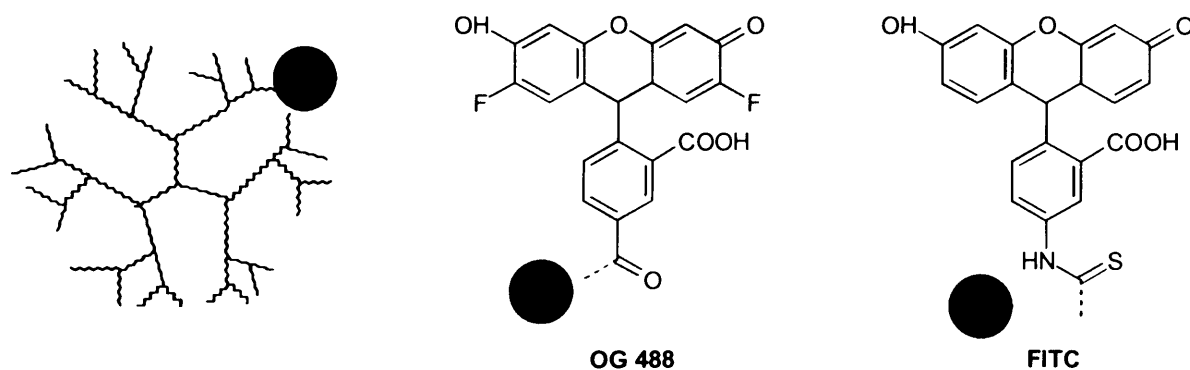


**Figure [1.12]:** Types of fluorophores linked statistically (one to a few) to the surface of dendrimers.<sup>[81]</sup>

Recently, this concept of statistical conjugating has been used as a multifunctional platform by introducing up to five different terminal groups on the dendritic structure. In most cases these types of compounds were synthesised from PAMAM dendrimers (except one example based on PPI dendrimers<sup>[94]</sup>) for various biological applications, like imaging and tumour treatment.<sup>[81]</sup> However, the statistical loading of fluorophores into the periphery of dendrimers has problems, like fluorescent quenching, in addition to the difficulties of controlling stoichiometry,<sup>[95-96]</sup> and the possibilities of changing biological function or transport.<sup>[97]</sup> These potential disadvantages can be addressed by loading the fluorophore into the core of dendron.

### 1.2.1.4. Dendrimers with fluorescent cores

Phthalocyanines and porphyrin fluorophores have been used as a fluorescent core in many known families of dendrimers. It is assumed that the dendrons protect the fluorescent core from any outer environmental effects,<sup>[98]</sup> in particular by preventing aggregation and protecting it against quenching by water, but by using appropriate terminal groups, solubility in water is induced. The first examples of water-soluble porphyrins embedded in a dendrimer (Figure 1.13) were synthesised with the aim of providing synthetic models of natural enzymes, such as cytochrome-c.<sup>[99]</sup> Dendritic water-soluble phthalocyanines have closely related structures and properties to dendritic porphyrins.<sup>[100-106]</sup> Besides porphyrins and phthalocyanines, stilbene derivatives have also been used as fluorophores that can be used as the core of water-soluble dendrimers.<sup>[107-112]</sup>

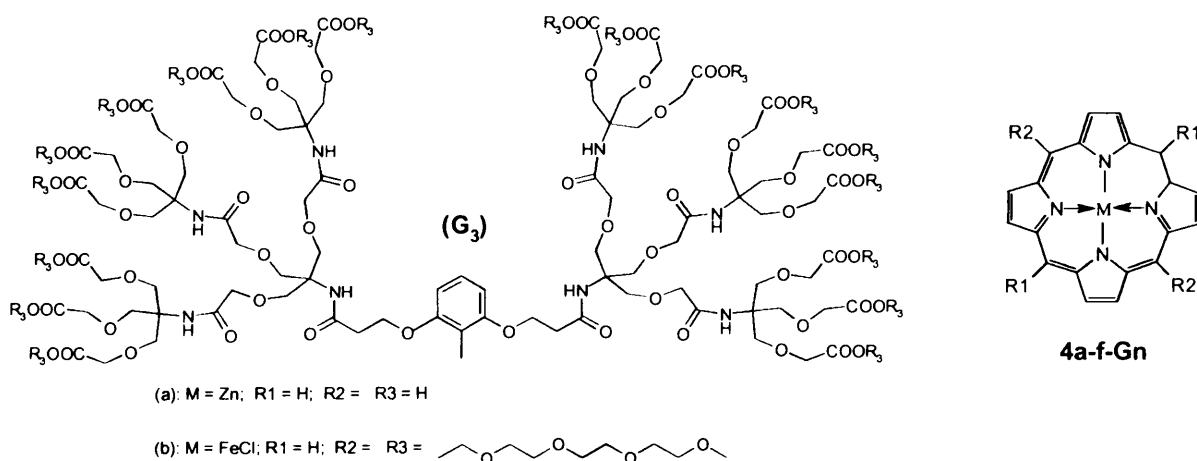


**Figure [1.13]:** Types of water-solubilising branches linked to a porphyrin core.

### 1.2.1.5. Dendritic wedges with fluorescent 'cores'.

In this case, the attached dendrons cannot fully protect the fluorophores against any environmental effects and aggregation, however, dendrons may be used simply to increase the solubility of the 'core' (or more correctly focal-point) unit in water, for

example, C<sub>60</sub> fullerene,<sup>[113-115]</sup> which is insoluble in aqueous and most polar media. A different kind of water soluble fullerene dendron was constructed using PAMAM dendrons. Due to the protonation of nitrogen in the internal structure, such compounds are water soluble in acidic conditions, even with methyl ester terminal groups (Figure 1.14).<sup>[57, 116]</sup> Other strongly fluorescent probes have been placed at the core of PAMAM dendritic wedges including: pyrene,<sup>[117-120]</sup> carbazole fluorophores<sup>[58]</sup> and dansyl fluorophores.<sup>[121-122]</sup>

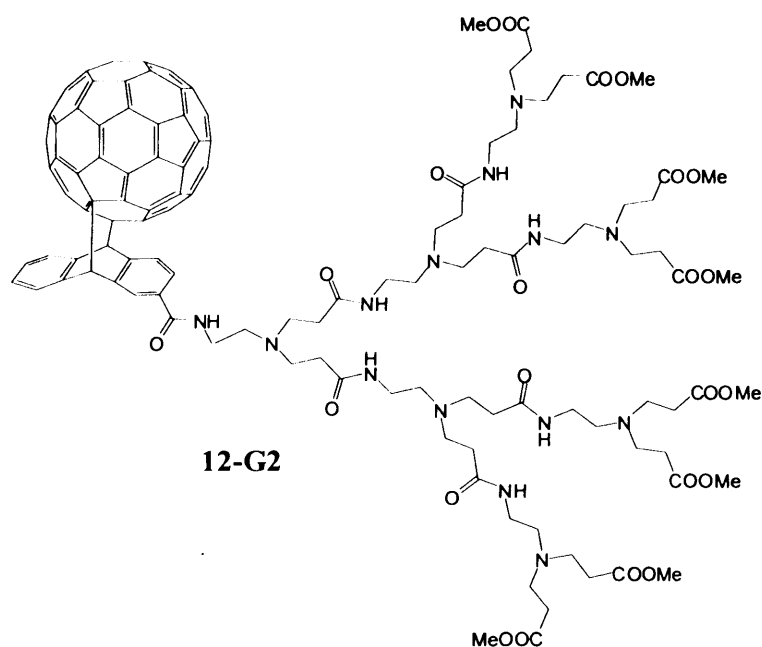


Figure [1.14]: Water soluble fullerodendron.

### 1.2.2. Applications of fluorescent dendrimers

Fluorescent dendrimers can be used for biological imaging. Of particular importance is their use in conjunction with novel one-photon<sup>[123]</sup> and two-photon<sup>[124-125]</sup> fluorescent tumor-sensing systems that have been developed to provide high spatial ( $\mu\text{M}$ ) resolution. For example, the two-photon optical fluorescence fibers technique together with a G5-PAMAM dendrimer conjugated to folic acid and the fluorescent probe 6-carboxytetramethylrhodamine succinic ester (6-TAMRA) has been used to image tumors *in-vivo*.<sup>[126-128]</sup> Fluorescent dansyl units have also been incorporated into

dendrimers and their cellular uptake and localization studied using confocal fluorescence microscopy.<sup>[129]</sup>

## 1.3. Fluorescent Compounds

### 1.3.1. Principles of fluorescence spectroscopy

#### 1.3.1.1. Fluorescence

All molecules have internal energy levels, in which an electron can transfer from the lower to higher level when the molecule absorbs a photon of light of equal energy to the energy difference between two energy level states (Figure 1.15).<sup>[130]</sup>

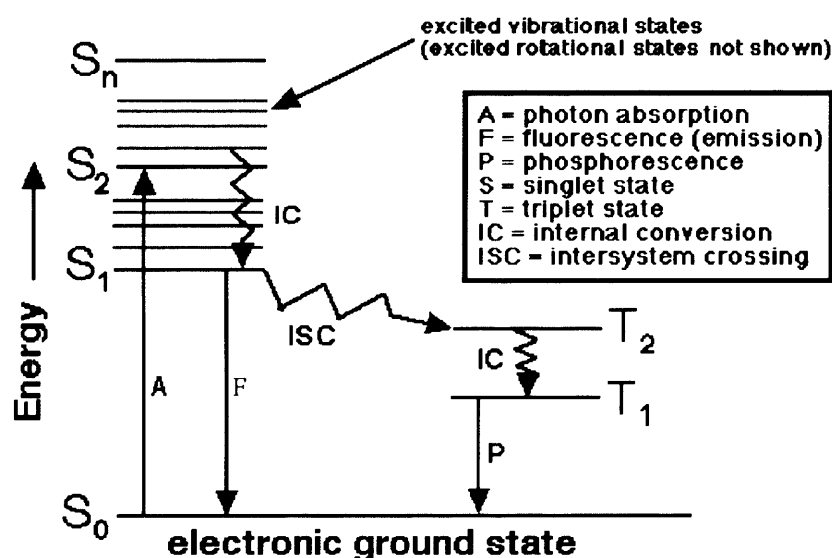


**Figure [1.15]:** Jablonski diagram of organic dyes: IC—internal conversion, ESA—excited state absorption, ISC—intersystem crossing.<sup>[131]</sup>

The fluorescence process involves instant emission of electromagnetic energy from the singlet state, while the related phosphorescence process occurs when the energy emission originates from an excited triplet state and is delayed relative to the fluorescence emission.<sup>[130]</sup>

### 1.3.1.2. Structural factors that determine fluorescence

Generally, strongly fluorescent molecules possess the ability to easily transfer between two transitional energy states via a small energy gap. Usually, aromatic compounds possess very strong fluorescence due to two reasons: the first is the presence of  $\pi$ - electrons system in which electrons are more easily transferred to higher  $\pi^*$  antibonding orbitals by light absorbance without affecting bonding. The second reason is the allowance of  $\pi$ - $\pi^*$  transition singlet states that are often involved in very strong fluorescence.<sup>[130]</sup> Fluorescence in an aliphatic compound is often insignificant except for carbonyl-containing compounds that can show signs of weak fluorescence due to  $n$ - $\pi^*$  transitions.<sup>[130]</sup> Rigid co-planarity is also a prerequisite for strong fluorescence as it favours  $\pi$ -  $\pi^*$  transitions singlet states. For example, (Figure 1.16) shows fluorescein which possesses rigid planarity so it strongly fluoresces, while phenolphthalein does not and has greater rotational freedom and dissipates its energy in solution.<sup>[130]</sup>

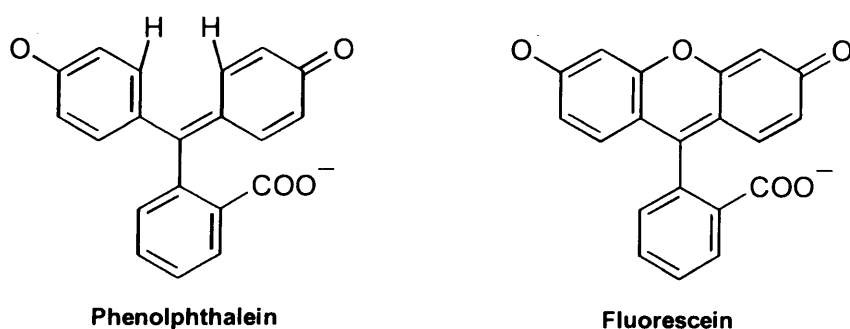
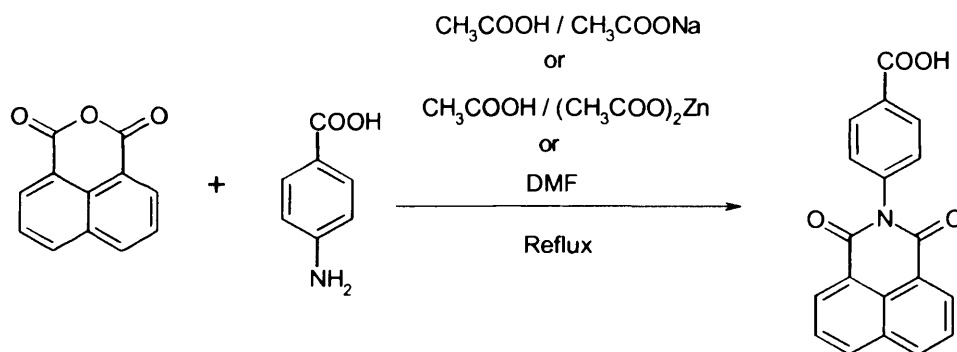


Figure [1.16]

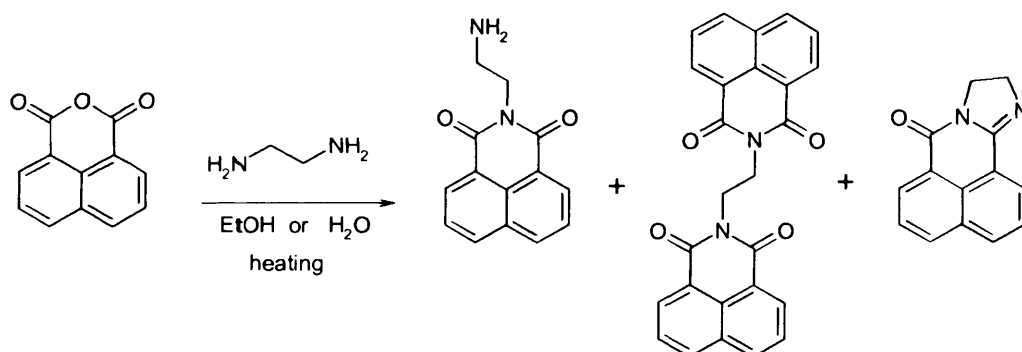
### 1.3.2. PAMAM conjugation to naphthalic anhydride derivatives

#### 1.3.2.1. Synthesis and Photoluminescence properties

There are many references concerned with the synthesis of N-aryl-naphthalimide derivatives<sup>[132-137]</sup> (Scheme 1.1) and N-alkyl-naphthalimide derivatives (Scheme 1.2).<sup>[138-145]</sup>



**Scheme [1.1]:** Example for synthesis of N-aryl-naphthalimide derivatives



**Scheme [1.2]:** Example for synthesis of N-alkyl-naphthalimide derivatives

Because of their strong fluorescence and good photostability, the 1,8-naphthalimide derivatives have found application in a number of areas including colouration of polymers,<sup>[146-150]</sup> laser active media,<sup>[151-152]</sup> photosensitive biological units,<sup>[153]</sup> fluorescent markers in biology,<sup>[154]</sup> analgesics in medicine,<sup>[155]</sup> light emitting diodes,<sup>[156-158]</sup> photo-induced electron transfer sensors,<sup>[159-163]</sup> fluorescence switches,<sup>[164-166]</sup> and ion probes.<sup>[167]</sup> Also, some N-alkyl-1,8-naphthalimide derivatives have been characterised by Lewis *et al.* as photo-chemotherapeutic inhibitors.<sup>[168-172]</sup>

The colour of 1,8-naphthalimide derivatives usually depends on the presence and type of substituent at the 4-position of the naphthalimide ring. For example, electron-donating amino groups<sup>[163, 173-176]</sup> cause a red-shift in the visible adsorption band with an increase in the quantum yield of fluorescence. It has been concluded that the fluorescent character of 1,8-naphthalimides also depends on the polarisation of the naphthalimide molecule due to the electron-acceptor donor interaction occurring between the carbonyl groups and the C-4 substituents of the chromophoric system (Figure 1.17).<sup>[177-178]</sup>

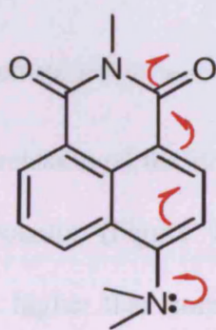


**Figure [1.17]:** intramolecular charge-transfer analogue of 4-amino-1,8-naphthalimide derivatives.<sup>[177]</sup>

### 1.3.2.2. PAMAM conjugates

1,8-Naphthalimide **6** and the dendronized dyes **7** and **8** (Figure 1.18), represent good model structures for the concept of “fluorophore-spacer-receptor” where the 4-amino-1,8-naphthalimide moiety is the fluorophore and the terminal ester or amino dendrons are the proton receptors, while the ethylenediamine spacer separates the fluorophore and dendron unit. The fluorescence emission of the 1,8-naphthalimide unit is quenched by the PET process (an electron transfer from the amine receptor to the excited state of the fluorophore), which represent the “off-state” of the system.

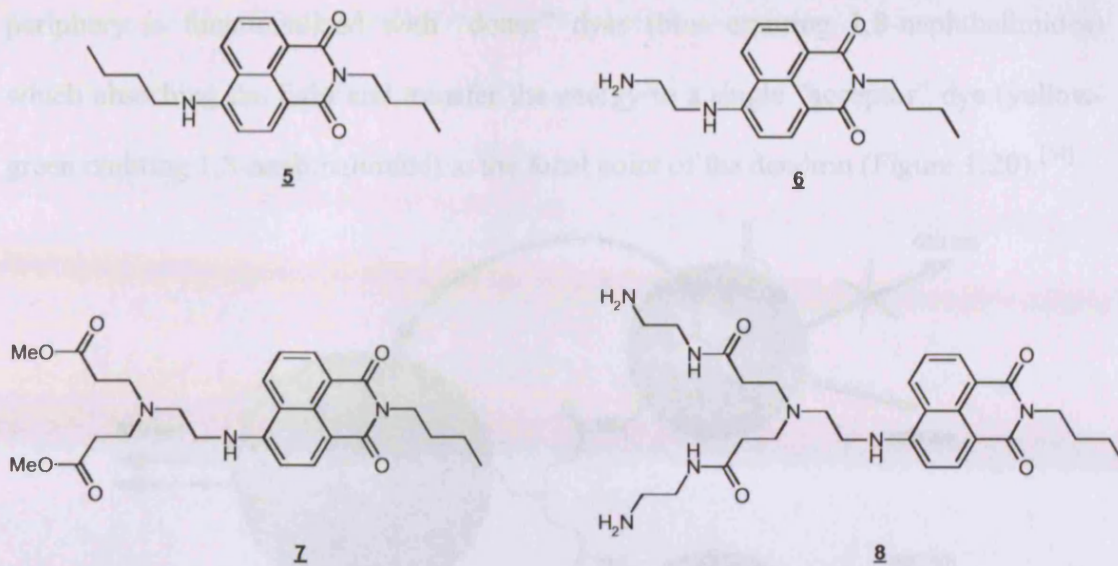


Figure [1.18]: compound structures 5, 6, 7 and 8.

In acidic solution, fluorescence emission of the compounds is “switched on” due to the protonation of the amine receptor (Figure 1.19).<sup>[174, 179-180]</sup> The fluorescence quantum yields of compound 5 is higher than compounds 6–8 due to the absence of PET process which quenches the fluorescence emission.<sup>[181-183]</sup>

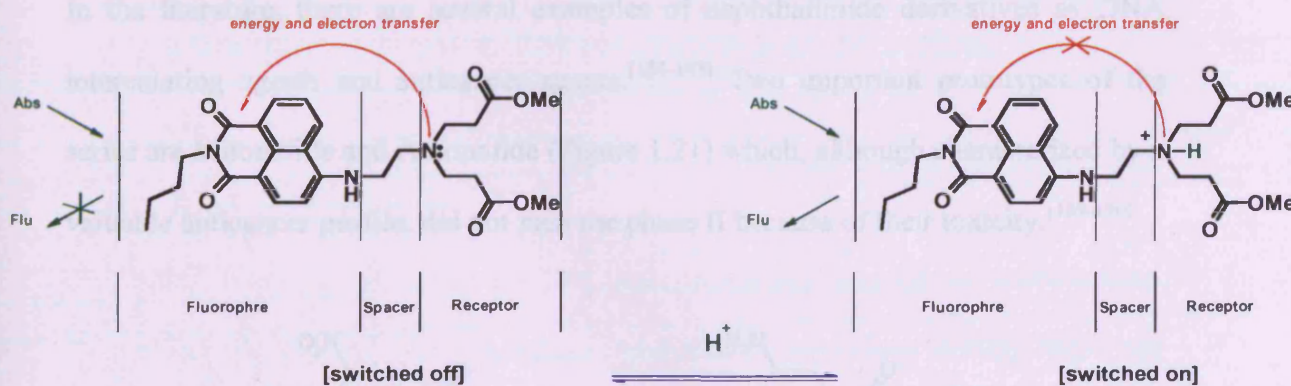


Figure [1.19]: “Fluorophore-spacer-receptor” model with indicating “off – on” switcher for PET process in present and absence of acidic media

Bojinov and co-workers used 1,8-naphthalimide derivatives to design, a novel PAMAM dendron 9, which was substituted at both core and periphery with 1,8-naphthalimide fluorophores. In this new-light harvesting antenna compound 9, the

periphery is functionalized with “donor” dyes (blue emitting 1,8-naphthalimides) which absorbing the light and transfer the energy to a single “acceptor” dye (yellow-green emitting 1,8-naphthalimide) at the focal point of the dendron (Figure 1.20).<sup>[54]</sup>

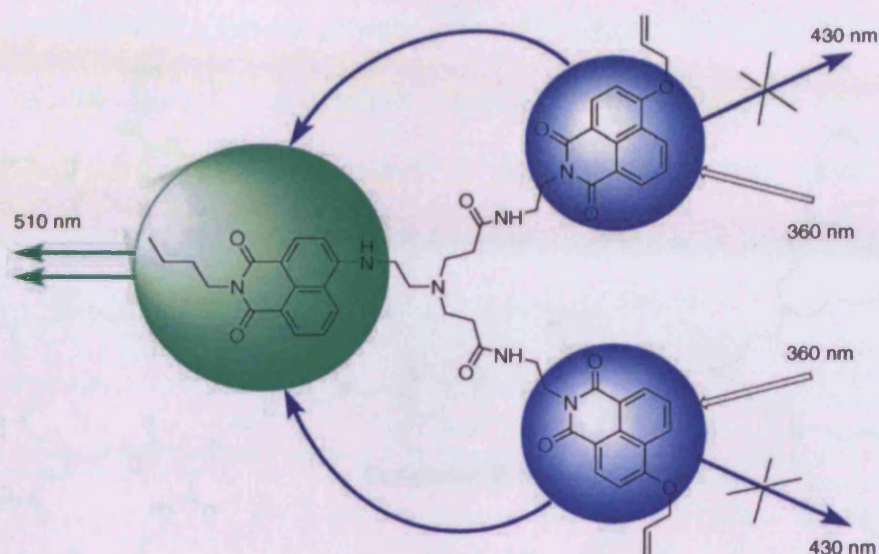


Figure [1.20]: Compound 9.<sup>[54]</sup>

### 1.3.2.3 Chemotherapeutic applications

In the literature, there are several examples of naphthalimide derivatives as DNA intercalating agents and anticancer agents.<sup>[184-188]</sup> Two important prototypes of the series are Mitonafide and Amonafide (Figure 1.21) which, although characterized by a valuable anticancer profile, did not pass the phase II because of their toxicity.<sup>[189-190]</sup>

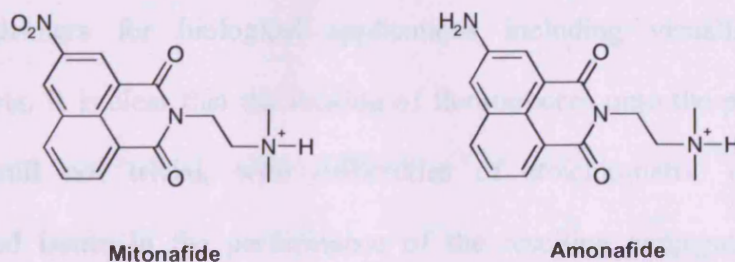
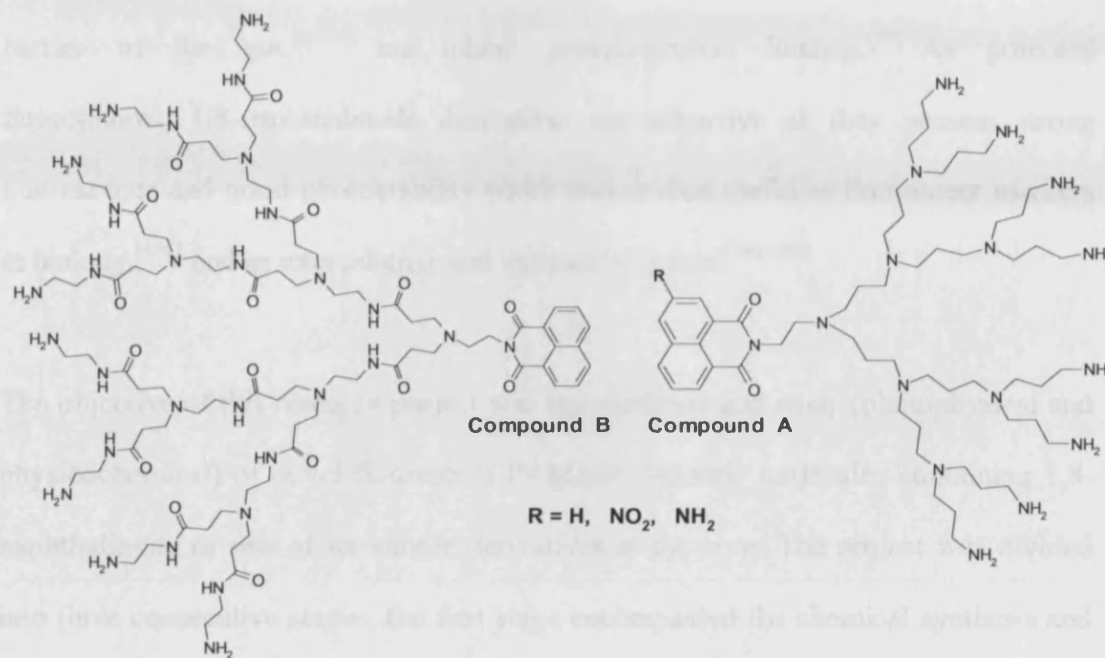


Figure [1.21]: Chemical structures of compound Mitonafide and Amonafide.

Therefore, PAMAM and PPI dendritic wedges, containing an intercalating 1,8-naphthalimide derivative at their core, have been employed in gene therapy and act as an antitumour agent (Figure 1.22).<sup>[141]</sup>



**Figure [1.22]:** Compound A: “PPI dendritic polyamines–(imide–DNA intercalator)” conjugates, Compound B: “PAMAM dendritic polyamines–(imide–DNA intercalator)”.<sup>[141]</sup>

## 1.4. Aim of Project

As noted above, recent literature indicates continuing interest in water-soluble fluorescent dendrimers for biological applications including visualisation and diagnostic imaging. It is clear that the loading of fluorophores onto the periphery of dendrimers is still not trivial, with difficulties of stoichiometric control for synthesis<sup>[95-96]</sup> and issues in the performance of the resulting conjugates such as fluorescent quenching. These disadvantages may be avoided by loading the fluorophore into the core (or focal point) of a dendron.

As well as being the first high-generation dendrimers and one of the most studied,<sup>[25]</sup> poly(amidoamine) (PAMAM) dendrimers are also considered one of the best potential drug delivery carriers due to their high biocompatibility. They are: hydrophilic, nanostructured, mimic globular proteins,<sup>[25]</sup> readily transported across the epithelial barrier of the gut,<sup>[26-28]</sup> and inhibit protein-protein binding.<sup>[29]</sup> As potential fluorophores, 1,8-naphthalimide derivatives are attractive as they possess strong fluorescence and good photostability which makes them useful as fluorescent markers in biology,<sup>[154]</sup> and as intercalating and anticancer agents.<sup>[184-188]</sup>

The objective of this research project was the synthesis and study (photophysical and physicochemical) of novel fluorescent PAMAM dendritic molecules containing 1,8-naphthalimide or one of its simple derivatives at the core. The project was divided into three consecutive stages, the first stage encompassed the chemical synthesis and photophysical studies of some 1,8-naphthalimide derivatives to investigate the fluorescent behaviour of these compounds. In the second stage, novel fluorescent PAMAM dendritic molecules were to be prepared with the optimised core selected from the initial work. Finally, in collaboration with other research groups the physicochemical properties, their transport through biological barriers and their binding to DNA was to be assessed.

# CHAPTER TWO

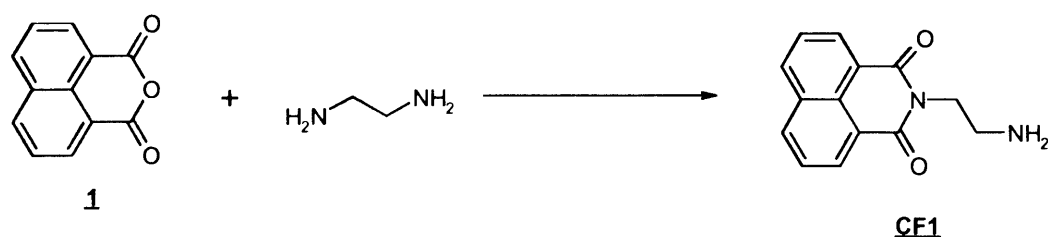
## FLUORESCENT CORES

2.1 Synthesis.....	24
2.2 Photoluminescence studies.....	29
2.3 Conclusions.....	36

## 2.1. Synthesis

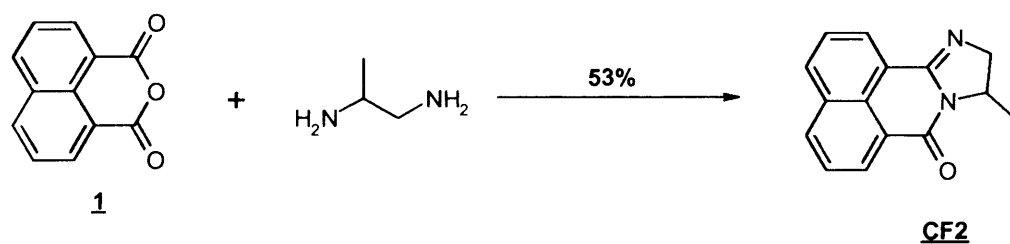
### 2.1.1 Synthesis of N-alkyl-1,8-Naphthalic anhydride derivatives

The routes to the synthesis of *N*-alkylamino-1,8-naphthalimide derivatives **CF1**-**CF3** are presented in (Schemes 2.1-2.3). Compound **CF1** was prepared according to a published procedure.<sup>[143]</sup>



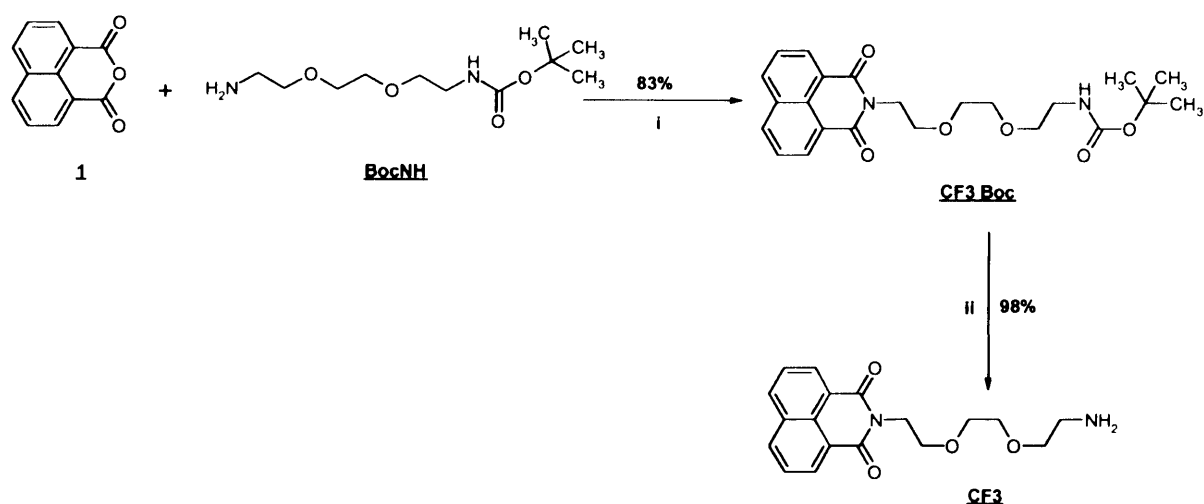
**Scheme [2.1]:** Synthesis of **CF1**. *Reagents and conditions:* EtOH, Reflux 8 h.<sup>[143]</sup>

Also by the analogue previous published procedure,<sup>[143]</sup> the reaction of 1,8-naphthalic anhydride **1** with 1,2-propanediamine in boiling ethanol gave the desired **CF2** (Scheme 2.2).



**Scheme [2.2]:** Synthesis of **CF2**. *Reagents and conditions:* EtOH, Reflux 8 h.

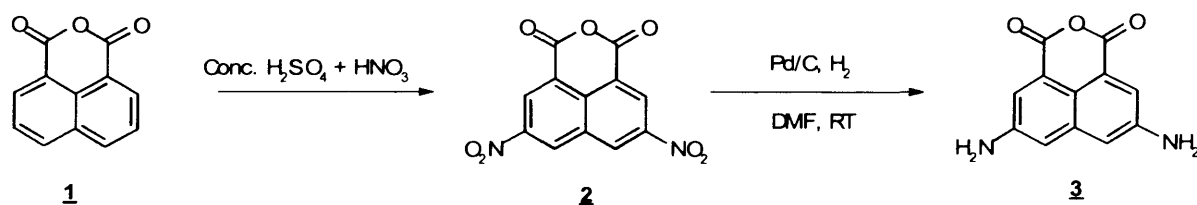
Compound **CF3** (Scheme 2.3) was obtained using a similar procedure utilising a Boc-terminated diamine (designated **BocNH**) which was prepared as previously reported.<sup>[191]</sup> The Boc-group was removed by treatment with TFA/DCM according to a standard procedure,<sup>[192]</sup> to give **CF3** as a new compound.



**Scheme [2.3]:** Synthesis of **CF3-Boc** and **CF3**. *Reagents and conditions:* (i) EtOH, 80 °C, 1 h; (ii) TFA/DCM, stirring 2 h.

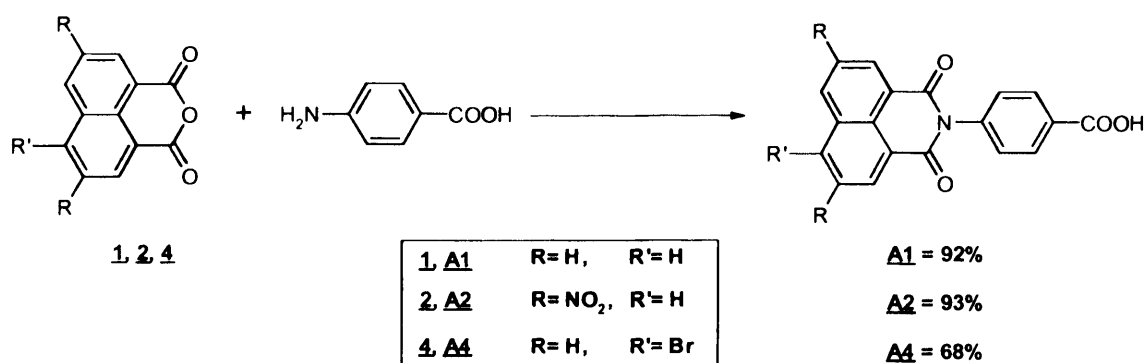
### 2.1.2 N-aryl-1,8-Naphthalic anhydride derivatives.

Precursor compounds 3,6-dinitro-1,8-naphthalic anhydride **2** and 3,6-diamino-1,8-naphthalic anhydride **3** were prepared according to published procedures<sup>[193]</sup> (Scheme 2.4).



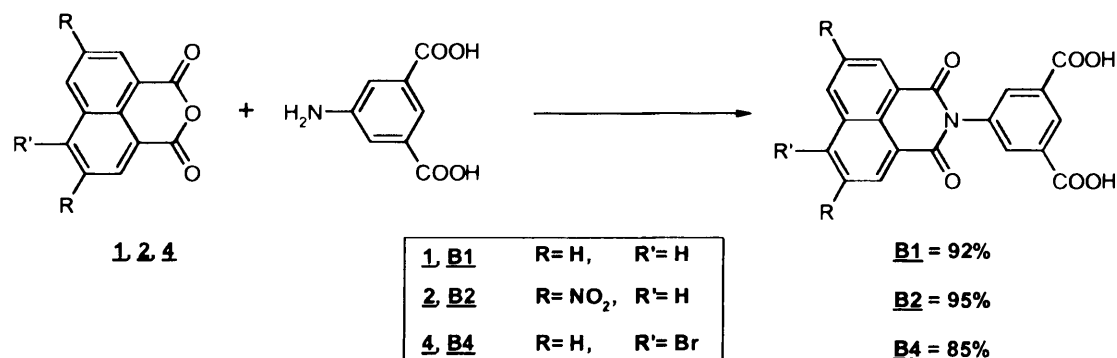
**Scheme [2.4]:** Reported synthesis of **2** and **3**. *Reagents and conditions:* (i) Conc. H<sub>2</sub>SO<sub>4</sub>/HNO<sub>3</sub>; (ii) DMF, Pd/C 10%, H<sub>2</sub>, stirring 16 h, RT.

*N*-phenyl-1,8-naphthalimide derivatives **A1**, **A2** and **A4** were synthesized by refluxing 1,8-naphthalic anhydride derivatives **1**, **2** and **4** with 4-aminobenzoic acid in the presence of glacial acetic acid and sodium acetate. **A1**, **A2** and **A4** were all obtained in good yield with high purity without any need for further purification (Scheme 2.5).



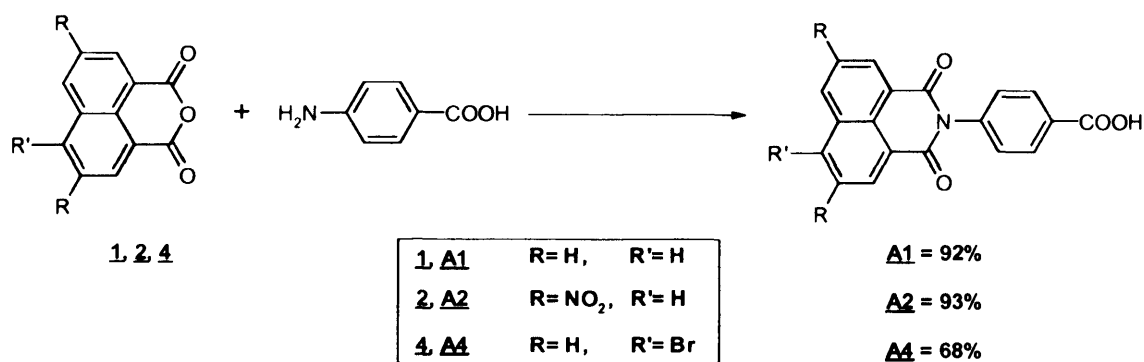
**Scheme [2.5]:** Synthesis of **A1**, **A2** and **A4**. *Reagents and conditions:* AcOH/AcONa, Reflux.

Compounds **B1**, **B2**, and **B4** were obtained using the same procedure by replacing 4-aminobenzoic acid with 5-aminoisophthalic acid (Scheme 2.6).



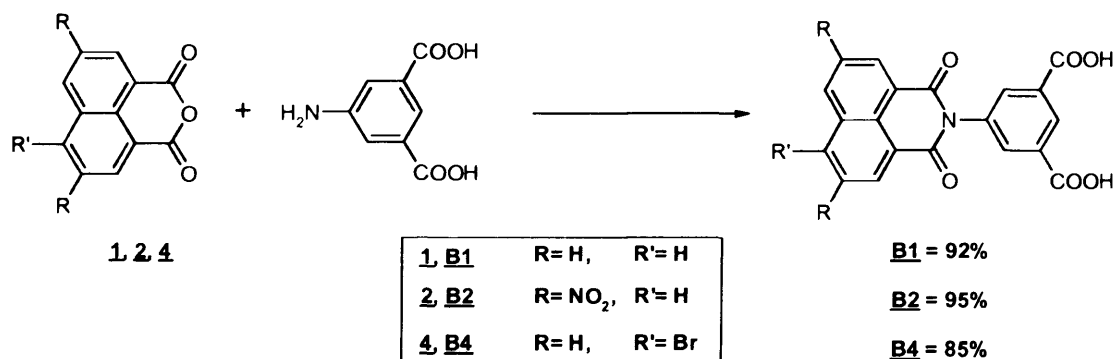
**Scheme [2.6]:** Synthesis of **B1**, **B2** and **B4**. *Reagents and conditions:* AcOH/AcONa, Reflux.

Compounds **C1**, **C2** and **C4** have been prepared by the same procedures as above (Scheme 2.7), however, their yields were much lower due to the formation of byproducts. Purification was achieved using flash column chromatography (CHCl<sub>3</sub> : MeOH : NH<sub>3</sub>; 9 : 1 : 0.1).



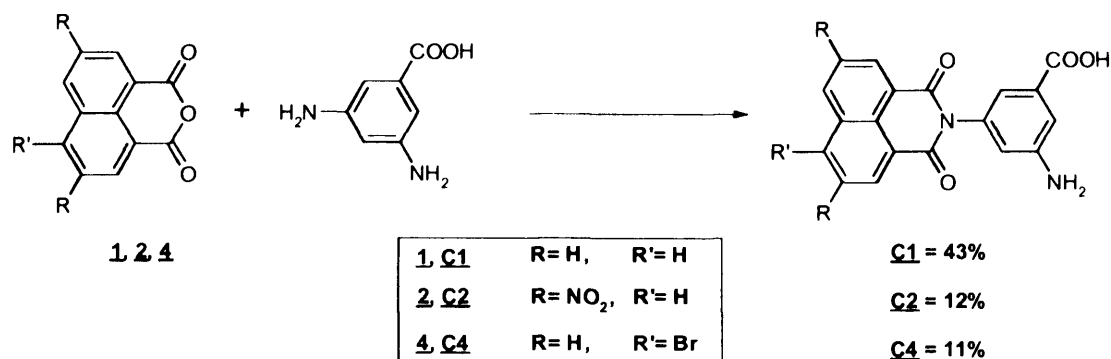
**Scheme [2.5]:** Synthesis of **A1**, **A2** and **A4**. *Reagents and conditions:* AcOH/AcONa, Reflux.

Compounds **B1**, **B2**, and **B4** were obtained using the same procedure by replacing 4-aminobenzoic acid with 5-aminoisophthalic acid (Scheme 2.6).



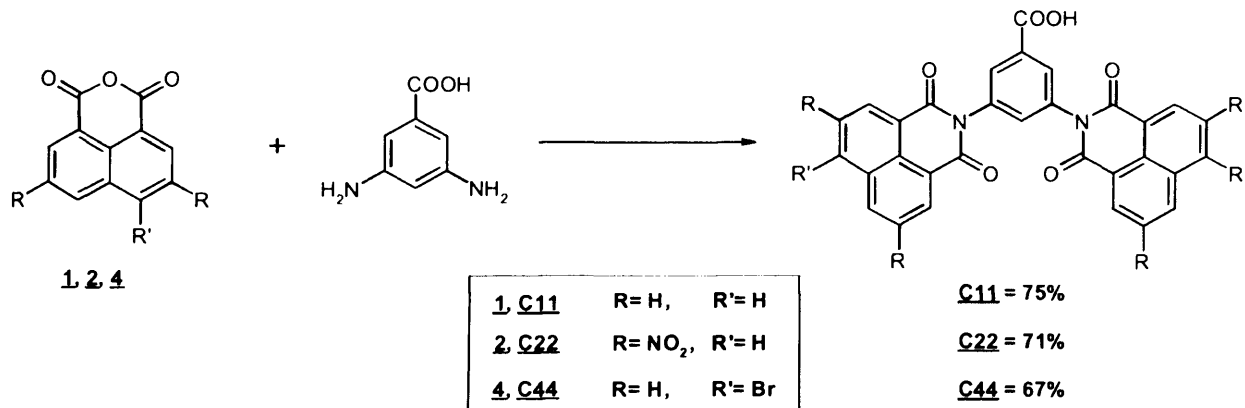
**Scheme [2.6]:** Synthesis of **B1**, **B2** and **B4**. *Reagents and conditions:* AcOH/AcONa, Reflux.

Compounds **C1**, **C2** and **C4** have been prepared by the same procedures as above (Scheme 2.7), however, their yields were much lower due to the formation of byproducts. Purification was achieved using flash column chromatography (CHCl<sub>3</sub> : MeOH : NH<sub>3</sub>; 9 : 1 : 0.1).



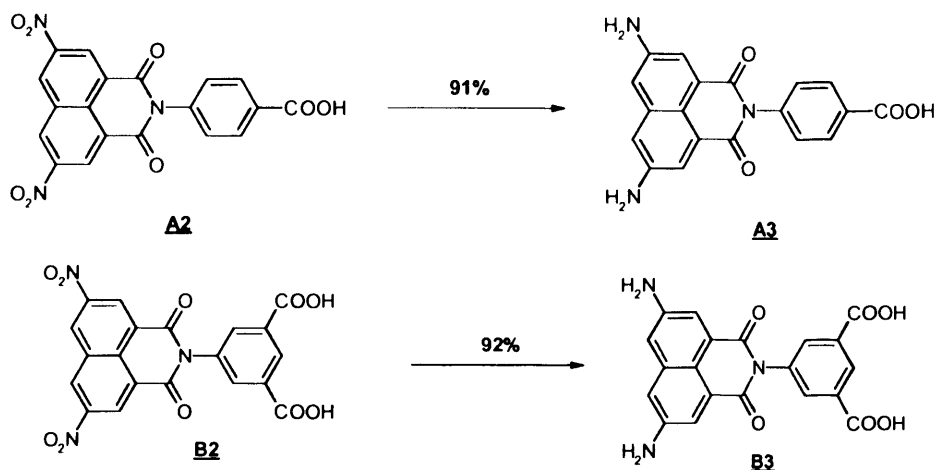
**Scheme [2.7]:** Synthesis of **C1**, **C2** and **C4**. *Reagents and conditions:* AcOH/AcONa, Reflux.

The byproducts of the previous reaction were found to be **C11**, **C22** and **C44**, however, these are all desirable and so were prepared using the same procedure but using double the amount of anhydride over an increased period of time. Separation was also achieved using flash chromatography (CHCl<sub>3</sub> : MeOH : NH<sub>3</sub>; 9 : 1 : 0.1) (Scheme 2.8).



**Scheme [2.8]:** Synthesis of **C11**, **C22** and **C44**. *Reagents and conditions:* AcOH/AcONa, Reflux.

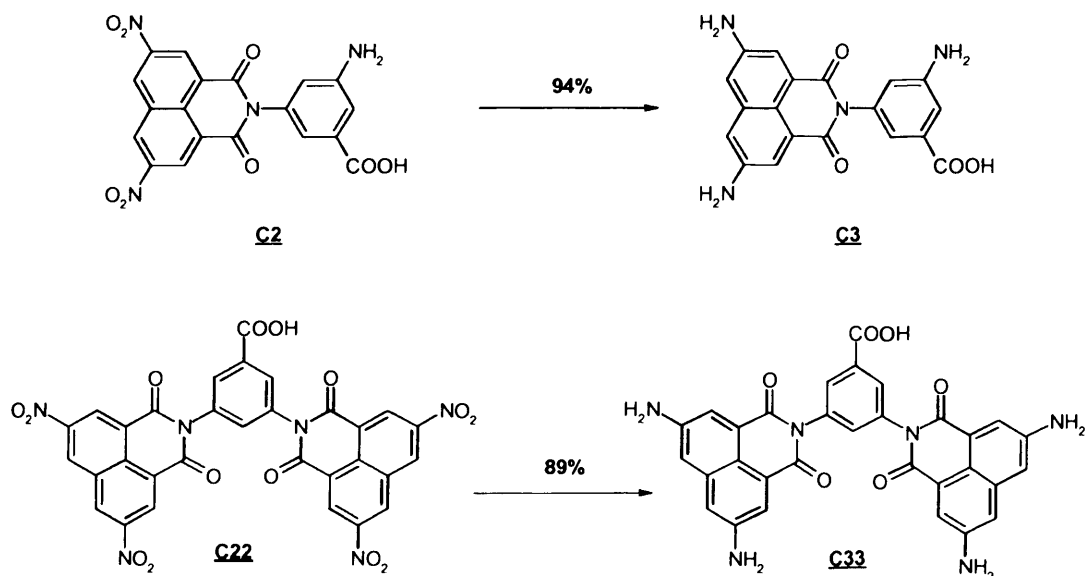
The 3,6-diamino-1,8-naphthalimide derivatives **A3**, **B3**, **C3** and **C33** were prepared according to an analogous reported procedure,<sup>[192]</sup> with slight modifications, for the hydrogenation of the nitro groups using Pd/C 10% in DMF solution (Scheme 2.9).



**Scheme [2.9]:** Synthesis of **A3** and **B3**. Reagents and conditions: DMF, Pd/C 10%, H<sub>2</sub>, stirring 16 h, RT.

The reaction was monitored by TLC and once complete the catalyst was filtered off and the filtrate poured into DCM (250 mL). The solid precipitate was then easily collected by filtration.

Compounds **C3** and **C33** were prepared by the same procedure over 24 hours, the final products were purified by flash chromatography (CHCl<sub>3</sub> : MeOH : AcOH; 8 : 2 : 0.5) (Scheme 2.10).



**Scheme [2.10]:** Synthesis of **C3** and **C33**. Reagents and conditions: DMF, Pd/C 10%, H<sub>2</sub>, stirring 24 h, RT.

## 2.2 Photophysical studies

### 2.2.1 UV-vis absorption spectra

As reported, precursor **1** has its longest wavelength UV-vis adsorption band  $\lambda_{max}$  at 330 nm; **2** at  $\lambda_{max} = 277$  due to the two nitro withdrawing groups in positions C-3 and C-6; **3** at  $\lambda_{max} = 439$  nm due to presence of two amino electron-donating groups in positions C-3 and C-6; **4** at  $\lambda_{max} = 340$  nm with the slight red-shift due to the bromine atom at position C-4. As expected due to the similarities of their basic chromophore, the derivatives of N-aryl-1,8-Naphthalic anhydride derivatives **A1-A4** (Figure 2.1), **B1-B4** (Figure 2.2), **C1-C4** (Figure 2.3) and **C11-C44** (Figure 2.4) have similar spectra to those of compounds **1-4**. The N-alkyleamino- and imidazole-based naphthalimide derivatives **CF1-CF3** (Figure 2.5) have  $\lambda_{max}$  at 340 nm.

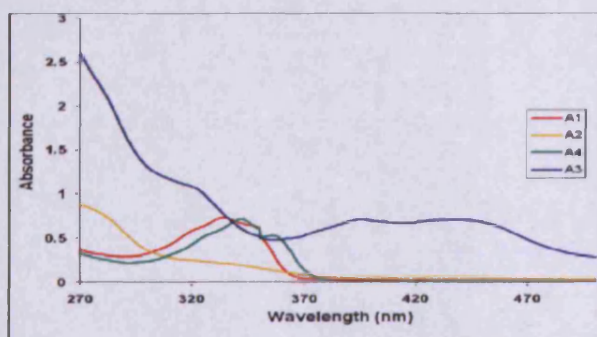


Figure [2.1]: UV absorbance spectra for compounds **A1-A4** in DMF solvent.

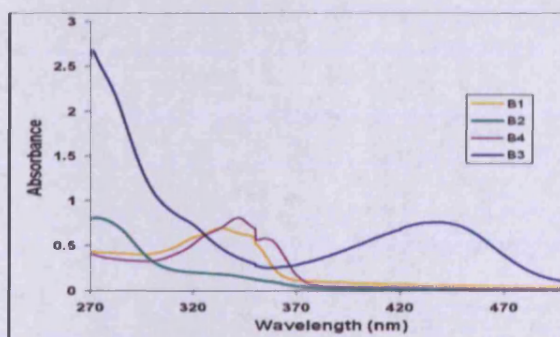


Figure [2.2]: UV absorbance spectra for compounds **B1-B4** in DMF solvent.

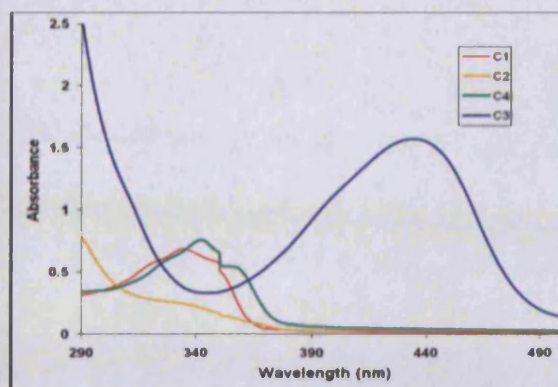


Figure [2.3]: UV absorbance spectra for compounds **C1-C4** in DMF solvent.

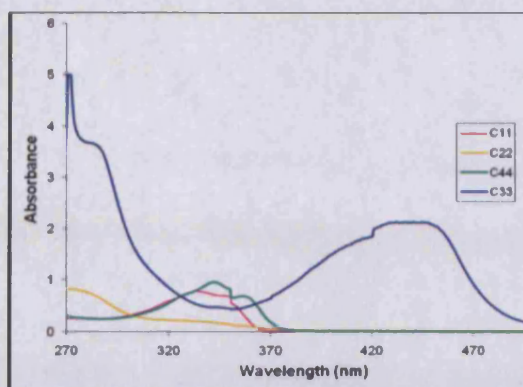


Figure [2.4]: UV absorbance spectra for compounds **C11-C44** in DMF solvent.

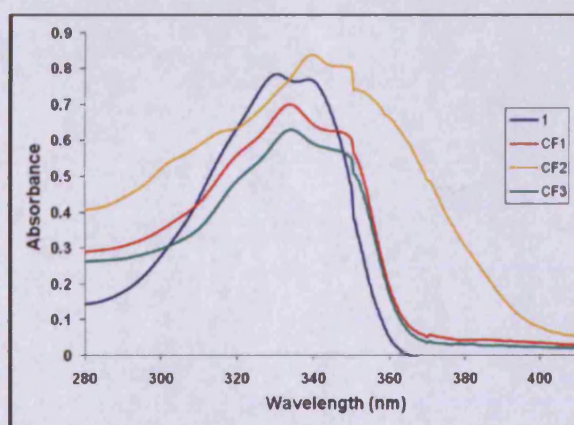


Figure [2.5]: UV absorbance spectra for compounds **1, CF1-CF3** in DMF solvent.

## 2.2.2 Relative fluorescence intensity (RFI)

All the compounds prepared for this study were soluble in DMF and the relative fluorescence intensity (RFI) was recorded at constant UV absorbance of 0.7 (Table 2.1).

**Table [2.1]:** Summary of fluorescent wavelengths and relative fluorescence emission intensity placed in order of increasing fluorescence intensity.

Compound	Wavelength (nm)	Fluorescence emission intensity
C22	342	16.19 x 10 <sup>-3</sup>
C1	422	20.20 x 10 <sup>-3</sup>
C4	428	26.50 x 10 <sup>-3</sup>
2	411	27.19 x 10 <sup>-3</sup>
A1	383	27.30 x 10 <sup>-3</sup>
C44	401	27.86 x 10 <sup>-3</sup>
A4	402	29.36 x 10 <sup>-3</sup>
C11	405	32.60 x 10 <sup>-3</sup>
C2	455	35.80 x 10 <sup>-3</sup>
CF1	425	35.84 x 10 <sup>-3</sup>
1	380	39.85 x 10 <sup>-3</sup>
A2	341	58.78 x 10 <sup>-3</sup>
B1	410	71.08 x 10 <sup>-3</sup>
4	455	79.26 x 10 <sup>-3</sup>
B4	408	90.60 x 10 <sup>-3</sup>
CF3	383	97.70 x 10 <sup>-3</sup>
B2	419	1409.4 x 10 <sup>-3</sup>
A3	518	3164.5 x 10 <sup>-3</sup>
B3	518	3434.9 x 10 <sup>-3</sup>
C3	521	4785.8 x 10 <sup>-3</sup>
3	518	6213.1 x 10 <sup>-3</sup>
C33	518	6489.4 x 10 <sup>-3</sup>
CF2	432	148310.0 x 10 <sup>-3</sup>

As was expected, the RFI order of *N*-arylamino-1,8-naphthalimide derivatives mainly depends on the intramolecular charge-transfer in the delocalized structures (Figure 2.8). This in turn depends on the type of functional groups present at the C-3 and C-6 positions (H, NO<sub>2</sub> or NH<sub>2</sub>), or the functional group on C-4 (e.g. Br) (Figure 2.6). The

RFI can be summarized by placing the following in ascending order  $\text{NO}_2 < \text{H} < \text{Br} < < < \text{NH}_2$ .

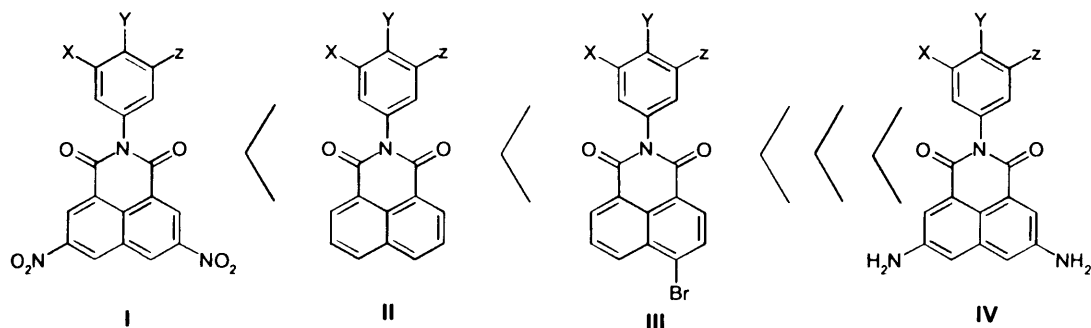


**Figure [2.6]:** Order of Relative fluorescent intensity of *N*-arylamino-1,8-naphthalimide derivatives

With regards to *N*-alkylamino-1,8-naphthalimide derivatives (Figure 2.7), their RFI mainly depends on the “fluorophore-spacer-receptor” model and Photoinduced Internal Electron Transfer (PIET) process.<sup>[181-183]</sup>

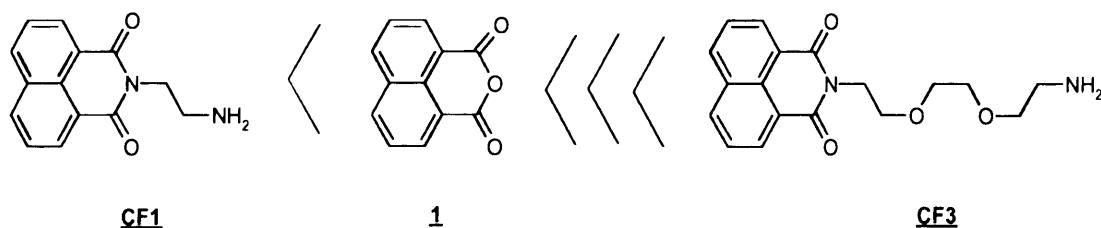


**Figure [2.7]:** Order of Relative fluorescent intensity of *N*-alkylamino-1,8-naphthalimide derivatives

The RFI of compound **CF1** is very low and close to that of compound **1** due to PET processes which quench the fluorescence of the anhydride moiety (Figure 2.8).

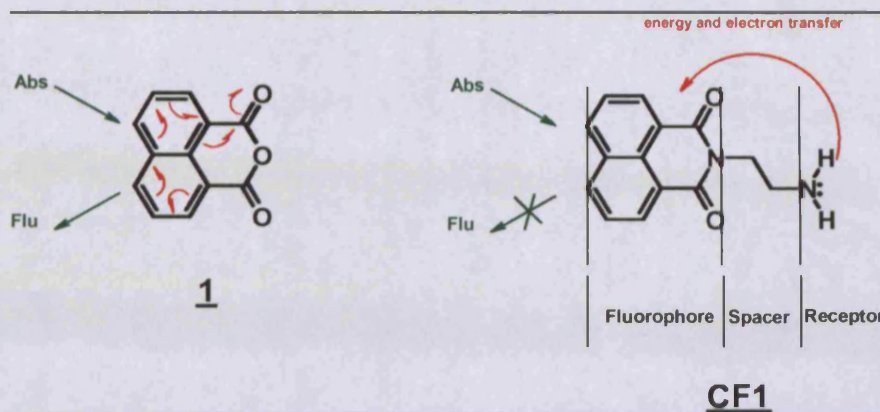


**Figure [2.8]:** (a) Conjugation process of compound **1**, (b) Fluorescent quenching process result from PET for compound **CF1**.

Compound **CF3** has a fluorescence intensity three times larger than that of **CF1** although it could potentially also suffer from a similar PET process as for **CF1**. A possible explanation for this is the length of the spacer in **CF3**, which is three times longer than in **CF1**. As a result, the possibility of **CF3** undergoing a PET process is less than the probability for **CF1** (Figure 2.8).<sup>[194]</sup>

Compound **CF2** (Scheme 2.2) possesses the highest RFI value, especially when compared to *N*-alkylamino and *N*-arylamino-1,8-naphthalimide derivatives. This high intensity of fluorescence might be interpreted according to two factors: firstly, there is no possibility for PET process, secondly, the nitrogen atom of the imidazole ring participates in the resonance conjugated anhydride system with a push-pull interaction via the  $\pi$  system. (Figure 2.9) shows the difference between the fluorescence of solutions of **CF1** and **CF2** under short-wavelength UV illumination.

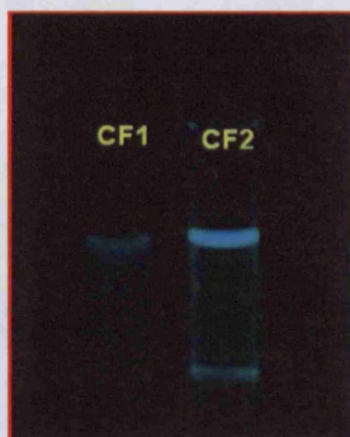


**Figure [2.9]:** Blue-green emitting for compounds **CF1** and **CF2** under short UV region.

The high fluorescence of compounds **A3**, **B3**, **C3**, **3**, **C33** (Figure 2.10) might be interpreted according to two points: firstly, there is no potential for PET, and secondly, the presence of the two amines (positions C-3 and C-6), which can interact with the imide ring via conjugation through the  $\pi$  system.<sup>[195-197]</sup>

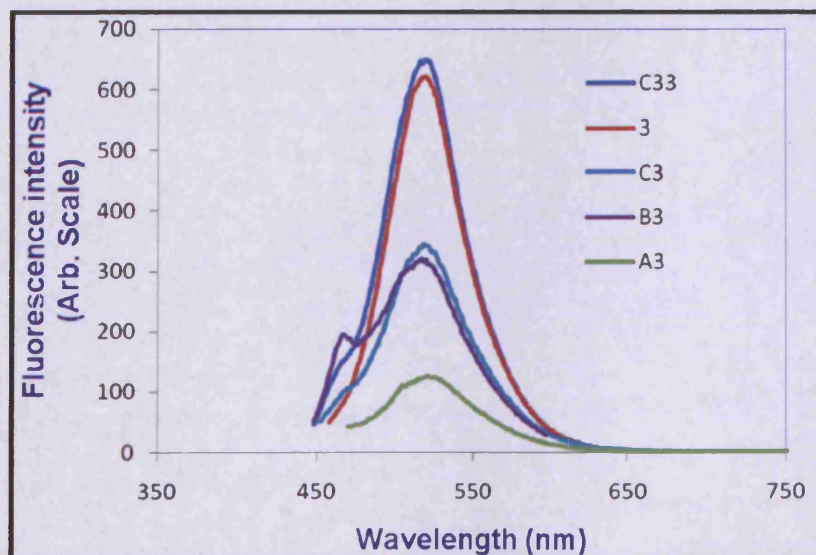


**Figure [2.10]:** Relative fluorescence emission spectra of compounds **3**, **A3**, **B3**, **C3**, and **C33**, when excited at wavelength  $\lambda_{\max}$  439 nm.

Figure (2.11) shows the difference between the fluorescence of solutions of **3**, **A3**, **B3**, **C3**, and **C33** under short-wavelength UV illumination.

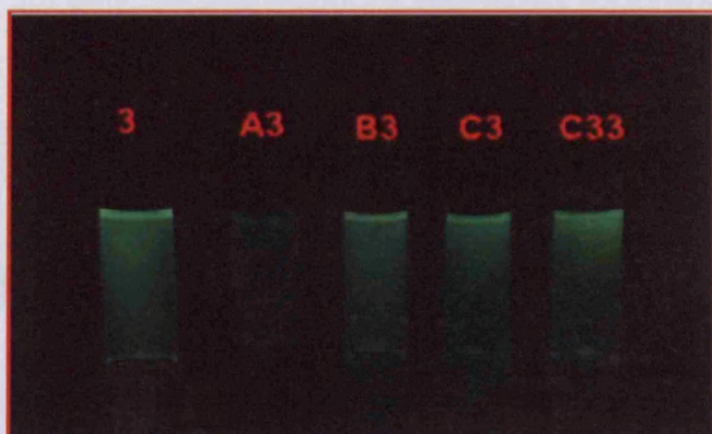


Figure [2.11]: Green emission for compounds 3, A3, B3, C3, C33 under short UV region.

## 2.2.2 Fluorescence quantum yield ( $\Phi_F$ )

The target compounds were designed as potential fluorescent cores for dendritic molecules with amino and carboxylic acid groups that can be functionalised. Hence, the fluorescence quantum yields  $\Phi_F$ , for the compounds possessing high RFI emission, were measured (Figure 2.12).

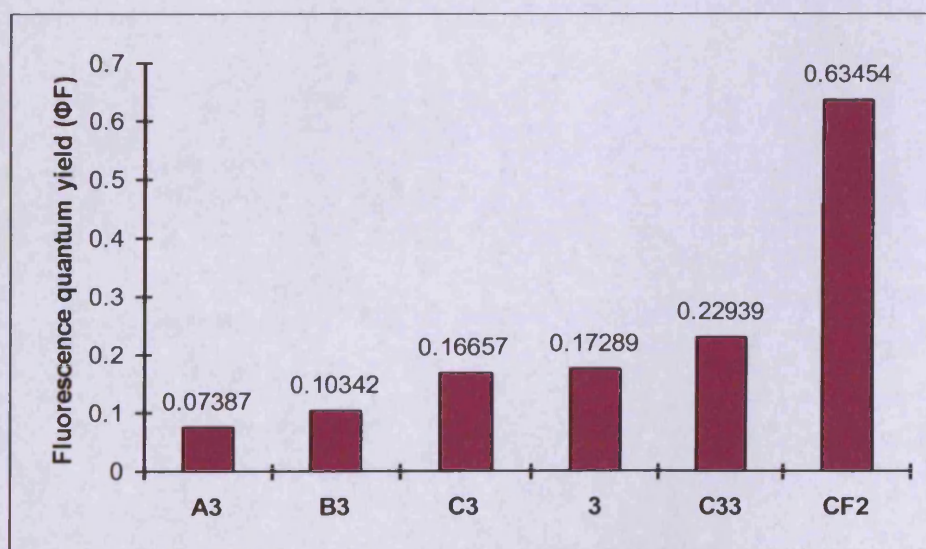


Figure [2.12]: Fluorescence quantum yield for compounds A3, B3, 3, C3, C33 and CF2, when excited at wavelength  $\lambda_{\max}$  439 nm.

## 2.3. Conclusions

Based upon these photophysical measurements it was decided to use readily modifiable derivatives of **CF2** as the fluorescent core in the design of highly fluorescent dendrons for pharmacological use.

# CHAPTER THREE

## FLUORESCENT PAMAM DENDRONS

3.1 Design and synthesis.....	37
3.2 Photophysical characterization studies.....	46
3.3 Physicochemical characterization studies.....	59
3.4 Conclusion.....	62

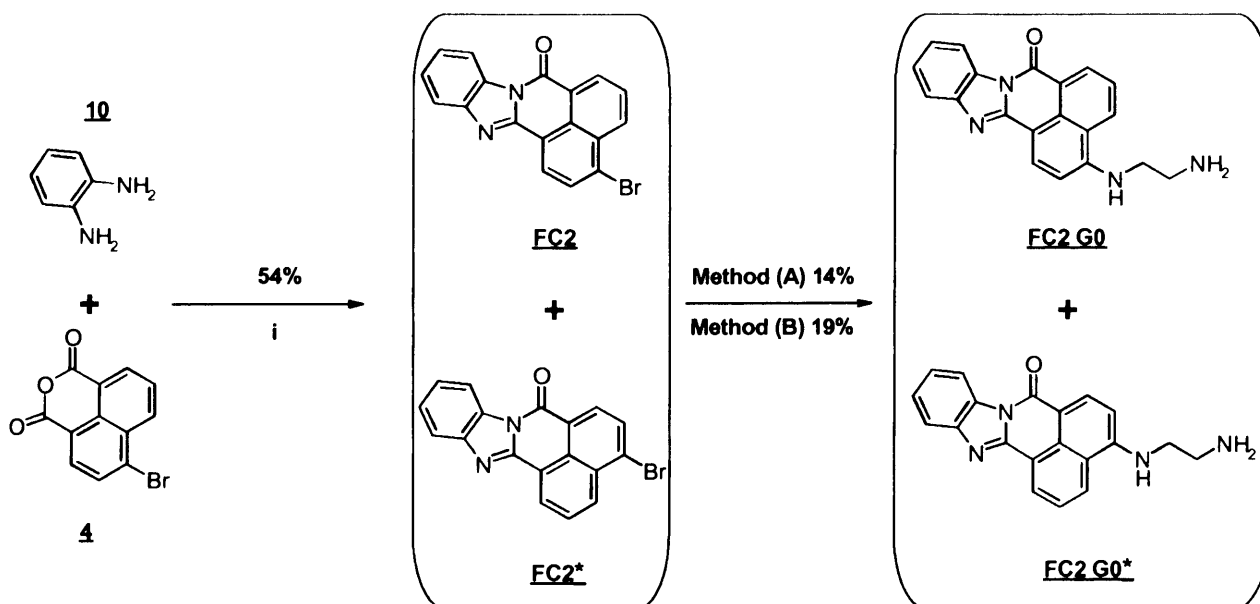
Recently, water-soluble fluorescent dendrimers have become an increasingly important class of labelling reagent for biological applications. Fluorescent labelling reagents are required to have high sensitivity, appropriate excitation and emission maxima, and specific functionality. Therefore, it is important to design and develop new fluorescent labelling reagents, which have high detection limits and appropriate fluorescent behaviour.<sup>[198]</sup>

### 3.1. Design and synthesis

Herein we report work on PAMAM dendritic wedges (i.e. dendrons) with a fluorescent label at their focal point or, to retain conventional dendrimer terminology, their 'core'. Based on the work in the preceding chapter, it was decided to design the dendrons on the highly fluorescent unit **FC2** because of its chemical stability and its strong fluorescence.<sup>[198-204]</sup> It should be noted that many similar derivatives of 1,8-naphthalic anhydride have been developed as fluorescent dyes and whitening agents,<sup>[205-206]</sup> but these suffer from being insoluble in aqueous and most polar media. So for our target materials the PAMAM dendron is used to enhance their solubility in water and, hopefully, their biocompatibility.

#### 3.1.1 Synthesis of fluorophore core (FC2 G0).

The synthesis of 3-(2-aminoethylamino)-7H-benz[de]benzimidazo[2,1-a]isoquinoline-7-one **FC2G0** (Scheme 3.1) was achieved by the reaction between *o*-phenylenediamine **10** and 4-bromo-1,8-naphthalenedicarboxylic anhydride **4** to give isomers **FC2** (3-bromo) and **FC2\*** (4-bromo), which were carefully separated by column chromatography.<sup>[198]</sup> **FC2** reacted with ethylenediamine by two different methods (A, B) to afford the corresponding substitution product **FC2G0** in low but sufficient yield.



**Scheme [3.1]:** Synthesis of **FC2** and **FC2G0**. *Reagents and conditions:* (i) AcOH, reflux 2 h; method (A) MeCN, EDA, reflux 3 days; method (B) EDA, heating 130 °C for 1 h.

Although there is significant literature about the synthesis, characterisation and potential applications of **FC2** and **FC2G0** or their derivatives, some of these references did not refer to the separation of the two isomers **FC2** and **FC2\***,<sup>[200, 207-213]</sup> whereas others discuss this in some detail due to the ultimate application of the compounds or their derivatives.<sup>[198-199, 204]</sup> We found it convenient to react a mixture of **FC2** and **FC2\*** with ethylene diamine (a nucleophilic aromatic substitution) and then separate the products by preparative HPLC as shown in (Scheme 3.1). (Figures 3.1-3.4) indicate the purity of the resulting product **FC2G0** and ester PAMAM dendrons **FC2G0.5**, **FC2G1.5**, **FC2G2.5**, respectively.

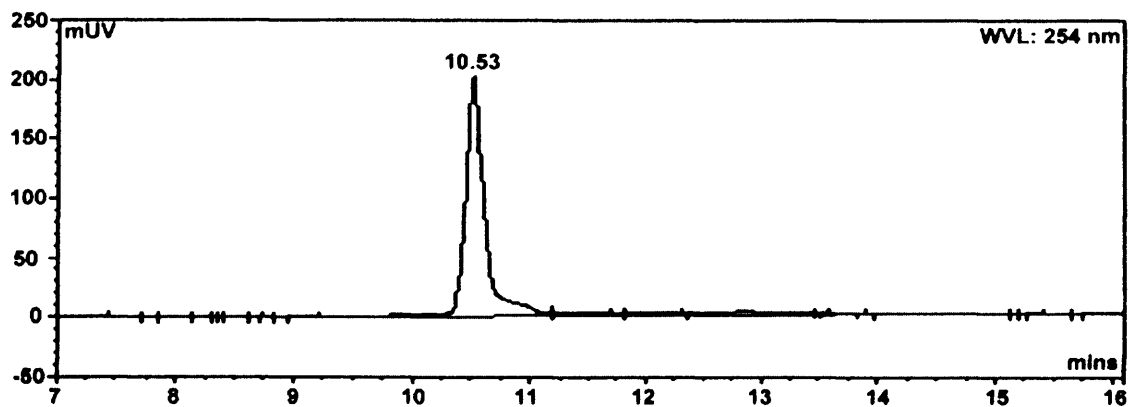


Figure [3.1]: Prep. HPLC Curve for FC2 G0 (10.533 min.)

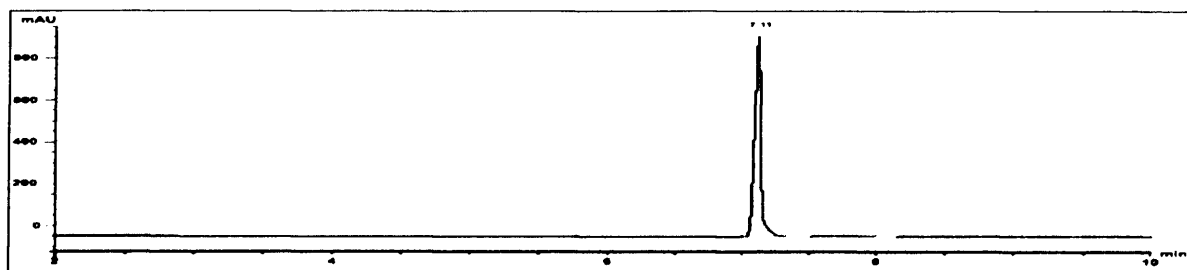


Figure [3.2]: Analytical HPLC Curve for FC2 G0.5 (7.118 min.)

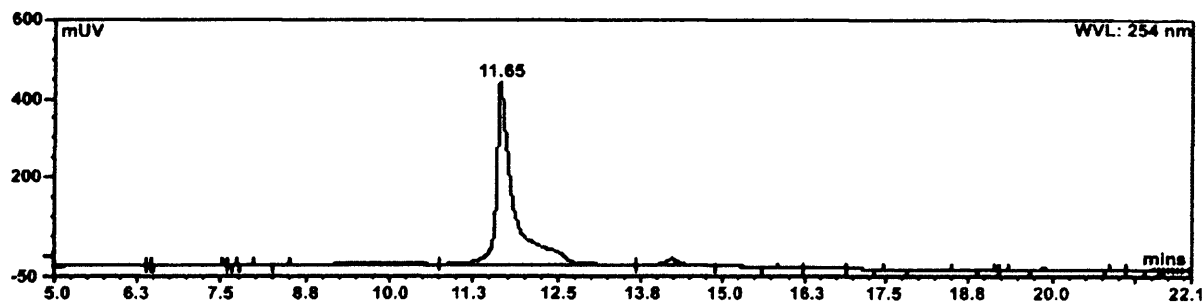


Figure [3.3]: Prep. HPLC Curve for FC2 G1.5 (11.650 min.)

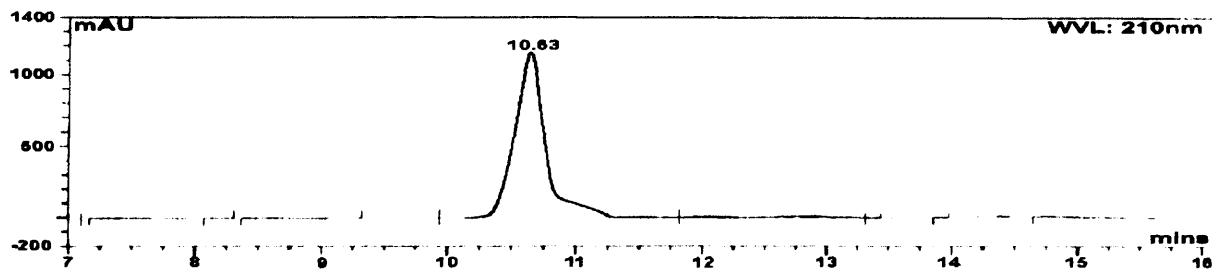
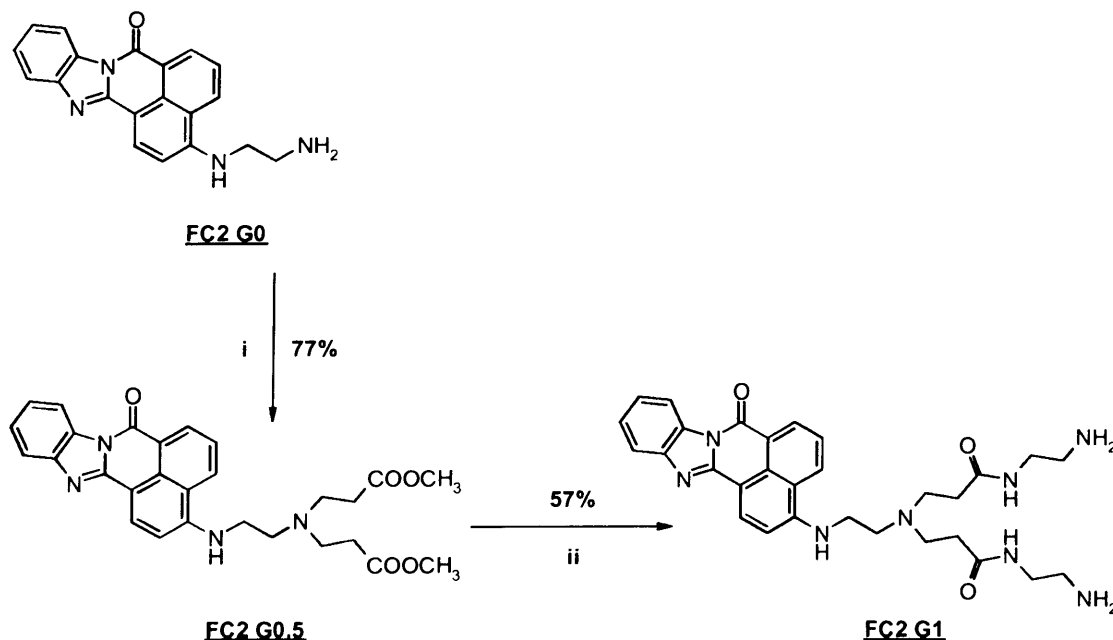


Figure [3.4]: Prep. HPLC Curve for FC2 G2.5 (10.633 min.)

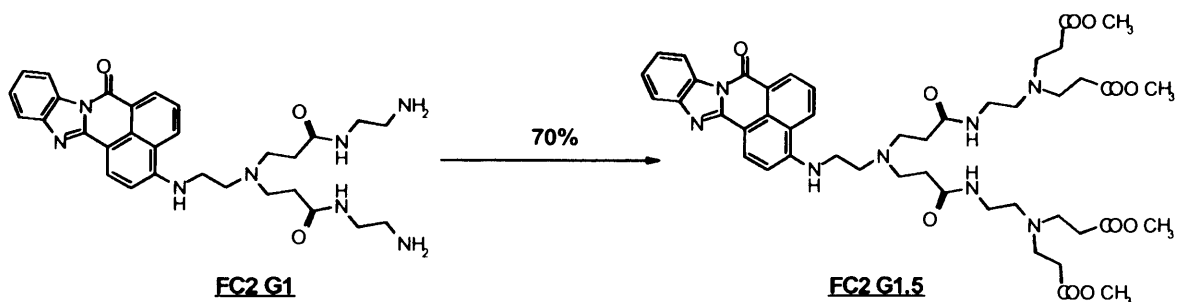
### 3.1.2. Synthesis of fluorescent PAMAM dendritic wedges FC2G0.5 – FC2G2.5 (COOMe, NH<sub>2</sub>).

To overcome the necessity for protection, it was decided to initiate a PAMAM synthesis from **FC2G0** (Scheme 3.2). The lone pairs on aromatic nitrogens are partially delocalised within the aromatic ring, resulting in a much reduced nucleophilicity when compared to the aliphatic nitrogen whose lone pair is free to react under the Michael conditions employed during PAMAM synthesis.<sup>[214]</sup> This means that the reaction between **FC2** and ethylenediamine addition occurs specifically on the aliphatic nitrogen, rather than the aromatic nitrogen. **FC2G0** was then further reacted with methyl acrylate by Michael addition<sup>[215]</sup> to yield **FC2G0.5**, followed by amidation with ethylenediamine to yield **FC2G1**. Repeating Michael additions and amidations resulted in dendrons of higher generations, **FC2G1.5** through **FC2G2.5** (Schemes 3.3, 3.4 and 3.5).



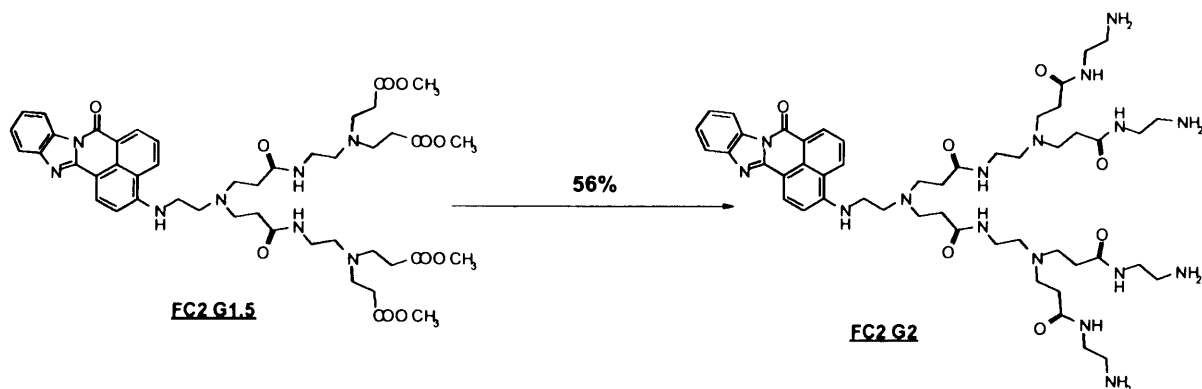
**Scheme [3.2]:** Synthesis of **FC2G0.5** and **FC2G1**. *Reagents and conditions:* (i) Methyl acrylate, MeOH, reflux 6 h, stirring 16 h, r.t; (ii) MeOH/DCM, EDA, stirring 2 days/N<sub>2</sub>.

For the Michael addition an excess of methyl acrylate (75 equiv. per primary amine), was used. For the amidation steps, a large excess of ethylenediamine (100 equiv. per ester function) was required to prevent dendron bridging and gelation. Repeating these two steps led to a controlled synthesis of the desired dendrons.



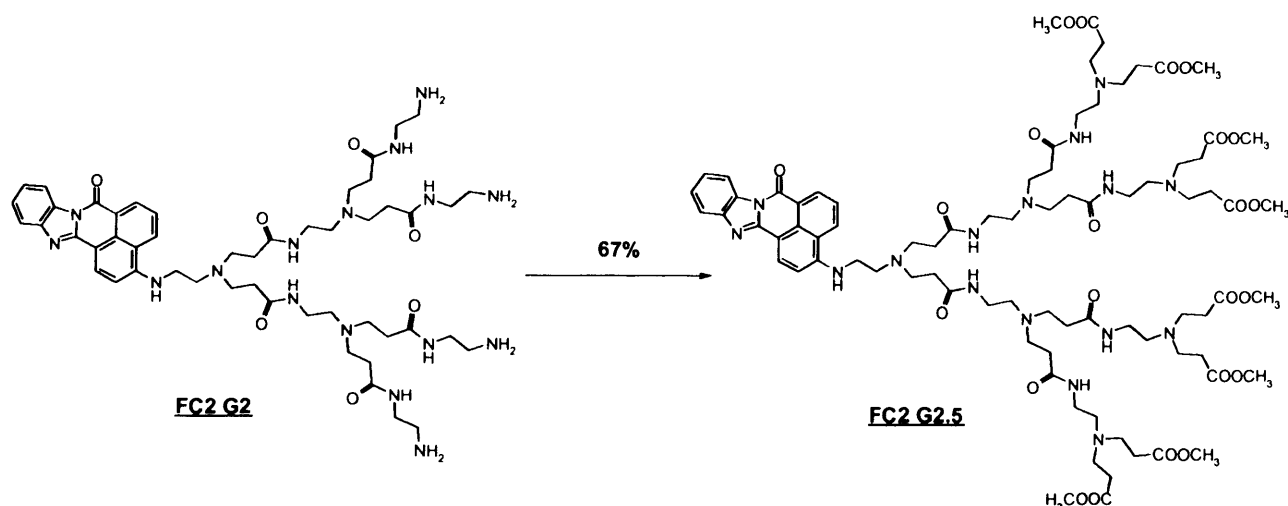
**Scheme [3.3]:** Synthesis of **FC2G1.5**. Reagents and conditions: Methyl acrylate, MeOH, reflux 24 h.

The dendrons terminated with methyl esters were easily purified with column chromatography (eluent DCM/MeOH) to give moderate or good yields (**FC2G0.5** = 77%, **FC2G1.5** = 70%, **FC2G2.5** = 67%). In each case the purity of the ester terminated dendrons, (i.e. **FC2G0.5**, **FC2G1.5** and **FC2G2.5**) was confirmed by HPLC (Figures 3.2-3.4). However, flash column chromatography could not be used to purify the amine species (**FC2G1**, **FC2G2**) because of their high polarity. Instead, the excess ethylenediamine (b.p. = 118 °C) was removed azeotropically using a toluene:methanol mixture (9:1) before the amines (**FC2G1**, **FC2G2**) were dried in vacuo. The amines were purified by flash column chromatography using a mixture of DCM and MeOH/NH<sub>4</sub>OH as eluent. They are then synthetically pure to use further.



**Scheme [3.4]:** Synthesis of **FC2G2**. Reagents and conditions: MeOH/DCM, EDA, stirring 5 days/ $N_2$ .

The structures of **FC2G0.5**, **FC2G1.5** and **FC2G2.5** were confirmed by FT-IR and  $^1H$  NMR spectroscopy. The most characteristic IR peak for structure identification is that originating from the carbonyl stretch at  $1730-1750\text{ cm}^{-1}$ . The IR data showed regular alternation of the absorbance of the carbonyl group in the fluorescent dendrons. In the case of the half generations (**FC2G0.5**, **FC2G1.5** and **FC2G2.5**), the ester carbonyl peak appeared around  $1730-1750\text{ cm}^{-1}$  and the ester C-O stretching peak appeared at around  $1260\text{ cm}^{-1}$ . For the full generations, methyl ester groups were converted to amide groups and the corresponding carbonyl peak shifted to  $1640-1660\text{ cm}^{-1}$ . The  $^1H$ -NMR data are summarized in the experimental section. They corroborated well with the FT-IR data to confirm the structure of the fluorescent dendrons. For example, the methyl ester proton peak ( $\delta\ 3.7$ ) appeared in all the NMR spectra of the half generation dendrons but was absent in the spectra of all the full generations.



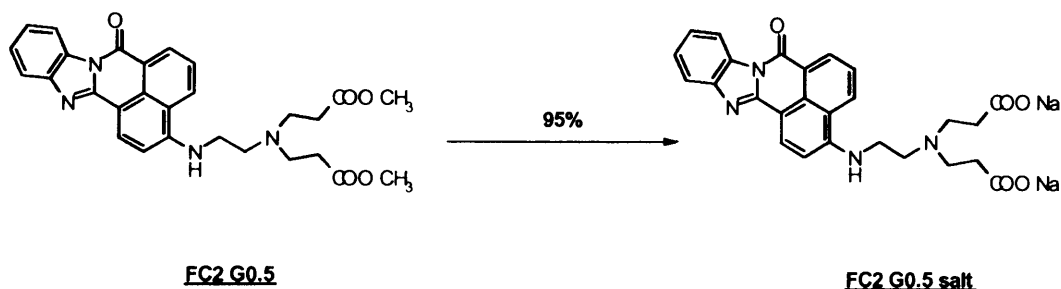
**Scheme [3.5]:** Synthesis of FC2G2.5. *Reagents and conditions:* Methyl acrylate, MeOH, reflux 2 days.

All the dendrons of interest were characterized and their structures verified by  $^1\text{H-NMR}$ ,  $^{13}\text{C-NMR}$ , EI-MS, and MALDI-TOF MS with all results agreeing with the proposed structures.<sup>[214]</sup>

### 3.1.3 Synthesis of fluorescent PAMAM dendritic wedge salts FC2G0.5, FC2G1.5 and FC2G2.5 (-COONa).

While PAMAM dendrimers have many biomedical applications, it is anionic PAMAM dendrimers which are of particular current interest as drug delivery vehicles.<sup>[216]</sup> This is because they have the important advantage of being non-cytotoxic compared to the cationic dendrimers,<sup>[217]</sup> whilst also being highly effective in transcellular transport and oral delivery applications. For example, previous studies in cancer cells have shown that efficacy of anionic PAMAM dendrimer–methotrexate (MTX) conjugates were significantly better than cationic PAMAM dendrimer–MTX conjugates.<sup>[218]</sup> This difference has been partially attributed to differences in lysosomal residence times and intracellular drug release from anionic and cationic dendrimer–drug conjugates. Hence anionic PAMAM dendrimers may be more effective in-vivo platforms for drug delivery

applications compared to cationic PAMAM dendrimers, because of their better cytotoxicity profiles, and reduced protein binding.<sup>[219]</sup> Therefore, conversion of **FC2G0.5** diester to the anionic **FC2G0.5** salt was attempted, and indeed achieved with very good yields (95%) by refluxing in ethanolic NaOH (Scheme 3.6).

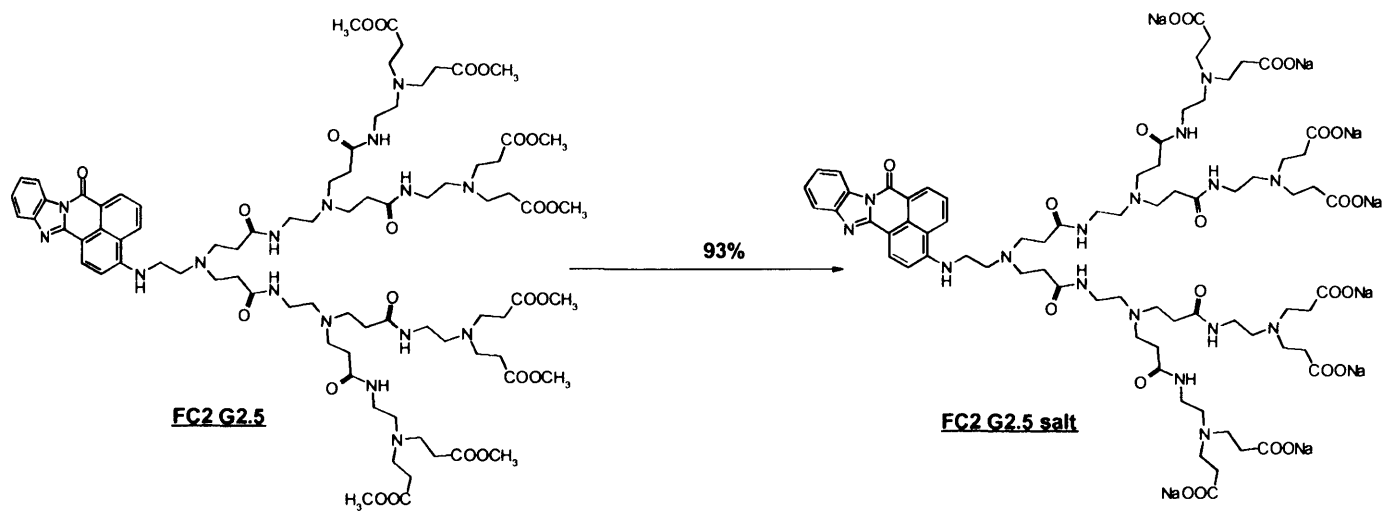


**Scheme [3.6]** Synthesis of **FC2G0.5** salt. *Reagents and conditions:* Ethanolic NaOH, EtOH, reflux 16 h.

Similarly, the other two anionic salts **FC2G1.5** and **FC2G1.5** were formed, in quantitative yield, by the alkaline hydrolysis of polyesters **FC2G1.5** and **FC2G1.5**, respectively, by stirring with ethanolic NaOH at room temperature (Schemes 3.7, 3.8). All the compounds were fully characterized using by <sup>1</sup>H-NMR, <sup>13</sup>C-NMR, EI-MS, and MALDI-TOF MS.



**Scheme [3.7]:** Synthesis of **FC2G1.5** salt. *Reagents and conditions:* NaOH, EtOH, stirring 24 h, rt.



**Scheme [3.8]:** Synthesis of **FC2G2.5 salt**. Reagents and conditions: NaOH, EtOH, stirring 24 h, rt.

## 3.2. Photophysical characterization

As noted in the introduction, 1,8-naphthalimide derivatives are good candidates for fluorescent studies because of their intrinsic photophysical and photochemical properties,<sup>[220]</sup> which account for their widespread use as fluorescent dyes<sup>[137, 221]</sup> and fluorescent markers.<sup>[151, 222-223]</sup>

### 3.2.1. UV-vis absorption properties

The UV/visible absorption spectrum of **FC2** in methanol at room temperature shows absorption in the near UV region at  $\lambda_{max} = 390$  nm. Substitution of the bromine atom at C-3 in **FC2** with an electron-donating alkylamino group (compounds **FC2G0** – **FC2G2.5** and their salts) results in a large bathochromic shift into the visible region at  $\lambda_{max} = 444$ -460 nm (Figure 3.5). This is a typical effect for conjugated organic compounds and agrees with the reported literature.<sup>[213]</sup>

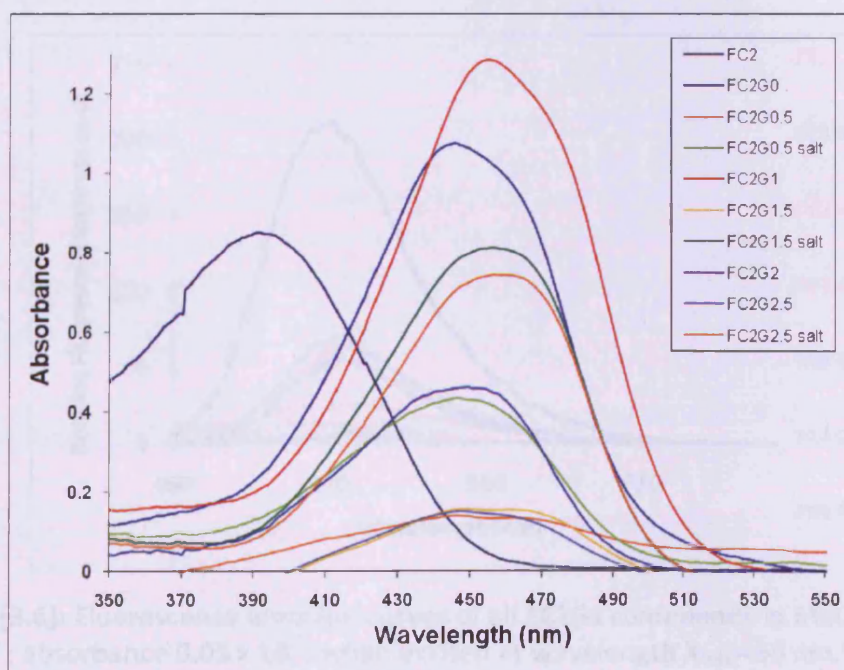
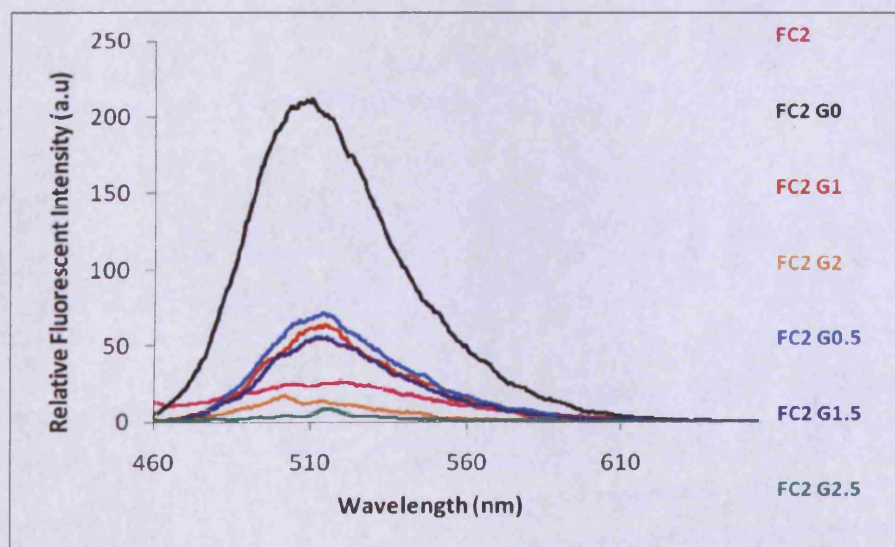


Figure [3.5]: UV absorbance spectra for **FC2** and **FC2Gs** in MeOH solvent.

### 3.2.2. Fluorescence measurements.

#### 3.2.2.1 Relative intensity of fluorescence for PAMAM terminated [-COOMe, -NH<sub>2</sub>].

As described earlier, the aminoethyl derivative **FC2G0-NH<sub>2</sub>** was chosen for study due to its suitability as a starting material for building PAMAM dendrons. The RFI characteristics of the fluorophore 3-aminobenzimidazo[2,1-a]benz[de]isoquinolin-7-one derivatives, **FC2** and **FC2G0-FC2G2.5**, in methanol are presented in (Figures 3.6, 3.7) and show that the fluorescence emissions are in the spectral region 502–516 nm (Table 3.1). The effect of the C-4 alkylamino substituent on the energy of the dyes' fluorescence maximum wavelength is negligible as reported.<sup>[224]</sup> In all cases the shape and maxima of the fluorescence band do not depend of the excitation wavelength, and the excitation spectra are identical to the corresponding absorption spectra.



**Figure [3.6]:** Fluorescence emission curves of all **FC2Gs** compounds in MeOH at UV absorbance  $0.05 \times 10^{-3}$ , when excited at wavelength  $\lambda_{\max}$  455 nm.

Despite the negligible effect on the wavelength of the fluorescence transitions, the fluorescence performance of compounds **FC2** and **FC2G0-FC2G2.5** is clearly influenced by the substituent at the C-3 position of the molecule (Figure 3.6, 3.7 and Table 3.1). The

fluorescence intensity of core **FC2** is very low in comparison with that of compounds **FC2G0**, **FC2G1** and **FC2G1.5**, but is stronger than that of higher generations **FC2G2**, **FC2G2.5**.

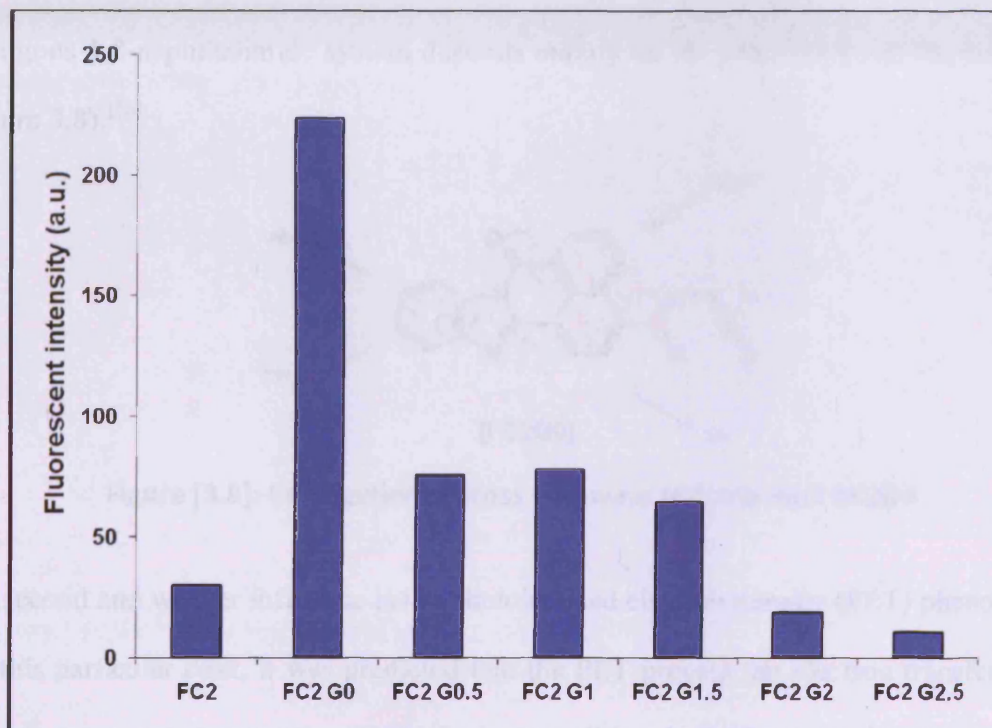


**Figure [3.7]:** Fluorescence Intensity values of all **FC2G** dendrons in MeOH at UV absorbance  $0.05 \times 10^{-3}$ , when excited at wavelength  $\lambda_{\max}$  455 nm

It has been explained previously that **FC2** has low fluorescent intensity due to the bromine derivative on its C-3 position, which affects polarization of the 1,8-naphthalimide chromophoric system.<sup>[177]</sup>

**Table [3.1]:** Fluorescence Intensity values of all **FC2Gs** compounds in MeOH at UV absorbance  $0.05 \times 10^{-3}$ , when excited at wavelength  $\lambda_{\max}$  455 nm

Compounds	FC2	FC2 G0	FC2 G0.5	FC2 G1	FC2 G1.5	FC2 G2	FC2 G2.5
Emission max (nm)	515.5	508.5	513.5	511.5	510	502	513
Fluorescence Intensity (a.u.)	31	224	81	79	65	21	11

It was found that the fluorescence intensity spectra of **FC2G0** in methanol solution is eight times higher than **FC2**. There are two opposite factors influencing the fluorescent spectra of **FC2G0**. The strongest influence, which increases the fluorescence, is the presence of the electron-donating amino group. It is known that the photophysical properties of the analogous 1,8-naphthalimide system depends mainly on the polarization of the molecule (Figure 3.8).<sup>[36]</sup>

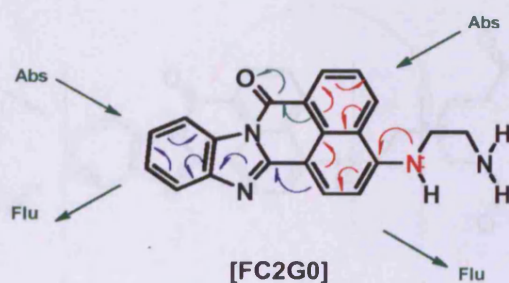


**Figure [3.8]:** Conjugation process pathways of compound **FC2G0**

The second and weaker influence is the photoinduced electron transfer (PET) phenomena. For this particular case, it was predicted that the PET process (an electron transfer from the primary amine receptor to the excited state of the fluorophore core) would quench fluorescence emission (Figure 3.9).<sup>[225]</sup> However, the possibility of PET happening is very low due to the receptor being a primary amine rather than a tertiary amine for which the PET process is more favoured.<sup>[226]</sup>

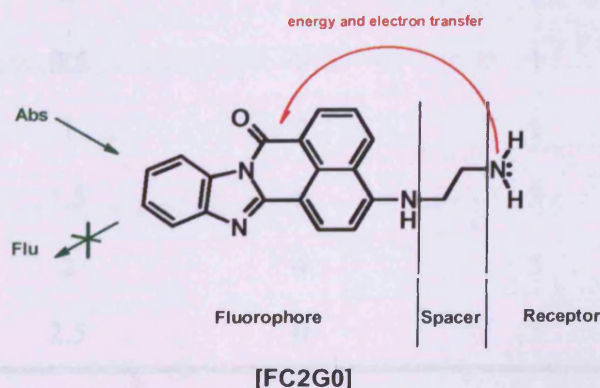


**Figure [3.9]:** Weak fluorescent quenching process result from PET in case of primary amine receptor.

As (Table 3.2) shows, the relative fluorescence intensity decreases from **FC2G0** >>> **FC2G0.5** = **FC2G1** > **FC2G1.5** > **FC2G2** > **FC2G2.5**. This trend is due to the effect of the tertiary amines within the PAMAM substituent, which can interact with the fluorophore core via the PET mechanism (Figure 3.10)<sup>[225]</sup> and, as the PAMAM generation increases, the number of amines also increases, which enhances the PET process (Table 3.2).<sup>[181-183]</sup>

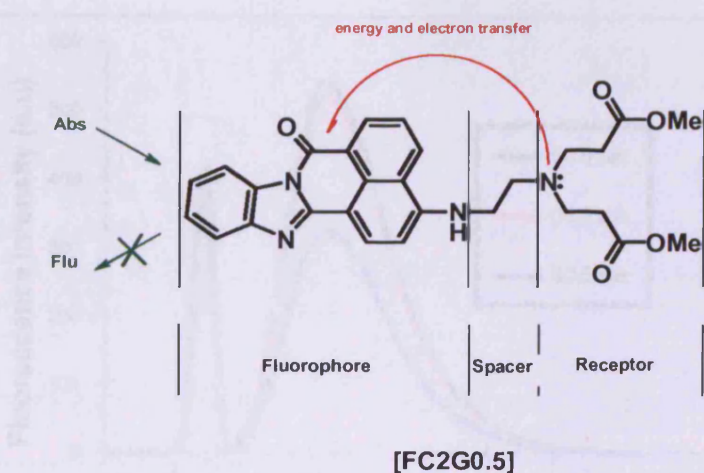


**Figure [3.10]:** Strong fluorescent quenching process resulting from PET in the case of tertiary amine receptor.

**Table [3.2]:** Number of primary, tertiary amines in all compounds FC2Gs.

Compounds Name	Generation Number	Primary amine -NH <sub>2</sub>	Tertiary amine =N-	Total no. of amines
FCG0	0	1	0	0
FC2G0.5	0.5	0	1	1
FC2G1	1	2	1	3
FC2G1.5	1.5	0	3	3
FC2G2	2	4	3	7
FC2G2.5	2.5	0	7	7

### 3.2.2.2 Relative intensity for fluorescent PAMAM terminated [-COONa].

Figures (3.12 and 3.13) show how the relative fluorescence intensity decreases for the carboxylate salts **FC2G0.5** > **FC2G1.5** >> **FC2G2.5** due to the previously mentioned PET effect. The extra tertiary amine groups in the scaffold quench the fluorescence as the generation increases.<sup>[194]</sup>

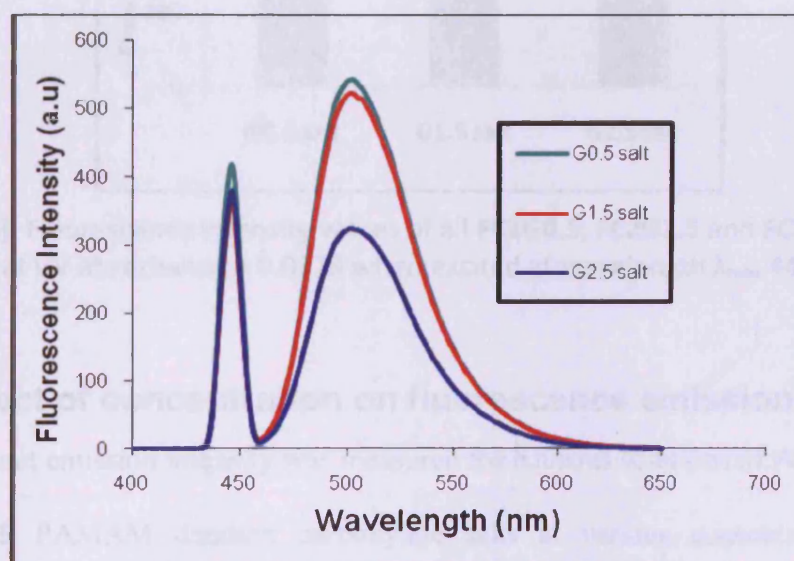


**Figure [3.12]:** Fluorescence emission curves for all **FC2G0.5**, **FC2G1.5** and **FC2G2.5** salts in  $H_2O$  at UV absorbance 0.0379 when excited at wavelength  $\lambda_{max}$  447 nm.

The RFI study of carboxylate terminated PAMAM dendron salts was carried out in water. This solvent was chosen due to its biological compatibility and its potential hydrogen-bonding capability with the terminal groups of the PAMAM dendrons. These H-bonds favour radiation-less transitions, which has previously been noted to cause a decrease of the fluorescence quantum yield of the analogous 1,8-naphthalimide fluorophore.<sup>[151, 227]</sup>

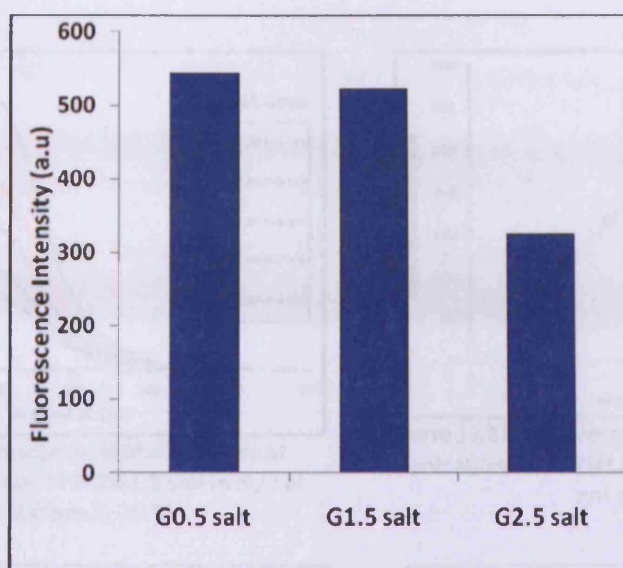


**Figure [3.13]:** Fluorescence intensity values of all FC2G0.5, FC2G1.5 and FC2G2.5 salts in H<sub>2</sub>O at UV absorbance = 0.0379 when excited at wavelength  $\lambda_{\max}$  447 nm.

### 3.2.3 Effect of concentration on fluorescence emission intensity

The fluorescent emission intensity was measured for aqueous solutions of FC2G0.5, FC2G1.5 and FC2G2.5 PAMAM dendron carboxylate salts at various concentrations at room temperature. It was found that the emission intensity increased almost linearly with concentration (Figures 3.15, 3.17, 3.19). This result suggests that there is no effect of intermolecular interaction (i.e. self-quenching within aggregates) on the fluorescence properties of the dendrons over the concentration range  $0.83 \times 10^{-4} - 5.75 \times 10^{-4} \text{ mM L}^{-1}$ .<sup>[226]</sup>

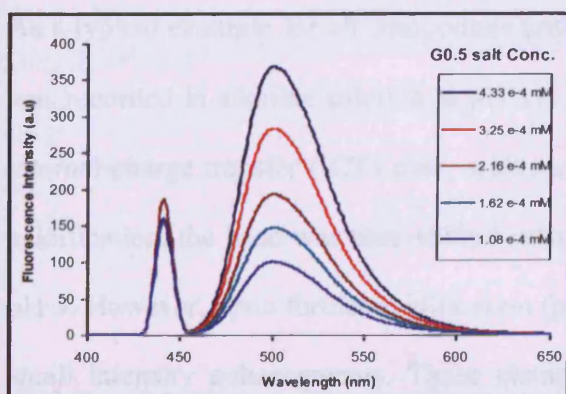


**Figure [3.14]:** Fluorescence Intensity curves at different concentrations of FC2G0.5 salt in H<sub>2</sub>O at emission 500 nm at 25 °C.

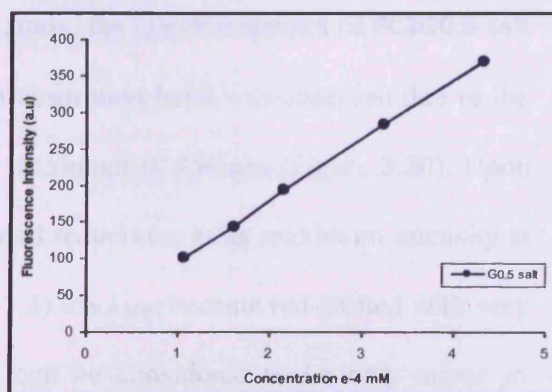


**Figure [3.15]:** Fluorescence Intensity at different concentrations of FC2G0.5 salt in H<sub>2</sub>O at emission 500 nm at 25 °C.

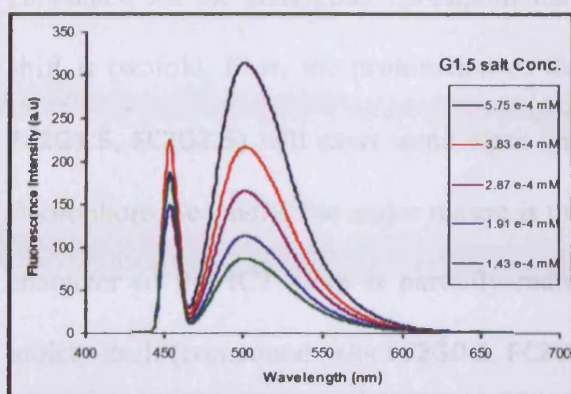


Figure [3.16]: Fluorescence Intensity curves at different concentrations of FC2G1.5 salt in H<sub>2</sub>O at emission 500 nm at 25 °C.

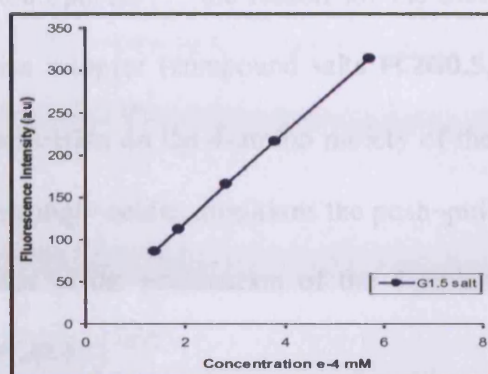


Figure [3.17]: Fluorescence Intensity at different concentrations of FC2G1.5 salt in H<sub>2</sub>O at emission 500 nm at 25 °C.

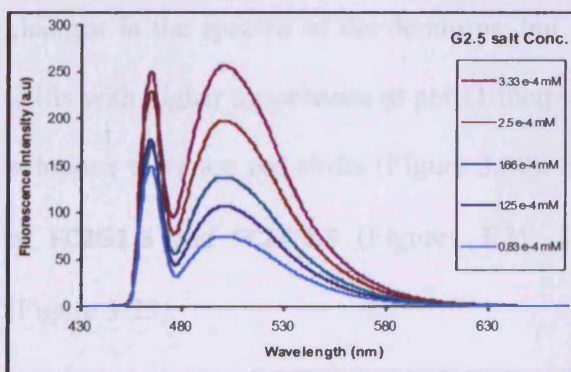


Figure [3.18]: Fluorescence Intensity curves at different concentrations of FC2G2.5 salt in H<sub>2</sub>O at emission 500 nm at 25 °C.

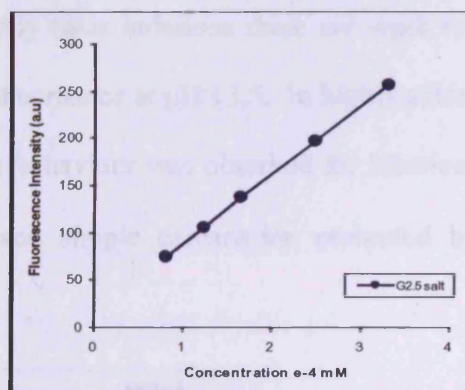


Figure [3.19]: Fluorescence Intensity at different concentrations of FC2G2.5 salt in H<sub>2</sub>O at emission 500 nm at 25 °C.

### 3.2.4 Influence of pH on the absorption and fluorescence characteristics

#### 3.2.4.1 UV-Visible Absorption Spectra

As a typical example for all compounds under study, the UV-Vis spectra of FC2G0.5 salt was recorded in alkaline solution at pH 11. An absorption band was observed due to the internal charge transfer (ICT) state, with  $\lambda_{MAX}$  maximum at 456 nm (Figure 3.20). Upon acidification, the band was blue-shifted with small reductions in its maximum intensity at pH 5. However, upon further acidification (pH 3.5) the  $\lambda_{MAX}$  became red-shifted with very small intensity enhancements. These changes can be considered to be only minor in comparison to the changes in the fluorescence spectra (see later). As Gunnlaugsson *et al.*

concluded for the analogous 1,8-naphthalimide fluorophores<sup>[164]</sup> the reason for the blue shift is twofold. First, the protonation of the amine receptor (compound salts **FC2G0.5**, **FC2G1.5**, **FC2G2.5**) will exert some weak charge repulsion on the 4-amino moiety of the fluorophore. Secondly, the major reason is that in strongly acidic conditions the push–pull character of the ICT state is partially reduced due to the protonation of the 4-amino moiety itself (compound salts **FC2G0.5**, **FC2G1.5**, **FC2G2.5**).<sup>[224]</sup>

To conclude, in neutral, weakly acidic and weakly basic solutions, there are only minor changes in the spectra of the dendrons, but in highly basic solutions there are weak red shifts with higher absorbance at pH 11 then weak absorbance at pH 13.5. In highly acidic solutions there are red shifts (Figure 3.20). Similar behaviour was observed for solutions of **FC2G1.5** and **FC2G2.5** (Figures 3.21, 3.22), and simple explanation presented by (Figure 3.23).

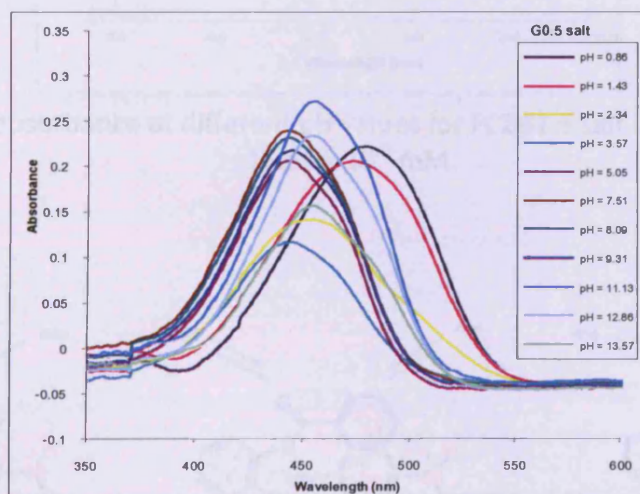


**Figure [3.20]:** UV absorbance at different pH values for **FC2G0.5** salt in H<sub>2</sub>O at concentration  $16.66 \times 10^{-3}$  mM.

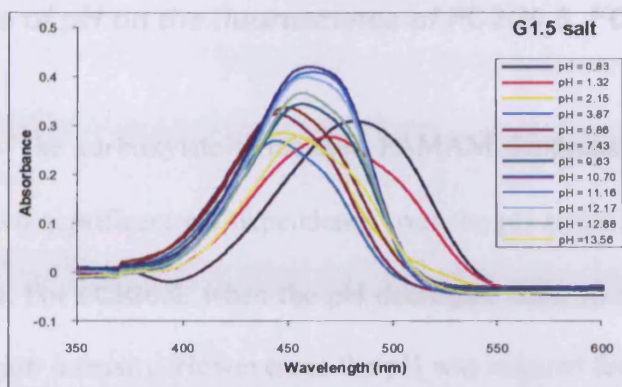


Figure [3.21]: UV absorbance at different pH values for FC2G1.5 salt in H<sub>2</sub>O at concentration  $16.66 \times 10^{-3}$  mM.

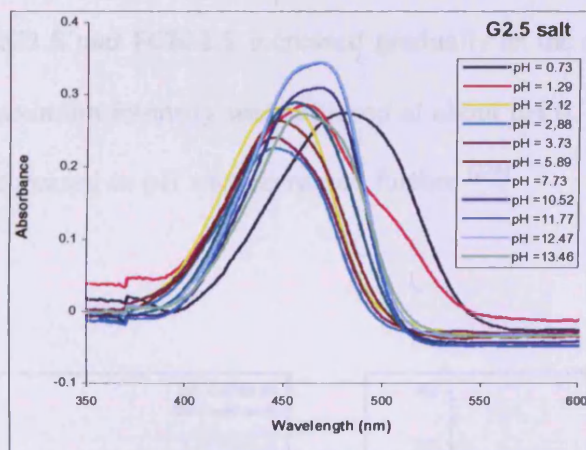


Figure [3.22]: UV absorbance at different pH values for FC2G2.5 salt in H<sub>2</sub>O at concentration  $16.66 \times 10^{-3}$  mM.

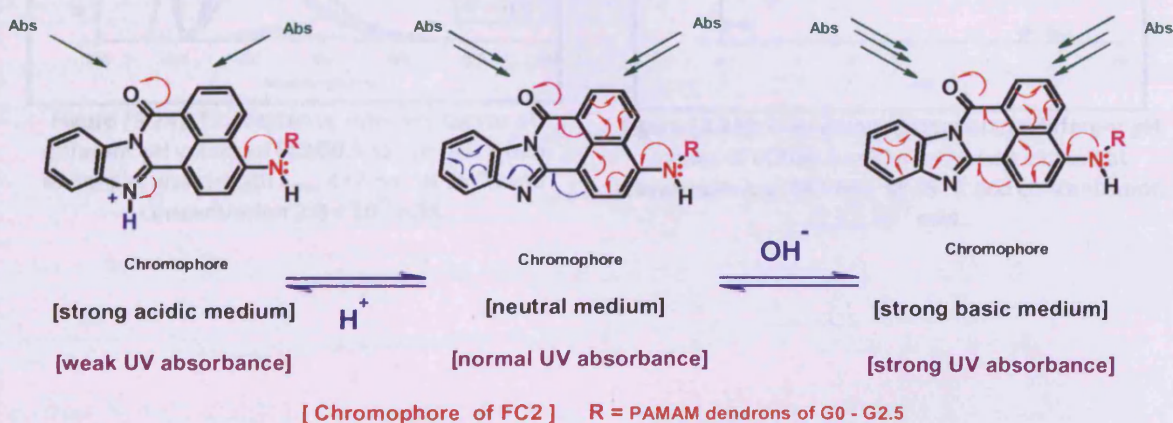
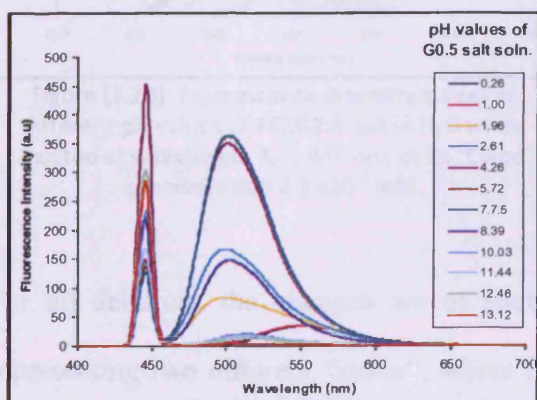


Figure [3.23]

### 3.2.4.2 Influence of pH on the fluorescence of FC2G0.5, FC2G1.5 and FC2G2.5 salts

The fluorescence of the carboxylate-terminated PAMAM dendrons (FC2G0.5, FC2G1.5 and FC2G2.5) showed significant pH dependence over the pH range 13 to 1 as shown in (Figures 3.24–3.29). For FC2G0.5, when the pH decreased from 13 to 7, there was little change in the emission intensity. However, as the pH was reduced further, there appeared a rapid increase of fluorescence intensity, which reached a maximum at about pH 6; the emission band position scarcely changed during this process. Similarly, the fluorescence intensity of both FC2G1.5 and FC2G2.5 increased gradually as the pH was lowered from 13 to 7, where the maximum intensity was achieved at about pH 6. Then the fluorescence intensity gradually decreased as pH was decreased further.<sup>[226]</sup>



**Figure [3.24]:** Fluorescence Intensity curves at different pH values of FC2G0.5 salt in H<sub>2</sub>O when excited at wavelength  $\lambda_{\max}$  447 nm. at 25 °C and concentration  $2.3 \times 10^{-3}$  mM.

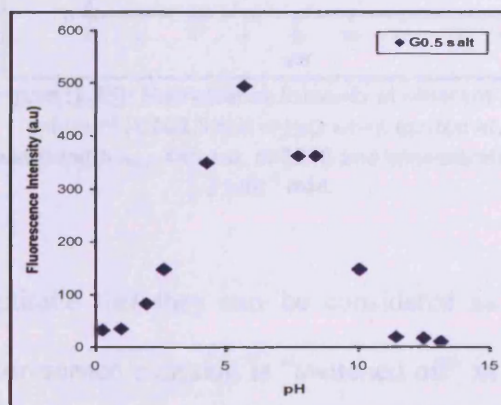


**Figure [3.25]:** Fluorescence Intensity at different pH values of FC2G0.5 salt in H<sub>2</sub>O when excited at wavelength  $\lambda_{\max}$  447 nm. at 25 °C and concentration  $2.3 \times 10^{-3}$  mM.

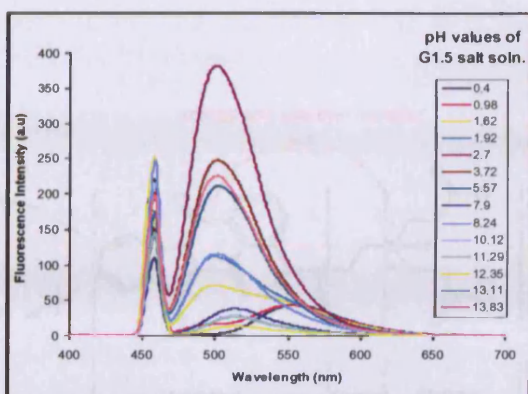


**Figure [3.26]:** Fluorescence Intensity curves at different pH values of FC2G1.5 salt in H<sub>2</sub>O when excited at wavelength  $\lambda_{\max}$  460 nm. at 25 °C and concentration  $2.3 \times 10^{-3}$  mM.

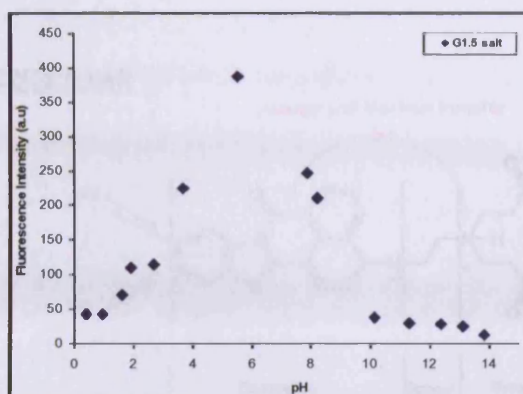


**Figure [3.27]:** Fluorescence Intensity at different pH values of FC2G1.5 salt in H<sub>2</sub>O when excited at wavelength  $\lambda_{\max}$  460 nm at 25 °C and concentration  $2.3 \times 10^{-3}$  mM.

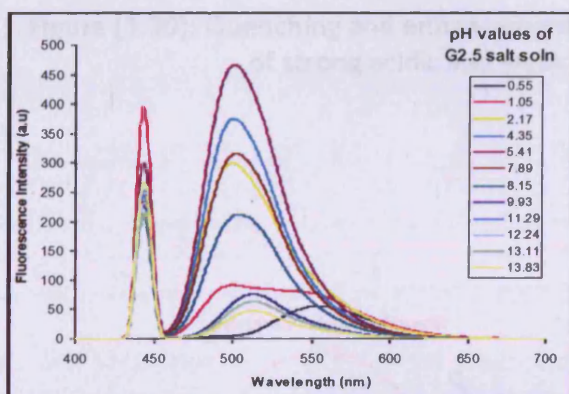


**Figure [3.28]:** Fluorescence Intensity curves at different pH values of FC2G2.5 salt in H<sub>2</sub>O when excited at wavelength  $\lambda_{\max}$  445 nm. at 25 °C and concentration  $2.3 \times 10^{-3}$  mM.

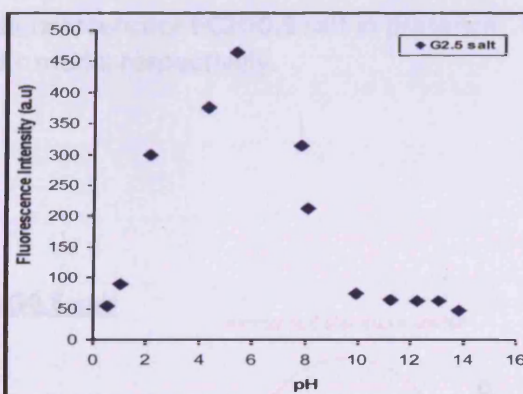


**Figure [3.29]:** Fluorescence Intensity at different pH values of FC2G2.5 salt in H<sub>2</sub>O when excited at wavelength  $\lambda_{\max}$  445 nm. at 25 °C and concentration  $2.3 \times 10^{-3}$  mM.

For all dendrons the changes are of such magnitude that they can be considered as representing two different “states”, where the fluorescence emission is “switched off” in alkaline solution or strongly acidic solution and “switched on” in mildly acidic solution (Figure 3.30, 3.31).<sup>[224]</sup> It is worth noting that pH 6 is the critical point in (Figures 3.25, 3.27, 3.29) which correlates well with the pKa value<sup>[228-229]</sup> of tertiary amines in PAMAM dendrimers. More acidic solutions (i.e. below pH 3) result in further protonation of the imidazole unit causing losses in fluorescence, as has been noted for other imidazole-containing fluorophores.<sup>[199-200, 203]</sup>

3.3. Physicochemical Characterization Studies

3.3.1. Pulsed Gradient Spin Echo (PGSE) NMR

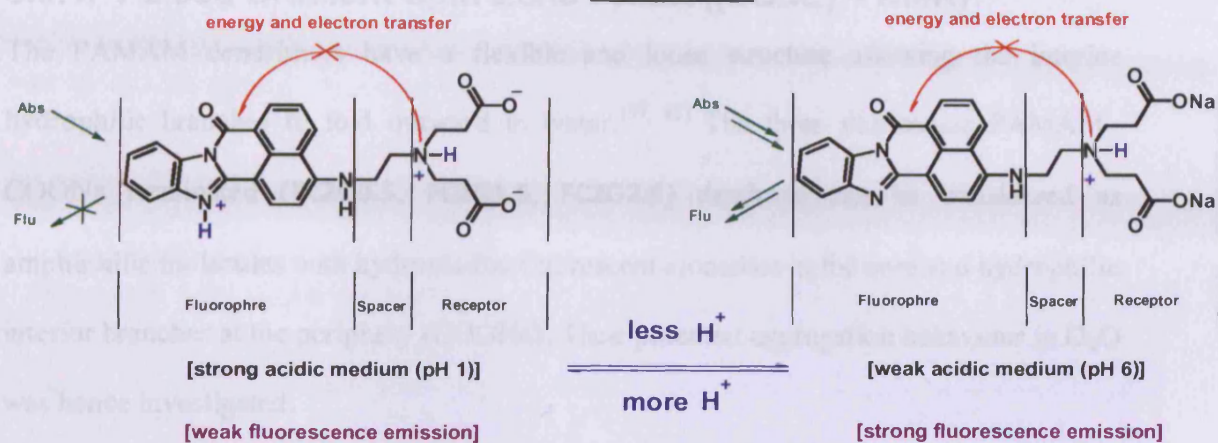


**Figure [3.30]:** Quenching and enhancement of fluorescence of FC2G0.5 salt in presence of strong acidic and weak acidic media respectively.

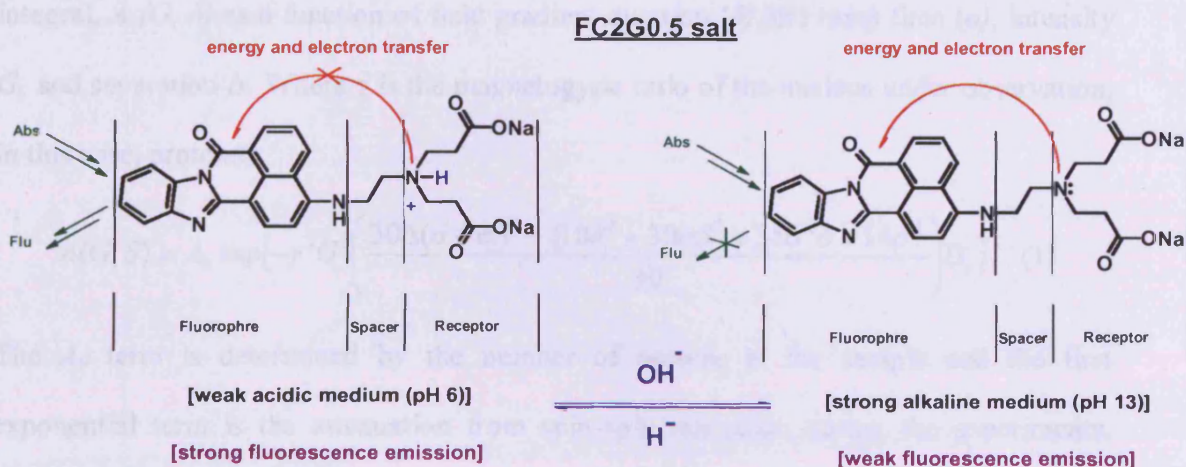


**Figure [3.31]:** Enhancement and quenching of fluorescence of FC2G0.5 salt in presence of weak acidic and strong basic media respectively.

### 3.3. Physicochemical Characterization Studies

#### 3.3.1. Pulsed Gradient Spin Echo - NMR ((PGSE) – NMR)

The PAMAM dendrimers have a flexible and loose structure allowing the interior hydrophilic branches to fold outward in water.<sup>[55, 88]</sup> The three fluorescent PAMAM–COONa terminated (**FC2G0.5**, **FC2G1.5**, **FC2G2.5**) dendrons can be considered as amphiphilic molecules with hydrophobic fluorescent aromatics at the core and hydrophilic interior branches at the periphery (COONa). Their potential aggregation behaviour in D<sub>2</sub>O was hence investigated.

##### 3.3.1.1 Self-diffusion Coefficient ( $D_s$ ).

Using data acquired from pulsed gradient spin echo (PGSE) NMR by PhD student Abdulhakim Jangher of the group of Dr. Peter Griffiths (Cardiff University), the self-diffusion coefficient,  $D_s$ , are calculated from equation (1) using the measured peak integral,  $A(G, \delta)$  as a function of field gradient duration ( $\delta$ ) and ramp time ( $\sigma$ ), intensity  $G$ , and separation  $\Delta$ . Where  $\gamma$  is the magnetogyric ratio of the nucleus under observation, in this case, protons.

$$A(G, \delta) = A_0 \exp\left[-\gamma^2 G^2 \left(\frac{30\Delta(\delta + \sigma)^2 - (10\delta^3 + 30\sigma\delta^2 + 35\sigma^2\delta + 14\sigma^3)}{30}\right) D_s\right] \quad (1)$$

The  $A_0$  term is determined by the number of protons in the sample and the first exponential term is the attenuation from spin-spin relaxation during the experiments. Typically values of  $\delta$ ,  $\Delta$  and  $\sigma$  for the polymer systems studied here are ( $d_4$ ) = 200  $\mu$ sec, ( $d_2$ ) = 400 msec.

Table (3.3) and (Figure 3.32) show the diffusion coefficient ( $D_s$ ) values for **FC2G0.5**, **FC2G1.5** and **FC2G2.5** fluorescent dendrons at different concentrations (9.0 - 23 mM L<sup>-1</sup>).

In each case a modest decrease of the diffusion coefficient ( $D_s$ ) is observed as the

concentration increases. In the case of **FC2G0.5**, the values of the diffusion coefficient ( $D_s$ ) are relatively large compared to those of **FC2G1.5** and **FC2G2.5** which are very similar to each other.

**Table [3.3]:** Self diffusion coefficient ( $D_s$ ) values of **FC2G0.5**, **FC2G1.5** and **FC2G2.5** fluorescent dendron salts in  $D_2O$  at 25 °C at different concentrations (9.0 - 23 mM L<sup>-1</sup>) at pH (9.3 – 9.8).

<b>FC2G0.5</b>		<b>FC2G1.5</b>		<b>FC2G2.5</b>	
Concentration (mM L <sup>-1</sup> )	$D_s / m^2 s^{-1}$	Concentration(mM L <sup>-1</sup> )	$D_s / m^2 s^{-1}$	Concentration(mM L <sup>-1</sup> )	$D_s / m^2 s^{-1}$
9.0	$1.92 \times 10^{-10}$	9.5	$1.40 \times 10^{-10}$	9.3	$1.38 \times 10^{-10}$
14.65	$1.85 \times 10^{-10}$	14.65	$1.37 \times 10^{-10}$	14.6	$1.27 \times 10^{-10}$
18.90	$1.76 \times 10^{-10}$	19.20	$1.36 \times 10^{-10}$	18.9	$1.25 \times 10^{-10}$
23.5	$1.69 \times 10^{-10}$	22.15	$1.31 \times 10^{-10}$	23.5	$1.15 \times 10^{-10}$

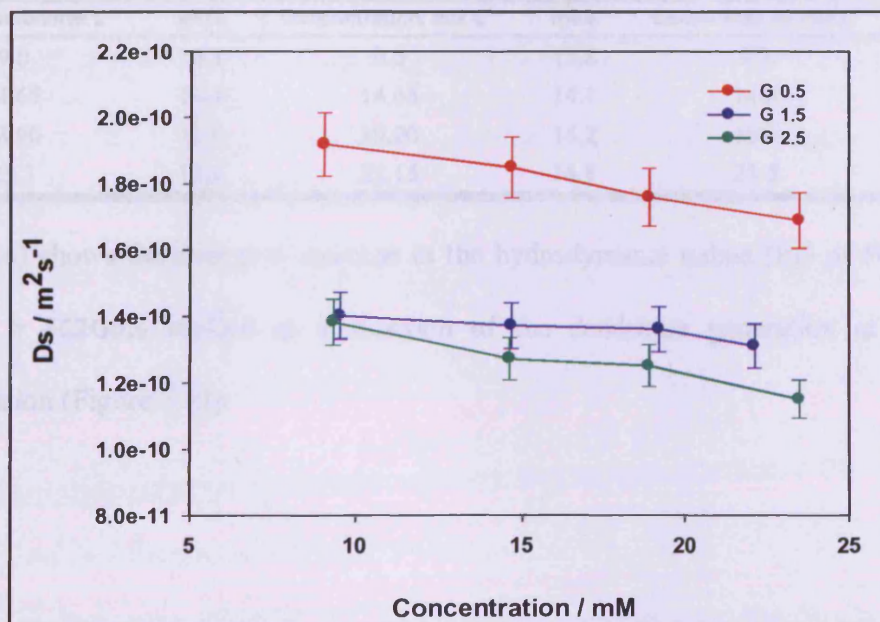


**Figure [3.32]:** Self diffusion coefficient ( $D_s$ ) curves of **FC2G0.5**, **FC2G1.5** and **FC2G2.5** fluorescent dendron salts in  $D_2O$  at 25 °C at different concentrationse (9.0 - 23 Mm L<sup>-1</sup>).

### 3.3.1.2 Hydrodynamic radii ( $R_h$ ).

The hydrodynamic radius ( $R_h$ ) values of the three fluorescent PAMAM–COONa terminated (**FC2G0.5**, **FC2G1.5**, **FC2G2.5**) dendrons as a function of concentration was also investigated by diffusion NMR. As a characteristic length, the hydrodynamic radius is calculated by Stokes-Einstein equation (2).

$$D = \frac{k_B T}{6\pi\eta R_h} \quad (2)$$

Where  $k_B$  is the Boltzmann constant,  $T$  is the temperature in Kelvin,  $\eta$  is the viscosity of the solvent and  $R_h$  is the hydrodynamic radius of the fluorescent dendron.

**Table [3.4]:** Hydrodynamic radii ( $R_h$ ) values of **FC2G0.5**, **FC2G1.5** and **FC2G2.5** fluorescent dendrons salt in  $D_2O$  at 25 °C at different concentrations (9.0 – 23  $mM L^{-1}$ ).

<b>FC2G0.5</b>		<b>FC2G1.5</b>		<b>FC2G2.5</b>	
Concentration/ $mM L^{-1}$	$R_h/\text{Å}$	Concentration/ $mM L^{-1}$	$R_h/\text{Å}$	Concentration/ $mM L^{-1}$	$R_h/\text{Å}$
9.0	10.1	9.5	13.8	9.3	14.0
14.65	10.4	14.65	14.1	14.6	15.2
18.90	11.0	19.20	14.2	18.9	15.5
23.5	11.4	22.15	14.8	23.5	16.8

Table (3.4) shows the expected increase in the hydrodynamic radius ( $R_h$ ) of **FC2G2.5** > **FC2G1.5** > **FC2G0.5** studied as a function of the dendrimer generation at constant concentration (Figure 3.33).

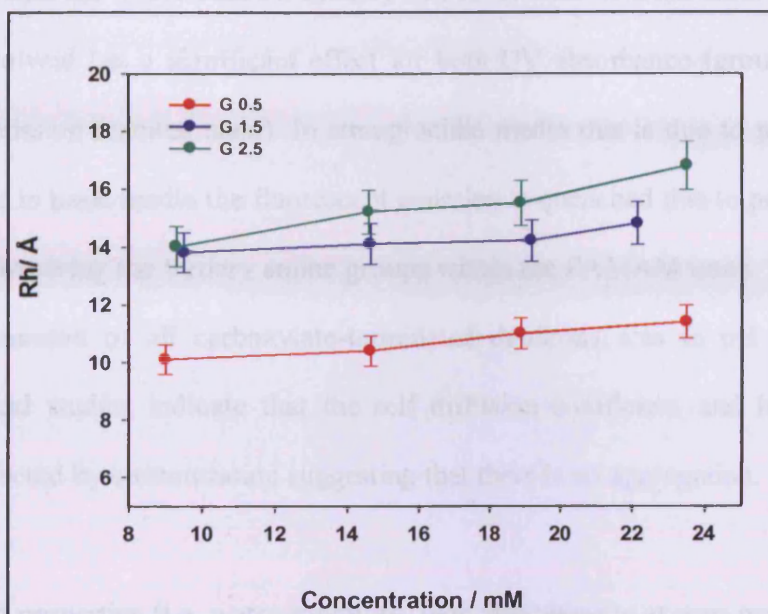


**Figure [3.33]:** Hydrodynamic radii ( $R_h$ ) curves of **FC2G0.5**, **FC2G1.5** and **FC2G2.5** fluorescent dendron salts in  $D_2O$  at  $25\text{ }^\circ\text{C}$  at different concentrations ( $9.0 - 23\text{ mM L}^{-1}$ ).

These studies demonstrate that over this relatively high concentration range (as compared to those used in the fluorescence studies) the diffusion coefficients of **FC2G0.5**, **FC2G1.5** and **FC2G2.5** do not vary significantly so there is no sign of aggregation. The hydrodynamic radii have been obtained using the Stokes-Einstein equation extrapolated to infinite dilution  $D_s$ . The size of the dendrons were not significantly altered at different concentrations.

### 3.4. Conclusion

In conclusion, we designed and prepared several new water soluble fluorescent dendrons and studied their photophysical and physicochemical properties. The dendrons are all fluorescent due to the core but this is modulated by PET process which increases with higher PAMAM dendron generation.

For all compounds the fluorescence is linearly correlated with concentration and the pH of the aqueous solvent has a significant effect for both UV absorbance (ground state) and fluorescent emission (excited state). In strong acidic media this is due to protonation of the core, while in basic media the fluorescent emission is quenched due to presence of the PET process involving the tertiary amine groups within the PAMAM units. The strongest fluorescent emission of all carboxylate-terminated dendrons was in pH 6. Generally physicochemical studies indicate that the self diffusion coefficient and hydrodynamic radii are unaffected by concentration suggesting that there is no aggregation.

The confirmed properties (i.e. water solubility, high fluorescence at near neutral pH, and no aggregation) suggest these new dendron are promising for the collaborative biological studies described in (Appendix A).

# CHAPTER FOUR

## EXPERIMENTAL

<b>4.1</b>	<b>Experimental techniques.....</b>	<b>64</b>
<b>4.2</b>	<b>General experimental procedures.....</b>	<b>66</b>
<b>4.3</b>	<b>Experimental procedures.....</b>	<b>68</b>
<b>4.3</b>	<b>Experimental Appendix.....</b>	<b>97</b>

## 4.1 Experimental techniques

### 4.1.1 Materials

Commercially available chemicals were purchased from Sigma-Aldrich or Acros Organics/Fisher Scientific and solvents were used without further purification. Anhydrous dichloromethane was obtained by distillation over calcium hydride under nitrogen atmosphere. Anhydrous *N,N*-dimethylformamide was received from Aldrich. All reactions involving air/moisture sensitive reagents were performed in oven-dried, under a nitrogen atmosphere. TLC analysis refers to analytical thin layer chromatography, using aluminum-backed plates coated with Merck Kieselgel 60 GF254. Product spots were viewed by the quenching of UV fluorescence. Flash chromatography was performed on silica gel 60A (35-70 micron) chromatography grade (Fisher Scientific).

### 4.1.2 Instruments

#### Melting Point

Melting points were recorded using a Gallenkamp Melting Point Apparatus.

#### Infra Red spectra (IR)

Infrared spectra were recorded in the range 4000-600  $\text{cm}^{-1}$  using a Perkin-Elmer 1600 series FTIR instrument either as a thin film or as a nujol mull between sodium chloride plates. All absorptions are quoted in  $\text{cm}^{-1}$ .

#### Nuclear Magnetic Resonance (NMR)

$^1\text{H}$  and  $^{13}\text{C}$  NMR spectra were recorded in  $\text{DMSO-d}_6$  (unless otherwise stated) using an Avance Bruker DPX 400 instrument (400 MHz) or an Avance Bruker DPX 500 (500 MHz). All chemical shifts reported in ( $\delta$ , ppm) with referenced to (TMS,  $\delta$  0.0).

### **Mass spectrometry**

Low-resolution mass spectrometric data were determined using a Fisons VG Platform II quadrupole instrument using electrospray ionisation (ES) unless otherwise stated. High-resolution mass spectrometric data were obtained in electrospray (ES) mode unless otherwise reported, on a Waters Q-TOF micromass spectrometer. Matrix Assisted Laser Desorption - time of flight Mass Spectrometry (MALDI-TOF) is available using a Waters Maldi Micro MX research grade instrument.

### **Elemental analyses**

Elemental analyses were obtained from University of Warwick Analytical Service facility. CHN Analysis CE440 Elemental Analyser, Bromine is analysed using classical oxygen flask methods. The methods have been fully developed to allow for interference correction from other elements including mixed halogens.

### **Ultra Violet (UV)**

Absorption spectra were recorded on a JASCO (V-570) UV/Vis/NIR spectrophotometer.

### **Luminescence fluorometer**

Fluorescence emission spectra were measured in the range 200-900  $\text{cm}^{-1}$  with a Perkin-Elmer (LS 55 precisely) Luminescence spectrometer.

### **High Performance Liquid Chromatography (HPLC)**

HPLC (UVD 170U) used for separation, column [250 X 10.00 nm, 10 micro – Silica C<sub>18</sub>].

Compounds **FC2 G0.5, G1.5, G2.5** were purified by preparative HPLC according to the following setup programme for Pharmacokinetic studies.

	Time	%CH <sub>3</sub> CN	TFA (0.02%)	H <sub>2</sub> O
1	0.00	4.0	1.0	95
2	5.00	4.0	1.0	95
3	12.00	98.0	1.0	1.0
4	14.00	98.0	1.0	1.0
5	16.00	4.0	1.0	95

Compounds **FC2 G0, G1, G2** were purified by preparative HPLC according to the following setup programme for DNA binding studies.

	Time	%MeOH	TFA (0.02%)	H <sub>2</sub> O
1	0.00	4.0	1.0	95
2	5.00	4.0	1.0	95
3	12.00	98.0	1.0	1.0
4	18.00	98.0	1.0	1.0
5	20.00	4.0	1.0	95

## 4.2. General experimental procedures

### 4.2.1. Photoluminescence study procedures

#### 4.2.1.1. Quantum yield determination

The compounds under study were prepared as solutions in DMF at concentrations that give a UV absorbance value of 0.7. The fluorescence quantum yields of the compounds were measured according to the comparative method of Williams et al.<sup>[230]</sup> which involves the use of well characterised standard samples with known fluorescence quantum yield ( $\Phi_F$ ) values. Using 2-aminopyridine as the reference compound ( $\Phi_F = 60 \times 10^{-2}$  in 0.1M H<sub>2</sub>SO<sub>4</sub>)<sup>[231]</sup> for compound **CF2** and fluorescein as the reference compound ( $\Phi_F = 79 \times 10^{-2}$  in 0.1M NaOH)<sup>[232]</sup> for compounds **3, A3, B3, C3, C33**. Standard 10 mm path length fluorescence cuvette was used for running the fluorescence measurements with the concentration range never exceeding an effective

adsorption of 0.1 at the maximum excitation wavelength. In order to minimise re-absorption effects (Dhami et al.),<sup>[233]</sup> the fluorescence spectra of all compounds were determined under the same operation conditions and settings with 2.5 slit widths. Fluorescence quantum yields were determined by comparing the integral areas of the fluorescence emission for the different compounds.

#### 4.2.1.2 pH measurements

For the first sample, the pH was lowered below 1 and fluorescent spectra were collected approximately every 1 pH unit until the pH reached around 13. pH adjustments were made using NaOH and HCl 0.1M (Merck) to avoid possible fluorescent interference from buffers. To decrease the dilution problem, small amounts of concentrated NaOH and HCl were spiked. The volume of the samples was 20 mL and the additions never exceeded 100  $\mu$ L, which represents <1% of the initial volume.<sup>[234]</sup>

#### 4.2.1.3 Fluorescent measurements

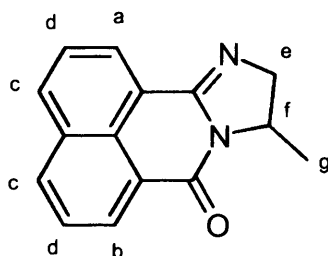
The samples were run on a Perkin-Elmer LS50B Luminescence Spectrometer connected to a personal computer and fitted with a xenon lamp with 20 kW pulses for 8 ms duration. The quartz cell can contain 3mL of sample. Fifty individual emission spectra were collected at excitation wavelengths 5 nm apart between 200 and 450 nm, and emission wavelengths ranging from 300 to 600 nm. The scanning speed was selected at 500 nm min<sup>-1</sup>, and band pass widths were 15 nm for excitation and emission. Fluorescence emission intensities were done in arbitrary units and always automatically corrected by the measurement system for variations in the excitation lamp spectral profile and any temporal intensity variation. Fluorescence

measurements were made at a regulated temperature, 231°C, because fluorescence is temperature-dependent.<sup>[234]</sup>

## 4.3. Experimental procedures

### 4.3.1. Organic synthesis procedures

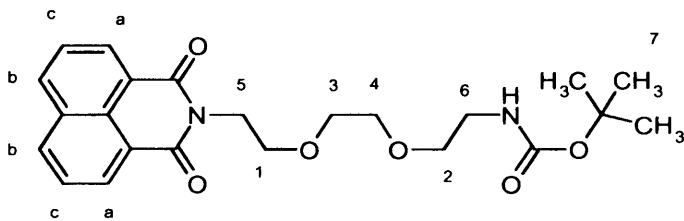
2-(1-aminopropan-2-yl)-1H-benzo[de]isoquinoline-1,3(2H)-dione [CF2].



1,8-Naphthalic anhydride [1] (4.80 g, 24 mmol) was added in portions to a solution of 1,2-propanediamine (2.45 mL, 28.8 mmol) in EtOH (250 mL) and the mixture was heated at reflux for 8 h. The mixture was filtered under partial vacuum and the filtrate was evaporated under reduced pressure. The residue was purified by flash column chromatography [CHCl<sub>3</sub>, MeOH, (10 : 0.1)] followed by HPLC (eluent: MeOH, H<sub>2</sub>O; 90:10) to yield [CF2] as a bright yellow oil (3.27 g, 53%). UV ( $\lambda_{\text{max}}$ , nm): 432 (DMF); IR (Neat NaCl, cm<sup>-1</sup>): 3059, 2968, 2921, 1668, 1629, 1595; <sup>1</sup>H-NMR (500 MHz; CDCl<sub>3</sub>):  $\delta$  8.37 (d, 1H<sub>a</sub>,  $J$  = 7.2 Hz), 8.28 (d, H<sub>b</sub>,  $J$  = 7.2 Hz), 7.93 (d, 2H<sub>c</sub>,  $J$  = 7.2 Hz), 7.51 (t, 2H<sub>d</sub>), 4.38 (m, 2H<sub>e</sub>), 4.12 (t, 1H<sub>f</sub>), 1.32 (d, 3H<sub>g</sub>); <sup>13</sup>C-NMR (125 MHz; CDCl<sub>3</sub>):  $\delta$  160.3 (C=O), 153.3 (C), 132.8 (CH), 132.1 (CH), 131.6 (CH), 129.0 (C), 128.4 (CH), 126.7 (C), 126.5 (CH), 126.4 (CH), 124.3 (CH), 120.9 (C), 61.0 (CH<sub>2</sub>), 50.6 (CH), 22.2 (Me); Anal. Calcd for (C<sub>15</sub>H<sub>12</sub>N<sub>2</sub>O): C, 76.25; H, 5.12; N,

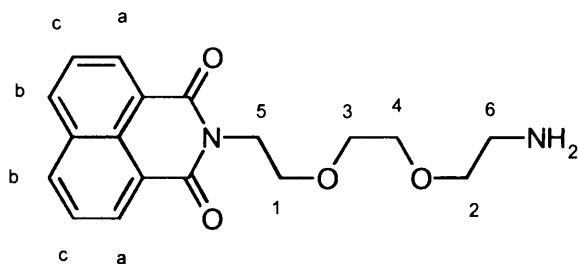
11.20. Found: C, 75.97; H, 4.83; N, 11.13; **HRMS** (EI+):  $m/z = 235.9801$  ( $M^+$ , 100%).

**tert-butyl 2-(2-(2-(1,3-dioxo-1H benzo[de]isoquinolin-2(3H)yl)ethoxy)ethoxy)ethylcarbamate [CF3 Boc].**



1,8-Naphthalic anhydride [**1**] (1.00 g, 5 mmol) was added in portions to a solution of *tert*-butyl 2-(2-(2-aminoethoxy)ethoxy)ethylcarbamate [**Boc NH**] (1.55 g, 6.25 mmol) in EtOH (30 mL) and the mixture was heated at 80 °C for 1 h. The mixture was filtered under vacuum and the filtrate was evaporated under reduced pressure. The residue was purified by flash column chromatography [toluene, acetone, (10 : 0.5)] to give [**CF3 Boc**] as a pale yellow oil (1.78 g, 83%). **IR** (Neat NaCl,  $\text{cm}^{-1}$ ): 3374, 3063, 2973, 2928, 1701, 1663, 1590, 1236;  **$^1\text{H-NMR}$**  (400 MHz;  $\text{CDCl}_3$ ):  $\delta$  8.39 (d, 2H<sub>a</sub>,  $J = 7.3$  Hz), 7.98 (d, 2H<sub>b</sub>,  $J = 7.3$  Hz), 7.53 (t, 2H<sub>c</sub>,  $J = 7.3$  Hz), 5.02 (s, 1H), 4.29 (t, 2H<sub>1</sub>), 3.71 (t, 2H<sub>2</sub>), 3.58 (t, 2H<sub>3</sub>), 3.49 (t, 2H<sub>4</sub>), 3.36 (t, 2H<sub>5</sub>), 3.12 (t, 2H<sub>6</sub>) 1.30 (s, 9H<sub>7</sub>);  **$^{13}\text{C-NMR}$**  (100 MHz;  $\text{CDCl}_3$ ):  $\delta$  164.1 (C=O), 156.0 (CONH), 133.9 (CH), 131.1 (CH), 129.0 (CH), 128.2 (C), 126.8 (C), 125.3 (C), 79.0 (C), 70.2 (CH<sub>2</sub>), 68.0 (CH<sub>2</sub>), 40.4 (CH<sub>2</sub>), 39.0 (CH<sub>2</sub>), 28.4 (Me); **Anal. Calcd** for ( $\text{C}_{23}\text{H}_{28}\text{N}_2\text{O}_6$ ): C, 64.47; H, 6.59; N, 6.54. Found: C, 64.47; H, 6.64; N, 6.53; **HRMS** (ES+):  $m/z = 429.2046$  ( $M + \text{H}^+$ , 100%), 446.2456 ( $M + \text{NH}_4^+$ , 43%).

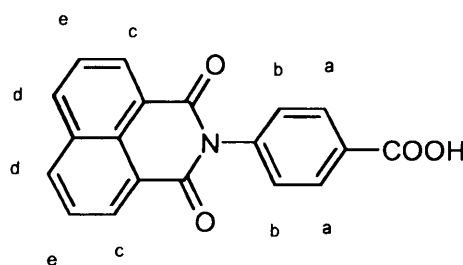
**2-(2-(2-(2-aminoethoxy)ethoxy)ethyl)-1H-benzo[de]isoquinoline-1,3(2H)-dione [CF3].**



A solution of [CF3 Boc] (9.50 g, 22.1 mmol) in dichloromethane (15 mL) was added dropwise to trifluoroacetic acid (15 mL) at 0 °C. The reaction was allowed to warm to room temperature and stirred for 2 h under a nitrogen atmosphere, then the solvent was evaporated under reduced pressure. The residue was dissolved in an aqueous solution of potassium carbonate and extracted with dichloromethane (3 × 200 mL). The combined organic layers were dried with magnesium sulfate, filtered and evaporated under reduced pressure. The residue was purified by flash column chromatography [CHCl<sub>3</sub> : MeOH : NH<sub>3</sub> (9 : 1 : 0.1)] to afford [CF3] as a pale brown oil (7.00 g, 98%). **UV** ( $\lambda_{max}$ , nm): 383 (DMF); **IR** (Neat NaCl, cm<sup>-1</sup>): 3373, 3313, 3061, 2869, 1698, 1660, 1587, 1113; **<sup>1</sup>H-NMR** (400 MHz; CDCl<sub>3</sub>):  $\delta$  8.25 (d, 2H<sub>a</sub>,  $J$  = 7.1 Hz), 7.90 (d, 2H<sub>b</sub>,  $J$  = 7.1 Hz), 7.42 (t, 2H<sub>c</sub>,  $J$  = 7.1 Hz), 4.17 (t, 2H<sub>1</sub>), 3.58 (t, 2H<sub>2</sub>), 3.48 (t, 2H<sub>3</sub>), 3.32 (t, 2H<sub>4</sub>), 3.19 (t, 2H<sub>5</sub>), 2.51 (t, 2H<sub>6</sub>) 1.06 (s, 2H); **<sup>13</sup>C-NMR** (100 MHz; CDCl<sub>3</sub>):  $\delta$  164.0 (C=O), 133.8 (CH), 131.3 (CH), 131.0 (CH), 127.9 (C), 126.8 (C), 122.3 (C), 73.4 (CH<sub>2</sub>), 70.2 (CH<sub>2</sub>), 67.8 (CH<sub>2</sub>), 41.7 (CH<sub>2</sub>), 38.9 (CH<sub>2</sub>); **Anal. Calcd** for (C<sub>18</sub>H<sub>20</sub>N<sub>2</sub>O<sub>4</sub>): C, 65.84; H, 6.14; N, 8.53. Found: C, 65.73; H, 6.03; N, 8.21; **HRMS** (EI<sup>+</sup>):  $m/z$  = 328.1425 (M<sup>+</sup>, 81%), 329.1537 (M+H<sup>+</sup>, 17%).

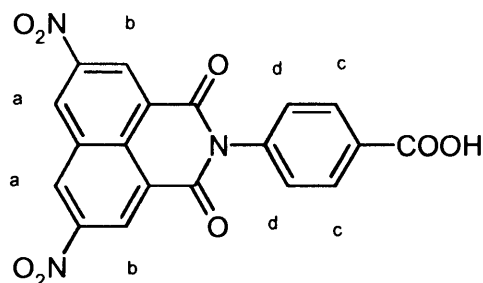
**General procedure (A) for synthesis of naphthalimide derivatives.**

To a stirred solution of naphthalic anhydride derivative (1 equiv.) in glacial acetic acid was added, under an N<sub>2</sub> atmosphere, the primary amine derivative (1 equiv.) and sodium acetate (3 equiv.). The reaction mixture was brought to reflux and the reaction's progress was monitored by TLC (CH<sub>2</sub>Cl<sub>2</sub>:MeOH:AcOH; 9:1:0.1). The resulting precipitate was collected by hot filtration, washed with hot glacial acetic acid then with hot distilled water. The final products were dried in vacuum for 24 h.

**4-(1,3-dioxo-1H,3H-benzo[de]isoquinolin-2-yl)-benzoic acid [A1].**

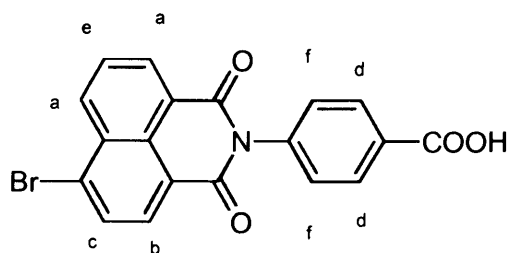
Following general procedure (A), 1,8-naphthalic anhydride **[1]** (1.98 g, 10 mmol), 4-aminobenzoic acid (1.37 g, 10 mmol) and AcONa (2.48 g, 30 mmol) were reacted in glacial acetic acid (60 mL) to afford **[A1]** as a off-white solid that was used without further purification (2.91 g, 92%). **mp**: > 300 °C; **UV** ( $\lambda_{max}$ , nm): 383 (DMF); **IR** (KBr, cm<sup>-1</sup>): 3404, 3113, 1713, 1675, 1654, 1587, 1237; **<sup>1</sup>H-NMR** (400 MHz; DMSO-d<sub>6</sub>):  $\delta$  8.52 (d, 2H<sub>a</sub>, *J* = 2.7 Hz), 8.50 (d, 2H<sub>b</sub>, *J* = 2.7 Hz), 8.10. (d, 2H<sub>c</sub>, *J* = 7.7 Hz), 7.91 (t, 2H<sub>d</sub>, *J* = 7.7 Hz), 7.55 (t, 2H<sub>e</sub>); **<sup>13</sup>C-NMR** (100 MHz; DMSO-d<sub>6</sub>):  $\delta$  166.8 (COO), 163.5 (C=O), 140.1(C), 134.5 (CH), 131.4 (CH), 130.7 (CH), 130.6 (CH), 129.8 (C), 129.5 (C), 127.8 (C), 127.2 (CH), 122.4 (C); **Anal. Calcd** for (C<sub>19</sub>H<sub>11</sub>NO<sub>4</sub>): C, 71.92; H, 3.49; N, 4.41. Found: C, 71.48; H, 3.40; N, 4.30; **HRMS** (ES<sup>+</sup>): *m/z* = 316.0552 (M-H<sup>+</sup>, 100%).

## 4-(5,8-dinitro-1,3-dioxo-1H,3H-benzo[de]isoquinolin-2-yl)-benzoic acid [A2].



Following general procedure (A), 3,6-dinitro-1,8-naphthalic anhydride [2] (2.88 g, 10 mmol), 4-aminobenzoic acid (1.37 g, 10 mmol) and AcONa (2.48 g, 30 mmol) were reacted in glacial acetic acid (60 mL) to afford [A2] as a bright yellow solid that was used without further purification (3.78 g, 93%). **mp:** > 300 °C; **UV** ( $\lambda_{\max}$ , nm): 341 (DMF); **IR** (KBr,  $\text{cm}^{-1}$ ): 3413, 3075, 1714, 1675, 1663, 1609, 1522, 1342;  **$^1\text{H-NMR}$**  (400 MHz; DMSO- $d_6$ ):  $\delta$  9.75 (d, 2H<sub>a</sub>,  $J = 2.0$  Hz), 9.06 (d, 2H<sub>b</sub>,  $J = 2.0$  Hz), 8.09 (d, 2H<sub>c</sub>,  $J = 8.3$  Hz), 7.54 (d, 2H<sub>d</sub>,  $J = 8.3$  Hz);  **$^{13}\text{C-NMR}$**  (100 MHz; DMSO- $d_6$ ):  $\delta$  166.7 (COO), 161.7 (C=O), 147.1 (C-NO<sub>2</sub>), 147.0 (CH), 139.1 (C), 131.8 (CH), 131.5 (CH), 129.1 (C), 127.6 (C), 125.7 (C), 125.0 (CH); **Anal. Calcd** for (C<sub>19</sub>H<sub>9</sub>N<sub>3</sub>O<sub>8</sub>): C, 56.03; H, 2.23; N, 10.32. Found: C, 55.98; H, 2.06; N, 10.01; **HRMS** (EI<sup>+</sup>):  $m/z = 407.0391$  (M<sup>+</sup>, 100%).

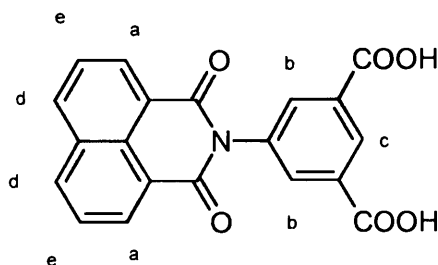
## 4-(6-bromo-1,3-dioxo-1H-benzo[de]isoquinolin-2(3H)-yl)benzoic acid [A4].



Following general procedure (A), 4-bromo-1,8-naphthalic anhydride [4] (2.77 g, 10 mmol), 4-aminobenzoic acid (1.37 g, 10 mmol) and AcONa (2.48 g, 30 mmol) were

reacted in glacial acetic acid (60 mL) to afford **[A4]** as a pale yellow solid that was used without further purification (2.69 g, 68%). **mp**: above 300 °C; **UV** ( $\lambda_{max}$ , nm): 402 (DMF); **IR** (KBr,  $\text{cm}^{-1}$ ): 3418, 3070, 1710, 1681, 1607, 1610, 551;  **$^1\text{H-NMR}$**  (500 MHz; DMSO- $d_6$ ):  $\delta$  8.54 (m, 2H<sub>a</sub>), 8.30 (d, 1H<sub>b</sub>,  $J = 7.8$  Hz), 8.20 (d, 1H<sub>c</sub>,  $J = 7.8$  Hz), 8.10 (d, 2H<sub>d</sub>,  $J = 8.3$  Hz), 7.99 (t, 1H<sub>e</sub>,  $J = 7.2$  Hz), 7.55 (d, 2H<sub>f</sub>,  $J = 8.3$  Hz);  **$^{13}\text{C-NMR}$**  (125 MHz; DMSO- $d_6$ ):  $\delta$  166.8 (COO), 162.9 (C=O), 139.7 (C), 132.7 (CH), 131.5 (CH), 131.3 (CH), 130.9 (C-Br), 130.8 (CH), 129.8 (CH), 129.3 (C), 128.7 (C), 128.6 (C), 123.1 (CH), 122.3 (C); **Anal. Calcd** for (C<sub>19</sub>H<sub>10</sub>BrNO<sub>4</sub>): C, 57.60; H, 2.54; Br, 20.17; N, 3.54. Found: C, 57.33; H, 2.44; Br, 19.80; N, 3.44; **HRMS** (EI<sup>+</sup>):  $m/z = 393.9583$  (M<sup>71+</sup>, 100%),  $395.9583$  (M<sup>81+</sup>, 98%).

#### 5-(1,3-dioxo-1H,3H-benzo[de]isoquinolin-2-yl)-isophthalic acid **[B1]**.

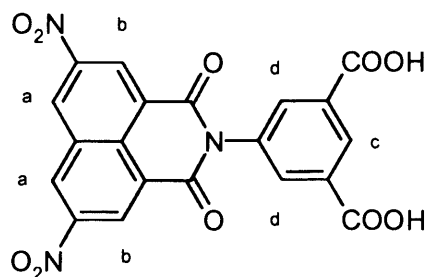


Following general procedure (A), 1,8-naphthalic anhydride **[1]** (1.98 g, 10 mmol), 5-aminoisophthalic acid (1.81 g, 10 mmol) and AcONa (2.48 g, 30 mmol) were reacted in glacial acetic acid (60 mL) to afford **[B1]** as an off-white solid that was used without further purification (2.93 g, 92%). **mp**: > 300 °C; **UV** ( $\lambda_{max}$ , nm): 410 (DMF); **IR** (KBr,  $\text{cm}^{-1}$ ): 3440, 3071, 1770, 1698, 1626, 1587;  **$^1\text{H-NMR}$**  (400 MHz; DMSO- $d_6$ ):  $\delta$  8.55 (d, 2H<sub>a</sub>,  $J = 6.2$  Hz), 8.52 (s, 2H<sub>b</sub>), 8.50 (s, 1H<sub>c</sub>), 7.92 (d, 2H<sub>d</sub>,  $J = 6.2$  Hz), 7.85 (t, 2H<sub>e</sub>);  **$^{13}\text{C-NMR}$**  (100 MHz; DMSO- $d_6$ ):  $\delta$  169.2 (COO), 164.0 (C=O), 140.4 (CH), 136.9 (CH), 134.8 (C), 132.3 (C), 131.7 (CH), 128.2 (C), 127.5 (CH), 125.1

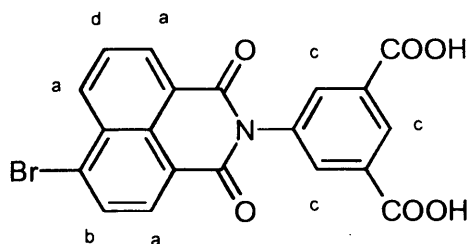
(C), 122.9 (CH), 114.6 (C); **Anal. Calcd** for (C<sub>20</sub>H<sub>11</sub>NO<sub>6</sub>): C, 66.44; H, 3.07; N, 3.88.

Found: C, 66.17; H, 3.15; N, 3.43; **HRMS** (EI+):  $m/z = 361.0585$  (M<sup>+</sup>, 64%).

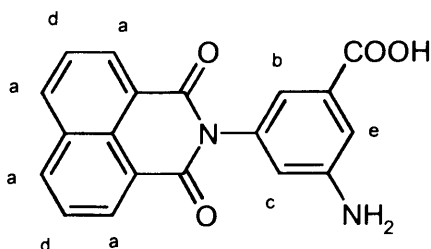
**5-(5,8-dinitro-1,3-dioxo-1H,3H-benzo[de]isoquinolin-2-yl)-isophthalic acid [B2].**



Following general procedure (A), 3,6-dinitro-1,8-naphthalic anhydride [2] (2.88 g, 10 mmol), 5-aminoisophthalic acid (1.81 g, 10 mmol) and AcONa (2.48 g, 30 mmol) were reacted in glacial acetic acid (60 mL) to afford [B2] as a pale yellow solid that was used without further purification (4.28 g, 95%). **mp**: > 300 °C; **UV** ( $\lambda_{\max}$ , nm): 419 (DMF); **IR** (KBr, cm<sup>-1</sup>): 3439, 3073, 1706, 1680, 1678, 1611, 1539, 1345; **<sup>1</sup>H-NMR** (400 MHz; DMSO-d<sub>6</sub>):  $\delta$  9.83 (d, 2H<sub>a</sub>,  $J = 1.9$  Hz), 9.09 (d, 2H<sub>b</sub>,  $J = 1.9$  Hz), 8.58 (s, 1H<sub>c</sub>), 8.27 (s, 2H<sub>d</sub>); **<sup>13</sup>C-NMR** (100 MHz; DMSO-d<sub>6</sub>):  $\delta$  165.8 (COO), 161.9 (C=O), 147.0 (C-NO<sub>2</sub>), 136.0 (CH), 134.1 (CH), 132.3 (C), 131.9 (C), 131.5 (C), 130.7 (C), 130.0 (C), 125.6 (CH), 125.2 (CH); **Anal. Calcd** for (C<sub>20</sub>H<sub>9</sub>N<sub>3</sub>O<sub>10</sub>): C, 53.23; H, 2.01; N, 9.31. Found: C, 52.92; H, 2.51; N, 9.14; **HRMS** (EI+):  $m/z = 451.0290$  (M<sup>+</sup>, 6%).

**5-(6-bromo-1,3-dioxo-1H-benzo[de]isoquinolin-2(3H)-yl)isophthalic acid [B4].**

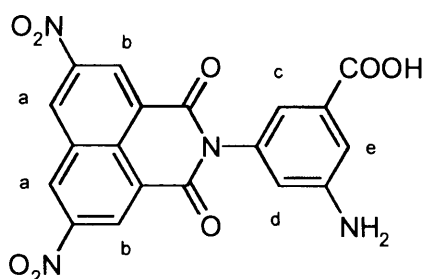
Following general procedure (A), 4-bromo-1,8-naphthalic anhydride **[4]** (2.77 g, 10 mmol), 5-aminoisophthalic acid (1.81 g, 10 mmol) and AcONa (2.48 g, 30 mmol) were reacted in glacial acetic acid (60 mL) to afford **[B4]** as a pale yellow solid that was used without further purification (3.74 g, 85%). **mp:** > 300 °C, **UV** ( $\lambda_{max}$ , nm): 408 (DMF), **IR** (KBr,  $\text{cm}^{-1}$ ): 3392, 3086, 1713, 1670, 1585, 1610, 688;  **$^1\text{H-NMR}$**  (400 MHz; DMSO- $d_6$ ):  $\delta$  8.60 (m, 3H<sub>a</sub>), 8.35 (d, 1H<sub>b</sub>,  $J = 7.7$  Hz), 8.29 (m, 3H<sub>c</sub>), 8.03 (t, 1H<sub>d</sub>,  $J = 7.7$  Hz);  **$^{13}\text{C-NMR}$**  (125 MHz; DMSO- $d_6$ ):  $\delta$  166.0 (COO), 163.1 (C=O), 136.5 (C), 134.3 (CH), 132.7 (C), 132.1 (C-Br), 131.5 (CH), 130.8 (C), 129.7 (C), 129.2 (CH), 128.7 (C), 123.4 (CH), 122.6 (C); **Anal. Calcd** for (C<sub>20</sub>H<sub>10</sub> BrNO<sub>6</sub>): C, 54.57; H, 2.29; Br, 18.15; N, 3.18. Found: C, 54.67; H, 2.33; Br, 18.31; N, 3.25; **HRMS** (EI<sup>+</sup>):  $m/z = 438.9684$  (M<sup>71+</sup>, 78%), 440.9741 (M<sup>81+</sup>, 76%).

**3-amino-5-(1,3-dioxo-1H,3H-benzo[de]isoquinolin-2-yl)-benzoic acid [C1].**

Following general procedure (A), 1,8-naphthalic anhydride **[1]** (1.98 g, 10 mmol), 3,5-diaminobenzoic acid (1.52 g, 10 mmol) and AcONa (2.48 g, 30 mmol) were reacted in glacial acetic acid (60 mL). The residue was purified by flash column

chromatography ( $\text{CHCl}_3$  : MeOH :  $\text{NH}_3$ ; 9 : 1 : 0.1) to afford [C1] as an off-white solid (1.42 g, 43%). **mp**: above 300 °C; **UV** ( $\lambda_{\text{max}}$ , nm): 422 (DMF); **IR** (KBr,  $\text{cm}^{-1}$ ): 3472, 3317, 3125, 1731, 1705, 1663, 1613, 1236;  **$^1\text{H-NMR}$**  (400 MHz; DMSO- $d_6$ ):  $\delta$  10.31 (s, 1H), 8.52 (m, 4H<sub>a</sub>), 8.22 (s, 1H<sub>b</sub>), 7.92 (s, 1H<sub>c</sub>), 7.85 (t, 2H<sub>d</sub>), 7.67 (s, 1H<sub>e</sub>);  **$^{13}\text{C-NMR}$**  (100 MHz; DMSO- $d_6$ ):  $\delta$  166.8 (COO), 166.4 (C=O), 164.1 (C-NH<sub>2</sub>), 137.2 (CH), 134.9 (C), 134.8 (C), 132.5 (C), 131.8 (C), 131.1 (C), 27.5 (CH), 123.7 (CH), 123.0 (CH); **Anal. Calcd** for (C<sub>19</sub>H<sub>12</sub>N<sub>2</sub>O<sub>2</sub>): C, 68.67; H, 3.64; N, 8.43. Found: C, 68.64; H, 3.60; N, 8.65; **HRMS** (EI<sup>+</sup>):  $m/z$  = 332.0800 ( $M^+$ , 100%).

**3-amino-5-(5,8-dinitro-1,3-dioxo-1H,3H-benzo[de]isoquinolin-2-yl)-benzoic acid [C2].**

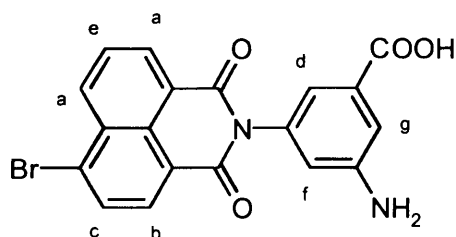


Following general procedure (A), 3,6-dinitro-1,8-naphthalic anhydride [2] (2.88 g, 10 mmol), 3,5-diaminobenzoic acid (1.52 g, 10 mmol) and AcONa (2.48 g, 30 mmol) were reacted in glacial acetic acid (60 mL). The residue was purified by flash column chromatography ( $\text{CHCl}_3$  : MeOH :  $\text{NH}_3$ ; 9 : 1 : 0.1) to afford [C2] as a pale brown solid (0.50 g, 12%). **mp**: > 300 °C; **UV** ( $\lambda_{\text{max}}$ , nm): 455 (DMF); **IR** (KBr,  $\text{cm}^{-1}$ ): 3368, 3077, 1720, 1676, 1633, 1577, 1413, 1336;  **$^1\text{H-NMR}$**  (500 MHz; DMSO- $d_6$ ):  $\delta$  10.21 (s, 1H), 9.81 (d, 2H<sub>a</sub>,  $J$  = 2.1 Hz), 9.08 (d, 2H<sub>b</sub>,  $J$  = 2.1 Hz), 8.02 (s, 1H<sub>c</sub>), 7.99 (s, 1H<sub>d</sub>), 7.58 (s, 1H<sub>e</sub>), 2.08 (s, 2H);  **$^{13}\text{C-NMR}$**  (125 MHz; DMSO- $d_6$ ):  $\delta$  171.9 (COO), 168.7 (C=O), 166.4 (C=O), 166.0 (C-NO<sub>2</sub>), 161.8 (C-NH<sub>2</sub>), 147.0 (C), 146.9 (CH), 140.0 (CH), 133.9 (C), 131.9 (C), 130.6 (C), 125.7 (C), 124.2 (CH), 123.2 (C), 119.6

(C); **Anal. Calcd** for (C<sub>19</sub>H<sub>10</sub>N<sub>4</sub>O<sub>8</sub>): C, 54.04; H, 2.39; N, 13.27. Found: C, 54.37; H, 2.75; N, 13.57; **HRMS** (EI<sup>+</sup>):  $m/z = 422.0489$  (M<sup>+</sup>, 100%).

### 3-amino-5-(6-bromo-1,3-dioxo-1H-benzo[de]isoquinolin-2(3H)-yl)benzoic acid

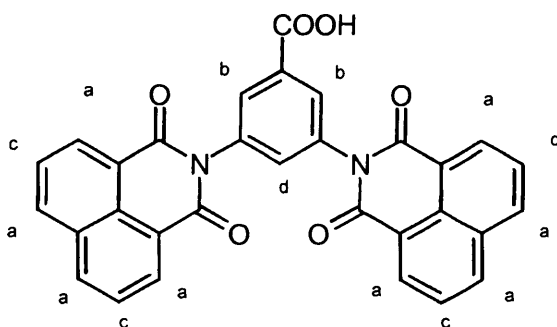
[C4].



Following general procedure (A) 4-bromo-1,8-naphthalic anhydride **[4]** (2.77 g, 10 mmol), 3,5-diaminobenzoic acid (1.52 g, 10 mmol) and AcONa (2.48 g, 30 mmol) were reacted in glacial acetic acid (60 mL). The residue was purified by flash column chromatography (CHCl<sub>3</sub> : MeOH : NH<sub>3</sub>; 9 : 1 : 0.1) to afford **[C4]** as a deep yellow solid (0.45 g, 11%). **mp**: > 300 °C; **UV** ( $\lambda_{\text{max}}$ , nm): 428 (DMF); **IR** (KBr, cm<sup>-1</sup>): 3445, 3337, 3076, 1728, 1707, 1669, 1613, 872; **<sup>1</sup>H-NMR** (400 MHz; DMSO-d<sub>6</sub>):  $\delta$  10.05 (s, 1H), 8.60 (m, 2H<sub>a</sub>), 8.37 (d, 1H<sub>b</sub>,  $J = 7.8$  Hz), 8.28 (d, 1H<sub>c</sub>,  $J = 7.8$  Hz), 8.09 (s, 1H<sub>d</sub>), 8.04 (t, 1H<sub>e</sub>), 7.81 (s, 1H<sub>f</sub>), 7.52 (s, 1H<sub>g</sub>), 2.05 (s, 2H); **<sup>13</sup>C-NMR** (100 MHz; DMSO-d<sub>6</sub>):  $\delta$  168.7 (COO), 166.5 (C=O), 163.0 (C), 140.0 (CH), 136.2 (CH), 132.7 (C), 131.95 (CH), 131.5 (C-Br), 131.3 (C), 130.8 (CH), 129.8 (C), 129.1 (C), 128.8 (C), 124.6 (C), 123.5 (CH), 122.6 (CH), 119.5 (CH); **Anal. Calcd** for (C<sub>19</sub>H<sub>11</sub>BrN<sub>2</sub>O<sub>4</sub>): C, 55.50; H, 2.70; Br, 19.43; N, 6.81. Found: C, 55.19; H, 2.93; Br, 19.31; N, 6.67; **HRMS** (EI<sup>+</sup>):  $m/z = 409.9912$  (M<sup>71+</sup>, 100%), 411.9868 (M<sup>81+</sup>, 98%).

**General procedure (B) for synthesis of naphthalimide derivatives.**

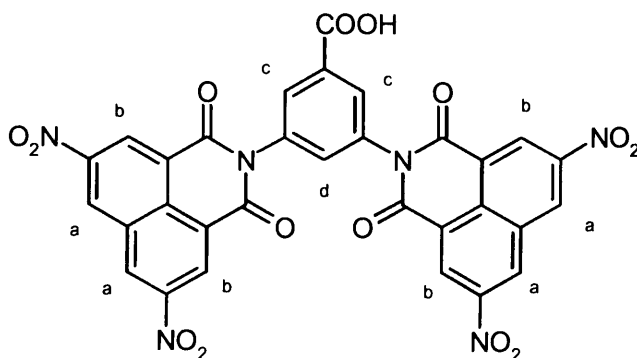
To a stirred solution of naphthalic anhydride derivative (2 equiv) in glacial acetic acid was added, under an N<sub>2</sub> atmosphere, the primary amine derivative (1 equiv.) and sodium acetate (6 equiv.). The reaction mixture was heated to reflux and the reaction progress was monitored by TLC (CH<sub>3</sub>Cl : MeOH : AcOH; 9 : 1 : 0.1). The resulting precipitate was collected by hot filtration, washed with hot glacial acetic acid then with hot distilled water. The final products were dried in vacuum for 48 h.

**3,5-bis-(1,3-dioxo-1H,3H-benzo[de]isoquinolin-2-yl)- benzoic acid [C11].**

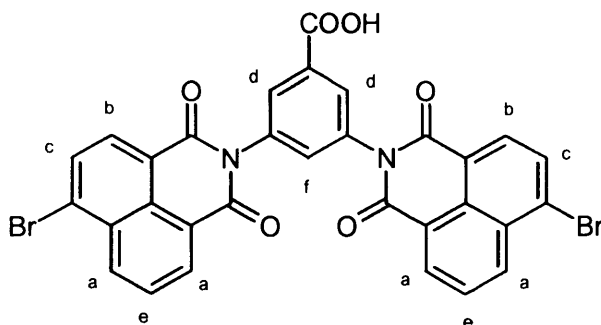
Following general procedure (B), 1,8-naphthalic anhydride [1] (3.96 g, 20 mmol), 3,5-diaminobenzoic acid (1.52 g, 10 mmol) and AcONa (4.96 g, 60 mmol) were reacted in glacial acetic acid (100 mL). The residue was purified by flash column chromatography (CHCl<sub>3</sub> : MeOH : NH<sub>3</sub>; 9 : 1 : 0.1) to afford [C11] as a pale yellow solid (3.84 g, 75%). **Mp** > 300 °C; **UV** ( $\lambda_{max}$ , nm): 405 (DMF); **IR** (KBr, cm<sup>-1</sup>): 3460, 3072, 1695, 1673, 1626, 1587; **<sup>1</sup>H-NMR** (400 MHz; DMSO-d<sub>6</sub>):  $\delta$  10.83 (s, 1H), 8.51 (m, 8H<sub>a</sub>), 8.23 (s, 2H<sub>b</sub>), 7.80 (m, 4H<sub>c</sub>), 7.54 (s, 1H<sub>d</sub>); **<sup>13</sup>C-NMR** (100 MHz; DMSO-d<sub>6</sub>):  $\delta$  172.0 (COO), 169.1 (C=O), 166.7 (C=O), 140.4 (CH), 137.0 (CH), 134.8 (C), 131.1 (C), 130.6 (CH), 127.6 (C), 125.1 (C), 124.0 (C), 122.9 (CH), 119.8 (CH);

**Anal. Calcd** for (C<sub>31</sub>H<sub>16</sub>N<sub>2</sub>O<sub>6</sub>): C, 72.66; H, 3.15; N, 5.47. Found: C, 72.60; H, 3.05; N, 5.77; **HRMS** (EI<sup>+</sup>):  $m/z = 512.1020$  (M<sup>+</sup>, 38%).

**3,5-bis-(5,8-dinitro-1,3-dioxo-1H,3H-benzo[de]isoquinolin-2-yl)-benzoic acid [C22].**



Following general procedure (B), 3,6-dinitro-1,8-naphthalic anhydride [2] (5.76 g, 20 mmol), 3,5-diaminobenzoic acid (1.52 g, 10 mmol) and AcONa (4.96 g, 60 mmol) were reacted in glacial acetic acid (100 mL). The residue was purified by flash column chromatography (CHCl<sub>3</sub> : MeOH : NH<sub>3</sub>; 9 : 1 : 0.1) to afford [C22] as a pale yellow solid (4.91 g, 71%). **mp**: > 300 °C; **UV** ( $\lambda_{\max}$ , nm): 342 (DMF); **IR** (KBr, cm<sup>-1</sup>): 3399, 3079, 1725, 1686, 1612, 1535, 1315; **<sup>1</sup>H-NMR** (400 MHz; DMSO-d<sub>6</sub>):  $\delta$  9.75 (s, 4H<sub>a</sub>), 9.12 (s, 4H<sub>b</sub>), 8.22 (s, 2H<sub>c</sub>), 7.82 (s, 1H<sub>d</sub>); **<sup>13</sup>C-NMR** (100 MHz; DMSO-d<sub>6</sub>):  $\delta$  172.0 (COO), 166.4 (C=O), 162.3 (C-NO<sub>2</sub>), 147.3 (CH), 136.3 (CH), 133.1 (C), 132.3 (C), 131.9 (C), 131.1 (C), 130.8 (C), 126.1 (CH), 125.4 (CH); **Anal. Calcd** for (C<sub>31</sub>H<sub>12</sub>N<sub>6</sub>O<sub>14</sub>): C, 53.77; H, 1.75; N, 12.14. Found: C, 53.48; H, 1.76; N, 11.74; **HRMS** (EI<sup>+</sup>):  $m/z = 692.0405$  (M<sup>+</sup>, 3%).

**3,5-bis(6-bromo-1,3-dioxo-1H-benzo[de]isoquinolin-2(3H)-yl)benzoic acid [C44].**

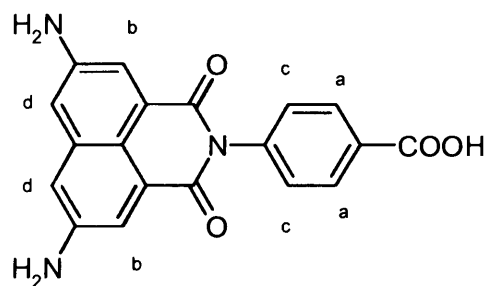
Following general procedure (B), 4-bromo-1,8-naphthalic anhydride **[4]** (5.54 g, 20 mmol), 3,5-diaminobenzoic acid (1.52 g, 10 mmol) and AcONa (4.96 g, 60 mmol) were reacted in glacial acetic acid (100 mL). The residue was purified by flash column chromatography (CHCl<sub>3</sub> : MeOH : NH<sub>3</sub>; 9 : 1 : 0.1) to afford **[C44]** as a bright yellow solid (4.49 g, 67%). **mp**: > 300 °C; **UV** ( $\lambda_{max}$ , nm): 401 (DMF); **IR** (KBr, cm<sup>-1</sup>): 3418, 3094, 1709, 1677, 1586, 672; **<sup>1</sup>H-NMR** (400 MHz; DMSO-d<sub>6</sub>):  $\delta$  8.61 (m, 4H<sub>a</sub>), 8.38 (d, 2H<sub>b</sub>,  $J = 7.9$  Hz), 8.28 (d, 2H<sub>c</sub>,  $J = 7.9$  Hz), 8.14 (s, 2H<sub>d</sub>), 8.03 (dd, 2H<sub>e</sub>,  $J = 7.5$ ,  $J = 0.8$  Hz), 7.73 (s, 1H<sub>f</sub>); **<sup>13</sup>C-NMR** (100 MHz; DMSO-d<sub>6</sub>):  $\delta$  168.6 (COO), 166.5 (C=O), 163.1 (C=O), 140.0 (CH), 136.3 (CH), 132.8 (CH), 131.6 (C), 131.3 (CH), 130.9 (C-Br), 130.3 (CH), 129.9 (C), 129.2 (C), 128.8 (C), 124.6 (C), 123.4 (CH), 122.6 (CH); **Anal. Calcd** for (C<sub>31</sub>H<sub>14</sub>BrN<sub>2</sub>O<sub>6</sub>): C, 55.55; H, 2.11; Br, 23.84; N, 4.18. Found: C, 54.98; H, 2.01; Br, 23.31; N, 4.19; **HRMS** (EI<sup>+</sup>):  $m/z =$  393.9831 (M<sup>79+</sup>, 100%), 395.9892 (M<sup>81+</sup>, 98%), 668.9410 (M<sup>158+</sup>, 18%), 669.9470 (M<sup>160+</sup>, 29%), 671.9366 (M<sup>162+</sup>, 16%).

**General procedure (C) for synthesis of naphthalimide derivatives.**

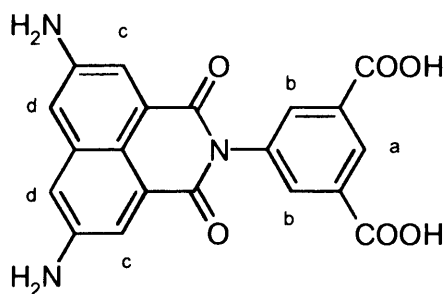
A mixture of 3,6-dinitro-1,8-naphthalimide derivative (0.339 mmol), Pb/C 10% (0.05 g) and DMF (30 mL) was hydrogenated using hydrogen contained in a balloon at room temperature with vigorous stirring from 16 - 24 h. The progress of the reaction

was monitored by TLC (CHCl<sub>3</sub>:MeOH:AcOH; 8:2:0.5). The catalyst was filtered off and the filtrate was poured into DCM (250 mL) with stirring. The solid precipitate was collected by filtration.

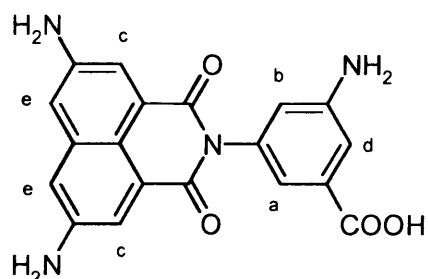
**4-(5,8-diamino-1,3-dioxo-1H,3H-benzo[de]isoquinolin-2-yl)-benzoic acid [A3].**



Following general procedure (C), [A2] (0.138 g, 0.339 mmol) and Pb/C 10% (0.05 g) were hydrogenated in DMF (30 mL) for 16 h to afford [A3] as a deep brown solid without further purification (0.10 g, 91%). **mp:** > 300 °C; **UV** ( $\lambda_{max}$ , nm): 518 (DMF); **IR** (KBr, cm<sup>-1</sup>): 3438, 3349, 3224, 3066, 1703, 1666, 1605; **<sup>1</sup>H-NMR** (400 MHz; DMSO-d<sub>6</sub>):  $\delta$  8.09 (d, 2H<sub>a</sub>,  $J$  = 8.5 Hz), 7.58 (d, 2H<sub>b</sub>,  $J$  = 2.0 Hz), 7.47 (d, 2H<sub>c</sub>,  $J$  = 8.5 Hz), 6.99 (d, 2H<sub>d</sub>,  $J$  = 2.0 Hz) 5.72 (br s, 4H); **<sup>13</sup>C-NMR** (100 MHz; DMSO-d<sub>6</sub>):  $\delta$  166.9 (COO), 164.2 (C=O), 162.2 (C-NH<sub>2</sub>), 147.6 (C), 140.4 (CH), 135.6 (C), 130.7 (C), 129.5 (CH), 122.6 (C), 117.0 (CH), 114.9 (CH), 109.9 (C); **Anal. Calcd** for (C<sub>19</sub>H<sub>13</sub>N<sub>3</sub>O<sub>4</sub>): C, 65.70; H, 3.77; N, 12.10. Found: C, 65.34; H, 4.20; N, 11.87; **HRMS** (ES<sup>+</sup>):  $m/z$  = 347.0905 (M<sup>+</sup>, 100%).

**5-(5,8-diamino-1,3-dioxo-1H,3H-benzo[de]isoquinolin-2-yl)-isophthalic acid [B3].**

Following general procedure (C), **[B2]** (0.153 g, 0.339 mmol) and Pb/C 10% (0.05 g) were hydrogenated in DMF (30 mL) for 16 h to afford **[B3]** as a yellowish brown solid that was used without further purification (0.12 g, 92%). **Mp** > 300 °C; **UV** ( $\lambda_{\text{max}}$ , nm): 518 (DMF); **IR** (KBr,  $\text{cm}^{-1}$ ): 3462, 3382, 3224, 3083, 1694, 1626, 1567; **<sup>1</sup>H-NMR** (500 MHz; DMSO- $d_6$ ):  $\delta$  8.51 (s, 1H<sub>a</sub>), 8.12 (s, 2H<sub>b</sub>), 7.60 (d, 2H<sub>c</sub>,  $J = 1.3$  Hz), 6.98 (d, 2H<sub>d</sub>,  $J = 1.3$  Hz) 5.5 (br s, 4H); **<sup>13</sup>C-NMR** (125 MHz; DMSO- $d_6$ ):  $\delta$  166.1 (COO), 164.1 (C=O), 162.2 (C-NH<sub>2</sub>), 147.5 (C), 140.4 (CH), 135.6 (C), 130.7 (CH), 129.5 (CH), 122.7 (C), 118.0 (CH), 114.9 (CH), 110.7 (C); **Anal. Calcd** for (C<sub>20</sub>H<sub>13</sub>N<sub>3</sub>O<sub>6</sub>): C, 61.38; H, 3.35; N, 10.74. Found: C, 61.17; H, 3.64; N, 11.10; **LRMS** (ES<sup>+</sup>):  $m/z = 391.34$  (M<sup>+</sup>, 19%).

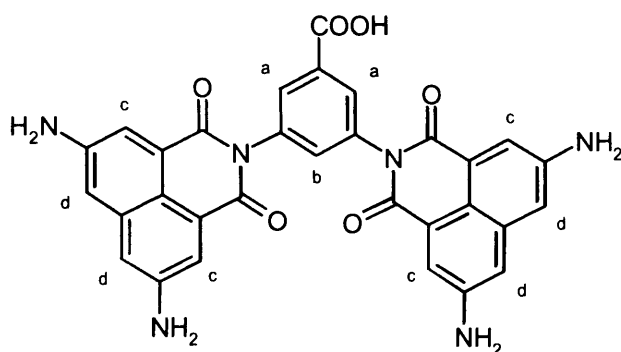
**3-amino-5-(5,8-diamino-1,3-dioxo-1H-benzo[de]isoquinolin-2(3H)-yl)benzoic acid [C3].**

Following general procedure (C), **[C2]** (0.143 g, 0.339 mmol) and Pb/C 10% (0.05 g) were hydrogenated in DMF (30 mL) for 24 h to afford **[C3]** as a yellow solid (0.11 g,

94%), after purification by flash chromatography (CHCl<sub>3</sub>:MeOH:AcOH; 8:2:0.5). **mp** > 300 °C; **UV** ( $\lambda_{max}$ , nm): 521 (DMF); **IR** (KBr, cm<sup>-1</sup>): 3459, 3365, 3228, 3092, 1697, 1657, 1625; **<sup>1</sup>H-NMR** (500 MHz; DMSO-d<sub>6</sub>):  $\delta$  8.24 (s, 1H<sub>a</sub>), 7.78. (s, 1H<sub>b</sub>), 7.60 (d, 2H<sub>c</sub>,  $J$  = 1.8 Hz), 7.58 (s, 1H<sub>d</sub>), 6.98 (d, 2H<sub>e</sub>,  $J$  = 1.8 Hz), 5.77 (br s, 6H); **<sup>13</sup>C-NMR** (125 MHz; DMSO-d<sub>6</sub>):  $\delta$  168.6 (COO), 164.0 (C=O), 147.6 (C-NH<sub>2</sub>), 139.9 (C-NH<sub>2</sub>), 136.7 (C), 135.6 (C), 124.6 (C), 123.4 (C), 122.6 (C), 122.6 (CH), 119.3 (CH), 117.0 (CH), 114.9 (C), 109.8 (CH); **Anal. Calcd** for (C<sub>19</sub>H<sub>14</sub>N<sub>4</sub>O<sub>4</sub>): C, 62.98; H, 3.89; N, 15.46. Found: C, 62.65 ; H, 3.95 ; N, 15.72 ; **HRMS** (EI<sup>+</sup>):  $m/z$  = 362.1026 (M<sup>+</sup>, 16%).

### 3,5-bis(5,8-diamino-1,3-dioxo-1H-benzo[de]isoquinolin-2(3H)-yl)benzoic acid

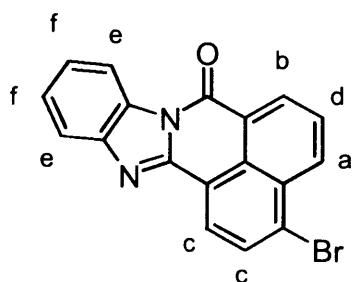
[C33].



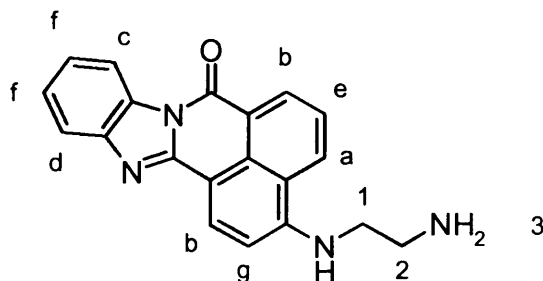
Following general procedure (C), [C22] (0.234 g, 0.339 mmol) and Pb/C 10% (0.10 g) were hydrogenated in DMF (60 mL) for 24 h to afford [C33] as a greenish yellow solid (0.17 g, 89%), after purification by flash chromatography (CHCl<sub>3</sub>:MeOH:AcOH; 8:2:0.5). **mp**: above 300 °C; **UV** ( $\lambda_{max}$ , nm): 518 (DMF); **IR** (KBr, cm<sup>-1</sup>): 3442, 3361, 3228, 3079, 1698, 1660, 1625; **<sup>1</sup>H-NMR** (500 MHz; DMSO-d<sub>6</sub>):  $\delta$  8.01 (s, 2H<sub>a</sub>), 7.63. (s, 1H<sub>b</sub>), 7.60 (d, 4H<sub>c</sub>,  $J$  = 1.7 Hz), 6.97 (d, 4H<sub>d</sub>,  $J$  = 1.7 Hz), 5.78 (s br, 8H); **<sup>13</sup>C-NMR** (125 MHz; DMSO-d<sub>6</sub>):  $\delta$  173.5 (COO), 166.3 (C=O), 164.0 (C=O), 147.6 (C-NH<sub>2</sub>), 136.9 (C), 135.6 (CH), 130.0 (C), 129.3 (C),

122.6 (CH), 120.3 (CH), 116.9 (CH), 114.9 (CH), 109.8 (C); **Anal. Calcd** for (C<sub>31</sub>H<sub>20</sub>N<sub>6</sub>O<sub>6</sub>): C, 65.03; H, 3.52; N, 14.68. Found: C, 64.90; H, 3.74; N, 14.95; **HRMS** (EI<sup>+</sup>):  $m/z = 572.3426$  (M<sup>+</sup>, 11%).

### 3-bromo-7H-benz[de]benzimidazo[2,1-a]isoquinoline-7-one. [FC2].



The mixture of 4-bromo-1,8-naphthalic anhydride (0.277 g, 0.001 mol) and *o*-phenylenediamine (0.2 g, 0.002 mol) was dissolved in acetic acid (50 mL). The resulting solution was allowed to reflux for 2 h, the mixture was cooled to room temperature, and then poured into distilled water to precipitate the product as a bright yellow powder. About (0.18 g, 54%) of [FC2] was obtained after twice recrystallised from toluen. **mp**: 253-254 °C according to Lit.;<sup>[199]</sup> **UV** ( $\lambda_{max}$ , nm): 390 (MeOH); **IR** (KBr, cm<sup>-1</sup>): 1696 (C=O), 746 (C-Br); **<sup>1</sup>H-NMR** (500 MHz; CDCl<sub>3</sub>):  $\delta$  8.86 (dd, 1H<sub>a</sub>,  $J = 1.4$  and 7.2 Hz), 8.68 (dd, 1H<sub>b</sub>,  $J = 1.4$  and 7.2 Hz), 8.56 (m, 2H<sub>c</sub>), 8.10 (t, 1H<sub>d</sub>), 7.91 (d, 2H<sub>e</sub>,  $J = 7.2$  Hz), 7.49 (t, 2H<sub>f</sub>); **<sup>13</sup>C-NMR** (125 MHz; CDCl<sub>3</sub>):  $\delta$  193.3 (C=O), 144.0 (C), 143.4(C), 141.3 (CH), 138.4 (C), 133.7 (CH), 133.1 (CH), 131.4 (C), 131.2 (C), 130.5 (C), 130.2 (CH), 128.9 (CH), 128.6 (C), 127.5 (C-Br), 127.4 (CH), 123.2 (CH), 115.3 (CH); **HRMS** (EI<sup>+</sup>):  $m/z = 347.9909$  (M<sup>71+</sup>, 100%), 351.03 (M<sup>81+</sup>+H, 98%).

**3-(2-aminoethylamino)-7H-benz[de]benzimidazo[2,1-a]isoquinoline-7-one.****[FC2G0].****Method [A]**

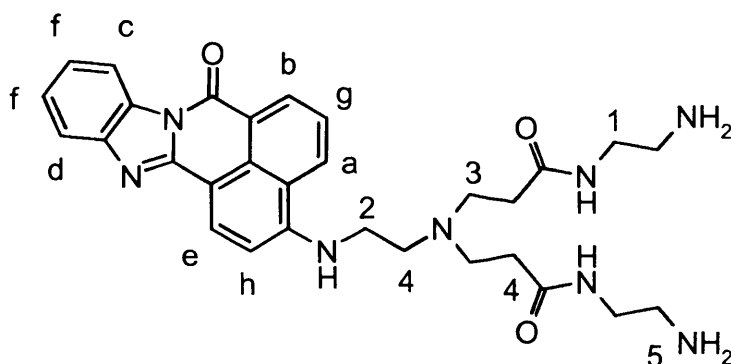
Compound **[FC2]** (0.6099 g, 1.747 mmol) and ethylenediamine (1.2 mL, 18.02 mmol) were stirred in refluxing MeCN (10 mL) for 3 days. The orange precipitate was collected by hot filtration and stirred in ether for 16 h, then filtered, and dried. The orange solid was recrystallized from toluene to give (0.084 g, 14%) a pale orange powder **[FC2G0]** after flash column chromatography (DCM:MeOH; 10:0 - 8:2).

**Method [B]**

Compound **[FC2]** (0.6022 g, 0.002 mol) was suspended in ethylenediamine (6.68 mL, 0.1 mol) and the resulting suspension was heated to 130 °C for 1 h., the mixture was cooled to 95 °C and poured into distilled water at 90 °C. After stirring and cooling to room temperature, the deep red suspension was filtered and washed with water. The solid was dried and recrystallized from toluene twice to give (0.12 g, 19%) as deep red crystals **[FC2G0]** after flash column chromatography (DCM:MeOH; 10:0 - 8:2), It was purified further by HPLC as described in the Section 4.1.2. **mp**: 212-213 °C; **UV** ( $\lambda_{\max}$ , nm): 433 (MeOH); **IR** (KBr,  $\text{cm}^{-1}$ ): 3530(-NH<sub>2</sub>), 2900 (-CH<sub>2</sub>-), 1677 (C=O); **<sup>1</sup>H-NMR** (500 MHz; MeOD):  $\delta$  8.82 (d, 1H<sub>a</sub>,  $J = 7.3$  Hz), 8.66 – 8.54 (m,

2H<sub>b</sub>), 8.04 (d, 1H<sub>c</sub>,  $J = 8.3$  Hz), 7.90 (d, 1H<sub>d</sub>,  $J = 8.3$  Hz), 7.67 (t, 1H<sub>e</sub>), 7.47 (t, 2H<sub>f</sub>), 6.71 (d, 1H<sub>g</sub>,  $J = 8.5$  Hz), 6.31 (s, 1H<sub>h</sub>), 3.37 (q, 2H<sub>1</sub>), 3.17 (t, 2H<sub>2</sub>), 1.31 (br s, 2H<sub>3</sub>); <sup>13</sup>C-NMR (125 MHz; MeOD):  $\delta$  142.5 (C), 141.4 (C), 141.1 (C), 135.2 (C), 133.7 (CH), 130.6 (C), 128.4 (C), 127.6 (CH), 124.5 (CH), 124.0 (CH), 123.9 (C), 123.1 (CH), 122.0 (CH), 121.8 (C), 116.1 (CH), 111.9 (CH), 45.7 (CH<sub>2</sub>), 39.5 (CH<sub>2</sub>); HRMS (ES<sup>+</sup>):  $m/z = 329.1401$  (MH<sup>+</sup>, 100%).

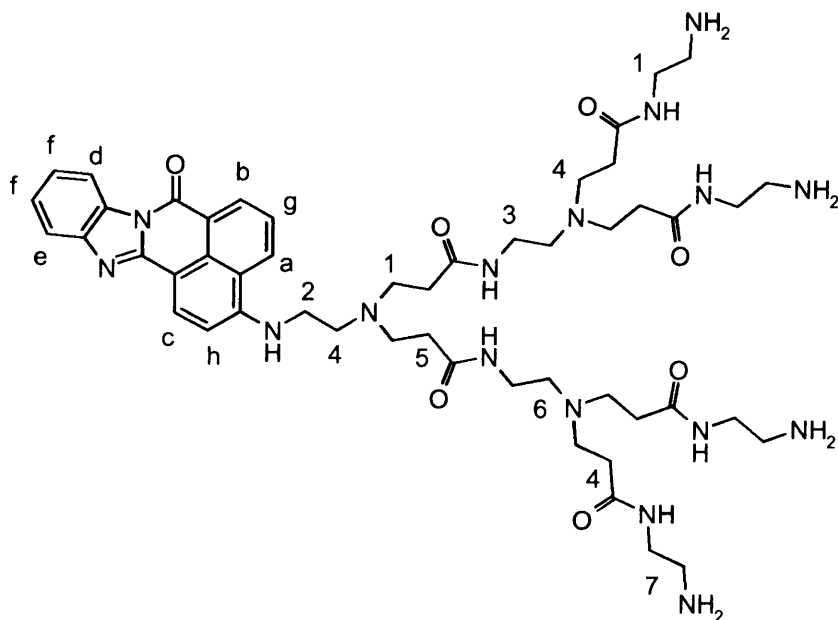
### FC - PAMAM Dendron - G1



A solution of [FC2G0.5] (0.5 g, 0.001 mol) in (MeOH:DCM; 5:15 mL) was added dropwise over 30 min to a cooled (0 °C) solution of ethylenediamine (13.38 mL, 0.2 mol) (100 equiv/COOMe) in MeOH (30 mL) and a small amount of DCM was added until the solution cleared. The reaction was stirred for 2 days under nitrogen at room temperature. The bulk of the solvent and excess ethylenediamine were removed via rotary evaporation. Final traces of excess ethylenediamine were removed azeotropically using a mixture of toluene and MeOH (9:1) (this was repeated several times until all traces of ethylenediamine had been removed). The product was dried thoroughly under high vacuum (1 mmHg) then was purified by flash column chromatography (DCM:MeOH:NH<sub>4</sub>OH; 9: 1: 0.2) to obtain (0.32 g, 57%) of [FC2G1] as a pink oil, It

was purified further by HPLC as described in the Section 4.1.2. UV ( $\lambda_{max}$ , nm): 445 (MeOH); IR (Neat,  $\text{cm}^{-1}$ ): 3284 ( $-\text{NH}_2$ ), 3075 (Ar-H), 2942 ( $-\text{CH}_2-$ ), 1675 ( $\text{N}-\text{C}=\text{O}$ ), 1572 ( $\text{NH}-\text{C}=\text{O}$ );  $^1\text{H-NMR}$  (500 MHz; MeOD):  $\delta$  8.14 (d, 1H<sub>a</sub>,  $J = 7.3$  Hz), 7.98 (d, 1H<sub>b</sub>,  $J = 7.3$  Hz), 7.76 (d, 1H<sub>c</sub>,  $J = 8.6$  Hz), 7.70 (d, 1H<sub>d</sub>,  $J = 8.6$  Hz), 7.54 (d, 1H<sub>e</sub>,  $J = 8.7$  Hz), 7.28 (t, 2H<sub>f</sub>), 7.08 (t, 1H<sub>g</sub>), 6.02 (d, 1H<sub>h</sub>,  $J = 8.7$  Hz), 3.22 (t, 4H<sub>i</sub>), 3.03 (t, 2H<sub>j</sub>), 2.82 (t, 4H<sub>k</sub>), 2.69 (m, 6H<sub>l</sub>), 2.41 (t, 4H<sub>m</sub>);  $^{13}\text{C-NMR}$  (125 MHz; MeOD):  $\delta$  173.6 (CONH), 159.5 (C), 150.9 (C), 149.0 (C), 142.5 (C), 134.4 (CH), 131.1 (C), 127.6 (C), 126.3 (CH), 125.1 (CH), 124.6 (CH), 123.8 (C), 123.7 (CH), 119.8 (CH), 118.2 (C), 115.4 (CH), 107.6 (CH), 103.6 (CH), 49.3 ( $\text{CH}_2$ ), 48.5 ( $\text{CH}_2$ ), 43.3 ( $\text{CH}_2$ ), 41.6 ( $\text{CH}_2$ ), 40.6 ( $\text{CH}_2$ ), 33.3 ( $\text{CH}_2$ ); HRMS Calc. for ( $\text{C}_{30}\text{H}_{36}\text{N}_8\text{O}_3$ ): 556.2983, found 556.2977 ( $\text{M}^+$ , 100%).

## FC - PAMAM Dendron - G2

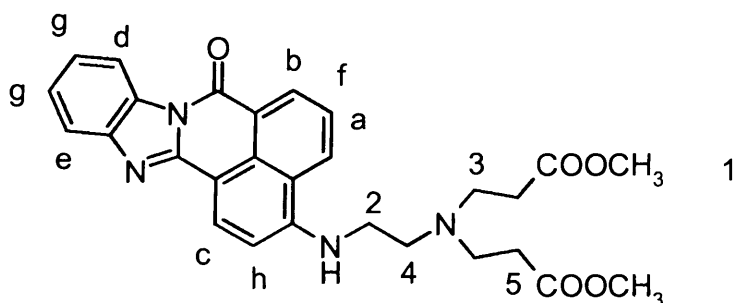


A solution of [FC2G1.5] (0.9 g, 0.001 mol) in MeOH (30 mL) was added dropwise over 30 min to a cooled (0 °C) solution of ethylenediamine (26.76 mL, 0.4 mol) (100

equiv/COOMe) in MeOH (70 mL). The reaction was stirred for 5 days under nitrogen at room temperature. The bulk of the solvent and excess ethylenediamine were removed via rotary evaporator. Final traces of excess ethylenediamine were removed azeotropically using a mixture of toluene and MeOH (9:1) (this was repeated several times until all traces of ethylenediamine had been removed). The product was dried thoroughly under high vacuum (1 mmHg) then was purified by flash column chromatography (DCM:MeOH:NH<sub>4</sub>OH; 9: 1: 0.2) to obtain (0.57 g, 56%) of polyamine [FC2G2] as a red oil, It was purified further by HPLC as described in the Section 4.1.2. UV ( $\lambda_{max}$ , nm): 433 (MeOH); IR (Neat, cm<sup>-1</sup>): 3262 (-NH<sub>2</sub>), 3075 (Ar-H), 2929 (-CH<sub>2</sub>-), 1675 (N-C=O), 1557 (NH-C=O); <sup>1</sup>H-NMR (500 MHz; MeOD):  $\delta$  8.21 (d, 1H<sub>a</sub>, *J* = 6.7 Hz), 8.12 (d, 1H<sub>b</sub>, *J* = 6.7 Hz), 7.92 (d, 1H<sub>c</sub>, *J* = 7.3 Hz), 7.84 (d, 1H<sub>d</sub>, *J* = 6.9 Hz), 7.59 (d, 1H<sub>e</sub>, *J* = 6.9 Hz), 7.34 (t, 2H<sub>f</sub>), 7.20 (t, 1H<sub>g</sub>), 6.12 (d, 1H<sub>h</sub>, *J* = 7.3 Hz), 3.22 (t, 12H<sub>1</sub>), 3.07 (t, 2H<sub>2</sub>), 2.83 (t, 4H<sub>3</sub>), 2.70 (t, 18H<sub>4</sub>), 2.48 (t, 4H<sub>5</sub>), 2.41 (t, 4H<sub>6</sub>), 2.28 (t, 8H<sub>7</sub>); <sup>13</sup>C-NMR (125 MHz; MeOD):  $\delta$  173.5 (CONH), 173.0 (CONH), 164.4 (C), 159.6 (C), 151.1 (C), 149.2 (C), 142.8 (CH), 134.6 (C), 131.3 (C), 127.8 (CH), 126.5 (CH), 126.4 (CH), 124.7 (C), 124.0 (CH), 120.0 (CH), 118.4 (C), 115.5 (CH), 107.8 (CH), 103.8 (CH), 52.1 (CH<sub>2</sub>), 49.7 (CH<sub>2</sub>), 49.4 (CH<sub>2</sub>), 48.6 (CH<sub>2</sub>), 43.6 (CH<sub>2</sub>), 41.7 (CH<sub>2</sub>), 40.8 (CH<sub>2</sub>), 37.3 (CH<sub>2</sub>), 33.4 (CH<sub>2</sub>); MALDI-TOF [LD<sup>+</sup>] Calc. for (C<sub>50</sub>H<sub>76</sub>N<sub>16</sub>O<sub>7</sub>): 1013.6170, found 1013.674 (M<sup>+</sup>, 100%).

**General procedure (D) for synthesis of polyesters G0.5, G1.5, G2.5**

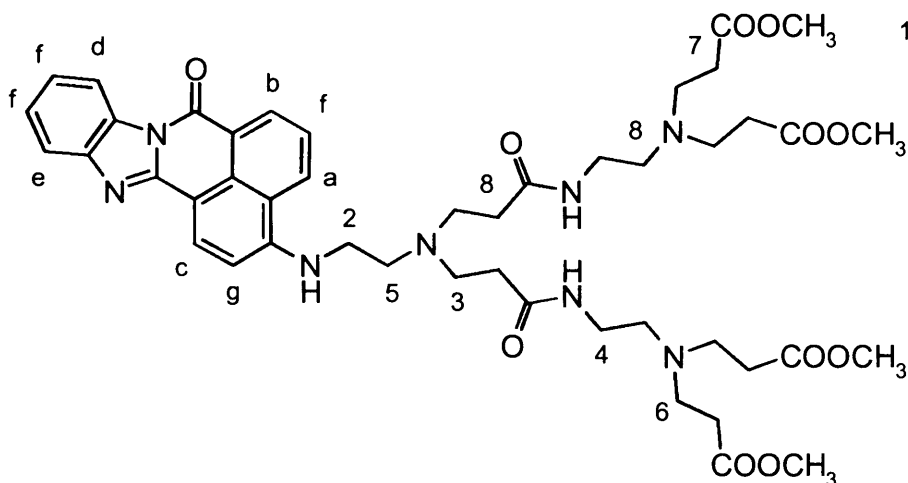
Methyl acrylate (75 equiv/ $\text{NH}_2$  function) was added to a solution of conjugate with amine terminal groups and the mixture was heated to reflux. MeOH and the excess of methylacrylate were eliminated to yield the polyester after chromatography using silica gel as substrate and a mixture of  $\text{CHCl}_3$  and MeOH (10:0.1) as eluent.

**FC - PAMAM Dendron – G0.5**

Methyl acrylate (6.75 mL, 0.075 mol) was added to a solution of [FC2G0] (0.328 g, 0.001 mol) in MeOH (40 mL) and the mixture was heated to reflux for 6 h, then stirred for 16 h at room temperature, filtered, washing with MeOH, and dried. The orange solid was recrystallized from MeOH to give (0.084 g, 77%) a bright orange solid [FC2G0.5] after flash column chromatography (DCM:MeOH; 10:0 – 10:0.2), It was purified further by HPLC as described in the (Section 4.1.2). **mp**: 170-171 °C; **UV** ( $\lambda_{max}$ , nm): 445 (MeOH); **IR** (KBr,  $\text{cm}^{-1}$ ): 3413 (-NH), 3058 (Ar-H), 2950 (-CH<sub>2</sub>-), 2848 (-OCH<sub>3</sub>), 1734 (-COOCH<sub>3</sub>), 1681 (N-C=O), 1581 (NH-C=O); **<sup>1</sup>H-NMR** (400 MHz;  $\text{CDCl}_3$ ):  $\delta$  8.54 (d, 1H<sub>a</sub>,  $J = 7.2$  Hz), 8.46 (d, 1H<sub>b</sub>,  $J = 7.2$  Hz), 8.24 (d, 1H<sub>c</sub>,  $J = 7.2$  Hz), 7.93 (d, 1H<sub>d</sub>,  $J = 8.4$  Hz), 7.74 (d, 1H<sub>e</sub>,  $J = 8.4$  Hz), 7.38 (t, 1H<sub>f</sub>), 7.30 (t, 2H<sub>g</sub>), 6.30 (d, 1H<sub>h</sub>,  $J = 7.2$  Hz), 6.09 (s, 1H), 3.40 (s, 6H<sub>1</sub>), 3.05 (t, 2H<sub>2</sub>), 2.61 (t, 4H<sub>3</sub>),

2.52 (t, 2H<sub>4</sub>), 2.29 (t, 4H<sub>5</sub>); <sup>13</sup>C-NMR (100 MHz; CDCl<sub>3</sub>): δ 172.7 (COO), 160.5 (C), 150.6 (C), 149.8 (C), 143.7 (C), 134.9 (CH), 131.9 (C), 128.3 (C), 126.8 (CH), 124.9 (CH), 124.8 (CH), 124.5 (C), 120.5 (CH), 119.9 (CH), 119.3 (C), 115.9 (CH), 109.4 (CH), 104.3 (CH), 51.5 (Me), 51.4 (CH<sub>2</sub>), 48.8 (CH<sub>2</sub>), 40.1 (CH<sub>2</sub>), 32.4 (CH<sub>2</sub>); **LRMS** (ES<sup>+</sup>): *m/z* = 501.21 (MH<sup>+</sup>, 100%), 502.22 (33%), 503.22 (6%); **HRMS** Calc. for (C<sub>28</sub>H<sub>28</sub>N<sub>4</sub>O<sub>5</sub>): 500.2060, found 500.2139 (M<sup>+</sup>, 100%).

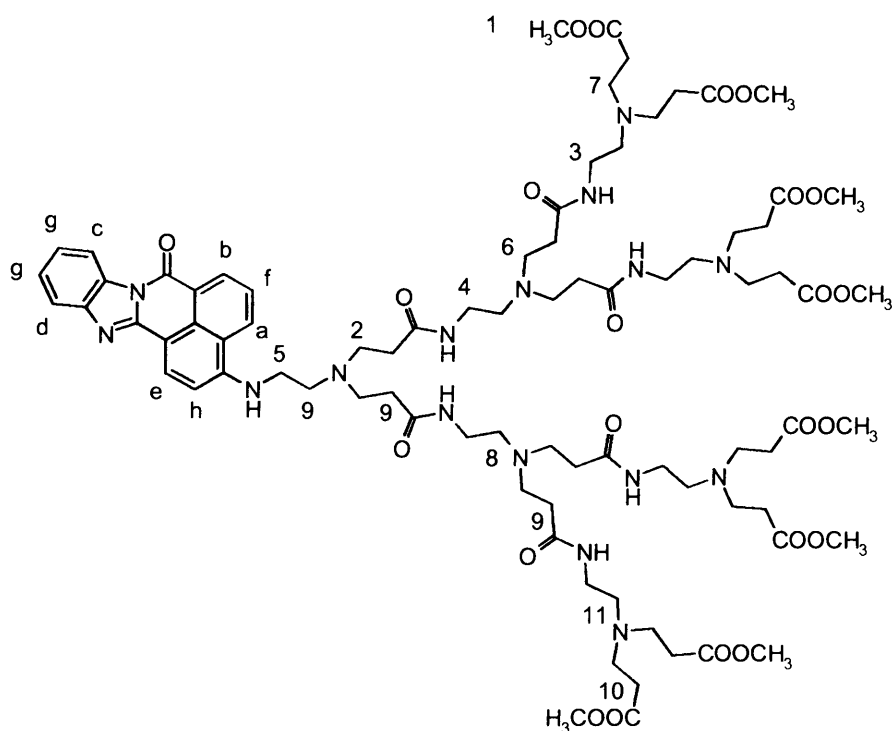
### FC - PAMAM Dendron – G1.5



Methyl acrylate (13.5 mL, 0.15 mol) was added to a solution of [FC2G1] (0.556 g, 0.001 mol) in MeOH (30 mL) and the mixture was heated to reflux for 24 h, then stirred for 16 h at room temperature. MeOH and excess of methylacrylate were eliminated by heating under reduced pressure to yield the [FC2G1.5] as a deep orange oil (0.63 g, 70%) after purification by flash column chromatography (DCM:MeOH; 10:0 – 10:0.3), It was purified further by HPLC as described in the (Section 4.1.2). **UV** ( $\lambda_{max}$ , nm): 445 (MeOH); **IR** (KBr, cm<sup>-1</sup>): 3306 (-NH), 3039 (Ar-H), 2918 (-CH<sub>2</sub>-), 2851 (-OCH<sub>3</sub>), 1729 (-COOCH<sub>3</sub>), 1674 (N-C=O), 1589 (NH-C=O); **<sup>1</sup>H-NMR** (400

MHz; MeOD):  $\delta$  8.16 (d, 1H<sub>a</sub>,  $J$  = 7.5 Hz), 8.13 (d, 1H<sub>b</sub>,  $J$  = 7.5 Hz), 7.93 (d, 1H<sub>c</sub>,  $J$  = 0.54 Hz), 7.86 (d, 1H<sub>d</sub>,  $J$  = 8.5 Hz), 7.49 (d, 1H<sub>e</sub>,  $J$  = 8.5 Hz), 7.19 (m, 3H<sub>f</sub>), 6.30 (d, 1H<sub>g</sub>,  $J$  = 0.54 Hz), 3.40 (s, 12H<sub>1</sub>), 3.03 (t, 2H<sub>2</sub>), 2.97 (t, 4H<sub>3</sub>), 2.67 (t, 4H<sub>4</sub>), 2.57 (t, 2H<sub>5</sub>), 2.42 (t, 8H<sub>6</sub>), 2.23 (m, 8H<sub>7</sub>), 2.14 (t, 8H<sub>8</sub>); <sup>13</sup>C-NMR (100 MHz; MeOD):  $\delta$  173.2 (CONH), 173.1 (COO), 159.9 (C), 151.3 (C), 149.4 (C), 142.7 (C), 134.8 (CH), 131.3 (C), 128.0 (C), 126.6 (CH), 125.6 (CH), 124.8 (CH), 124.0 (C), 120.2 (CH), 118.6 (CH), 118.3 (C), 115.5 (CH), 107.9 (CH), 104.0 (CH), 52.2 (CH<sub>2</sub>), 51.0 (CH<sub>2</sub>), 50.7 (Me), 49.3 (CH<sub>2</sub>), 48.9 (CH<sub>2</sub>), 40.9 (CH<sub>2</sub>), 37.0 (CH<sub>2</sub>), 33.3 (CH<sub>2</sub>), 32.0 (CH<sub>2</sub>); HRMS (EI<sup>+</sup>) Calc. for (C<sub>46</sub>H<sub>60</sub>N<sub>8</sub>O<sub>11</sub>): 900.4454, found 900.4453 (M<sup>+</sup>, 100%).

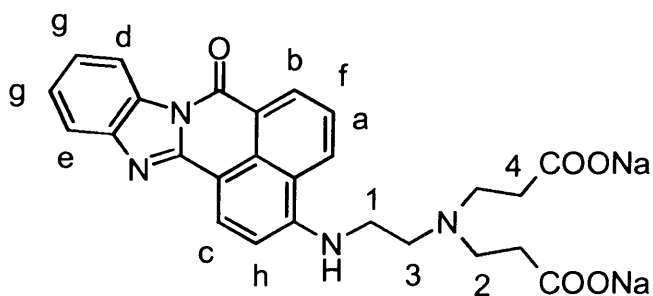
#### FC - PAMAM Dendron - G2.5



Methyl acrylate (27 mL, 0.30 mol) was added to a solution of [FC2G2] (1.01 g, 0.001 mol) in MeOH (30 mL) and the mixture was heated to reflux for 2 days. MeOH and excess of methylacrylate were eliminated by heating under reduced pressure to yield

the [FC2G2.5] as a deep orange oil (1.3 g, 76%) after flash column chromatography (DCM:MeOH; 10:0 - 10:0.3), It was purified further by HPLC as described in the (Section 4.1.2). UV ( $\lambda_{\max}$ , nm): 445 (MeOH); IR (KBr,  $\text{cm}^{-1}$ ): 3422 (-NH), 3043 (Ar-H), 2924 (-CH<sub>2</sub>-), 2850 (-OCH<sub>3</sub>), 1736 (-COOCH<sub>3</sub>), 1681 (N-C=O), 1581 (NH-C=O); <sup>1</sup>H-NMR (400 MHz; MeOD):  $\delta$  8.46 (d, 1H<sub>a</sub>,  $J = 7.2$  Hz), 8.40 (d, 1H<sub>b</sub>,  $J = 7.2$  Hz), 8.24 (d, 1H<sub>c</sub>,  $J = 8.5$ ), 8.20 (d, 1H<sub>d</sub>,  $J = 8.5$  Hz), 7.72 (d, 1H<sub>e</sub>,  $J = 8.8$  Hz), 7.49 (t, 1H<sub>f</sub>), 7.42 (t, 2H<sub>g</sub>), 6.50 (d, 1H<sub>h</sub>,  $J = 8.8$  Hz), 3.62 (s, 24H<sub>i</sub>), 3.25 (t, 4H<sub>2</sub>), 3.20 (t, 8H<sub>3</sub>), 2.90 (t, 4H<sub>4</sub>), 2.83 (t, 2H<sub>5</sub>), 2.74 (t, 8H<sub>6</sub>), 2.68 (t, 16H<sub>7</sub>), 2.54 (t, 4H<sub>8</sub>), 2.48 (t, 14H<sub>9</sub>), 2.39 (t, 16H<sub>10</sub>), 2.31 (t, 8H<sub>11</sub>); <sup>13</sup>C-NMR (100 MHz; MeOD):  $\delta$  173.2 (CONH), 173.1 (CONH), 173.0 (COO), 160.0 (C), 151.4 (C), 149.5 (C), 142.8 (C), 135.0 (CH), 131.4 (C), 128.3 (C), 126.8 (CH), 125.8 (CH), 124.9 (CH), 124.4 (C), 124.2(CH), 120.4 (CH), 118.9 (C), 115.6 (CH), 108.1 (CH), 104.2 (CH), 52.3 (CH<sub>2</sub>), 52.0 (CH<sub>2</sub>), 51.1 (Me), 50.8 (CH<sub>2</sub>), 49.5 (CH<sub>2</sub>), 49.0 (CH<sub>2</sub>), 40.6 (CH<sub>2</sub>), 37.2 (CH<sub>2</sub>), 37.0 (CH<sub>2</sub>), 33.4 (CH<sub>2</sub>), 33.2 (CH<sub>2</sub>), 32.1 (CH<sub>2</sub>), 29.5 (CH<sub>2</sub>); MALDI-TOF [LD<sup>+</sup>] Calc. for (C<sub>82</sub>H<sub>124</sub>N<sub>16</sub>O<sub>23</sub>): 1701.9554, found 1701.969 (M<sup>+</sup>, 100%).

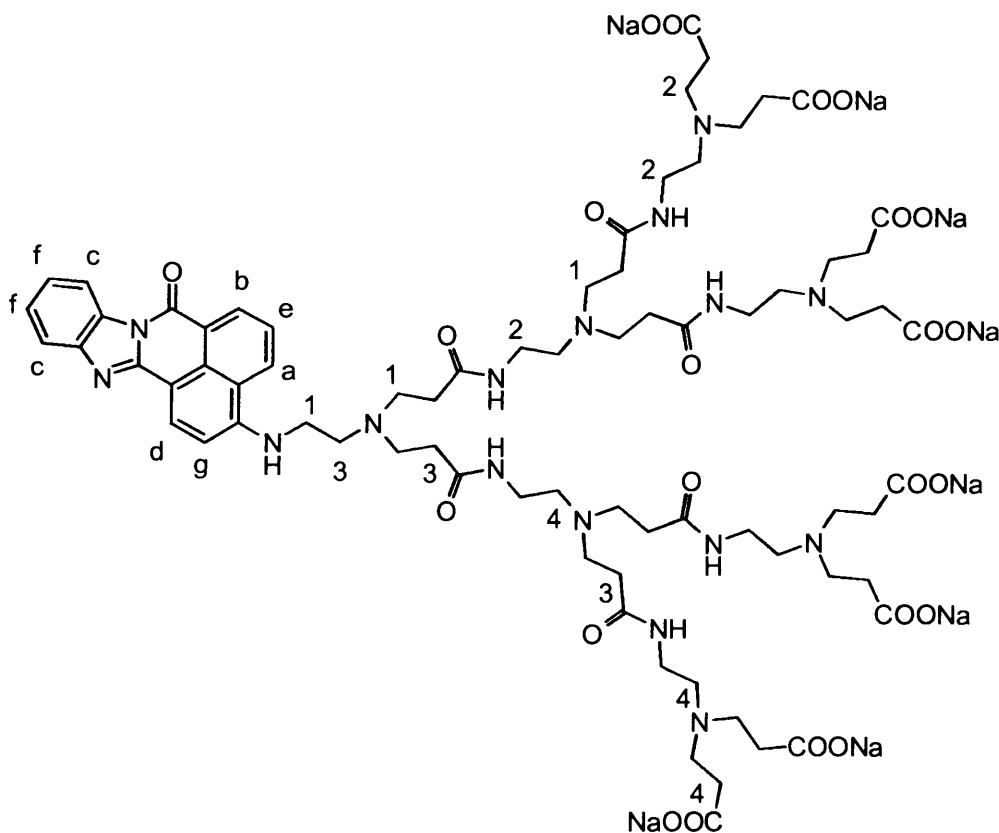
### FC - PAMAM Dendron – G0.5 salt



To NaOH (0.5 g, 12.5 mmol), dissolved in hot EtOH (40 mL), was added a solution of the **[FC2G0.5]** (1.2 g, 2.4 mmol) in EtOH (10 mL). The mixture was heated to reflux for 16 h. After cooling, a the precipitate was collected by filtration and recrystallized from wet EtOH to yield **[FC2G0.5 salt]** as a pale yellow solid (0.92 g, 95%). Mp > 300 °C decomposed at 315 °C (TGA); UV ( $\lambda_{max}$ , nm): 445 (MeOH); IR (KBr,  $\text{cm}^{-1}$ ): 3380 (-NH), 3067 (Ar-H), 2956 (-CH<sub>2</sub>-), 1666 (-COONa), 1681 (N-C=O), 1571 (NH-C=O); <sup>1</sup>H-NMR (400 MHz; MeOD):  $\delta$  8.47 (dd, 1H<sub>a</sub>,  $J = 7.3, J = 0.7$  Hz), 8.38 (d, 1H<sub>b</sub>,  $J = 7.3$  Hz), 8.33 (d, 1H<sub>c</sub>,  $J = 8.7$ ), 8.28 (d, 1H<sub>d</sub>,  $J = 8.6$  Hz), 7.69 (d, 1H<sub>e</sub>,  $J = 8.6$  Hz), 7.56 (t, 1H<sub>f</sub>), 7.45-7.35 (m, 2H<sub>g</sub>), 6.60 (d, 1H<sub>h</sub>,  $J = 8.7$  Hz), 3.44 (t, 2H<sub>i</sub>), 2.95 (t, 4H<sub>2</sub>), 2.89 (t, 2H<sub>3</sub>), 2.48 (t, 4H<sub>4</sub>); <sup>13</sup>C-NMR (100 MHz; MeOD):  $\delta$  179.9 (COO), 160.3 (C), 151.9 (C), 149.5 (C), 142.6 (C), 135.2 (CH), 131.3 (C), 128.3 (C), 126.8 (CH), 126.1 (CH), 124.8 (CH), 124.3 (C), 124.0 (CH), 120.5 (CH), 118.5 (C), 118.2 (CH), 115.5 (CH), 107.5 (CH), 50.7 (CH<sub>2</sub>), 50.4 (CH<sub>2</sub>), 40.5 (CH<sub>2</sub>), 35.1 (CH<sub>2</sub>); LRMS (ES<sup>+</sup>):  $m/z = 473.18$  (MH<sup>+</sup>, 100%); HRMS Calc. for (C<sub>26</sub>H<sub>24</sub>N<sub>4</sub>O<sub>5</sub>): 472.1872, found 473.1840 (MH<sup>+</sup>, 100%).



## FC - PAMAM Dendron - G2.5 salt



To NaOH (3.0 g, 75 mmol), dissolved in absolute EtOH (150 mL), was added a solution of [FC2G2.5] (4.23 g, 2.4 mmol) in EtOH (10 mL). The mixture was stirring for 24 h. at room temperature and the precipitate was collected by filtration and was recrystallized from EtOH to yield [FC2G2.5 salt] as a deep orange solid (3.9 g, 93%).  
**mp:** 269 °C; **UV** ( $\lambda_{max}$ , nm): 445 (MeOH); **IR** (KBr,  $\text{cm}^{-1}$ ): 3412 (-NH-), 3091 (Ar-H), 2956 (-CH<sub>2</sub>-), 1655 (-COONa), 1681 (N-C=O), 1571 (NH-C=O); **<sup>1</sup>H-NMR** (500 MHz; MeOD):  $\delta$  8.52 (d, 1H<sub>a</sub>,  $J = 7.2$  Hz), 8.43 (d, 1H<sub>b</sub>,  $J = 7.2$  Hz), 8.33 (m, 2H<sub>c</sub>), 7.72 (d, 1H<sub>d</sub>,  $J = 7.5$  Hz), 7.56 (t, 1H<sub>e</sub>), 7.42 (m, 2H<sub>f</sub>), 6.60 (d, 1H<sub>g</sub>,  $J = 7.5$  Hz), 3.32 (m, 14H<sub>1</sub>), 2.85 (m, 28H<sub>2</sub>), 2.59 (m, 14H<sub>3</sub>), 2.37 (m, 28H<sub>4</sub>); **<sup>13</sup>C-NMR** (125 MHz; MeOD):  $\delta$  181.4 (COO), 174.7 (CONH), 174.6 (CONH), 161.9 (C), 153.4 (C), 151.1 (C), 144.3 (C), 142.5 (CH), 136.9 (C), 132.9 (C), 128.7 (CH), 127.6 (CH), 126.4 (CH), 125.6 (C), 122.2 (CH), 120.4 (CH), 119.9 (C), 117.0 (CH), 109.4 (CH), 105.8

(CH), 58.3 (CH<sub>2</sub>), 53.3 (CH<sub>2</sub>), 52.0 (CH<sub>2</sub>), 50.9 (CH<sub>2</sub>), 42.2 (CH<sub>2</sub>), 38.5 (CH<sub>2</sub>), 38.4 (CH<sub>2</sub>), 36.5 (CH<sub>2</sub>), 34.8 (CH<sub>2</sub>), 34.5 (CH<sub>2</sub>); **MALDI-TOF [LD<sup>+</sup>]** Calc. for (C<sub>74</sub>H<sub>108</sub>N<sub>16</sub>O<sub>23</sub>): 1588.7773, found 1588.27 (M<sup>+</sup>, 100%).

## 4.4. Experimental Appendix

**Table [4.1]:** UV maximum absorbance for **FC2** and **FC2Gs** in MeOH solvent.

Compounds	FC2	FC2G0	FC2G0.5	FC2G1	FC2G1.5	FC2G2	FC2G2.5
UV max (nm)	383	444	447	455	449	460	447

**Table [4.2]:** Fluorescence Intensity at different concentrations of **FC2G0.5** salt in H<sub>2</sub>O at max wavelength 443 nm at 25 °C.

Concentration e-4 mM	1.08	1.62	2.16	3.25	4.33
Fluorescence Intensity	99.86	142.8	192.84	282.21	368.06

**Table [4.3]:** Fluorescence Intensity at different concentrations of **FC2G1.5** salt in H<sub>2</sub>O at max wavelength 456 nm at 25 °C.

Concentration e-4 mM	1.43	1.91	2.87	3.83	5.75
Fluorescence Intensity	85.58	112.1	164.91	215.98	313.36

**Table [4.4]:** Fluorescence Intensity at different concentrations of **FC2G2.5** salt in H<sub>2</sub>O at max wavelength 467 nm at 25 °C.

Concentration e-4 mM	0.83	1.25	1.66	2.5	3.33
Fluorescence Intensity	73.33	105	136.74	196.99	255.45

**Table [4.5]:** UV absorbance at different pH values for **FC2G0.5** salt in H<sub>2</sub>O at concentration  $16.66 \times 10^{-3}$  mM.

pH	0.86	1.43	2.34	3.57	5.05	7.51	8.09	9.31	11.13	12.86	13.57
$\lambda_{MAX}$ (nm)	479	474	455	442	443	443	444	445	456	454	455
Abs .	0.22	0.20	0.14	0.11	0.20	0.23	0.23	0.21	0.27	0.23	0.15

**Table [4.6]:** UV absorbance at different pH values for **FC2G1.5** salt in H<sub>2</sub>O at concentration  $16.66 \times 10^{-3}$  mM.

<b>pH</b>	0.83	1.32	2.15	3.87	5.86	7.43	9.63	10.7	11.16	12.17	12.88	13.56
<b><math>\lambda_{MAX}</math> (nm)</b>	482	470	447	443	445	448	457	460	462	459	457	455
<b>Abs .</b>	0.30	0.27	0.28	0.26	0.32	0.33	0.34	0.42	0.40	0.39	0.36	0.27

**Table [4.7]:** UV absorbance at different pH values for **FC2G2.5** salt in H<sub>2</sub>O at concentration  $16.66 \times 10^{-3}$  mM.

<b>pH</b>	0.73	1.29	2.12	2.88	3.73	5.89	7.71	10.52	11.77	12.47	13.46
<b><math>\lambda_{MAX}</math> (nm)</b>	479	461	447	445	445	448	455	467	468	468	459
<b>Abs.</b>	0.27	0.28	0.28	0.22	0.24	0.26	0.28	0.30	0.34	0.34	0.27

**Table [4.8]:** Fluorescence Intensity at different pH values of **FC2G0.5** salt in H<sub>2</sub>O at max wavelength 447 nm at 25 °C and concentration  $2.3 \times 10^{-3}$  mM.

<b>pH values</b>	0.26	1.0	1.96	2.61	4.26	5.72	7.75	8.39	10.03	11.44	12.46	13.12
<b>Flu Intensity</b>	33.55	34.21	82.58	146.5	349.1	493.6	361.7	361.1	146.6	20.31	16.66	11.45
<b>Flu Em max</b>	554	549	497	499	501	501	501	501	503	516	516	516

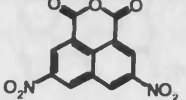
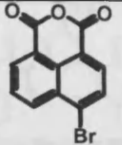
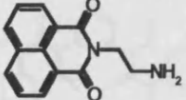
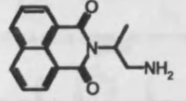
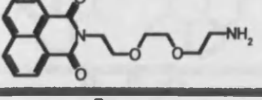
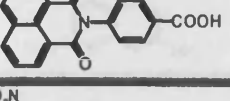
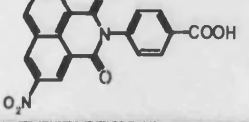
**Table [4.9]:** Fluorescence Intensity at different pH values of **FC2G1.5** salt in H<sub>2</sub>O at max wavelength 447 nm at 25 °C and concentration  $2.3 \times 10^{-3}$  mM.

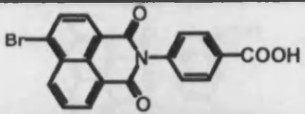
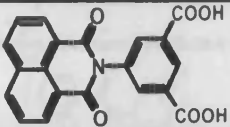
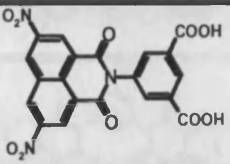
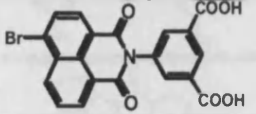
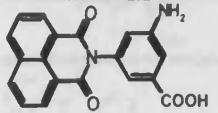
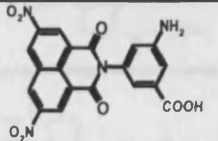
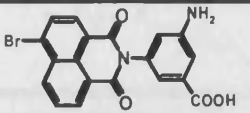
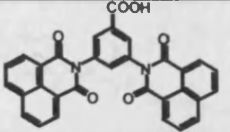
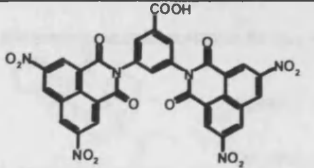
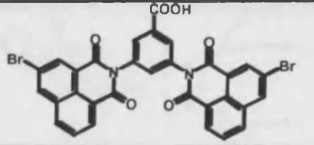
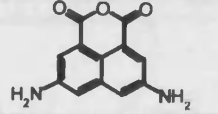
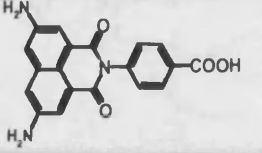
<b>pH values</b>	0.4	0.98	1.62	1.92	2.7	3.72	5.57	7.9	8.24	10.12	11.29	12.35	13.11	13.83
<b>Flu Intensity</b>	42.8	42.57	70.19	110.5	113.8	224.5	380.7	246.4	209.3	37.27	29.15	28.99	24.94	12.3
<b>Flu Em max</b>	554.	550.5	502.5	500.5	502.5	503	502.5	503	502.5	516	515	515	513.5	515.5

**Table [4.10]:** Fluorescence Intensity at different pH values of FC2G2.5 salt in H<sub>2</sub>O at max wavelength 447 nm at 25 °C and concentration  $2.3 \times 10^{-3}$  mM.

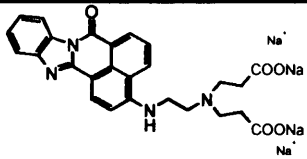
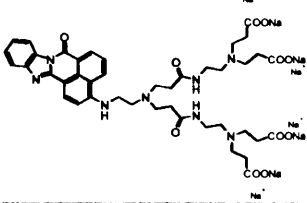
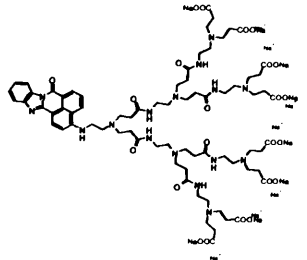
pH values	0.55	1.05	2.17	4.35	5.41	7.89	8.15	9.93	11.29	12.24	13.11	13.83
Flu Intensity	55.04	90.78	298.6	375.3	464.9	315.3	211.8	75.49	64.43	63.62	62.56	47.03
Flu Em max	553.5	501	500.5	500	501	503	504.5	514.5	515	513	513.5	515

**Table [4.11]:** Extinction Coefficient of all thesis' compounds.

Comp. No.	Structure	UV $\lambda_{\text{max abso}}$ (nm)	Extinction Coefficient ( $\text{L mol}^{-1} \text{cm}^{-1}$ )
<b>1</b>		330	13066.83
<b>2</b>		277	30865.96
<b>3</b>		278	33537.6
<b>4</b>		339.5	13029.4
<b>CF1</b>		334	13997.8
<b>CF2</b>		339.5	13946.66
<b>CF3</b>		334	12574.0
<b>A1</b>		334	14693.6
<b>A2</b>		269.5	44050.5

<b>A4</b>		342	17801.0
<b>B1</b>		334	17344.5
<b>B2</b>		272.5	32368.8
<b>B4</b>		342	16317.0
<b>C1</b>		334.5	13785.8
<b>C2</b>		269.5	12012.6
<b>C4</b>		342	18880.5
<b>C11</b>		334.5	27678.246
<b>C22</b>		272	75707.27
<b>C44</b>		342	33701.402
<b>3</b>		278	33537.6
<b>A3</b>		440	46648.3

<b>B3</b>		438	3959.77
<b>C3</b>		432	6809.62
<b>C33</b>		435	14107.1
<b>FC2</b>		395	12429.4
<b>FC260</b>		457	8018.56
<b>FC261</b>		454	18645.0
<b>FC262</b>		460	9623.43
<b>FC260.5</b>		457	12591.8
<b>FC261.5</b>		461	23311.5
<b>G2.5</b>		461	16069.8

<b>FC2G0.5 salt</b>		442	6399.78
<b>FC2G1.5 salt</b>		444	14979.2
<b>FC2G2.5 salt</b>		450	19209.6

#### 4.4.1. Relative Fluorescence Intensity by comparison to standard Fluorescein salt.

The compounds under study were prepared as solutions in distillate H<sub>2</sub>O at concentrations that give a UV absorbance value of  $0.1 \times 10^{-5}$ . Compounds (**FC2G0.5 salt**, **FC2G1.5 salt** and **FC2G2.5 salt**) were excited at UV max wavelength 445 nm while **Fluorescein salt** was excited at UV max wavelength 481 nm. Standard 10 mm path length fluorescence cuvette was used for running the fluorescence measurements with the concentration range never exceeding an effective adsorption of 0.1 at the maximum excitation wavelength. In order to minimise re-absorption effects (Dhami et al.),<sup>[233]</sup> the fluorescence spectra of all compounds were determined under the same operation conditions and settings with 7.5 slit widths. Fluorescence quantum yields were determined by comparing the integral areas of the fluorescence emission for the different compounds.

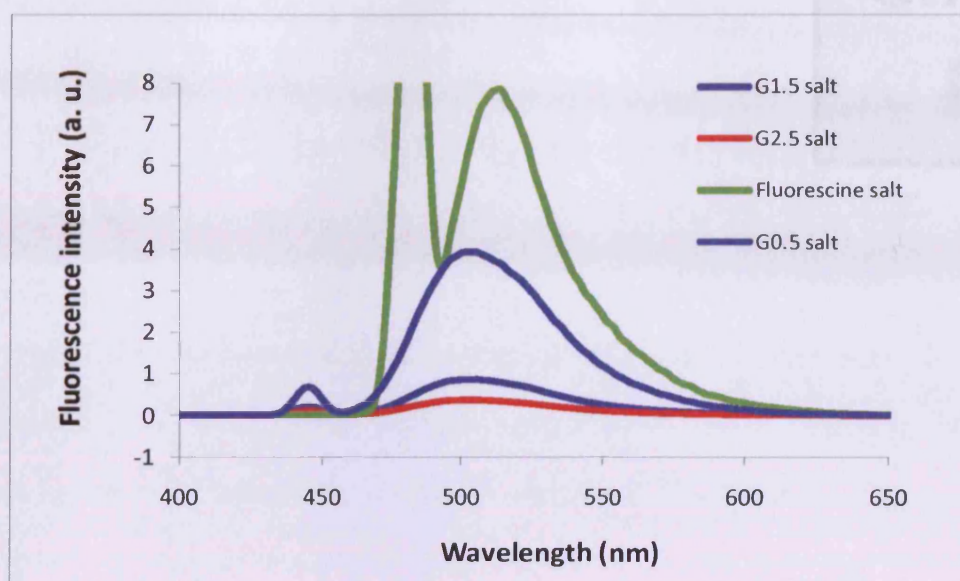


**Figure [4.1]:** Fluorescence emission curves for all FC2G0.5, FC2G1.5, FC2G2.5 salts (when excited at wavelength  $\lambda_{\max}$  447 nm), and Fluorescein salt (when excited at wavelength  $\lambda_{\max}$  481 nm) in  $H_2O$  at UV absorbance  $0.1 \times 10^{-5}$ .

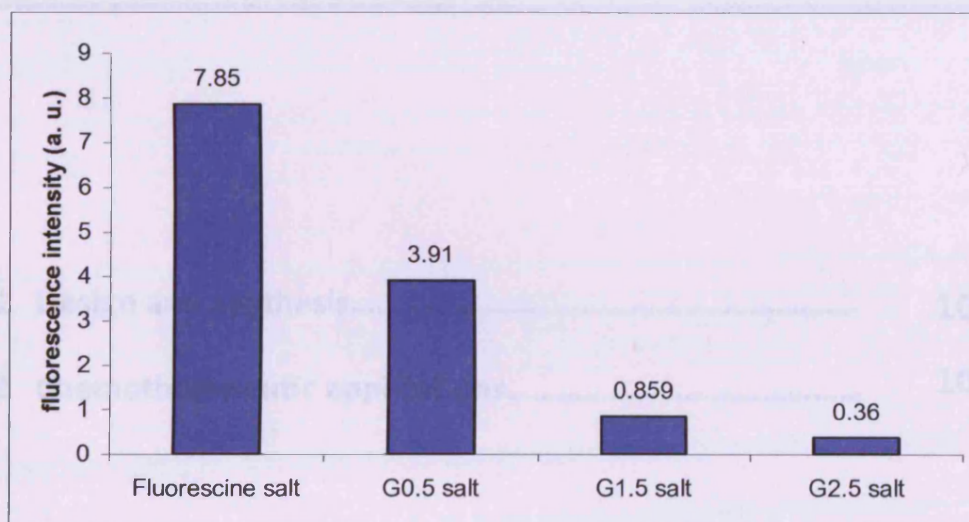


**Figure [4.2]:** Fluorescence intensity values of all FC2G0.5, FC2G1.5, FC2G2.5 salts (when excited at wavelength  $\lambda_{\max}$  447 nm), and Fluorescein salt (when excited at wavelength  $\lambda_{\max}$  481 nm) in  $H_2O$  at UV absorbance  $0.1 \times 10^{-5}$ .

# CHAPTER FIVE

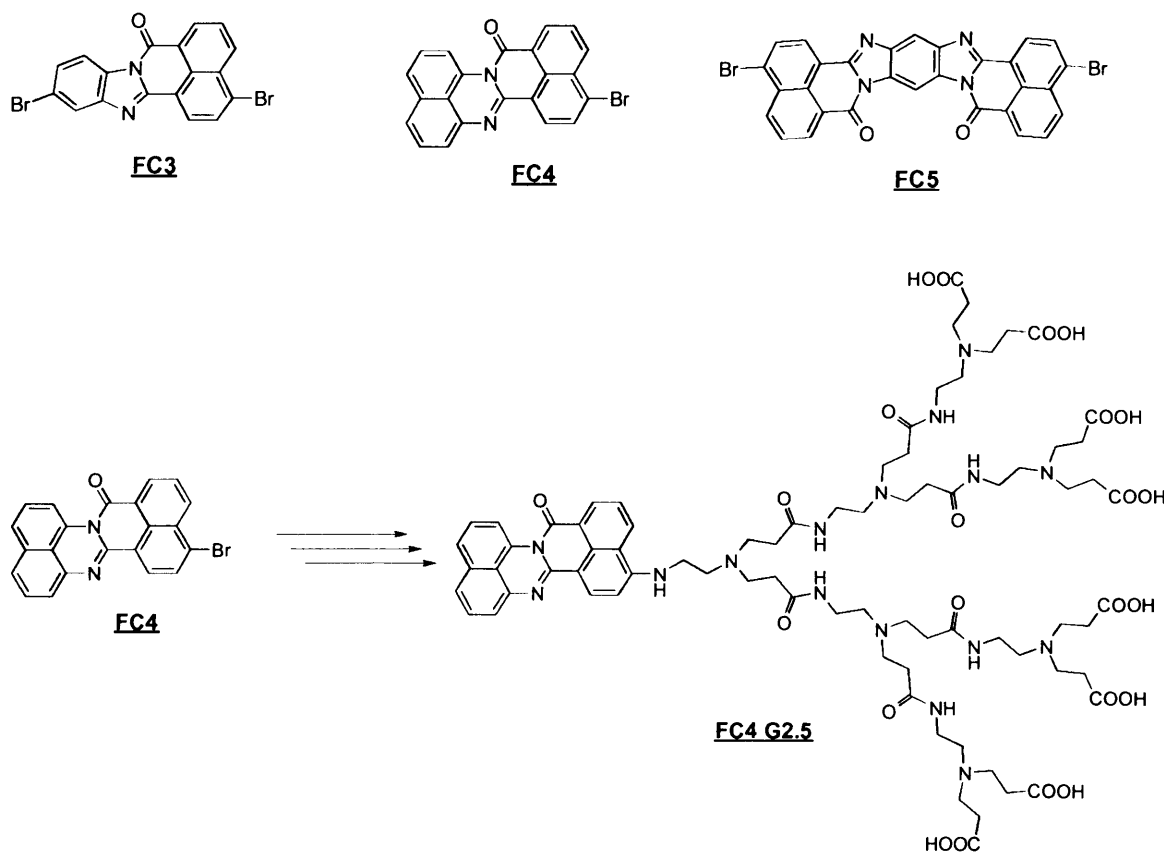
## FUTURE WORK

5.1 Design and synthesis.....	104
5.2 Chemotherapeutic applications.....	107

## 5.1. Design and synthesis

### 5.1.1. Synthesis of new fluorescent dendritic wedges.

The new fluorescent cores described in this thesis were designed to possess specific features including (a) functional groups to build up multi PAMAM dendritic wedges, (b) high fluorescence emission and (c) biological activity especially for DNA intercalation, anticancer activity, and/or as special protein binding inhibitor. Further examples that could be used for this purpose are given in (Scheme 5.1).



**Scheme [5.1]:** New fluorescent cores **FC3**, **FC4**, **FC5** and an example of a new fluorescent PAMAM dendritic wedge **FC4 G2.5**.

## 5.1.2 Synthesis of fluorescent PAMAM dendritic multi-wedges.

The cores **FC3** and **FC5** can be used to prepare bow-tie dendrimers. For example, **FC3G2.5** and **FC5G2.5** can be prepared by a divergent pathway. Similarly, compound **FC5G2.5** can be prepared via a convergent method; this route gives more facility to loading different dendritic wedges or different conjugated moieties (Figure 5.1).

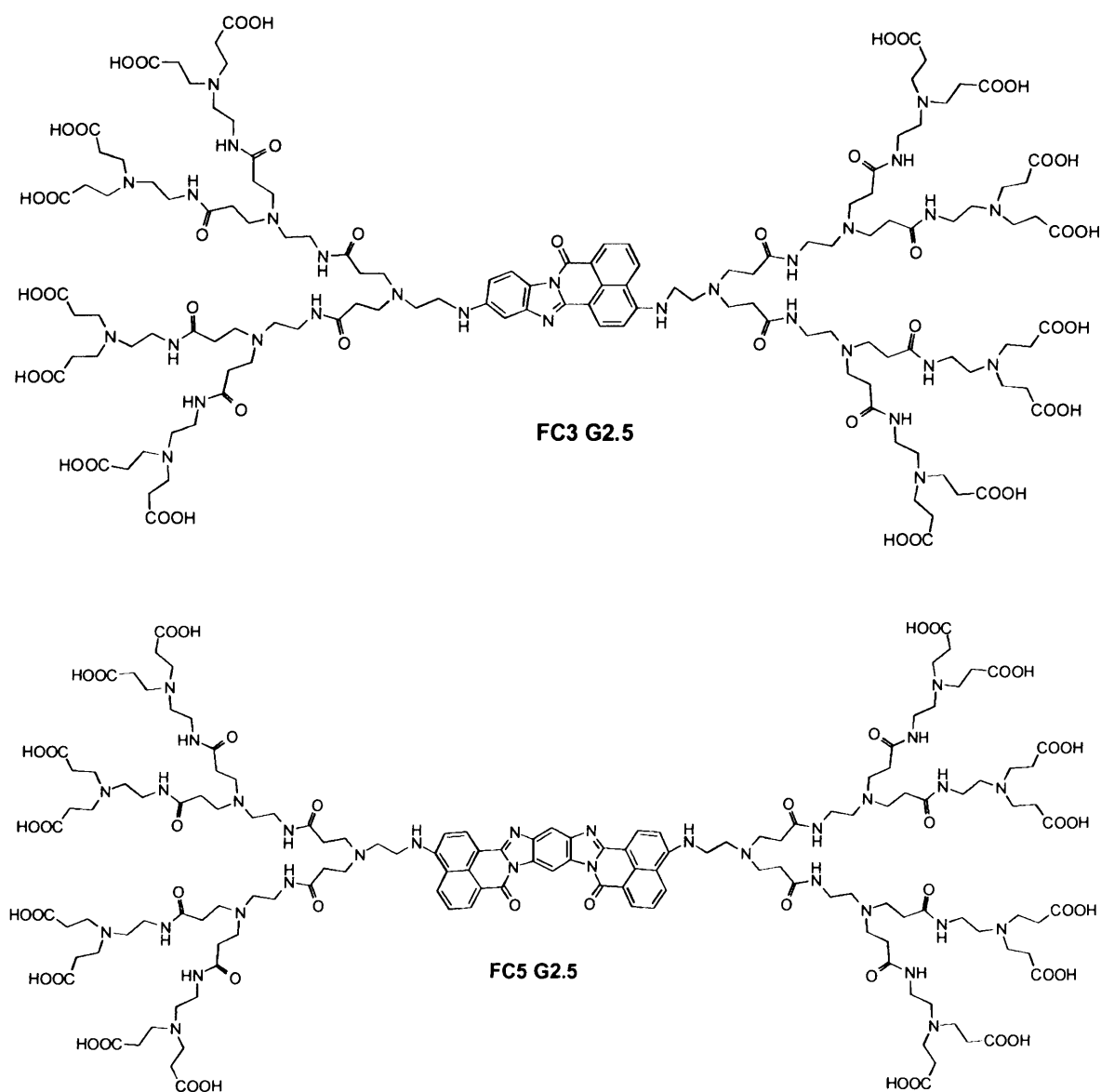


**Figure [5.1]:** New fluorescent PAMAM dendritic double wedges **FC3G2.5**, **FC5G2.5**

### 5.1.3 Self assembled core of fluorescent PAMAM Dendritic wedges.

Dendron self assembly can result from weak noncovalent interactions (e.g. van der Waals, hydrophobic forces,  $\pi - \pi$  interactions, hydrogen bonds) as opposed to more "classical" covalent, ionic or metallic bonds. It would be of interest to use intermolecular self-assembly to form a supradendrimer assembly (Figure 5.3) with enhanced fluorescence emission. Of particular interest will be the use of  $\pi - \pi$  interactions and hydrogen bonding for self-assembly.

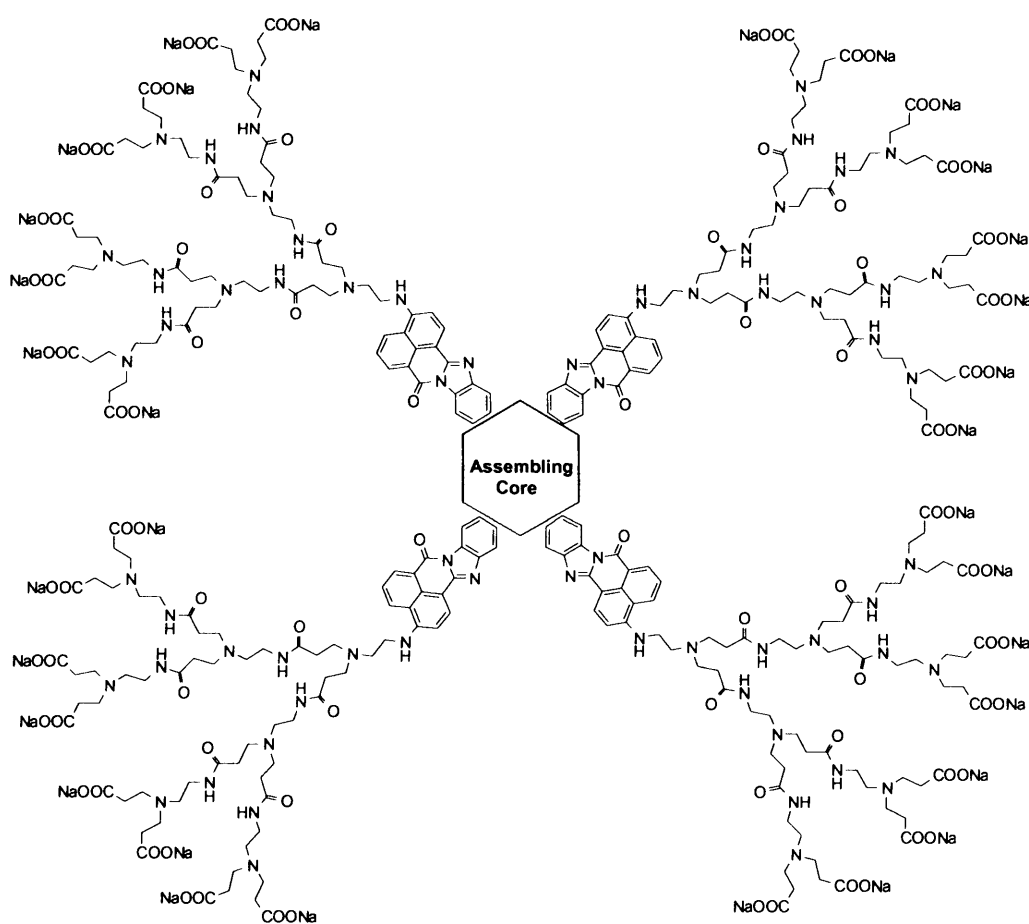
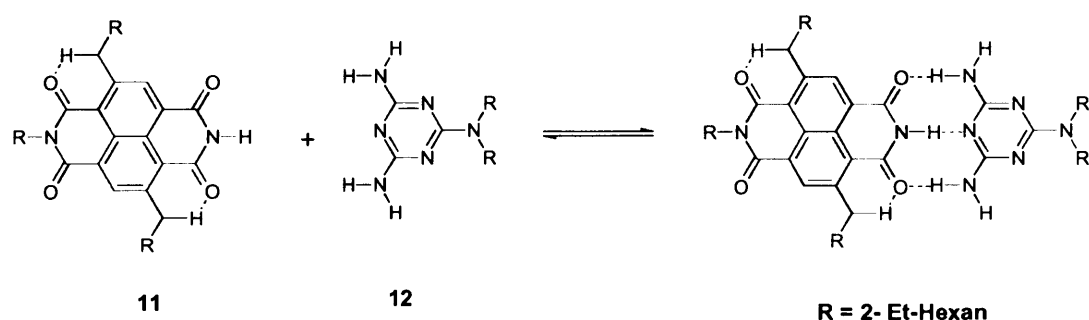


Figure [5.2]: Possible structure for self assembly fluorescent core dendrimer.

For example, melamine-based systems compounds are proven H-bonding units that have been used for the self assembly of fluorescent core derived from naphthalene derivatives (Scheme 5.3).<sup>[235]</sup> We are more interested in  $\pi$ - $\pi$  interactions because they act strongly on flat polycyclic aromatic hydrocarbons such those uses for fluorescent cores.



**Scheme [5.3]:** Formation of a hydrogen bonded complex of 1 : 1 stoichiometry between the monotopic naphthalene bisimide **11** and melamine **12**.

## 5.2 Chemotherapeutic applications

Through new and continued co-operation with other research groups, we would be interested in developing the applications of our fluorescent dendron in the following areas.

### 5.2.1 Inhibitor of protein aggregation.

Some diseases are related to large insoluble protein aggregates resulting from abnormal protein folding and protein binding behaviour. Twyman's group have recently developed a dendrimer-based methodology for studying the various contributing factors to protein-protein interactions instead of the conventional small molecule approach.<sup>[236]</sup> For example it was found that PAMAM dendrimers bind more strongly to proteins of similar size (e.g. cytochrome-c to G2 and PAMAM

chymotrypsin to G3 PAMAM) (Figure 5.4) so that the dendrimer that binds best has a maximum addressable area of similar dimensions to the interfacial area of the protein.<sup>[29]</sup>

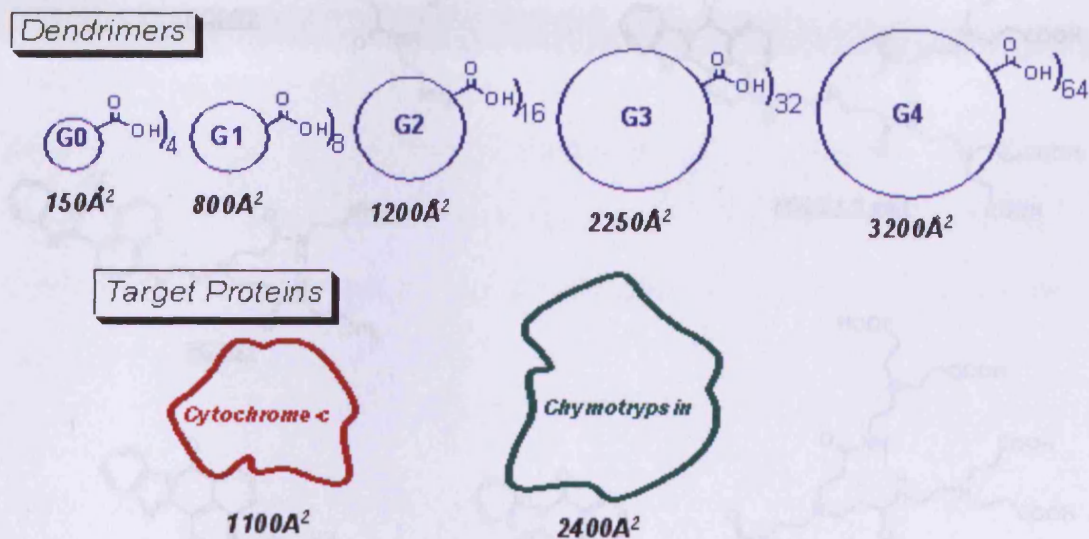


**Figure [5.4]:** Schematic showing the relative size of PAMAM dendrimers and proteins used for binding studies. The maximum addressable and interfacial areas are shown below each dendrimer and protein respectively.<sup>[29]</sup>

A similar methodology could be applied to the same two proteins but by using different generations of our fluorescent PAMAM dendritic systems terminated with  $-\text{COOH}$  or  $\text{NH}_2$  (Figure 5.5) to be used as a protein inhibitor and biosensor simultaneously.

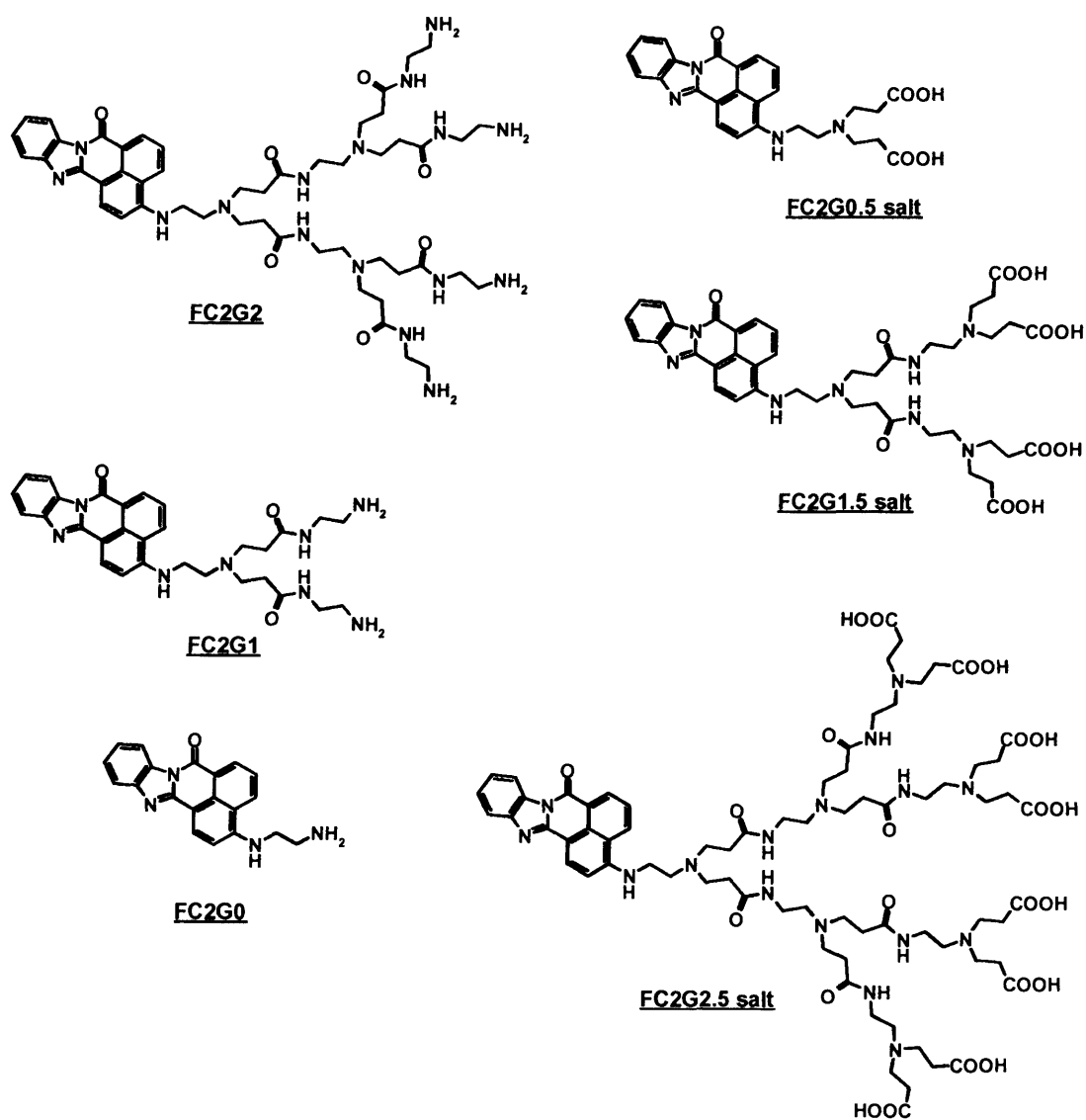
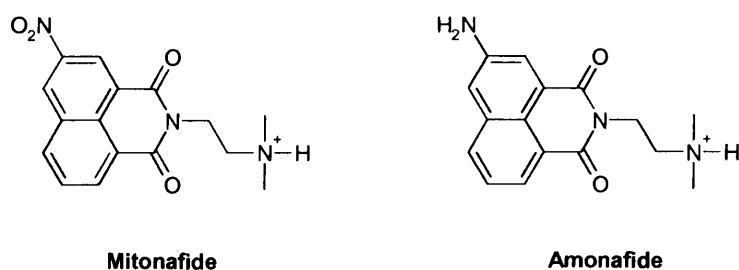


Figure [5.5]: Fluorescent poly(amidoamine) (PAMAM) dendrons (FC2G0 - FC2G2.5)

### 5.2.2. Anticancer activity studies.

Recently, much effort has been made by researchers to discover and produce new anticancer drugs with no undesirable side effects.<sup>[237]</sup> DNA intercalators are new potential anticancer agents,<sup>[184]</sup> which are mostly described as planar heterocyclic molecules with approximately the same size and shape of a DNA base pair.<sup>[238]</sup> DNA intercalators interact with DNA by inserting perpendicularly into DNA and their stability depends on van der Waals, hydrophobic, hydrogen bonding, and charge transfer forces.<sup>[239]</sup> The results of this interaction can cause disfiguration of the DNA double helix, affecting the process of cell replication and leading to cellular passing away and special genotoxic effects.<sup>[240]</sup>

There are very strong interactions between protonated polyamines and DNA phosphate residues,<sup>[241]</sup> hence there are many examples of naphthalimide derivatives as anticancer agents.<sup>[184-188]</sup> These examples are where the aromatic system is inserted between the DNA base pairs whilst the protonated amine base interacts with grooves.<sup>[242]</sup> Compounds Mitonafide and Amonafide (Figure 5.6) are the most famous trial compounds of the naphthalimide series for anticancer activity, but they are highly toxic.<sup>[189-190]</sup> Hence, the desire for analogues.<sup>[243-245]</sup>



**Figure [5.6]:** Chemical structures of compound Mitonafide and Amonafide.

Derivatives of naphthalimide and naphthalimide polyamine conjugates are currently under investigation for use as anti-tumor agents.<sup>[246]</sup> Due to the strong interactions between DNA and protonated polyamines, many interesting assemblages of polyamines and DNA intercalators can be employed as linear,<sup>[247-248]</sup> macrocyclic,<sup>[249]</sup> or dendronic polyamines.<sup>[141]</sup>

Dendritic polyamine–(imide–DNA intercalator) conjugates have been modified to conjugate naphthalimide derivatives with the chromophore as antitumour compound (Figure 5.7).<sup>[141]</sup>

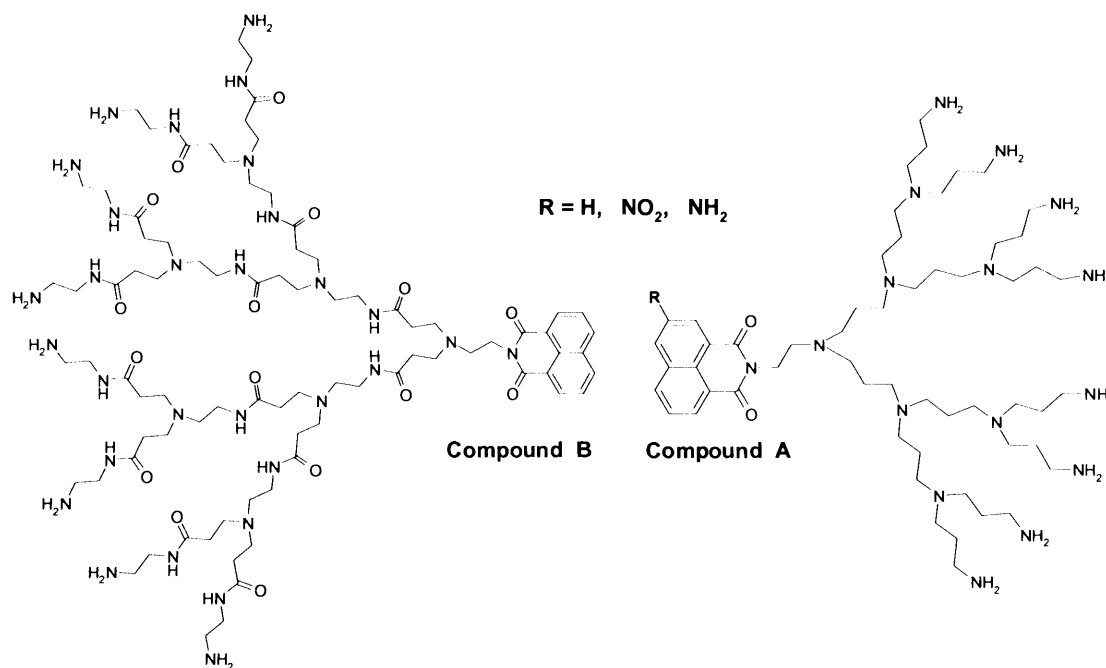


**Figure [5.7]:** Compound A: “PAMAM dendritic polyamines–(imide–DNA intercalator)” conjugates, Compound B: “PPI dendritic polyamines–(imide–DNA intercalator)”.<sup>[141]</sup>

The PAMAM dendritic wedges that contain fluorescent cores studied in this project have yet to be investigated for this application. Thus, the pharmacological activity of such compounds could be significant, especially they show strong DNA binding.<sup>[246]</sup>

# REFERENCES

---

## References

1. Moorefield, C.N. and G.R. Newkome, *Unimolecular micelles: supramolecular use of dendritic constructs to create versatile molecular containers*. C. R. Chim., 2003. **6**(8-10): p. 715-724.
2. Jansen, J.F.G.A., E.M.M. de Brabander van den Berg, and E.W. Meijer, *Encapsulation of guest molecules into a dendritic box*. Science (Washington, D. C.), 1994. **266**(5188): p. 1226-9.
3. Morgan, M.T., et al., *Dendritic Molecular Capsules for Hydrophobic Compounds*. J. Am. Chem. Soc., 2003. **125**(50): p. 15485-15489.
4. Vutukuri, D.R., S. Basu, and S. Thayumanavan, *Dendrimers with both polar and apolar nanocontainer characteristics*. J. Am. Chem. Soc., 2004. **126**(48): p. 15636-15637.
5. Adronov, A. and J.M.J. Frechet, *Light-harvesting dendrimers*. Chem. Commun. (Cambridge), 2000(18): p. 1701-1710.
6. Grayson, S.M. and J.M.J. Frechet, *Convergent Dendrons and Dendrimers: from Synthesis to Applications*. Chem. Rev. (Washington, D. C.), 2001. **101**(12): p. 3819-3867.
7. Ihre, H.R., et al., *Polyester Dendritic Systems for Drug Delivery Applications: Design, Synthesis, and Characterization*. Bioconjugate Chem., 2002. **13**(3): p. 443-452.
8. Gitsov, I., et al., *Synthesis and properties of novel linear-dendritic block copolymers. Reactivity of dendritic macromolecules toward linear polymers*. Macromolecules, 1993. **26**(21): p. 5621-7.
9. Gillies, E.R. and J.M.J. Frechet, *Designing Macromolecules for Therapeutic Applications: Polyester Dendrimer-Poly(ethylene oxide) "Bow-Tie" Hybrids with Tunable Molecular Weight and Architecture*. J. Am. Chem. Soc., 2002. **124**(47): p. 14137-14146.
10. Gillies, E.R., et al., *Biological Evaluation of Polyester Dendrimer: Poly(ethylene oxide) "Bow-Tie" Hybrids with Tunable Molecular Weight and Architecture*. Mol. Pharm., 2005. **2**(2): p. 129-138.
11. Lee, C.C., S.M. Grayson, and J.M.J. Frechet, *Synthesis of narrow-polydispersity degradable dendronized aliphatic polyesters*. J. Polym. Sci., Part A Polym. Chem., 2004. **42**(14): p. 3563-3578.
12. Yoshida, M., et al., *Efficient Divergent Synthesis of Dendronized Polymers with Extremely High Molecular Weight: Structural Characterization by SEC-MALLS and SFM and Novel Organic Gelation Behavior*. Macromolecules, 2005. **38**(2): p. 334-344.
13. Helms, B., et al., *Dendronized Linear Polymers via "Click Chemistry"*. J. Am. Chem. Soc., 2004. **126**(46): p. 15020-15021.
14. Gillies, E.R. and J.M.J. Frechet, *Dendrimers and dendritic polymers in drug delivery*. Drug Discovery Today, 2005. **10**(1): p. 35-43.
15. Medina, S.H. and M.E.H. El-Sayed, *Dendrimers as Carriers for Delivery of Chemotherapeutic Agents*. Chem. Rev. (Washington, DC, U. S.), 2009. **109**(7): p. 3141-3157.
16. Morgan, M.T., et al., *Dendrimer-Encapsulated Camptothecins: Increased Solubility, Cellular Uptake, and Cellular Retention Affords Enhanced Anticancer Activity In vitro*. Cancer Res., 2006. **66**(24): p. 11913-11921.
17. Grinstaff, M.W., *Biodendrimers: new polymeric biomaterials for tissue engineering*. Chem.--Eur. J., 2002. **8**(13): p. 2838-2846.

18. Goodwin, A.P., S.S. Lam, and J.M.J. Frechet, *Rapid, Efficient Synthesis of Heterobifunctional Biodegradable Dendrimers*. J. Am. Chem. Soc., 2007. **129**(22): p. 6994-6995.
19. Padilla De Jesus, O.L., et al., *Polyester Dendritic Systems for Drug Delivery Applications: In Vitro and In Vivo Evaluation*. Bioconjugate Chem., 2002. **13**(3): p. 453-461.
20. Mulders, S.J.E., et al., *Synthesis of a novel amino acid based dendrimer*. Tetrahedron Lett., 1997. **38**(4): p. 631-634.
21. McGrath, D.V., M.-J. Wu, and U. Chaudhry, *An approach to highly functionalized dendrimers from chiral, non-racemic synthetic monomers*. Tetrahedron Lett., 1996. **37**(34): p. 6077-6080.
22. Ozawa, C., et al., *Efficient Sequential Segment Coupling Using N-Alkylcysteine-Assisted Thioesterification for Glycopeptide Dendrimer Synthesis*. Org. Lett., 2008. **10**(16): p. 3531-3533.
23. Patri, A.K., I.J. Majoros, and J.R. Baker, *Dendritic polymer macromolecular carriers for drug delivery*. Curr. Opin. Chem. Biol., 2002. **6**(4): p. 466-471.
24. Lee, J.W., et al., *Synthesis of symmetrical and unsymmetrical PAMAM dendrimers by fusion between azide- and alkyne functionalized PAMAM dendrons*. Bioconjugate Chem., 2007. **18**(2): p. 579-584.
25. Esfand, R. and D.A. Tomalia, *Poly(amidoamine) (PAMAM) dendrimers: from biomimicry to drug delivery and biomedical applications*. Drug Discovery Today, 2001. **6**(8): p. 427-436.
26. Wiwattanapatapee, R., et al., *Anionic PAMAM dendrimers rapidly cross adult rat intestine in vitro: a potential oral delivery system?* Pharm. Res., 2000. **17**(8): p. 991-998.
27. El-Sayed, M., et al., *Transepithelial transport of poly(amidoamine) dendrimers across Caco-2 cell monolayers*. J. Controlled Release, 2002. **81**(3): p. 355-365.
28. El-Sayed, M., et al., *Influence of surface chemistry of poly(amidoamine) dendrimers on caco-2 cell monolayers*. J. Bioact. Compat. Polym., 2003. **18**(1): p. 7-22.
29. Chiba, F., et al., *Dendritic macromolecules as inhibitors to protein-protein binding*. Macromol. Symp., 2010. **287**(Macro- and Supramolecular Architectures and Materials): p. 37-41.
30. Wang, D., T. Imae, and M. Miki, *Fluorescence emission from PAMAM and PPI dendrimers*. J. Colloid Interface Sci., 2007. **306**(2): p. 222-227.
31. Grabchev, I., et al., *Synthesis and photophysical properties of 1,8-naphthalimide-labelled PAMAM as PET sensors of protons and of transition metal ions*. Polymer, 2002. **43**(21): p. 5731-5736.
32. Grabchev, I., et al., *Poly(amidoamine) dendrimers peripherally modified with 4-ethylamino-1,8-naphthalimide. Synthesis and photophysical properties*. Tetrahedron, 2003. **59**(48): p. 9591-9598.
33. Grabchev, I., et al., *Poly(amidoamine) dendrimers peripherally modified with 1,8-naphthalimides. Photodegradation and photostabilization on polyamide matrix*. Eur. Polym. J., 2004. **40**(6): p. 1249-1254.
34. Grabchev, I., D. Staneva, and R. Betcheva, *Sensor activity, photodegradation and photostabilization of a PAMAM dendrimer comprising 1,8-naphthalimide functional groups in its periphery*. Polym. Degrad. Stab., 2006. **91**(10): p. 2257-2264.

35. Sali, S., et al., *Selective sensors for Zn<sup>2+</sup> cations based on new green fluorescent poly(amidoamine) dendrimers peripherally modified with 1,8-naphthalimides*. Spectrochim. Acta, Part A, 2006. **65A**(3-4): p. 591-597.
36. Grabchev, I., et al., *Synthesis and spectral properties of new green fluorescent poly(propyleneimine) dendrimers modified with 1,8-naphthalimide as sensors for metal cations*. Polymer, 2007. **48**(23): p. 6755-6762.
37. Yang, S.-P., et al., *The fluorescence of polyamidoamine dendrimers peripherally modified with 1,8-naphthalimide groups: Effect of the rare earth ions and protons*. J. Lumin., 2007. **126**(2): p. 515-530.
38. Li, W.-S., et al., *Synthesis and energy-transfer properties of poly(amidoamine) dendrons modified with naphthyl and dansyl groups*. Tetrahedron Letters, 2008. **49**(12): p. 1988-1992.
39. Waengler, C., et al., *PAMAM structure-based multifunctional fluorescent conjugates for improved fluorescent labelling of biomacromolecules*. Chem.--Eur. J., 2008. **14**(27): p. 8116-8130.
40. Tomalia, D.A., et al., *A new class of polymers: starburst-dendritic macromolecules*. Polym. J. (Tokyo), 1985. **17**(1): p. 117-32.
41. Twyman, L.J., et al., *The synthesis of water soluble dendrimers, and their application as possible drug delivery systems*. Tetrahedron Lett., 1999. **40**(9): p. 1743-1746.
42. Pittelkow, M. and J.B. Christensen, *Convergent Synthesis of Internally Branched PAMAM Dendrimers*. Org. Lett., 2005. **7**(7): p. 1295-1298.
43. Kim, Y., F. Zeng, and S.C. Zimmerman, *Peptide dendrimers from natural amino acids*. Chem.--Eur. J., 1999. **5**(7): p. 2133-2138.
44. Romagnoli, B., et al., *Chiral poly(aromatic amide ester) dendrimers bearing an amino acid derived C<sub>3</sub>-symmetric core - synthesis and properties*. Eur. J. Org. Chem., 2004(20): p. 4148-4157.
45. Twyman, L.J., A.E. Beezer, and J.C. Mitchell, *The synthesis of chiral dendritic molecules based on the repeat unit L-glutamic acid*. Tetrahedron Lett., 1994. **35**(25): p. 4423-4.
46. Rannard, S., N. Davis, and H. McFarland, *Synthesis of dendritic polyamides using novel selective chemistry*. Polym. Int., 2000. **49**(9): p. 1002-1006.
47. Brouwer, A.J., S.J.E. Mulders, and R.M.J. Liskamp, *Convergent synthesis and diversity of amino acid based dendrimers*. Eur. J. Org. Chem., 2001(10): p. 1903-1915.
48. Vinogradov, S.A., L.-W. Lo, and D.F. Wilson, *Dendritic polyglutamic porphyrins: probing porphyrin protection by oxygen-dependent quenching of phosphorescence*. Chem.--Eur. J., 1999. **5**(4): p. 1338-1347.
49. Lee, J.W., J.H. Kim, and B.-K. Kim, *Synthesis of azide-functionalized PAMAM dendrons at the focal point and their application for synthesis of PAMAM-like dendrimers*. Tetrahedron Lett., 2006. **47**(16): p. 2683-2686.
50. Lee, J.W., et al., *Convergent synthesis of PAMAM dendrimers using click chemistry of azide-functionalized PAMAM dendrons*. Tetrahedron, 2006. **62**(39): p. 9193-9200.
51. King, A.S.H., I.K. Martin, and L.J. Twyman, *Synthesis and aggregation of amine cored polyamidoamine dendrons synthesized without invoking a protection/deprotection strategy*. Polym. Int., 2006. **55**(7): p. 798-807.
52. Zhang, X.-Q., et al., *In vitro gene delivery using polyamidoamine dendrimers with a trimesyl core*. Biomacromolecules, 2005. **6**(1): p. 341-350.

53. Brana, M.F., et al., *Synthesis and antitumour activity of new dendritic polyamines-(imide-DNA-intercalator) conjugates: potent Lck inhibitors*. Eur. J. Med. Chem., 2002. **37**(7): p. 541-551.
54. Bojinov, V.B., N.I. Georgiev, and P.S. Nikolov, *Design and synthesis of core and peripherally functionalized with 1,8-naphthalimide units fluorescent PAMAM dendron as light harvesting antenna*. Journal of Photochemistry and Photobiology A: Chemistry, 2008. **197**(2-3): p. 281-289.
55. Wang, D. and T. Imae, *Fluorescence Emission from Dendrimers and Its pH Dependence*. J. Am. Chem. Soc., 2004. **126**(41): p. 13204-13205.
56. Takaguchi, Y., et al., *Facile and reversible synthesis of an acidic water-soluble poly(amidoamine) fullerodendrimer*. Tetrahedron Lett., 2003. **44**(31): p. 5777-5780.
57. Hirano, C., et al., *Fabrication and Properties of Fullerodendron Thin Films*. Langmuir, 2005. **21**(1): p. 272-279.
58. Wang, B.-B., et al., *Self-assembly and supramolecular transition of poly(amidoamine) dendrons focally modified with aromatic chromophores*. J. Colloid Interface Sci., 2007. **314**(1): p. 289-296.
59. A. D'Emanuele, D. Attwood, and R. A. Rmaileh, *Dendrimers*. In: J. Swarbrick and J.C. Boylan, Editors,. Encyclopedia of Pharmaceutical Technology, Marcel Dekker 2003: p. pp. 1-21.
60. Duncan, R. and L. Izzo, *Dendrimer biocompatibility and toxicity*. Adv. Drug Delivery Rev., 2005. **57**(15): p. 2215-2237.
61. Tomalia, D.A., et al., *Dendritic macromolecules: synthesis of starburst dendrimers*. Macromolecules, 1986. **19**(9): p. 2466-8.
62. Tomalia, D.A., A.M. Naylor, and W.A. Goddard, III, *Starburst dendrimers: control of size, shape, surface chemistry, topology and flexibility in the conversion of atoms to macroscopic materials*. Angew. Chem., 1990. **102**(2): p. 119-57.
63. Malik, N., E.G. Evagorou, and R. Duncan, *Dendrimer-platinate: a novel approach to cancer chemotherapy*. Anti-Cancer Drugs, 1999. **10**(8): p. 767-776.
64. Haensler, J. and F.C. Szoka, Jr., *Polyamidoamine cascade polymers mediate efficient transfection of cells in culture*. Bioconjugate Chem., 1993. **4**(5): p. 372-9.
65. Yoo, H., P. Sazani, and R.L. Juliano, *PAMAM dendrimers as delivery agents for antisense oligonucleotides*. Pharm. Res., 1999. **16**(12): p. 1799-1804.
66. Buhleier, E., W. Wehner, and F. Voegtle, *"Cascade"- and "nonskid-chain-like" syntheses of molecular cavity topologies*. Synthesis, 1978(2): p. 155-8.
67. Chauhan, A.S., et al., *Solubility enhancement of poorly water soluble molecules using dendrimers*. Mater. Matters (Milwaukee, WI, U. S.), 2007. **2**(1): p. 24-26.
68. Bhadra, D., et al., *A PEGylated dendritic nanoparticulate carrier of fluorouracil*. Int. J. Pharm., 2003. **257**(1-2): p. 111-124.
69. Patri, A.K., J.F. Kukowska-Latallo, and J.R. Baker, *Targeted drug delivery with dendrimers: Comparison of the release kinetics of covalently conjugated drug and non-covalent drug inclusion complex*. Adv. Drug Delivery Rev., 2005. **57**(15): p. 2203-2214.
70. Kojima, C., et al., *Synthesis of Polyamidoamine Dendrimers Having Poly(ethylene glycol) Grafts and Their Ability To Encapsulate Anticancer Drugs*. Bioconjugate Chem., 2000. **11**(6): p. 910-917.

71. Rihova, B., et al., *Doxorubicin bound to a HPMA copolymer carrier through hydrazone bond is effective also in a cancer cell line with a limited content of lysosomes*. J. Controlled Release, 2001. **74**(1-3): p. 225-232.
72. Wiener, E.C., et al., *Dendrimer-based metal chelates: a new class of magnetic resonance imaging contrast agents*. Magn. Reson. Med., 1994. **31**(1): p. 1-8.
73. Margerum, L.D., et al., *Gadolinium(III) DO3A macrocycles and polyethylene glycol coupled to dendrimers. Effect of molecular weight on physical and biological properties of macromolecular magnetic resonance imaging contrast agents*. J. Alloys Compd., 1997. **249**(1-2): p. 185-190.
74. Ziemer, L.S., et al., *Oxygen distribution in murine tumors: characterization using oxygen-dependent quenching of phosphorescence*. J. Appl. Physiol., 2005. **98**(4): p. 1503-1510.
75. Lee, C.C., et al., *Designing dendrimers for biological applications*. Nat. Biotechnol., 2005. **23**(12): p. 1517-1526.
76. Nishikawa, M., Y. Takakura, and M. Hashida, *Pharmacokinetic evaluation of polymeric carriers*. Adv. Drug Delivery Rev., 1996. **21**(2): p. 135-155.
77. Tomalia, D.A. and J.M.J. Frechet, *Discovery of dendrimers and dendritic polymers: a brief historical perspective*. J. Polym. Sci., Part A Polym. Chem., 2002. **40**(16): p. 2719-2728.
78. Tekade, R.K., P.V. Kumar, and N.K. Jain, *Dendrimers in Oncology: An Expanding Horizon*. Chem. Rev. (Washington, DC, U. S.), 2009. **109**(1): p. 49-87.
79. Tomalia, D.A., A.M. Naylor, and W.A. Goddard, *Starburst Dendrimers: Molecular-Level Control of Size, Shape, Surface Chemistry, Topology, and Flexibility from Atoms to Macroscopic Matter*. Angewandte Chemie International Edition in English, 1990. **29**(2): p. 138-175.
80. Bouit, P.-A., et al., *Dendron-decorated cyanine dyes for optical limiting applications in the range of telecommunication wavelengths*. New J. Chem., 2009. **33**(5): p. 964-968.
81. Caminade, A.-M., A. Hameau, and J.-P. Majoral, *Multicharged and/or Water-Soluble Fluorescent Dendrimers: Properties and Uses*. Chem.--Eur. J., 2009. **15**(37): p. 9270-9285.
82. Caminati, G., N.J. Turro, and D.A. Tomalia, *Photophysical investigation of starburst dendrimers and their interactions with anionic and cationic surfactants*. J. Am. Chem. Soc., 1990. **112**(23): p. 8515-22.
83. Larson, C.L. and S.A. Tucker, *Intrinsic fluorescence of carboxylate-terminated polyamidoamine dendrimers*. Appl. Spectrosc., 2001. **55**(6): p. 679-683.
84. Lee, W.I., Y. Bae, and A.J. Bard, *Strong Blue Photoluminescence and ECL from OH-Terminated PAMAM Dendrimers in the Absence of Gold Nanoparticles*. J. Am. Chem. Soc., 2004. **126**(27): p. 8358-8359.
85. Huang, J.-F., et al., *Hydrophobic Bronsted Acid-Base Ionic Liquids Based on PAMAM Dendrimers with High Proton Conductivity and Blue Photoluminescence*. J. Am. Chem. Soc., 2005. **127**(37): p. 12784-12785.
86. Jayamurugan, G., C.P. Umesh, and N. Jayaraman, *Inherent Photoluminescence Properties of Poly(propyl ether imine) Dendrimers*. Org. Lett., 2008. **10**(1): p. 9-12.
87. Al-Jamal, K.T., et al., *An intrinsically fluorescent dendrimer as a nanoprobe of cell transport*. J. Drug Targeting, 2006. **14**(6): p. 405-412.

88. Wang, B.-B., et al., *Poly(amidoamine) dendrimers with phenyl shells: fluorescence and aggregation behavior*. *Polymer*, 2004. **45**(25): p. 8395-8402.
89. Martinez-Ferrero, E., et al., *Optical properties of hybrid dendritic-mesoporous titania nanocomposite films*. *Chem.--Eur. J.*, 2008. **14**(25): p. 7658-7669.
90. Lartigue, M.-L., et al., *Phosphorus-containing dendrimers: synthesis of macromolecules with multiple tri- and tetrafunctionlization*. *Chem.--Eur. J.*, 1996. **2**(11): p. 1417-1426.
91. Fuchs, S., et al., *A surface-modified dendrimer set for potential application as drug delivery vehicles: synthesis, in vitro toxicity, and intracellular localization*. *Chem.--Eur. J.*, 2004. **10**(5): p. 1167-1192.
92. Yoo, H. and R.L. Juliano, *Enhanced delivery of antisense oligonucleotides with fluorophore-conjugated PAMAM dendrimers*. *Nucleic Acids Res.*, 2000. **28**(21): p. 4225-4231.
93. Seib, F.P., A.T. Jones, and R. Duncan, *Comparison of the endocytic properties of linear and branched PEIs, and cationic PAMAM dendrimers in B16f10 melanoma cells*. *J. Controlled Release*, 2007. **117**(3): p. 291-300.
94. Stasko, N.A., et al., *Cytotoxicity of Polypropylenimine Dendrimer Conjugates on Cultured Endothelial Cells*. *Biomacromolecules*, 2007. **8**(12): p. 3853-3859.
95. Hayek, A., et al., *Conjugation of a New Two-Photon Fluorophore to Poly(ethylenimine) for Gene Delivery Imaging*. *Bioconjugate Chem.*, 2007. **18**(3): p. 844-851.
96. Talanov, V.S., et al., *Dendrimer-Based Nanoprobe for Dual Modality Magnetic Resonance and Fluorescence Imaging*. *Nano Lett.*, 2006. **6**(7): p. 1459-1463.
97. Puckett, C.A. and J.K. Barton, *Fluorescein Redirects a Ruthenium-Octaarginine Conjugate to the Nucleus*. *J. Am. Chem. Soc.*, 2009. **131**(25): p. 8738-8739.
98. Hecht, S. and J.M.J. Frechet, *Dendritic encapsulation of function: applying nature's site isolation principle from biomimetics to materials science*. *Angew. Chem., Int. Ed.*, 2001. **40**(1): p. 74-91.
99. Dandliker, P.J., et al., *Water-soluble dendritic iron porphyrins: synthetic models of globular heme proteins*. *Angew. Chem., Int. Ed. Engl.*, 1996. **34**(23/24): p. 2725-8.
100. Kimura, M., et al., *Dendritic metallophthalocyanines: synthesis and characterization of a zinc(II) phthalocyanine[8]3-arborol*. *Chem. Commun. (Cambridge)*, 1997(13): p. 1215-1216.
101. Ng, A.C.H., X.-y. Li, and D.K.P. Ng, *Synthesis and Photophysical Properties of Nonaggregated Phthalocyanines Bearing Dendritic Substituents*. *Macromolecules*, 1999. **32**(16): p. 5292-5298.
102. Leclaire, J., et al., *Nanometric Sponges Made of Water-Soluble Hydrophobic Dendrimers*. *J. Am. Chem. Soc.*, 2004. **126**(8): p. 2304-2305.
103. Leclaire, J., et al., *Octasubstituted Metal-Free Phthalocyanine as Core of Phosphorus Dendrimers: A Probe for the Properties of the Internal Structure*. *J. Am. Chem. Soc.*, 2005. **127**(45): p. 15762-15770.
104. Leclaire, J., et al., *Metallated phthalocyanines as the core of dendrimers - synthesis and spectroscopic studies*. *Eur. J. Inorg. Chem.*, 2007(18): p. 2890-2896.
105. Maszewska, M., et al., *Water-Soluble Polycationic Dendrimers with a Phosphoramidothioate Backbone: Preliminary Studies of Cytotoxicity and*

- Oligonucleotide/Plasmid Delivery in Human Cell Culture*. Oligonucleotides, 2003. **13**(4): p. 193-205.
106. Suelue, M., A. Altindal, and O. Bekaroglu, *Synthesis, characterization and electrical and CO<sub>2</sub> sensing properties of triazine containing three dendritic phthalocyanine*. Synth. Met., 2005. **155**(1): p. 211-221.
107. Hayakawa, J., et al., *Solvent Effect on the Photochemical Properties of Symmetrically Substituted trans-3,3',5,5'-Tetramethoxystilbene*. J. Phys. Chem. A, 2006. **110**(46): p. 12566-12571.
108. Schmidt, C.D., C. Bottcher, and A. Hirsch, *Synthesis and aggregation properties of water-soluble Newkome-dendronized perylenetetracarboxydiimides*. Eur. J. Org. Chem., 2007(33): p. 5497-5505.
109. Denk, W., J.H. Strickler, and W.W. Webb, *Two-photon laser scanning fluorescence microscopy*. Science, 1990. **248**(4951): p. 73-6.
110. Krishna, T.R., et al., *Water-soluble dendrimeric two-photon tracers for in vivo imaging*. Angew. Chem., Int. Ed., 2006. **45**(28): p. 4645-4648.
111. Mongin, O., et al., *Brilliant organic nanodots: novel nano-objects for bionanophotonics*. Proc. SPIE, 2008. **7040**(Nanobiosystems: Processing, Characterization, and Applications): p. 704006/1-704006/12.
112. Almutairi, A., et al., *Monitoring the biodegradation of dendritic near-infrared nanoprobe by in vivo fluorescence imaging*. Mol Pharm, 2008. **5**(6): p. 1103-10.
113. Sun, Y.P., P. Wang, and N.B. Hamilton, *Fluorescence spectra and quantum yields of buckminsterfullerene (C<sub>60</sub>) in room-temperature solutions. No excitation wavelength dependence*. J. Am. Chem. Soc., 1993. **115**(14): p. 6378-81.
114. Texier, I., et al., *Photophysics and Photochemistry of a Water-Soluble C<sub>60</sub> Dendrimer: Fluorescence Quenching by Halides and Photoinduced Oxidation of I*. J. Phys. Chem. A, 2001. **105**(45): p. 10278-10285.
115. Sarova, G.H., et al., *Testing electron transfer within molecular associates built around anionic C<sub>60</sub> and C<sub>70</sub> dendrofullerenes and a cationic zinc porphyrin*. Chem.--Eur. J., 2008. **14**(10): p. 3137-3145.
116. Takaguchi, Y., et al., *Reversible binding of C<sub>60</sub> to an anthracene bearing a dendritic poly(amidoamine) substituent to give a water-soluble fullerodendrimer*. Angew. Chem., Int. Ed., 2002. **41**(5): p. 817-819.
117. Cardona, C.M., et al., *Dendrimers Functionalized with a Single Pyrene Label: Synthesis, Photophysics, and Fluorescence Quenching*. J. Phys. Chem. B, 2002. **106**(34): p. 8649-8656.
118. Mohanty, S.K., et al., *Self-Association of Protected Newkome-Type Second-Generation Dendrimers at Nanomolar Level Concentrations in Aqueous Solution*. Macromolecules, 2004. **37**(14): p. 5364-5369.
119. Mohanty, S.K., et al., *Photophysical properties of Newkome-type dendrimers in aqueous medium*. Photochem. Photobiol. Sci., 2007. **6**(11): p. 1164-1169.
120. Ogawa, M., A. Momotake, and T. Arai, *Water-soluble poly(aryl ether) dendrimers as a potential fluorescent detergent to form micelles at very low CMC*. Tetrahedron Lett., 2004. **45**(46): p. 8515-8518.
121. Cardona, C.M., et al., *Dendrimers functionalized with a single fluorescent dansyl group attached "off center": synthesis and photophysical studies*. J. Am. Chem. Soc., 2000. **122**(26): p. 6139-6144.

122. Qualmann, B., et al., *Synthesis of boron-rich lysine dendrimers as protein labels in electron microscopy*. *Angew. Chem., Int. Ed. Engl.*, 1996. **35**(8): p. 909-911.
123. Barker, S.L.R., et al., *Cellular Applications of a Sensitive and Selective Fiber-Optic Nitric Oxide Biosensor Based on a Dye-Labeled Heme Domain of Soluble Guanylate Cyclase*. *Anal. Chem.*, 1999. **71**(11): p. 2071-2075.
124. Parthenopoulos, D.A. and P.M. Rentzepis, *Three-dimensional optical storage memory*. *Science (Washington, D. C., 1883-)*, 1989. **245**(4920): p. 843-5.
125. Denk, W., J.H. Strickler, and W.W. Webb, *Two-photon laser scanning fluorescence microscopy*. *Science (Washington, D. C., 1883-)*, 1990. **248**(4951): p. 73-6.
126. Thomas, T.P., et al., *Tissue distribution and real-time fluorescence measurement of a tumor-targeted nanodevice by a two photon optical fiber fluorescence probe*. *Proc. SPIE-Int. Soc. Opt. Eng.*, 2006. **6095**(Nanobiophotonics and Biomedical Applications III): p. 60950Q/1-60950Q/7.
127. Majoros, I.J., et al., *Poly(amidoamine) dendrimer-based multifunctional engineered nanodevice for cancer therapy*. *J. Med. Chem.*, 2005. **48**(19): p. 5892-5899.
128. Thomas, T.P., et al., *Investigation of tumor cell targeting of a dendrimer nanoparticle using a double-clad optical fiber probe*. *J. Biomed. Opt.*, 2008. **13**(1): p. 014024/1-014024/6.
129. Fuchs, S., et al., *Fluorescent dendrimers with a peptide cathepsin B cleavage site for drug delivery applications*. *Chem. Commun. (Cambridge, U. K.)*, 2005(14): p. 1830-1832.
130. Guilbault, G.G., *Principles of luminescence spectroscopy. Luminescent determination of clinically and agriculturally important samples*. *Pure Appl. Chem.*, 1985. **57**(3): p. 495-514.
131. Zimmermann, J., A. Zeug, and B. Roeder, *A generalization of the Jablonski diagram to account for polarization and anisotropy effects in time-resolved experiments*. *Phys. Chem. Chem. Phys.*, 2003. **5**(14): p. 2964-2969.
132. Babinski, K., et al., *Methods using benzoisoquinolines and benzoindoles for modulating neurotrophin-mediated activity*. 2007, (Painceptor Pharma Corporation, Can.). Application: WO
- WO. p. 136 pp.
133. Ahn, C., R.F. Campbell, and K.S. Feldman, *Zinc acetate as a catalyst for di- and triimide formation from 1,8-naphthalic anhydride and aromatic polyamines*. *Bull. Korean Chem. Soc.*, 1997. **18**(4): p. 441-442.
134. Cao, H., et al., *Matrix Screening of Substituted N-Aryl-1,8-naphthalimides Reveals New Dual Fluorescent Dyes and Unusually Bright Pyridine Derivatives*. *J. Org. Chem.*, 2005. **70**(13): p. 4929-4934.
135. Du, P., et al., *Dendron-Functionalized Macromolecules: Enhancing Core Luminescence and Tuning Carrier Injection*. *Macromolecules*, 2004. **37**(12): p. 4387-4398.
136. Cao, H., et al., *Matrix Screening of Substituted N-Aryl-1,8-naphthalimides Reveals New Dual Fluorescent Dyes and Unusually Bright Pyridine Derivatives*. *The Journal of Organic Chemistry*, 2005. **70**(13): p. 4929-4934.
137. Qian, X., Z. Zhu, and K. Chen, *The synthesis, application and prediction of Stokes shift in fluorescent dyes derived from 1,8-naphthalic anhydride*. *Dyes Pigm.*, 1989. **11**(1): p. 13-20.

138. Wen, G.-T., et al., *Studies on the transition metal ion induced fluorescence enhancement of 1,8-naphthalimide derivatives*. *Chin. J. Chem.*, 2006. **24**(9): p. 1230-1237.
139. Zee-Cheng, R.K.Y. and C.C. Cheng, *N-(Aminoalkyl)imide antineoplastic agents. Synthesis and biological activity*. *J. Med. Chem.*, 1985. **28**(9): p. 1216-22.
140. Girouard, S., et al., *Synthesis and Characterization of Dimaleimide Fluorogens Designed for Specific Labeling of Proteins*. *J. Am. Chem. Soc.*, 2005. **127**(2): p. 559-566.
141. Braña, M.F., et al., *Synthesis and antitumour activity of new dendritic polyamines-(imide-DNA-intercalator) conjugates: potent Lck inhibitors*. *European Journal of Medicinal Chemistry*, 2002. **37**(7): p. 541-551.
142. Koner, A.L., et al., *Selective sensing of citrate by a supramolecular 1,8-naphthalimide/calix[4]arene assembly via complexation-modulated pKa shifts in a ternary complex*. *J. Org. Chem.*, 2007. **72**(10): p. 3889-3895.
143. Licchelli, M., et al., *Excimer emission induced by metal ion coordination in 1,8-naphthalimide-tethered iminopyridine ligands*. *Dalton Trans.*, 2003(23): p. 4537-4545.
144. Cho, D.W., et al., *Intramolecular Exciplex and Intermolecular Excimer Formation of 1,8-Naphthalimide-Linker-Phenothiazine Dyads*. *J. Phys. Chem. B*, 2006. **110**(10): p. 4576-4582.
145. Zhang, J., et al., *Synthesis and photochemical protein crosslinking studies of hydrophilic naphthalimides*. *Bioorg. Med. Chem. Lett.*, 2002. **12**(6): p. 853-856.
146. Patrick, L.G.F. and A. Whiting, *Synthesis and application of some polycondensable fluorescent dyes*. *Dyes Pigm.*, 2002. **52**(2): p. 137-143.
147. Grabchev, I. and R. Betcheva, *Copolymerization and photostabilization of methyl methacrylate with 1,8-naphthalimide fluorescent brighteners*. *J. Photochem. Photobiol., A*, 2001. **142**(1): p. 73-78.
148. Grabchev, I., et al., *Photochemistry of some 1,8-naphthalic anhydride derivatives*. *Dyes Pigm.*, 1997. **35**(4): p. 361-366.
149. Patrick, L.G.F. and A. Whiting, *Synthesis of some polymerisable fluorescent dyes*. *Dyes Pigm.*, 2002. **55**(2-3): p. 123-132.
150. Konstantinova, T. and R. Lazarova, *On the properties of some naphthalimide dyes and their copolymers with methyl methacrylate*. *J. Univ. Chem. Technol. Metall.*, 2003. **38**(2): p. 281-284.
151. Martin, E., R. Weigand, and A. Pardo, *Solvent dependence of the inhibition of intramolecular charge-transfer in N-substituted 1,8-naphthalimide derivatives as dye lasers*. *J. Lumin.*, 1996. **68**(2-4): p. 157-164.
152. Gruzinskii, V.V., et al., *Spectral-luminescence and lasing properties of several morpholine derivatives of naphthalimide in different solvents*. *J. Appl. Spectrosc.*, 1998. **64**(5): p. 616-619.
153. Tao, Z.-F. and X. Qian, *Naphthalimide hydroperoxides as photonucleases: substituent effects and structural basis*. *Dyes Pigm.*, 1999. **43**(2): p. 139-145.
154. Stewart, W.W., *Synthesis of 3,6-disulfonated 4-aminonaphthalimides*. *J. Am. Chem. Soc.*, 1981. **103**(25): p. 7615-20.
155. De Souza, M.M., et al., *4-Nitro-1,8-naphthalimides exhibit antinociceptive properties*. *Pharmazie*, 2002. **57**(6): p. 430-431.

156. Bouche, C.M., et al., *Side-chain electroluminescent polymers*. Synth. Met., 1996. **81**(2-3, 2nd Japan-France Joint Forum (JFJF'2) on Organic Materials and Optoelectronic Devices, 1995): p. 191-195.
157. Morgado, J., et al., *4-AcNI - a new polymer for light-emitting diodes*. Synth. Met., 1998. **95**(2): p. 113-117.
158. Zhu, W., et al., *Luminescent properties of copolymeric dyad compounds containing 1,8-naphthalimide and 1,3,4-oxadiazole*. Synth. Met., 1998. **96**(2): p. 151-154.
159. Tian, H., et al., *Positive and negative fluorescent imaging induced by naphthalimide polymers*. J. Mater. Chem., 2002. **12**(5): p. 1262-1267.
160. Grabchev, I., J.M. Chovelon, and X. Qian, *A copolymer of 4-N,N-dimethylaminoethylene-N-allyl-1,8-naphthalimide with methylmethacrylate as a selective fluorescent chemosensor in homogeneous systems for metal cations*. J. Photochem. Photobiol., A, 2003. **158**(1): p. 37-43.
161. Grabchev, I., J.-M. Chovelon, and X. Qian, *A polyamidoamine dendrimer with peripheral 1,8-naphthalimide groups capable of acting as a PET fluorescent sensor for metal cations*. New J. Chem., 2003. **27**(2): p. 337-340.
162. Grabchev, I., et al., *Novel heterogeneous PET fluorescent sensors selective for transition metal ions or protons: polymers regularly labeled with naphthalimide*. New J. Chem., 2002. **26**(7): p. 920-925.
163. Tian, H., et al., *Two-path photoinduced electron transfer in naphthalimide-based model compound*. J. Chem. Soc., Perkin Trans. 2, 1999(3): p. 545-550.
164. Gunnlaugsson, T., et al., *Towards the development of controllable and reversible "on-off" luminescence switching in soft-matter; synthesis and spectroscopic investigation of 1,8-naphthalimide-based PET (photoinduced electron transfer) chemosensors for pH in water-permeable hydrogels*. ARKIVOC (Gainesville, FL, U. S.), 2003(7): p. 216-228.
165. Poteau, X., et al., *Fluorescence switching in 4-amino-1,8-naphthalimides: "on-off-on" operation controlled by solvent and cations*. Dyes Pigm., 2000. **47**(1-2): p. 91-105.
166. Jia, L., et al., *A novel chromatism switcher with double receptors selectively for Ag<sup>+</sup> in neutral aqueous solution: 4,5-diaminoalkeneamino-N-alkyl-1,8-naphthalimides*. Tetrahedron Lett., 2004. **45**(20): p. 3969-3973.
167. Cosnard, F. and V. Wintgens, *A new fluoroionophore derived from 4-amino-N-methyl-1,8-naphthalimide*. Tetrahedron Lett., 1998. **39**(18): p. 2751-2754.
168. Chanh, T.C., et al., *Inhibition of retrovirus-induced syncytium formation by photoproducts of a brominated 1,8-naphthalimide compound*. Antiviral Res., 1994. **25**(2): p. 133-46.
169. Chang, S.C., et al., *4-Alkylamino-3-bromo-N-alkyl-1,8-naphthalimides: new photochemically activatable antiviral compounds*. Bioorg. Med. Chem. Lett., 1993. **3**(4): p. 555-6.
170. Chang, S.-C., R.E. Utecht, and D.E. Lewis, *Synthesis and bromination of 4-alkylamino-N-alkyl-1,8-naphthalimides*. Dyes Pigm., 1999. **43**(2): p. 83-94.
171. Lewis, D.E., et al., *Nonazo naphthalimide dyes, their preparation, and their uses*. 1993, (Microbiomed Corp., USA). Application: US  
US. p. 46 pp.
172. Baughman, R.G., et al., *Two related potent antiviral compounds: 3-bromo-N-butyl-4-butylamino-1,8-naphthalenedicarboximide (1) and 4-amino-3-bromo-N-butyl-1,8-naphthalenedicarboximide (2)*. Acta Crystallogr., Sect. C Cryst. Struct. Commun., 1995. **C51**(6): p. 1189-93.

156. Bouche, C.M., et al., *Side-chain electroluminescent polymers*. Synth. Met., 1996. **81**(2-3, 2nd Japan-France Joint Forum (JFJF'2) on Organic Materials and Optoelectronic Devices, 1995): p. 191-195.
157. Morgado, J., et al., *4-AcNI - a new polymer for light-emitting diodes*. Synth. Met., 1998. **95**(2): p. 113-117.
158. Zhu, W., et al., *Luminescent properties of copolymeric dyad compounds containing 1,8-naphthalimide and 1,3,4-oxadiazole*. Synth. Met., 1998. **96**(2): p. 151-154.
159. Tian, H., et al., *Positive and negative fluorescent imaging induced by naphthalimide polymers*. J. Mater. Chem., 2002. **12**(5): p. 1262-1267.
160. Grabchev, I., J.M. Chovelon, and X. Qian, *A copolymer of 4-N,N-dimethylaminoethylene-N-allyl-1,8-naphthalimide with methylmethacrylate as a selective fluorescent chemosensor in homogeneous systems for metal cations*. J. Photochem. Photobiol., A, 2003. **158**(1): p. 37-43.
161. Grabchev, I., J.-M. Chovelon, and X. Qian, *A polyamidoamine dendrimer with peripheral 1,8-naphthalimide groups capable of acting as a PET fluorescent sensor for metal cations*. New J. Chem., 2003. **27**(2): p. 337-340.
162. Grabchev, I., et al., *Novel heterogeneous PET fluorescent sensors selective for transition metal ions or protons: polymers regularly labeled with naphthalimide*. New J. Chem., 2002. **26**(7): p. 920-925.
163. Tian, H., et al., *Two-path photoinduced electron transfer in naphthalimide-based model compound*. J. Chem. Soc., Perkin Trans. 2, 1999(3): p. 545-550.
164. Gunnlaugsson, T., et al., *Towards the development of controllable and reversible "on-off" luminescence switching in soft-matter; synthesis and spectroscopic investigation of 1,8-naphthalimide-based PET (photoinduced electron transfer) chemosensors for pH in water-permeable hydrogels*. ARKIVOC (Gainesville, FL, U. S.), 2003(7): p. 216-228.
165. Poteau, X., et al., *Fluorescence switching in 4-amino-1,8-naphthalimides: "on-off-on" operation controlled by solvent and cations*. Dyes Pigm., 2000. **47**(1-2): p. 91-105.
166. Jia, L., et al., *A novel chromatism switcher with double receptors selectively for Ag<sup>+</sup> in neutral aqueous solution: 4,5-diaminoalkeneamino-N-alkyl-1,8-naphthalimides*. Tetrahedron Lett., 2004. **45**(20): p. 3969-3973.
167. Cosnard, F. and V. Wintgens, *A new fluoroionophore derived from 4-amino-N-methyl-1,8-naphthalimide*. Tetrahedron Lett., 1998. **39**(18): p. 2751-2754.
168. Chanh, T.C., et al., *Inhibition of retrovirus-induced syncytium formation by photoproducts of a brominated 1,8-naphthalimide compound*. Antiviral Res., 1994. **25**(2): p. 133-46.
169. Chang, S.C., et al., *4-Alkylamino-3-bromo-N-alkyl-1,8-naphthalimides: new photochemically activatable antiviral compounds*. Bioorg. Med. Chem. Lett., 1993. **3**(4): p. 555-6.
170. Chang, S.-C., R.E. Utecht, and D.E. Lewis, *Synthesis and bromination of 4-alkylamino-N-alkyl-1,8-naphthalimides*. Dyes Pigm., 1999. **43**(2): p. 83-94.
171. Lewis, D.E., et al., *Nonazo naphthalimide dyes, their preparation, and their uses*. 1993, (Microbiomed Corp., USA). Application: US  
US. p. 46 pp.
172. Baughman, R.G., et al., *Two related potent antiviral compounds: 3-bromo-N-butyl-4-butylamino-1,8-naphthalenedicarboximide (1) and 4-amino-3-bromo-N-butyl-1,8-naphthalenedicarboximide (2)*. Acta Crystallogr., Sect. C Cryst. Struct. Commun., 1995. **C51**(6): p. 1189-93.

173. Tian, H., et al., *Fluorescence properties of dyad compounds containing 1,8-naphthalimide and 1,3,4-oxadiazole*. J. Photochem. Photobiol., A, 1997. **109**(3): p. 213-215.
174. Prasanna de Silva, A. and T.E. Rice, *A small supramolecular system which emulates the unidirectional, path-selective photoinduced electron transfer of the bacterial photosynthetic reaction center*. Chem. Commun. (Cambridge), 1999(2): p. 163-164.
175. Prasanna de Silva, A., et al., *Luminescent PET signaling systems*. Mol. Supramol. Photochem., 2001. **7**(Optical Sensors and Switches): p. 93-151.
176. Alexiou, M.S., et al., *The UV-visible absorption and fluorescence of some substituted 1,8-naphthalimides and naphthalic anhydrides*. J. Chem. Soc., Perkin Trans. 2, 1990(5): p. 837-42.
177. Bojinov, V., et al., *Photophysical and photochemical properties of some 3-bromo-4-alkylamino-N-alkyl-1,8-naphthalimides*. Dyes Pigm., 2003. **58**(1): p. 65-71.
178. Gan, J.-A., et al., *1,8-Naphthalimides for non-doping OLEDs: the tunable emission color from blue, green to red*. J. Photochem. Photobiol., A, 2004. **162**(2-3): p. 399-406.
179. Prasanna de Silva, A., H.Q.N. Gunaratne, and C.P. McCoy, *A molecular photoionic AND gate based on fluorescent signalling*. Nature (London), 1993. **364**(6432): p. 42-4.
180. Prasanna de Silva, A., et al., *New fluorescent model compounds for the study of photoinduced electron transfer: the influence of a molecular electric field in the excited state*. Angew. Chem., Int. Ed. Engl., 1995. **34**(16): p. 1728-31.
181. Bissell, R.A., et al., *Molecular fluorescent signalling with 'fluor-spacer-receptor' systems: approaches to sensing and switching devices via supramolecular photophysics*. Chem. Soc. Rev., 1992. **21**(3): p. 187-95.
182. Bissell, R.A., et al., *Fluorescent PET (photoinduced electron transfer) sensors*. Top. Curr. Chem., 1993. **168**(Photoinduced Electron Transfer V): p. 223-64.
183. de Silva, A.P., et al., *Signaling recognition events with fluorescent sensors and switches*. Chem. Rev. (Washington, D. C.), 1997. **97**(5): p. 1515-1566.
184. Martinez, R. and L. Chacon-Garcia, *The search of DNA-intercalators as antitumoral drugs: What it worked and what did not work*. Curr. Med. Chem., 2005. **12**(2): p. 127-151.
185. Yen, S.F., E.J. Gabbay, and W.D. Wilson, *Interaction of aromatic imides with deoxyribonucleic acid. Spectrophotometric and viscometric studies*. Biochemistry, 1982. **21**(9): p. 2070-6.
186. Brana, M.F. and A. Ramos, *Naphthalimides as anti-cancer agents: synthesis and biological activity*. Curr. Med. Chem. Anti-Cancer Agents, 2001. **1**(3): p. 237-255.
187. Liu, Z.-R., K.H. Hecker, and R.L. Rill, *Selective DNA binding of(N-alkylamine)-substituted naphthalene imides and diimides to G+C-rich DNA*. J. Biomol. Struct. Dyn., 1996. **14**(3): p. 331-339.
188. Ingrassia, L., et al., *Naphthalimides and azonafides as promising anti-cancer agents*. Curr. Med. Chem., 2009. **16**(10): p. 1192-1213.
189. Diaz-Rubio, E., et al., *Phase I study of mitonafide with a 3-day administration schedule: early interruption due to severe central nervous system toxicity*. Invest New Drugs, 1994. **12**(4): p. 277-81.

190. Ratain, M.J., et al., *Paradoxical relationship between acetylator phenotype and amonafide toxicity*. Clin. Pharmacol. Ther. (St. Louis), 1991. **50**(5, Pt. 1): p. 573-9.
191. Jiang, W., et al., *An NBD fluorophore-based sensitive and selective fluorescent probe for zinc ion*. Chem. Commun. (Cambridge, U. K.), 2008(2): p. 259-261.
192. Brana, M.F., et al., *Bis-naphthalimides: a new class of antitumor agents*. Anti-Cancer Drug Des., 1993. **8**(4): p. 257-68.
193. Schneider, R., et al., *Design, synthesis, and biological evaluation of folic acid targeted tetraphenylporphyrin as novel photosensitizers for selective photodynamic therapy*. Bioorg. Med. Chem., 2005. **13**(8): p. 2799-2808.
194. Adronov, A. and J.M.J. Frechet, *Light-harvesting dendrimers*. Chemical Communications, 2000(18): p. 1701-1710.
195. Ramachandram, B., et al., *Unusually High Fluorescence Enhancement of Some 1,8-Naphthalimide Derivatives Induced by Transition Metal Salts*. J. Phys. Chem. B, 2000. **104**(49): p. 11824-11832.
196. Abad, S., et al., *Proton-induced fluorescence switching in novel naphthalimide-dansylamide dyads*. J. Org. Chem., 2005. **70**(25): p. 10565-10568.
197. Bojinov, V.B., N.I. Georgiev, and P.S. Nikolov, *Synthesis and photophysical properties of fluorescence sensing ester- and amidoamine-functionalized 1,8-naphthalimides*. J. Photochem. Photobiol., A, 2008. **193**(2-3): p. 129-138.
198. Nakaya, K.-I.T., Toshiyuki; Shirataki, Yoshiaki; Shiozaki, Hisayoshi; Funabiki, Kazumasa; Shibata, Katsuyoshi; Matsui, Masaki., *4-(2-Aminoethylamino)-7H-benz[de]benzimidazo[2,1-a]isoquinoline-7-one as a highly sensitive fluorescent labeling reagent for carnitine*. Bulletin of the Chemical Society of Japan, 2001. **74**(1): p. 173-177.
199. Podsiadly, R., J. Kolinska, and J. Sokolowska, *Study of free radical polymerization with dye photoinitiators containing a naphthoylenebenzimidazolone skeleton*. Color. Technol., 2008. **124**(2): p. 79-85.
200. Silva, A.P.d., et al., *Luminescence and charge transfer. Part 3. The use of chromophores with ICT (internal charge transfer) excited states in the construction of fluorescent PET (photoinduced electron transfer) pH sensors and related absorption pH sensors with aminoalkyl side chains*. 1993(9): p. 1611-1616.
201. Sakamoto, T. and C. Pac, *A "green" route to perylene dyes: direct coupling reactions of 1,8-naphthalimide and related compounds under mild conditions Using a "new" base complex reagent, t-BuOK/DBN*. J. Org. Chem., 2001. **66**(1): p. 94-98.
202. Qian, X., et al., *A study on the relationship between Stoke's shift and low frequency half-value component of fluorescent compounds*. Dyes Pigm., 1996. **32**(4): p. 229-235.
203. Kolinska, J., et al., *The photochemical behavior of naphthoylenebenzimidazolone dyes in 1-methyl-2-pyrrolidone*. Dyes Pigm., 2009. **82**(2): p. 238-243.
204. Lee, J.-F. and S.L.-C. Hsu, *Green polymer-light-emitting-diodes based on polyfluorenes containing N-aryl-1,8-naphthalimide and 1,8-naphthoylene-arylimidazole derivatives as color tuner*. Polymer, 2009. **50**(24): p. 5668-5674.

205. Peters, A.T. and M.J. Bide, *Amino derivatives of 1,8-naphthalic anhydride and derived dyes for synthetic-polymer fibres*. *Dyes and Pigments*, 1985. **6**(5): p. 349-375.
206. Grayshan, P.H., A.M. Kadhim, and A.T. Perters, *Heterocyclic derivatives of naphthalene-1,8-dicarboxylic anhydride. Part III. Benzo[*k,l*]thioxanthene-3,4-dicarboximides*. *Journal of Heterocyclic Chemistry*, 1974. **11**(1): p. 33-38.
207. Xuhong, Q., Z. Zhenghua, and C. Kongchang, *The synthesis, application and prediction of Stokes shift in fluorescent dyes derived from 1,8-naphthalic anhydride*. *Dyes and Pigments*, 1989. **11**(1): p. 13-20.
208. Peng, Q., et al., *Fabrication of Organic/Inorganic Hybrid Nanocomposite of 1,8-Naphthalimide and CdS in Self-Assembly Film*. *Crystal Growth & Design*, 2003. **3**(5): p. 623-626.
209. Carson, T.D.C., Sean M.; Iverson, Isaac K.; Seo, Wonwoo; Tam-Chang, Suk-Wah, *Materials and methods for the preparation of anisotropically-ordered solids using soluble orienting compounds*. *PCT Int. Appl.*, (2005): p. 108 pp.
210. Kaul, B.L. and J.-C. Graciet, *Dye monomers, their production and polymer compositions containing them*. 2002, (Clariant International Ltd., Switz.). Application: WO  
WO. p. 17 pp.
211. Kaul, B.L. and J.-C. Graciet, *Functionalized dyes, their production and their incorporation into polymeric materials*. 2002, (Clariant International Ltd., Switz.). Application: WO  
WO. p. 14 pp.
212. Carson, T.D., et al., *Materials and methods for the preparation of anisotropically-ordered solids using soluble orienting compounds*. 2005, (The Board of Regents of the University and Community College System of Nevada, USA). Application: WO  
WO. p. 108 pp.
213. Hekmatshoar, R., et al., *Synthesis and absorption properties of some 4-mercapto-1,8-naphthalimides, 4-mercapto-7H-benzimidazo[2,1-a]benz[d,e]isoquinolin-7-one, and 4-mercapto-7H-imidazo[2,1-a]benz[d,e]isoquinolin-7-one*. *Phosphorus, Sulfur Silicon Relat. Elem.*, 2006. **181**(7): p. 1521-1526.
214. King, A.S., I.K. Martin, and L.J. Twyman, *Synthesis and aggregation of amine-cored polyamidoamine dendrons synthesised without invoking a protection/deprotection strategy*. *Polymer International*, 2006. **55**(7): p. 798-807.
215. Tomalia, D.A., et al., *Dendritic macromolecules: synthesis of starburst dendrimers*. *Macromolecules*, 1986. **19**(9): p. 2466-2468.
216. Wiwattanapatapee, R., et al., *Anionic PAMAM Dendrimers Rapidly Cross Adult Rat Intestine In Vitro: A Potential Oral Delivery System?* *Pharmaceutical Research*, 2000. **17**(8): p. 991-998.
217. Malik, N., et al., *Dendrimers: Relationship between structure and biocompatibility in vitro, and preliminary studies on the biodistribution of 125I-labeled polyamidoamine dendrimers in vivo*. *J. Controlled Release*, 2000. **65**(1-2): p. 133-148.
218. Gurdag, S., et al., *Activity of Dendrimer-Methotrexate Conjugates on Methotrexate-Sensitive and -Resistant Cell Lines*. *Bioconjugate Chemistry*, 2006. **17**(2): p. 275-283.

219. Malik, N., et al., *Dendrimers:: Relationship between structure and biocompatibility in vitro, and preliminary studies on the biodistribution of 125I-labelled polyamidoamine dendrimers in vivo*. Journal of Controlled Release, 2000. **65**(1-2): p. 133-148.
220. Martin, E., et al., *Experimental and theoretical study of the intramolecular charge transfer on the derivatives 4-methoxy and 4-acetamide 1,8-naphthalimide N-substituted*. J. Photochem. Photobiol., A, 2005. **175**(1): p. 1-7.
221. Grabchev, I., C. Petkov, and V. Bojinov, *Synthesis and absorption properties of some new bis-1,8-naphthalimides*. Dyes Pigm., 2001. **48**(3): p. 239-244.
222. Stewart, W.W., *Lucifer dyes. Highly fluorescent dyes for biological tracing*. Nature (London), 1981. **292**(5818): p. 17-21.
223. Pardo, A., et al., *N-substituted 1,8-naphthalimide derivatives as high efficiency laser dyes*. J. Photochem. Photobiol., A, 1989. **48**(2-3): p. 259-63.
224. Bojinov, V.B., N.I. Georgiev, and P.S. Nikolov, *Synthesis and photophysical properties of fluorescence sensing ester- and amidoamine-functionalized 1,8-naphthalimides*. Journal of Photochemistry and Photobiology A: Chemistry, 2008. **193**(2-3): p. 129-138.
225. Georgiev, N.I., V.B. Bojinov, and P.S. Nikolov, *Design and synthesis of a novel pH sensitive core and peripherally 1,8-naphthalimide-labeled PAMAM dendron as light harvesting antenna*. Dyes and Pigments, 2009. **81**(1): p. 18-26.
226. Wang, D., T. Imae, and M. Miki, *Reprint of "Fluorescence emission from PAMAM and PPI dendrimers [J. Colloid Interface Sci. 306 (2007) 222-227]*. Journal of Colloid and Interface Science, 2007. **312**(1): p. 8-13.
227. Jasmine, M.J., M. Kavitha, and E. Prasad, *Effect of solvent-controlled aggregation on the intrinsic emission properties of PAMAM dendrimers*. Journal of Luminescence, 2009. **129**(5): p. 506-513.
228. Kleinman, M.H., et al., *Effect of Protonation and PAMAM Dendrimer Size on the Complexation and Dynamic Mobility of 2-Naphthol*. J. Phys. Chem. B, 2000. **104**(48): p. 11472-11479.
229. Manna, A., et al., *Synthesis of Dendrimer-Passivated Noble Metal Nanoparticles in a Polar Medium: Comparison of Size between Silver and Gold Particles*. Chem. Mater., 2001. **13**(5): p. 1674-1681.
230. Williams, A.T.R., S.A. Winfield, and J.N. Miller, *Relative fluorescence quantum yields using a computer-controlled luminescence spectrometer*. Analyst (London), 1983. **108**(1290): p. 1067-71.
231. Rusakowicz, R. and A.C. Testa, *2-Aminopyridine as a standard for low-wavelength spectrofluorimetry*. J. Phys. Chem., 1968. **72**(7): p. 2680-1.
232. Umberger, J.Q. and V.K. LaMer, *The kinetics of diffusion-controlled molecular and ionic reactions in solution as determined by measurements of the quenching of fluorescence*. J. Am. Chem. Soc., 1945. **67**: p. 1099-1109.
233. Dhimi, S., et al., *Phthalocyanine fluorescence at high concentration: dimers or reabsorption effect?* Photochem. Photobiol., 1995. **61**(4): p. 341-6.
234. Patel-Sorrentino, N., S. Mounier, and J.Y. Benaim, *Excitation-emission fluorescence matrix to study pH influence on organic matter fluorescence in the Amazon basin rivers*. Water Res., 2002. **36**(10): p. 2571-2581.
235. Thalacker, C., et al., *Hydrogen bond directed self-assembly of core-substituted naphthalene bisimides with melamines in solution and at the graphite interface*. Org. Biomol. Chem., 2005. **3**(3): p. 414-422.

236. Lo Conte, L., C. Chothia, and J. Janin, *The Atomic Structure of Protein-Protein Recognition Sites*. J. Mol. Biol., 1999. **285**(5): p. 2177-2198.
237. Chabner Bruce, A. and G. Roberts Thomas, Jr., *Timeline: Chemotherapy and the war on cancer*. Nat Rev Cancer, 2005. **5**(1): p. 65-72.
238. Persil, O. and N.V. Hud, *Harnessing DNA intercalation*. Trends Biotechnol., 2007. **25**(10): p. 433-436.
239. Tumiatti, V., et al., *Design, Synthesis, and Biological Evaluation of Substituted Naphthalene Imides and Diimides as Anticancer Agent*. J. Med. Chem., 2009. **52**(23): p. 7873-7877.
240. Ferguson, L.R. and W.A. Denny, *Genotoxicity of non-covalent interactions: DNA intercalators*. Mutat. Res., Fundam. Mol. Mech. Mutagen., 2007. **623**(1-2): p. 14-23.
241. Schneider, H.-J., *Ligand binding to nucleic acids and proteins: Does selectivity increase with strength?* Eur. J. Med. Chem., 2008. **43**(11): p. 2307-2315.
242. Streckowski, L. and B. Wilson, *Noncovalent interactions with DNA: An overview*. Mutat. Res., Fundam. Mol. Mech. Mutagen., 2007. **623**(1-2): p. 3-13.
243. Zhu, H., et al., *R16, a novel amonafide analogue, induces apoptosis and G2-M arrest via poisoning topoisomerase II*. Mol. Cancer Ther., 2007. **6**(2): p. 484-495.
244. Van Quaquebeke, E., et al., *2,2,2-Trichloro-N-({2-[2-(dimethylamino)ethyl]-1,3-dioxo-2,3-dihydro-1H-benzof[de]isoquinolin-5-yl}carbonyl)acetamide (UNBS3157), a Novel Nonhematotoxic Naphthalimide Derivative with Potent Antitumor Activity*. J. Med. Chem., 2007. **50**(17): p. 4122-4134.
245. Mijatovic, T., et al., *UNBS5162, a novel naphthalimide that decreases CXCL chemokine expression in experimental prostate cancers*. Neoplasia (Ann Arbor, MI, U. S.), 2008. **10**(6): p. 573-586.
246. Wang, C., et al., *Preparation of naphthalimide polyamine derivatives as antitumor agents*. 2010, (Henan University, Peop. Rep. China). Application: CN  
CN. p. 18pp.
247. Rodger, A., et al., *Multiple DNA binding modes of anthracene-9-carbonyl-N1-spermine*. Bioorg. Med. Chem., 1995. **3**(6): p. 861-72.
248. Ghaneolhosseini, H., W. Tjarks, and S. Sjoberg, *Synthesis of novel boronated acridines and spermidines as possible agents for BNCT*. Tetrahedron, 1998. **54**(15): p. 3877-3884.
249. Fenniri, H., M.W. Hosseini, and J.M. Lehn, *Molecular recognition of NADP(H) and ATP by macrocyclic polyamines bearing acridine groups*. Helv. Chim. Acta, 1997. **80**(3): p. 786-803.
250. Florence, A.T., T. Sakthivel, and I. Toth, *Oral uptake and translocation of a polylysine dendrimer with a lipid surface*. J. Controlled Release, 2000. **65**(1-2): p. 253-259.
251. Florence, A.T., *The oral absorption of micro- and nanoparticulates: neither exceptional nor unusual*. Pharm. Res., 1997. **14**(3): p. 259-266.
252. Irvine, J.D., et al., *MDCK (Madin-Darby canine kidney) cells: a tool for membrane permeability screening*. J. Pharm. Sci., 1999. **88**(1): p. 28-33.
253. Rothen-Rutishauser, B., et al., *MDCK cell cultures as an epithelial in vitro model: cytoskeleton and tight junctions as indicators for the definition of age-related stages by confocal microscopy*. Pharm. Res., 1998. **15**(7): p. 964-971.

- 
254. Saunders, M., *Transplacental transport of nanomaterials*. Wiley Interdiscip. Rev. Nanomed. Nanobiotechnol., 2009. **1**(6): p. 671-684.
  255. Irvine, J.D., et al., *MDCK (Madin-Darby canine kidney) cells: A tool for membrane permeability screening*. J Pharm Sci, 1999. **88**(1): p. 28-33.
  256. Lipschutz, J.H., et al., *Extracellular Signal-regulated Kinases 1/2 Control Claudin-2 Expression in Madin-Darby Canine Kidney Strain I and II Cells*. J. Biol. Chem., 2005. **280**(5): p. 3780-3788.
  257. Dufes, C., I.F. Uchegbu, and A.G. Schaetzlein, *Dendrimers in gene delivery*. Adv. Drug Delivery Rev., 2005. **57**(15): p. 2177-2202.
  258. Eichman, J.D., et al., *The use of PAMAM dendrimers in the efficient transfer of genetic material into cells*. Pharm. Sci. Technol. Today, 2000. **3**(7): p. 232-245.
  259. Bielinska, A.U., J.F. Kukowska-Latallo, and J.R. Baker, Jr., *The interaction of plasmid DNA with polyamidoamine dendrimers: mechanism of complex formation and analysis of alterations induced in nuclease sensitivity and transcriptional activity of the complexed DNA*. Biochim. Biophys. Acta, Gene Struct. Expression, 1997. **1353**(2): p. 180-190.
  260. Fant, K., et al., *DNA Condensation by PAMAM Dendrimers: Self-Assembly Characteristics and Effect on Transcription*. Biochemistry, 2008. **47**(6): p. 1732-1740.
  261. Kukowska-Latallo, J.F., et al., *Efficient transfer of genetic material into mammalian cells using Starburst polyamidoamine dendrimers*. Proc. Natl. Acad. Sci. U. S. A., 1996. **93**(10): p. 4897-4902.
  262. Boussif, O., et al., *A versatile vector for gene and oligonucleotide transfer into cells in culture and in vivo: polyethylenimine*. Proc. Natl. Acad. Sci. U. S. A., 1995. **92**(16): p. 7297-301.

# **APPENDICES**

# **APPENDIX A**

## **CHEMOTHERAPEUTIC APPLICATIONS**

<b>A.1. In-Vitro Permeability studies.....</b>	<b>128</b>
<b>A.2. DNA Binding studies.....</b>	<b>135</b>

All of the following work was accomplished by internal collaborations within Cardiff University. The “in-vitro permeability study” was carried out by PhD student Ghaith Al-Jayyous of the group of Dr. Mark Gumbleton (Welsh School of Pharmacy), while the “DNA binding study” was performed by PhD students Irina Dorin and Ismail Althagafi of the group of Dr. Niek Buurma (School of Chemistry).

## A.1. In-Vitro Permeability Studies

### A.1.1. Introduction

The rate of permeability of positively charged dendrimers of different generations across epithelial cell monolayers depends on their concentration, and on the generation; with the order of permeability being reported as  $G4 \gg G0 \approx G1 > G3 > G2$ .<sup>[27, 250]</sup> In addition to the generation size of the dendrimer, also the charge of peripheral groups of the dendrimer surface effects the efficiency of dendrimer transport, presumably by modulating the intercellular tight junctions. It is believed that adsorptive-mediated endocytosis is the probable mechanism of dendrimer transport across epithelial cells.<sup>[251]</sup> Recent studies by D’Emanuele *et al.* confirmed that conjugation of small molecular weight drugs (that are known to be p-glycoprotein [P-gp] substrates) to PAMAM dendrimers enhances their transport across P-gp expressing cells indicating that dendrimers are themselves not substrates for P-gp and that they can carry cargo into cells bypassing the plasma membrane P-gp efflux.

Recently, many reports have verified that the transport of PAMAM dendrimers across the epithelial barrier of the gut is influenced by the surface chemistry of the dendrimers.<sup>[26-28]</sup> Early studies propose that the way in which both cationic<sup>[27]</sup> and anionic<sup>[26, 28]</sup> charged dendrimers leak across epithelial barriers is related to their size. In case of PAMAM dendrimers terminated with  $-NH_2$ , transepithelial electrical

resistance (TEER) readings decreased and  $^{14}\text{C}$ -mannitol increased as the generation dendrimer increased. In contrast, TEER or  $^{14}\text{C}$ -mannitol transport was not influenced by PAMAM dendrimers terminated with OH groups; while, in case of PAMAM dendrimers terminated-COOH, decreased TEER and increased  $^{14}\text{C}$ -mannitol permeability within dendrimer generation size (G2.5 and G3.5).<sup>[27-28]</sup> These studies point to an optimum size and charge of PAMAM dendrimers that can effectively translocate drug molecules across the epithelial barrier of the gut. Conversely, a systematic correlation between the effect of charge, size, and degree of surface modification of these dendrimers on their permeability across the intestinal barrier has not been assessed.

The main purpose of our studies is to investigate the transport of our series of fluorescent poly(amidoamine) (PAMAM) dendrons (**FC2G0.5**, **FC2G1.5** and **FC2G2.5**) all with negatively charged surface groups across cell barriers. A test system for measuring membrane permeability has been developed using the MDCK (Madin–Darby Canine Kidney) cell line, to mimic the distal renal epithelium of a normal male cocker spaniel.<sup>[252]</sup> In case of inertly absorbed compounds, drug permeability across MDCK cells is analogous to permeability across Caco-2 cells.<sup>[252]</sup> Over 2–6 days, confluent MDCK monolayers form a tight junction network visible by confocal microscopy.<sup>[253]</sup> The cell lines used are similar except that they hold different numbers of tight junctions, such that their intercellular restrictiveness is different. For instance, the MDCK I cell line present high restrictiveness, e.g. TEER of  $2000\ \Omega\cdot\text{cm}^2$ , while the MDCK II cell line is more permeable with a TEER of  $200\ \Omega\cdot\text{cm}^2$ ; therefore, MDCK I is frequently used as a permeability model for the Blood Brain Barrier (BBB) while the MDCK II a model for the more permeable intestinal barrier.

## A.1.2. Results and Discussions

### A.1.2.1. Permeability of fluorescent core PAMAM dendrons across MDCK I, II cell monolayers

MDCK I, II cells were seeded at 45,000 cells/cm<sup>2</sup> onto polyester 24-well Transwell<sup>®</sup> filters of 0.8 μm mean pore size, 0.33 cm<sup>2</sup> surface area (Corning Incorporated, Corning, NY). MDCK I, II cells were maintained under appropriate incubation conditions described above and used for transport experiments after 4 days post-seeding. The transport of fluorescent core PAMAM dendrons was investigated in triplicate in the apical-to-basolateral (A-B) direction (Figure A.1) at a donor concentration of 1.0 mM. Permeability experiments were conducted in a humidified atmosphere of 37 °C. Samples were collected from the receiver chamber at 30, 60, 90 and 120 min. Permeability samples were analyzed using a Fluostar fluorometer with fluorescent-core PAMAM dendron samples being detected with an excitation

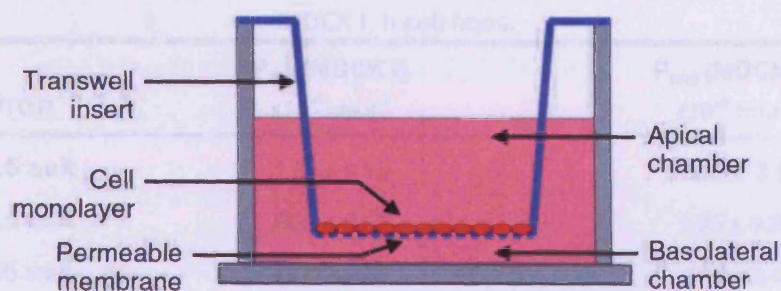


**Figure [A.1]:** Schematic of a Transwell<sup>®</sup> insert showing the separation of apical and basolateral chambers by a permeable membrane with a confluent cell monolayer on the apical surface.<sup>[254]</sup>

wavelength of 460 nm and an emission wavelength of 540 nm. The apparent permeability ( $P_{app}$ ) coefficients were calculated as follows:

$$P_{app} = \frac{\partial Q}{A \cdot C_0 \cdot \partial t} \quad (3)$$

Where  $A$  is the surface area of the membrane filter,  $C_0$  is the initial concentration in the donor chamber, and  $\partial Q/\partial t$  is the permeability rate.<sup>[255]</sup>

For MDCK I cell line,  $P_{app}$  to fluorescent PAMAM dendron **FC2G0.5** salt ( $P_{app}$   $1.81 \pm 0.17 \times 10^{-6}$  cm.sec<sup>-1</sup>) was significantly higher than the maximum possible  $P_{app}$  (based upon LLQ) for **FC2G1.5** salt of  $P_{app} < 0.58 \times 10^{-6}$  cm.sec<sup>-1</sup> and for **FC2G2.5** salt of  $P_{app} < 0.35 \times 10^{-6}$  cm.sec<sup>-1</sup> (Table 1). Similarly a decrease in  $P_{app}$  with increase in molecular size was observed for the MDCK II cell line where  $P_{app}$  of fluorescent PAMAM dendron **FC2G0.5** salt ( $P_{app}$   $8.93 \pm 2.1 \times 10^{-6}$  cm.sec<sup>-1</sup>) was significantly greater than **FC2G1.5** salt ( $P_{app}$   $1.38 \pm 0.24 \times 10^{-6}$  cm.sec<sup>-1</sup>) and **FC2G2.5** salt where the maximum possible  $P_{app}$  (based upon LLQ) was  $\times 10^{-6}$  cm.sec<sup>-1</sup> (Table A.1; Figure A.2).

**Table [A.1]:** Permeability Coefficient ( $10^{-6}$  cm.s<sup>-1</sup>) for dendron generations across MDCK I, II cell lines.

Dendron	$P_{app}$ (MDCK I) $\times 10^{-6}$ cm.s <sup>-1</sup>	$P_{app}$ (MDCK II) $\times 10^{-6}$ cm.s <sup>-1</sup>
<b>FC2G0.5 salt</b>	$1.81 \pm 0.17$	$8.93 \pm 2.1$
<b>FC2G1.5 salt</b>	$BLQ < 0.58$	$1.38 \pm 0.24$
<b>FC2G2.5 salt</b>	$BLQ < 0.35$	$BLQ < 3.48$

The correlation between monolayer permeability ( $P_{app}$ ) and TEER values with the PAMAM dendrons allows us to speculate that these fluorescent dendrons might have been transported across the epithelial cells via a paracellular route. The permeabilities of the dendrons across MDCK II cell line are higher over the permeability across MDCK I cell line was attributed to differences in restrictiveness where MDCK I cell line is more restrictive than MDCK II cell line due to the existence of greater concentration of tight junctions.<sup>[256]</sup>

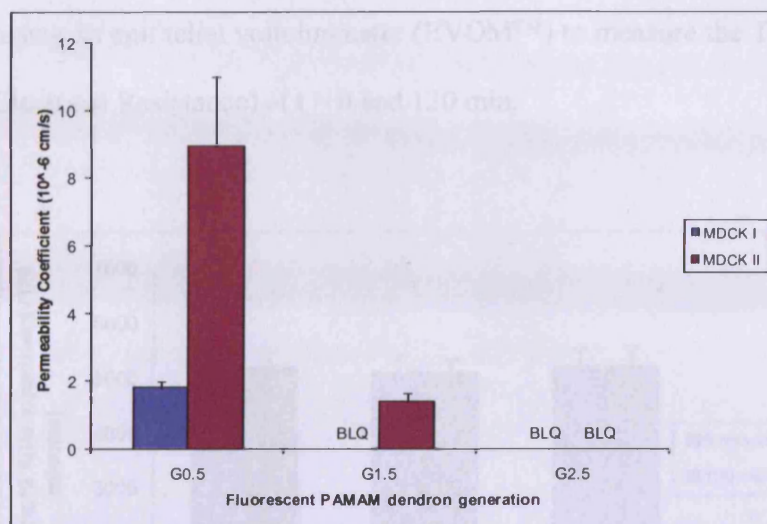


**Figure [A.2]:** The permeability of Fluorescent PAMAM dendrons across MDCK I, II cell monolayer in AB (apical-to-basolateral) directions at concentration 1mM.

#### **A.1.2.2. Effect on monolayer integrity by measuring transepithelial electrical resistance (TEER)**

MDCK I, II cells (passages 5-30) were seeded onto the polystyrene 24-well Transwell® filters at a density of  $1 \times 10^5$  cells/cm<sup>2</sup>. The cells were grown at 37 °C in an atmosphere of 5% CO<sub>2</sub> and 95% relative humidity. Cells were maintained in T-75 flasks using Dulbecco's Modified Eagle's Medium (DMEM) supplemented with 10% fetal bovine serum, 10,000 units/ml penicillin, 10,000 µg/ml streptomycin. Growth medium was changed every 2 days. Cells were passaged at 70-90% confluency using 0.25% trypsin/ethylenediamine tetraacetic acid (EDTA) solution. Transport medium consisted of DMEM-F12 invitrogen. Mean TEER value across the MDCK cell monolayers was found to be  $1000 \pm 58 \Omega \cdot \text{cm}^2$ . The effect of modified fluorescent core PAMAM dendrons on two MDCK cell lines monolayers was determined by measuring of the transepithelial electrical resistance across MDCK cells monolayers in presence of the fluorescent dendrons at donor concentrations of 1µg/mL and 10

$\mu\text{g/mL}$  upon both apical and basolateral incubation. The cell monolayer integrity was monitored using an epithelial voltohmmeter (EVOM™) to measure the TEER (Trans-Epithelial Electrical Resistance) at  $t = 0$  and 120 min.

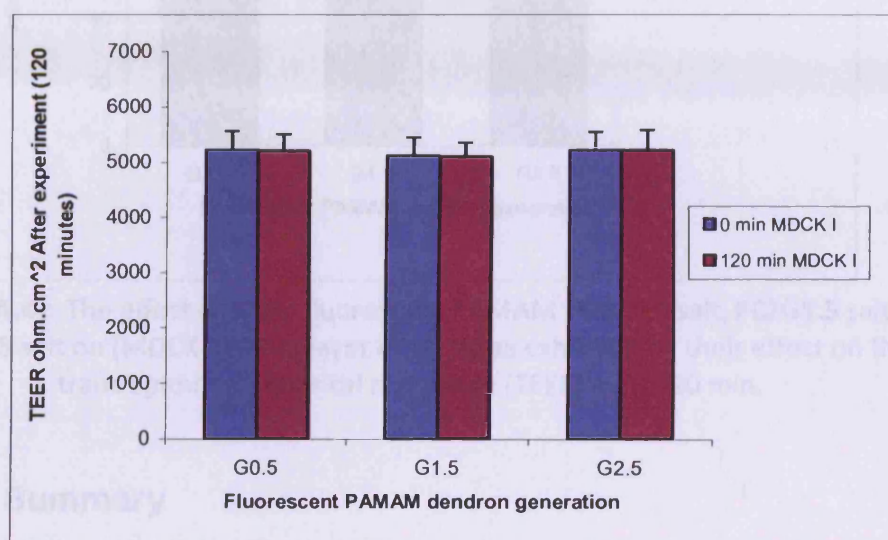


**Figure [A.3]:** The effect of 1mM fluorescent PAMAM FC2G0.5 salt, FC2G1.5 salt or FC2G2.5 salt on (MDCK I) monolayer integrity as exhibited by their effect on the trans epithelial electrical resistance (TEER) at 0, 120 min.

For both MDCK I and MDCK II cell line, the TEER studies indicate that the presence of any of the three fluorescent PAMAM dendrons does significantly change the TEER values. The constant TEER value was independent of dendrimer concentration and duration of incubation (Figures A.3, A.4).

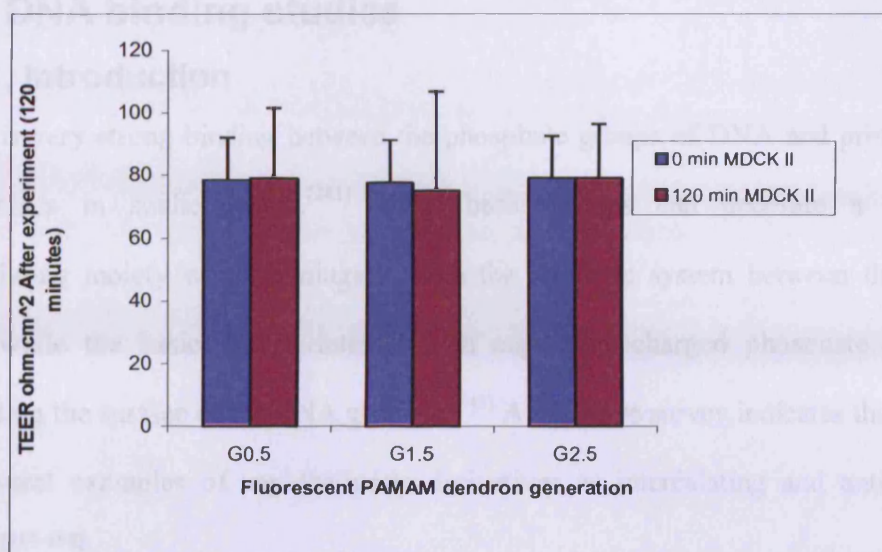


**Figure [A.4]:** The effect of 1mM fluorescent PAMAM FC2G0.5 salt, FC2G1.5 salt or FC2G2.5 salt on (MDCK II) monolayer integrity as exhibited by their effect on the trans epithelial electrical resistance (TEER) at 0, 120 min.

### A.1.3. Summary

In conclusion the results of this initial study suggest that the permeability of fluorescent core PAMAM dendrons across MDCK cell monolayers appear to be a function of the size of the dendrons. These studies pave the way for future detailed mechanistic and morphological studies to elucidate the nature of the interaction of fluorescent core PAMAM dendrons with epithelial cells.

## A.2. DNA binding studies

### A.2.1. Introduction

There is very strong binding between the phosphate groups of DNA and protonated polyamines in acidic media.<sup>[241]</sup> These basic groups can decorate a planar, intercalating moiety which conjugates with the aromatic system between the base pairs, while the basic groups interact with negatively charged phosphate groups decorating the surface of the DNA grooves.<sup>[242]</sup> A literature survey indicates that there are several examples of naphthalimide derivatives as intercalating and anticancer agents.<sup>[184-188]</sup>

Poly(amido amine) PAMAM dendrimers are one of the universal cationic polymer agents that bind to DNA by electrostatic interactions,<sup>[257-258]</sup> once bound PAMAM dendrimers supply protection against DNase activity and hinder gene expression in vitro.<sup>[259-260]</sup> Dendrimers have been applied in DNA binding and gene therapy<sup>[261-262]</sup> and the modification of PAMAM dendrons to incorporate a DNA intercalating naphthalimide chromophore within its core as to provide anti-tumour activity has been described<sup>[141]</sup> and an interesting pharmacological profile was discovered.

The aim of this study is to evaluate PAMAM dendrons/DNA interaction as a function of generation and charge density (cationic, neutral), in order to interrogate the characteristics of the binding event. For this purpose we have investigated the binding of a calf thymus DNA sample, fluorescent –COOH terminated PAMAM dendrons of generation **FC2G0.5**, **FC2G2.5** and **FC2G0**, and –NH<sub>2</sub> terminated **FC2G1**, **FC2G2** PAMAM dendrons using UV-visible spectroscopy.

## A.2.2. Results and discussion

The DNA-binding properties of 3-bromo-7*H*-benz[*de*]benzimidazo[2,1-*a*]isoquinoline-7-one **FC2** and its dendritic derivatives of different generations were studied using UV-visible titrations. Unfortunately, the aqueous solubility of **FC2** is negligible, which did not allow us to carry out UV-visible titrations. Aqueous solubility of **FC2G0**, however, is sufficient for UV-visible titrations (Figure A.5).

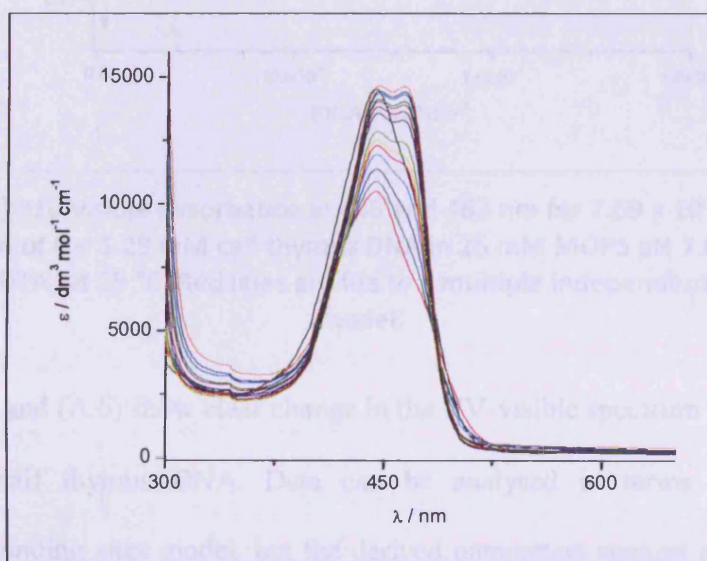


**Figure [A.5]:** UV-visible spectra for  $2.69 \times 10^{-2}$  mM **FC2G0** upon addition of 0 – 1.29 mM calf thymus DNA in 25 mM MOPS pH 7.0, 50 mM NaCl and 1 mM EDTA, at 25 °C.

Figure (A.5) shows an increase in extinction coefficient with increasing concentration of DNA, eventually leading to a spectrum with maxima at 446 and 463 nm. A titration curve can be extracted from the data (Figure A.6).

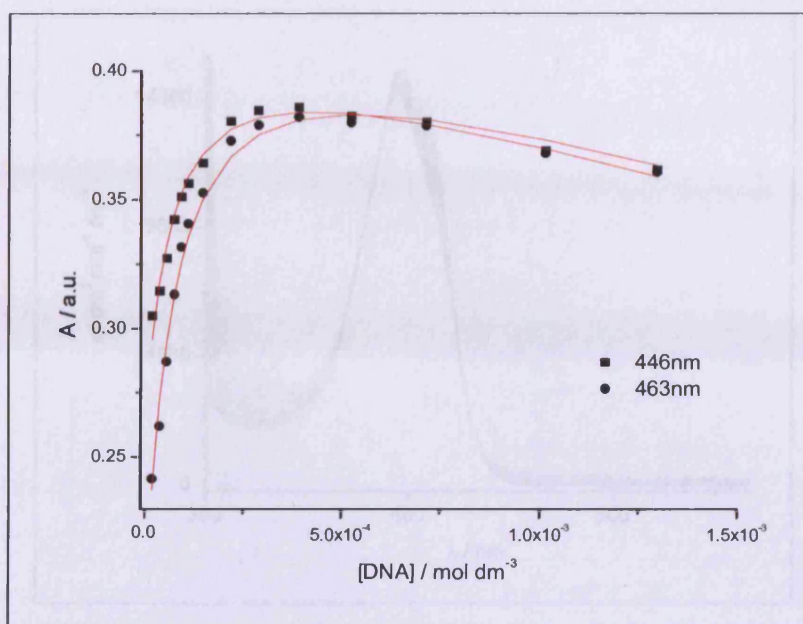


**Figure [A.6]:** UV-visible absorbance at 446 and 463 nm for  $2.69 \times 10^{-2}$  mM **FC2G0** upon addition of 0 – 1.29 mM calf thymus DNA in 25 mM MOPS pH 7.0, 50 mM NaCl and 1 mM EDTA, at 25 °C. Red lines are fits to a multiple independent binding sites model.

Figures (A.5) and (A.6) show clear change in the UV-visible spectrum of **FC2G0** upon addition of calf thymus DNA. Data can be analysed in terms of a multiple independent binding sites model, but the derived parameters suggest a problem with calculated concentrations (the model suggests that 10 ligand molecules bind to every base pair, which is unrealistic). In any case, DNA binding of **FC2G0** is relatively strong.

To investigate the effect of covalently-attached negatively-charged dendrimeric structures, we studied the interactions with calf thymus DNA of **FC2G0.5** carboxylate salt and **FC2G2.5** carboxylate salt, again using UV-visible titrations (Figures A.7 and A.8).

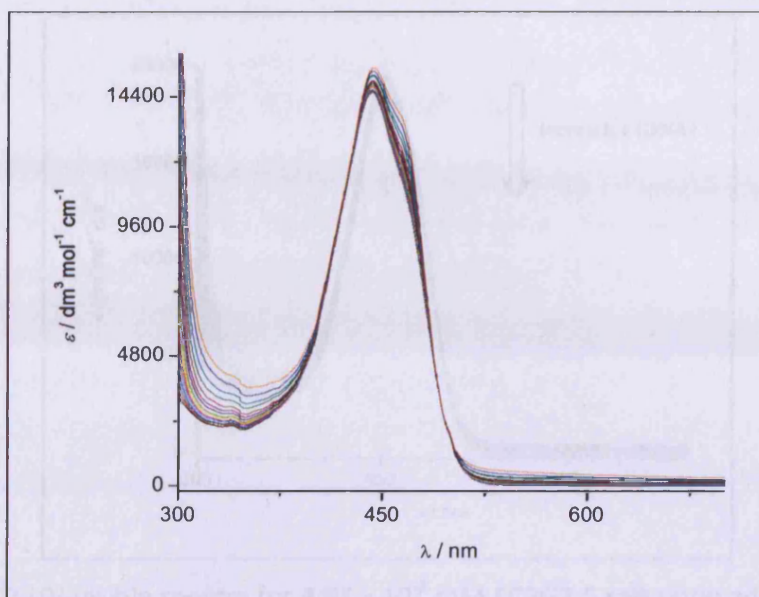


**Figure [A.7]:** UV-visible spectra for  $3.76 \times 10^{-2}$  mM **FC2G0.5** salt upon addition of 0 – 3.03 mM calf thymus DNA in 25 mM MOPS pH 7.0, 50 mM NaCl and 1 mM EDTA, at 25 °C.

Figure (A.7) shows a small increase in the extinction coefficient for **FC2G0.5** carboxylate upon addition of calf thymus DNA. The increase in extinction coefficient does not reach saturation even in the presence of 3.03 mM calf thymus DNA, indicating that the interaction of **FC2G0.5** with calf thymus DNA is considerably weaker than the interaction of **FC2G0** with calf thymus DNA. Nevertheless, the change in the absorption peak towards a shape reminiscent of that for fully DNA-bound **FC2G0** suggests that both molecules bind to DNA in a similar manner, but that binding is attenuated by the appended dendron. Both electrostatic and steric repulsion will undoubtedly play a role.

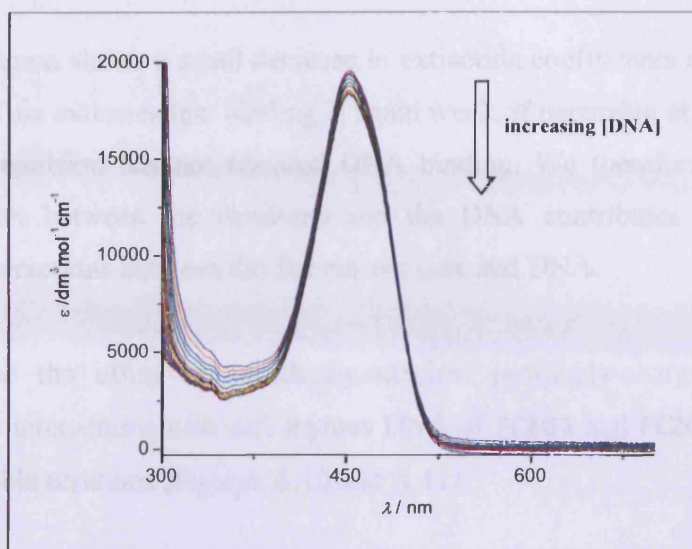


**Figure [A.8]:** UV-visible spectra for  $4.98 \times 10^{-2}$  mM FC2G2.5 salt upon addition of 0 – 4.44 mM calf thymus DNA in 25 mM MOPS pH 7.0, 50 mM NaCl and 1 mM EDTA, at 25 °C.

Figure (A.8) does not show increases in extinction coefficients. A small decrease in extinction coefficient is observed but this does not reach saturation: binding is weak, if any binding occurs at all.

To check whether binding could be switched back on by eliminating electrostatic repulsion, the interaction with DNA of FC2G2.5 ester was studied (Figure A.9)

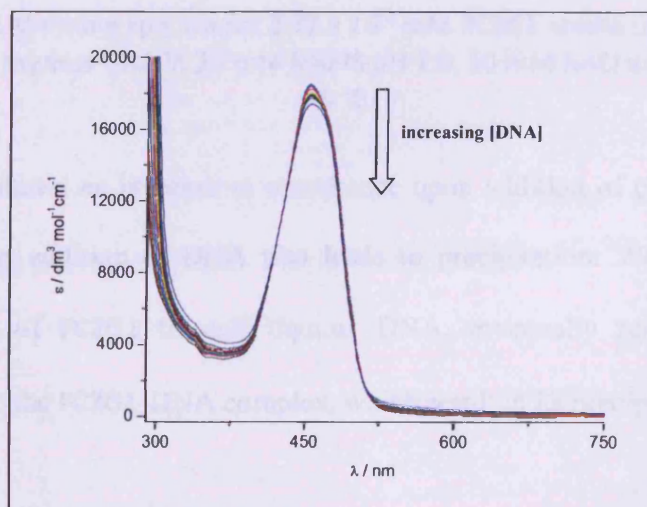


**Figure [A.9]:** UV-visible spectra for  $2.49 \times 10^{-2}$  mM FC2G2.5 ester upon addition of 0 – 0.26 mM calf thymus DNA in 25 mM MOPS pH 7.0, 50 mM NaCl and 1 mM EDTA, at 25 °C.

Figure (A.9) again shows a small decrease in extinction coefficients and saturation is not reached. This indicates that binding is again weak, if occurring at all. Eliminating electrostatic repulsion has not restored DNA binding. We therefore conclude that steric repulsion between the dendrons and the DNA contributes to the lack of observable interactions between the fluorescent core and DNA.

To investigate the effect of covalently-attached positively-charged dendrimeric structures, the interactions with calf thymus DNA of **FC2G1** and **FC2G2** were studied using UV-visible titrations (Figures A.10 and A.11).

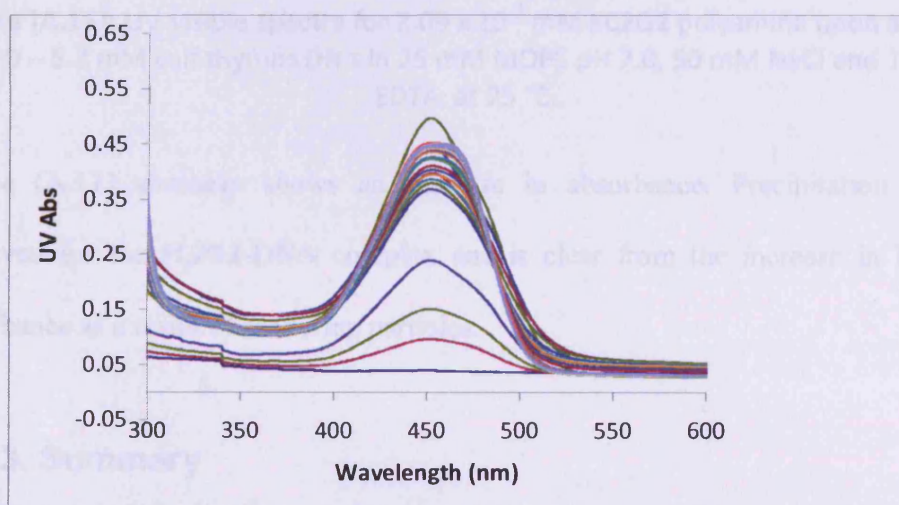


**Figure [A.10]:** UV-visible spectra for  $3.77 \times 10^{-2}$  mM **FC2G1** amine upon addition of 0 – 1.38 mM calf thymus DNA in 25 mM MOPS pH 7.0, 50 mM NaCl and 1 mM EDTA, at 25 °C.

Figure (A.10) shows an increase in absorbance upon addition of calf thymus DNA, but in this case, addition of DNA also leads to precipitation. We attribute this to strong binding of **FC2G1** to calf thymus DNA, eventually resulting in charge neutralization in the **FC2G1**-DNA complex, which result in its precipitation.

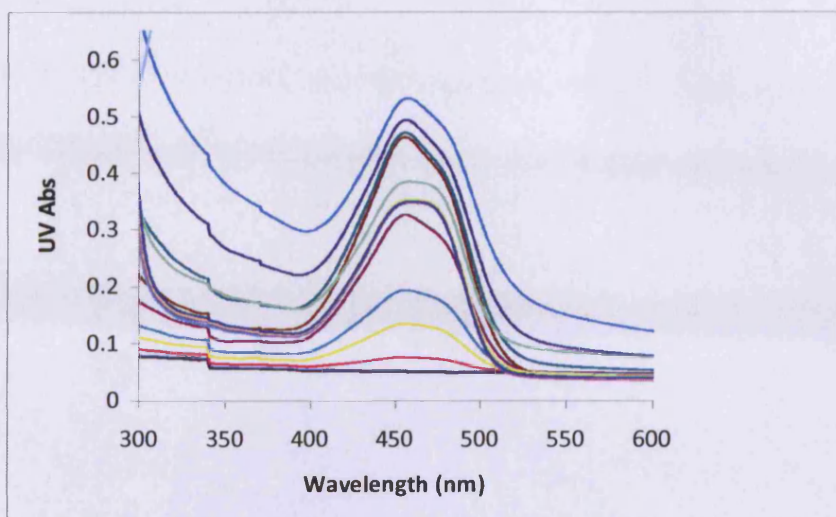


**Figure [A.11]:** UV-visible spectra for  $2.09 \times 10^{-2}$  mM **FC2G2** polyamine upon addition of 0 – 5.2 mM calf thymus DNA in 25 mM MOPS pH 7.0, 50 mM NaCl and 1 mM EDTA, at 25 °C.

Figure (A.11) similarly shows an increase in absorbance. Precipitation is also observed for the **FC2G2**-DNA complex and is clear from the increase in baseline absorbance as a result of scattering particles.

### A.2.3. Summary

The fluorescent core binds to DNA. Although we have not done any experiments to elucidate the binding mode, one would expect this type of flat aromatic molecule to be an intercalator. Addition of negatively charged dendrons results in a strong decrease in affinity for DNA. The affinity is not restored by esterification, highlighting contributions of both electrostatic repulsion but particularly steric interactions in blocking interactions. Coupling the fluorescent core to positively charged dendrons leads to strong binding accompanied by precipitation of the DNA complex. The latter observation is in line with the literature.<sup>[141, 257-258, 261-262]</sup>

